

**Investigating leaf development in moss (*P. patens*)
using Tnt1 insertional "*short-leaf (shlf)*" and
targeted knockout "*slender-leaf*" mutants**

A thesis

Submitted in partial fulfillment of the requirement

of the degree of

Doctor of Philosophy

by

Boominathan Mohanasundaram

20113123




INDIAN INSTITUTE OF SCIENCE EDUCATION AND RESEARCH, PUNE

2018

CERTIFICATE

Certified that the work incorporated in the thesis entitled, “**Investigating leaf development in moss (*P. patens*) using Tnt1 insertional “short-leaf (*shlf*)” and targeted knockout “slender- leaf” mutants**” submitted by **Mr. Boominathan Mohanasundaram** (Reg. No-20113123) was carried out by the candidate, under my supervision. The work presented here or part of it has not been included in any other thesis submitted previously for the award of any degree or diploma from any other University or Institution.

Date: 30th July, 2018



Dr. A. K. Banerjee

(Thesis supervisor)

डॉ. अंजन के. बॅनर्जी/Dr. Anjan K. Banerjee
सहयोगी प्राध्यापक एवं उप अध्यक्ष, जीवशास्त्र कार्यक्रम
Associate Prof. & Co-Chair, Biology Program
भारतीय विज्ञान शिक्षा एवं अनुसंधान संस्थान
Indian Institute of Science Education & Research
पुणे / Pune - 411 008, India

DECLARATION

I declare that this written submission represents my ideas in my own words and where others' ideas have been included; I have adequately cited and referenced the original sources. I also declare that I have adhered to all principles of academic honesty and integrity and have not misrepresented or fabricated or falsified any idea/data/fact/source in my submission. I understand that violation of the above will be cause for disciplinary action by the Institute and can also evoke penal action from the sources that have not been properly cited or from whom proper permission has not been taken when needed.

Date: 30th July, 2018

H. Boominathan

Boominathan Mohanasundaram
Reg. No. 20113123

Acknowledgement

I thank my Ph.D. supervisor Dr. Anjan K. Banerjee for his guidance and constant support to complete of my thesis work. His valuable suggestions and insights helped me to overcome major hurdles during my work. His interest towards scientific research and the tendency to help students to excel in their career has been a inspiration for me to continue in academia.

My sincere thanks to my RAC committee members Prof. Usha Vijayraghavan, Prof. Sanjeev Galande and Dr. Deepak Barua for evaluating my progress every year and helping me to shape my research work properly. I thank CSIR for my research fellowship and IISER-Pune for funding and infrastructure. I remain grateful to the EMBO travel awards and the Infosys foundation for providing me the financial assistance to attend the prestigious EMBO conference on the theme- "land plant evolution" in Lisbon,2018.

*My sincere thanks to the plant research community for sharing many biological reagents and transgenic lines which enabled me to complete my Ph.D. thesis. I would like to thank Prof. Hasebe, NIBB, Japan for sharing the moss knockout and overexpression constructs which are used in this study. Timely help from Prof. Meenu Kapoor, IP University, New Delhi enabled us to establish moss cultures in the lab. My sincere thanks to Prof. Pascal Ratet, CNRS, France and Prof. Thomas Guilfoyle, Univ., Missouri, USA for sharing the Tnt1 retrotransposon and soybean auxin-responsive promoter respectively. My sincere thanks to Prof. Luis Vidali, WPI, USA for providing the myosin 3x-mGFP lines. Prof. Takayuki Kohchi, Kyoto University, Japan helped us to establish *Marchantia polymorpha* in our lab. My sincere thanks to Dr. Bhushan Dholakia for proofreading the thesis.*

I thank Dr. Amey Bhide whose has significantly contributed to this project and helped me in various situations. I would like to thank Arati, Vyankatesh, Sukanya, Kavya, Sheeba, Gargi, Asmi, Navakrishna, Ravi and Montu for their contribution to standardize various protocols in the lab. I thank Shirsa for helping me during my experiments and taking forward moss research work. My sincere thanks to all the past and present members of the Plant Molecular Biology lab. I thank Harpreet, Amit, Kirti, Bhavani, Nilam, and Prajakta for their critical comments on my work. I am grateful to my seniors Arun, Senthil, Ameya, Sneha, Harsha, and Payal for helping me during my initial days at IISER-Pune. Constant help and support from my

friends at home: Mohan, Mahendran, Pal, Soundar, Karuppusamy, Ansar, Ram, Logesh, and Vishnu made my stay at Pune possible. I would like to thank my parents Eswari and Mohansundaram, my sister Kayalvizhi and my nephew Udhaya for their continuous support to continue my research work at Pune.

Boominathan. M

30th July, 2018

Contents

List of Figures	v
List of Tables	viii
Abbreviations	xi
Synopsis	xviii
1 Introduction	1
1.1 Evolution of leaves in plants	2
1.1.1 Phyllids (leaves) in bryophytes	4
1.2 Developmental events in SAM	5
1.2.1 Shoot meristem organization in plants	5
1.2.2 Shoot meristem maintenance and regulation	8
1.2.3 Events of leaf founder cells formation in SAM	8
1.2.4 Role of auxin in leaf founder cell formation in SAM	11
1.2.5 Molecular events in formation of leaf primordia	12
1.2.6 Understanding phyllotaxy in land plants	15
1.3 Leaf development: Acquisition of symmetry axes	16
1.3.1 Adaxial and abaxial polarity determination in leaves	16
1.3.2 Medial-Lateral Polarity determination in leaves	20
1.3.3 Proximal-distal polarity determination in leaves	20
1.4 Control of leaf size	22
1.4.1 Leaf complexity	25
1.4.2 Leaf vasculature	27
1.5 Diversity and development of phyllids in bryophytes	28
1.5.1 Lamina diversity in Bryophytes	29
1.5.2 Midrib diversity in bryophytes	31
1.5.3 The moss - <i>Physcomitrella patens</i> , as a suitable model organism to study evolutionary questions	31
1.5.4 Life cycle of moss (<i>P. patens</i>) and stem cells involved in its body plan	33
1.5.5 Resources available for <i>P. patens</i> research	34

1.6	Hypothesis and objectives	36
2	Development of Tnt1 retrotransposon as a mutagenesis tool and screening of <i>P. patens</i> mutants	38
2.1	Introduction	39
2.1.1	Tnt1 retrotransposon as a mutagenesis tool	39
2.1.2	<i>Physcomitrella patens</i> as a model organism to understand gametophyte evolution	40
2.1.3	Other mutagenesis tools in <i>P. patens</i>	40
2.2	Materials and methods	41
2.2.1	Moss culture and maintenance	41
2.2.2	Methionyl-tRNA _i sequence analysis	42
2.2.3	Cloning and moss transformation	42
2.2.4	Southern hybridization	44
2.2.5	Sequence Specific Amplified Polymorphism-PCR (SSAP-PCR)	44
2.2.6	Thermal Asymmetric Interlaced PCR (TAIL-PCR)	45
2.2.7	GC content analysis	45
2.2.8	Tnt1 retrotransposon expression analysis	46
2.2.9	Screening of Tnt1 insertion lines	46
2.3	Results	47
2.3.1	Tobacco Tnt1 is functional in <i>P. patens</i>	47
2.3.2	Tnt1 preferentially transposes into genes and GC-rich regions in <i>P. patens</i> genome	50
2.3.3	Tnt1 promoter expression is tissue-specific and inducible	54
2.3.4	Isolation of <i>P. patens</i> mutants impaired in gametophyte development	54
2.3.5	Viability of Tnt1 as a mutagenesis tool for <i>P. patens</i>	55
2.4	Discussion	58
3	Characterization of Tnt1 insertional <i>P. patens</i> mutant line, <i>short-leaf</i> (<i>shlf</i>), defective in leaf development	61
3.1	Introduction	62
3.1.1	Moss leaf development	62
3.1.2	Factors influencing leaf shape and size	62
3.1.3	Auxin metabolism, signaling and transport in <i>P. patens</i>	63

3.2	Materials and methods	64
3.2.1	Plant culture and maintenance	64
3.2.2	Phenotypic analysis of <i>shlf</i> mutant	65
3.2.3	Cloning and plant transformation	65
3.2.4	PEG-mediated transformation	66
3.2.5	GUS assay	67
3.2.6	Genome sequencing	67
3.2.7	qRT-PCR analysis	68
3.2.8	Plasmodesmata (PD) associated callose staining using aniline blue	68
3.2.9	Bioinformatic analysis	68
3.3	Results	69
3.3.1	Phenotypic characterization of <i>short-leaf</i> (<i>shlf</i>) mutant lines	69
3.3.2	The response of <i>shlf</i> gametophores to temperature and dark conditions	71
3.3.3	<i>shlf</i> mutant show reduced apical dominance	72
3.3.4	Analysis of auxin accumulation pattern in <i>shlf</i> gametophore	73
3.3.5	WGS and determination of causal gene for the <i>shlf</i> mutant	76
3.3.6	Bio-informatic analysis of <i>SHLF</i> gene	79
3.4	Discussion	86
3.4.1	Phenotypic and molecular characterization of <i>short-leaf</i> (<i>shlf</i>) mutant indicate differential auxin accumulation	86
3.4.2	<i>SHLF</i> is the causal gene of <i>short-leaf</i> mutant	88
3.4.3	<i>SHLF</i> represents a novel bryophyte-specific gene family	89
4	A reverse genetic approach to characterize the role of <i>SCARECROW</i> orthologs of <i>P. patens</i> in gametophore shoot development	91
4.1	Introduction	92
4.1.1	SCR is a GRAS domain transcription factor	93
4.1.2	Asymmetric divisions and moss gametophore development	93
4.2	Materials and methods	94
4.2.1	Phylogenetic tree construction	94
4.2.2	Moss culture and maintenance	95
4.2.3	Cloning and plant transformation	95

4.2.4	PEG-mediated protoplast transformation	95
4.2.5	qRT-PCR analysis	96
4.2.6	<i>in situ</i> hybridization	97
4.2.7	Microscopy	97
4.2.8	Histological analysis	98
4.3	Results	98
4.3.1	Identification of <i>P. patens</i> orthologs of <i>SCR</i>	98
4.3.2	<i>Ppscr3</i> knock out lines developed slender-leaves	100
4.3.3	Histological approach to understand the slender-leaf phenotype	102
4.3.4	Live cell imaging of myosin XI-3xEGFP line to study cell division pattern	105
4.4	Discussion	106
5	Summary and future directions	110
6	References	118
7	Annexure	141

List of Figures

1.1	The morphological variation of shoot and leaf among major clades of living land plants.	3
1.2	Independent origins of leaf evolution.	4
1.3	Different layers and zones of vascular shoot apical meristem (SAM)	6
1.4	Formation of the moss leaf apical cell and leaf growth	7
1.5	Interaction domains of critical players regulating shoot apical meristem (SAM) development	9
1.6	MP accumulates before convergent polar localization of PIN1 around incipient primordia	12
1.7	<i>Arabidopsis</i> mutant lines that are defective in organ primordia formation	13
1.8	Effect of loss of function pin mutant and perturbation of auxin concentration on phyllid and phyllotaxy of moss gametophores	13
1.9	Symmetries of a leaf	16
1.10	Surgical and genetic studies on the adaxial-abaxial polarity of a leaf	17
1.11	<i>Arabidopsis</i> mutants defective in adaxial-abaxial leaf patterning	19
1.12	Mutants defective in proximo-distal and M-L leaf patterning	21
1.12	continued	22
1.13	Phytohormones and genes involved in the regulation of the cell proliferation ‘arrest front’ dynamics	23
1.14	Regulation of angiosperm complexity by class I <i>KNOX</i> and <i>FLO/LFY</i>	26
1.15	Peak of leaf diversity	30
1.16	Phyllid diversity in bryophytes	30
1.17	The phylogenetic relationship among moss species is depicted in a cladogram	32
1.18	<i>P. patens</i> life cycle and the stem cells involved in it’s body plan	35
1.18	continued	36
2.1	<i>P. patens</i> has the necessary host factor for Tnt1 transposition activity	48
2.2	PCR screening of <i>P. patens</i> lines harboring a Tnt1 retrotransposon	48
2.3	Detection of Tnt1 transposition activity in mutant lines of moss generated by <i>Agrobacterium</i> -mediated transformation	49
2.4	Tnt1 retrotransposon insertions in <i>P. patens</i> genome determined by TAIL-PCR analysis	52

2.5	Tnt1 transposition sites are biased towards the regions of high local GC content in <i>P. patens</i> genome	53
2.6	Estimation of critical GC value (GC*) of <i>P. patens</i> genome	53
2.7	Tissue-specific inducible expression pattern of tobacco Tnt1 in <i>P. patens</i>	55
2.8	Novel phenotypes isolated from the Tnt1 insertional mutant population	56
2.9	SSAP analysis to assess the stability of Tnt1 insertional mutants	57
3.1	<i>shlf</i> mutant produces two times shorter leaves than WT	70
3.2	Both cell division and elongation are affected in <i>shlf</i> leaves	70
3.3	<i>shlf</i> gametophores and leaves are sensitive to the environmental changes	72
3.4	<i>shlf</i> gametophores exhibit reduced apical dominance.	73
3.5	Generation of <i>GH3::GUS</i> lines in WT and <i>shlf</i> backgrounds	74
3.6	Soybean <i>GH3::GUS</i> lines revealed the differential auxin accumulation patterns in <i>shlf</i> gametophores	74
3.7	Callose staining indicates that the plasmodesmata (PD) density could be low in <i>shlf</i> mutant leaves	75
3.8	PCR confirmation of Tnt1 insertion inside the locus Pp3c1_9390	77
3.9	PCR confirmation of Tnt1 insertion inside the locus Pp3c14_22870	78
3.10	Generation of Pp3c1_9390 over-expression lines in the <i>shlf</i> background	79
3.11	Generation of Pp3c14_22870 over-expression lines in the <i>shlf</i> background	80
3.12	Pp3c14_22870 overexpression rescues the <i>shlf</i> phenotype	80
3.13	Primary structure of <i>SHLF</i> gene and protein	81
3.14	Tandem DNA repeats of <i>SHLF</i>	82
3.15	Tandem amino acid repeats of SHLF	82
3.16	<i>SHLF</i> has N-terminal ER-targeting signal	83
3.17	<i>SHLF</i> is a bryophyte-specific gene	84
3.18	<i>SHLF</i> gene is conserved among lower streptophytes	85
3.19	Cross-species complementation of <i>SHLF</i>	86
4.1	Phylogenetic tree of GRAS domain containing transcription factors	99
4.2	Expression analysis of <i>P. patens</i> <i>SCARECROW</i> orthologs	99
4.3	<i>in situ</i> hybridization to detect the expression pattern of <i>PpSCR3</i>	100
4.4	Generation of <i>Ppscr3</i> knockout lines in moss	101

4.5	<i>Ppscr3</i> knockout moss lines produced slender-leaves	101
4.6	Understanding the slender-leaf phenotype with histological sections of leaves .	103
4.7	Serial cross section of a WT moss leaf from leaf tip to base	103
4.8	Serial cross-sections of a <i>Ppscr3</i> mutant leaf from it's tip to base	104
4.9	Serial cross-sections of a <i>Ppscr3</i> leaf at the middle of the proximal-distal axis .	104
4.10	Tracking cell division in protonemal filaments using myosin XI-3xEGFP lines .	106
4.11	Proposed model of cell division patterns and comparison between WT and <i>Pp- scr3</i> knockout lines	109

List of Tables

1.1	Conservation of crucial genetic players regulating SAM among plant lineages .	10
2.1	List of primers used in this study.	43
2.2	List of primers used in this study.	50
3.1	List of primers used in this study.	66
3.2	Tnt1 and T-DNA insertions in <i>shlf</i> mutant genome ascertained by WGS	76
3.3	Details of local protein BLAST results for SHLF homolog search.	85
3.4	Details of Marpolbase BLAST results for SHLF homolog search.	86
4.1	List of primers used in this study.	96

Abbreviations

1-Naphthaleneacetic acid	NAA
1-N-Naphthylphthalamic acid	NPA
2,4-Dichlorophenoxyacetic acid	2,4-D
2-Deoxy-D-Glucose	DDG
4-Nitrobluetetrazolium chloride	NBT
5-Bromo 4-chloro-3-indolyl-phosphate	BCIP
6-Benzylaminopurine	BAP
abscisic acid	ABA
<i>AINTEGUMENTA</i>	<i>ANT</i>
amino acid	aa
<i>ANGUSTIFOLIA3 GRF INTERACTING FACTOR</i>	<i>AN3/GIF1</i>
<i>Arabidopsis thaliana</i>	<i>A. thaliana</i>
<i>ASYMMETRIC LEAVES1</i>	<i>AS1</i>
<i>ASYMMETRIC LEAVES2</i>	<i>AS2</i>
<i>AUXIN RESPONSE FACTOR 3</i>	<i>ARF3</i>
<i>AUXIN RESPONSE FACTOR 4</i>	<i>ARF4</i>
<i>AUXIN-REGULATED GENE INVOLVED IN ORGAN SIZE</i>	<i>ARGOS</i>
<i>BABY BOOM</i>	<i>BBM</i>
<i>BIG BROTHER</i>	<i>BB</i>
<i>BREVIPEDICELLUS</i>	<i>BP</i>
central zone	CZ
class III <i>HOMEODOMAIN-LEUCINE ZIPPER</i>	<i>HD-ZIPIII</i>
critical GC value	GC*
<i>CUP-SHAPED COTYLEDON</i>	<i>CUC</i>
cytokinin	CK
dispersed meristematic cells	DMC
endoplasmic reticulum	ER
epidermal patterning factors	EPF
gibberellic acid	GA
<i>A. thaliana Gibberellin 20 oxidase 1</i>	<i>AtGA20ox1</i>
<i>A. thaliana Gibberellin2 – β – dioxygenase2</i>	<i>AtGA2ox2</i>

<i>GIBBERELLIN-INSENSITIVE</i>	<i>GAI</i>
<i>GRETCHEN HAGEN3</i>	<i>GH3</i>
<i>GROWTH-REGULATING FACTOR</i>	<i>GRF</i>
<i>INDETERMINATE GAMETOPHYTE1</i>	<i>IG1</i>
indole acetic acid	IAA
initiator methionyl-tRNA	Met-tRNA ^{Met}
internal peripheral zone	IPZ
International Moss Stock Center	IMSC
<i>KANADI</i>	<i>KAN</i>
<i>KNOTTED-like homeobox</i>	<i>KNOX</i>
leaf apical cells	LAC
long terminal repeats	LTR
medial-lateral	M-L
<i>MONOPTEROS</i>	<i>MP</i>
N-1-Naphthylphthalamic Acid	NPA
<i>NARROW SHEATH1</i>	<i>NS1</i>
<i>NARROW SHEATH2</i>	<i>NS2</i>
Organ primordia	OP
organizing center	OC
outer peripheral zone	OPZ
<i>P. patens SCR</i>	<i>PpSCR</i>
<i>PEAPOD</i>	<i>PPD</i>
peripheral zone	PZ
<i>PHABULOSA</i>	<i>PHB</i>
<i>phantastica</i>	<i>phan</i>
<i>PHAVOLUTA</i>	<i>PHV</i>
phosphate buffer saline	PBS
<i>Physcomitrella patens</i>	<i>P. patens</i>
<i>PHYTOCHROME A SIGNAL TRANSDUCTION1</i>	<i>PAT1</i>
<i>PINFORMED1</i>	<i>PIN1</i>
plasmodesmata	PD
<i>PLETHORA</i>	<i>PLT</i>
polar auxin transport	PAT
polymerase chain reaction	PCR

primer binding site	PBS
<i>REPRESSOR of ga1-3</i>	<i>RGA</i>
restriction enzyme	RE
<i>REVOLUTA</i>	<i>REV</i>
root apical meristem	RAM
<i>ROUGH SHEATH2</i>	<i>RS2</i>
saline sodium citrate	SSC
<i>SCARECROW</i>	<i>SCR</i>
shoot apical meristem	SAM
<i>SHOOT MERISTEMLESS</i>	<i>STM</i>
<i>SHORT INTERNODES/ STYLISH</i>	<i>SHI/ STY</i>
<i>short-leaf</i>	<i>shlf</i>
<i>SHORTROOT</i>	<i>SHR</i>
<i>TAA-1</i> related enzymes	<i>TARs</i>
<i>TEOSINTE BRANCHED1, CYCLOIDEA, PROLIFERATING</i>	<i>TCPs</i>
<i>CELL FACTORS</i>	
thermal asymmetric interlaced PCR	TAIL-PCR
transcription factor	TF
Transfer DNA	T-DNA
transfer RNA	tRNA
Ultraviolet C	UV-C
whole genome sequencing	WGS
wild-type	WT
<i>WUSCHEL</i>	<i>WUS</i>
<i>WUS-related homeobox</i>	<i>WOX</i>
β – glucuronidase	<i>GUS</i>

Synopsis

Investigating leaf development in moss (*P. patens*) using Tnt1 insertional "*short-leaf* (*shlf*)" and targeted knockout "*slender-leaf*" mutants

Name: Boominathan Mohanasundaram

Reg. No: 20113123

Name of the supervisor: Dr. Anjan K. Banerjee

Department: Biology

Date of registration: 1st August, 2011

Indian Institute of Science Education and Research (IISER), Pune, India.

Introduction

Leaves are highly specialized organs for light harvesting and photosynthesis. Leaf tissue is flattened to various degrees and arranged in a species-specific phyllotactic pattern in order to optimize the light-intercepting leaf area per unit biomass invested (Wright *et al.*, 2004). Due to the immense contribution of leaves for the survival of a plant, leaf-like organs have evolved independently across plant lineages multiple times, which are majorly classified as megaphylls, microphylls, and phyllids (Tomescu, 2009). It was proposed that microphylls form a monophyly, and they have evolved from the leafless ancestors of the extinct clade, zosterophylls. The enation theory has suggested that small enations found on the leafless stems of zosterophylls were vascularised and evolved into microphylls (Bower, 1935). Widely-accepted Zimmermann's telome theory states that megaphylls have evolved from the extinct leafless ancestors of trimerophytes (Zimmermann, 1952). However, the origin and evolution of miniature leaf-like organs (phyllids) of gametophytes in bryophyte (moss and liverworts) is not clear. In the bryophytes monophyly, moss and liverwort are closely related than hornworts (Puttick *et al.*, 2018). Nevertheless, it is not clear whether the phyllids (leaf) of moss and leafy-liverworts share a common origin or not? Thus, further studies through phylogenetics and functional genomics would give better insights to conclude about the origin of leaf like organs in bryophytes. Though vascular

plant leaves and moss leaves have evolved independently, their basic morphological, anatomical and functional features have converged. As commonly observed in the leaves of vascular plants, phyllids also have a midrib flanked by the flat leaf blades with different polarity axes and arranged on a predefined phyllotaxy. However, they vary entirely in their developmental events and genetic regulatory networks. Unlike sporophytic shoot, a single tetrahedral gametophore apical cell divides to form leaf apical in a spiral phyllotaxy, which is robust to exogenous hormone treatments (Crandall-Stotler, 1980; Harrison *et al.*, 2009; Bennett *et al.*, 2014; Kofuji and Hasebe, 2014). In contrast to flowering plants, moss leaf primordium is developed by a series of asymmetric cell division of leaf apical cell, hence, the total leaf area can be divided into asymmetric segments (Harrison *et al.*, 2009). The major genetic factors regulating shoot apices such as class I *KNOTTED-HOMEODOMAIN* (*KNOX*), *ASYMMETRIC LEAVES1*, *ROUGH SHEATH2*, *PHANTASTICA* (*ARP* genes) and *CUP-SHAPED COTYLEDON* (*CUC*) genes are either not involved in the gametophore shoot development or absent in the moss genome (Sundås-Larsson *et al.*, 1998; Harrison *et al.*, 2005; Floyd *et al.*, 2006; Sakakibara *et al.*, 2008). However, orthologs of *Arabidopsis* *AP2*-type genes, which are involved in regulating cell proliferation, root apical meristem (*RAM*) stem cell niche formation and embryogenesis, respectively, (Elliott *et al.*, 1996; Boutilier *et al.*, 2002; Aida *et al.*, 2004) are necessary for the moss gametophore apical cell formation (Aoyama *et al.*, 2012). These studies have suggested that haploid and diploid body plans are distinct. Hence, we hypothesize that forward genetics would be an ideal approach to study the moss gametophore shoot/leaf development. This would benefit from the haploid dominant life cycle of moss as well as the high preferential transposition of *Tnt1* into genic regions. Considering the role of orthologs of *AP2*-type transcription factors (*TFs*) in the moss gametophore apical cell development, orthologs of *SCARECROW* (*SCR*), which are part of the genetic network regulating *RAM* along with *AP2*-type genes, were also selected for a parallel reverse genetic study. Hence, the following objectives were selected for the present study.

1. To develop an efficient *Tnt1* retrotransposon-based mutagenesis protocol in moss for efficient gene discovery and screen for such mutants.
2. To characterize *Tnt1* insertional mutants defective in the gametophore shoot and leaf development.
3. To study the function of a *GRAS* domain *TFs* in the gametophore shoot development by a reverse genetic approach.

Chapter 2: Development of Tnt1 retrotransposon as a mutagenesis tool and screening of *P. patens* mutants

Literature survey suggested that the moss leaf regulatory network could be different from vascular plant leaves (Sakakibara *et al.*, 2008). Hence, we chose a forward genetic approach to study the moss gametophore shoot apex development. When we initiated this study, there was no efficient transposition protocol for *P. patens*. Earlier, it was demonstrated that tobacco Tnt1 retrotransposon actively transposes in several heterologous angiosperm hosts like *Arabidopsis* (Lucas *et al.*, 1995), Medicago (d'Erfurth *et al.*, 2003), soybean (Cui *et al.*, 2013) and potato (Duangpan *et al.*, 2013) and shown to preferably transpose into gene-rich regions. Hence, we attempted to use tobacco Tnt1 as a mutagenesis tool for *P. patens* to generate mutants.

Through bioinformatics analysis, we found that Tnt1 could be functional in all the sequenced-genomes of land plant species. We also performed Southern blotting and sequence-specific amplified polymorphism-PCR (SSAP-PCR) to detect Tnt1 transposition events in *P. patens*. Additionally, thermal asymmetric interlaced-PCR (TAIL-PCR) was performed to identify the genome coordinates of Tnt1 transpositions. Detailed analysis of this data suggested that Tnt1 preferentially transposed into gene- and GC-rich regions of *P. patens* genome. Long terminal repeat (LTR) promoter-reporter lines showed that LTR promoter was active in the moss gametophore apical cell. However, SSAP-PCR analysis confirmed that the LTR promoter activity did not reflect in the accumulation of mutagenic load in the mutant genome. Our forward genetic screen resulted into many mutants that were defective in the gametophyte development including a *short-leaf* mutant. Overall, we show that *Agrobacterium tumefaciens*-mediated Tnt1 insertional mutagenesis could also successfully generate mutants for forward genetic studies in moss.

Chapter 3: Characterization of Tnt1 insertional *P. patens* mutant line, *short-leaf* (*shlf*), defective in leaf development

Our forward genetic screen on Tnt1 insertional mutant population yielded a *short-leaf* (*shlf*) mutant, which had impaired leaf development. Literature review suggest that only the miniature leaves of class III *HOMEODOMAIN-LEUCINE ZIPPER* (*HD-ZIP III*) knockout lines to be phenotypically similar to *shlf* leaves (Yip *et al.*, 2016). However, leaves of *HD-ZIP III* knockdown lines had highly disoriented cell arrangements, while *shlf* had the proper cell ar-

rangements. Hence, we hypothesize that the *shlf* phenotype could be caused by a gene, which is yet to be characterized in *P. patens*. Therefore, we initiated a complete phenotypic characterization of *shlf* mutant.

Phenotypic analysis revealed that the *shlf* mutant had pleiotropic phenotypes such as small leaf size, shape, temperature sensitivity, early etiolation and reduced apical dominance. The mutant leaves were small due to the suppression of both cell division and cell elongation. Using soybean *GRETCHEN HAGEN3* (*GH3*) promoter, we analyzed the auxin accumulation patterns and how it changes upon treatment with callose biosynthesis inhibitor, 2-Deoxy-D-Glucose (DDG). *GH3::GUS* lines showed differential auxin accumulation patterns in the *shlf* mutant gametophores. In contrast to the wild-type (WT), *shlf* gametophores exhibited high GUS activity at the apex than base. We showed that this differential GUS activity in *shlf* could be reversed by the DDG treatment. Aniline blue staining of plasmodesmata (PD)-associated callose revealed that the *shlf* mutant leaves had a low density of PD connections. Whole genome sequencing (WGS) analysis indicated one T-DNA insertion and three Tnt1 insertions in the genome of *shlf* mutant. Two out of three Tnt1 insertions were inside the open reading frame. Two putative candidate genes (*EXTENSIN* and a gene of unknown function), disrupted by Tnt1 transposition, were overexpressed individually in the *shlf* background to rescue the phenotype. While extension (a protein involved in self-assembly of cell wall) did not rescue the phenotype, the gene of unknown functions rescued the short leaf phenotype. Preliminary sequence analyses of this gene showed 4 unique repeats of 513 bp (171 amino acid) in the genomic DNA, mRNA and protein sequences. Our bioinformatic analyses suggested that the *SHLF* could be specific for lower streptophytes. Additionally, we also attempted to rescue the *shlf* phenotype by overexpressing the *M. polymorpha* homolog to understand the functional conservation across plant lineages.

Chapter 4: A reverse genetic approach to characterize the role of *SCARECROW* orthologs of *P. patens* in gametophore shoot development

In parallel to the forward genetic approach, we also carried out a reverse genetic approach with key TFs that are associated with gametophyte shoot development. Literature review suggested that AP2-type TFs are necessary for the gametophore apical cell development in *P. patens* (Aoyama *et al.*, 2012). In *Arabidopsis*, *AINTEGUMENTA* (*ANT*), *PLETHORA* (*PLT*) and *BABY BOOM* (*BBM*) (*APB*) genes, collectively known as AP2-type genes, regulate cell

proliferation, root apical meristem (RAM) stem cell niche formation, and embryogenesis, respectively (Elliott *et al.*, 1996; Boutilier *et al.*, 2002; Aida *et al.*, 2004). *SCR* TF regulates an asymmetric cell division in RAM and is a member of the gene regulatory network governing the root development along with *AP2*-type TFs. Hence, we hypothesize that the members of this regulatory network could be conserved between *P. patens* and *Arabidopsis*. Therefore, *SCR* TFs were selected as potential candidates to study their role(s) in the moss gametophore shoot/leaf development.

To identify the orthologs of *SCR* TF, we constructed a phylogenetic tree of GRAS domain-containing proteins from *P. patens* and *Arabidopsis*. The phylogenetic analysis suggested that *P. patens* has three orthologs for the *Arabidopsis SCR*. The *in situ* hybridization analysis revealed that the expression of *PpSCR3* is not tissue specific. We generated knock-out lines for one of the orthologs of *PpSCR3* that developed a slender-leaf phenotype. Further analysis revealed that slender-leaf had less leaf lamina width and having a thick midrib. Histological sectioning of WT and *Ppscr3* leaves- indicated that the mutant leaves had very less anticlinal cell divisions causing slender-leaf formation. Based on these histological observations, we have proposed a model for moss midrib development, wherein, lack of asymmetric anticlinal divisions in *Ppscr3* mutants leads to the development of thick midrib. However, this cell-division model needs to be validated by live-imaging techniques. To further authenticate these findings, attempts were made to live-image the cell division patterns from the WT and *Ppscr3* leaves. Our findings suggest that the role of *SCR* TF in the regulation of asymmetric cell divisions could be conserved across the plant lineage and between haploid and diploid body plans.

Summary

In this thesis, we have demonstrated that *Agrobacterium*-mediated intact Tnt1 can be used to generate *P. patens* mutant population and identification of novel genes. As observed in flowering plants, Tnt1 preferentially transposes into gene-rich regions of *P. patens*. Though LTR promoter is active in the gametophore apical cells, the SSAP-PCR analysis has indicated that it does not reflect in the accumulation of mutagenic load in the mutant genome. Our forward genetic approach has yielded many mutants with interesting phenotypes. Characterization of one of the mutant *shlf* has revealed pleiotropic phenotypes including the reduced apical dominance. The *shlf* mutant appears to be defective in auxin transport in gametophore. WGS and

phenotype rescue analyses revealed that *shlf* phenotype is due to the disruption in a novel gene that may be conserved only among early streptophytes. A preliminary sequence analysis of this gene has shown 4 unique 513 bp repeats (171 amino acids) in the genomic DNA, mRNA and protein sequences. Thus, our forward genetic approach has led to the discovery of a novel lower streptophyte-specific gene family. In the parallel reverse genetic study, we have also generated knockout lines for one of the *P. patens* ortholog of *Arabidopsis* SCR TF, which produced slender-leaves. Based on histological studies, we have proposed a cell division-based model in moss to explain this phenotype. We would be validating this model using live-imaging methods in the future. This study has showed that the role of SCR TF in the regulation of asymmetric cell divisions might be conserved across plant lineages.

List of publications:

1. **Mohanasundaram B**, Rajmane VB, Jogdand SV, Bhide AJ and Banerjee AK, (2018). Analysis of Tnt1 transposition activity in moss (*Physcomitrella patens*) and isolation of mutants with impaired gametophyte development. (**Under revision in Molecular Genetics and Genomics**).
2. **Mohanasundaram B et al.**, (2018). *SHORT-LEAF (SHLF)* - a bryophyte-specific protein regulates auxin transport in *P. patens* gametophores. (**Manuscript under preparation**).

Reference

Aida, M., Beis, D., Heidstra, R., Willemsen, V., Blilou, I., Galinha, C., Nussaume, L., Noh, Y.-S., Amasino, R. and Scheres, B. (2004). The PLETHORA genes mediate patterning of the Arabidopsis root stem cell niche. *Cell* **119**, 109–120.

Aoyama, T., Hiwatashi, Y., Shigyo, M., Kofuji, R., Kubo, M., Ito, M. and Hasebe, M. (2012). AP2-type transcription factors determine stem cell identity in the moss *Physcomitrella patens*. *Development* **139**, 3120–3129.

Bennett, T.A., Liu, M.M., Aoyama, T., Bierfreund, N.M., Braun, M., Coudert, Y., Dennis, R.J., O'Connor, D., Wang, X.Y., White, C.D. et al. (2014). Plasma membrane-targeted PIN proteins drive shoot development in a moss. *Current Biology* **24**, 2776–2785.

Boutilier, K., Offringa, R., Sharma, V.K., Kieft, H., Ouellet, T., Zhang, L., Hattori, J., Liu, C.-M., van Lammeren, A.A., Miki, B.L. et al. (2002). Ectopic expression of BABY BOOM triggers a conversion from vegetative to embryonic growth. *The Plant Cell* **14**, 1737–1749.

Bower, F.O. (1935). Primitive land plants. Macmillan And Co.; London.

Crandall-Stotler, B. (1980). Morphogenetic Designs and a Theory of Bryophyte Origins and Divergence Barbara Crandall-Stotler. *BioScience* **30**, 580–585.

- Cui, Y., Barampuram, S., Stacey, M.G., Hancock, C.N., Findley, S., Mathieu, M., Zhang, Z., Parrott, W.A. and Stacey, G.** (2013). Tnt1 Retrotransposon Mutagenesis: A Tool for Soybean Functional Genomics. *Plant Physiology* **161**, 36–47.
- d’Erfurth, I., Cosson, V., Eschstruth, A., Lucas, H., Kondorosi, A. and Ratet, P.** (2003). Efficient transposition of the Tnt1 tobacco retrotransposon in the model legume *Medicago truncatula*. *The Plant Journal* **34**, 95–106.
- Duangpan, S., Zhang, W., Wu, Y., Jansky, S.H. and Jiang, J.** (2013). Insertional Mutagenesis Using Tnt1 Retrotransposon in Potato. *Plant Physiology* **163**, 21–29.
- Elliott, R.C., Betzner, A.S., Huttner, E., Oakes, M.P., Tucker, W., Gerentes, D., Perez, P. and Smyth, D.R.** (1996). AINTEGUMENTA, an APETALA2-like gene of Arabidopsis with pleiotropic roles in ovule development and floral organ growth. *The Plant Cell* **8**, 155–168.
- Floyd, S.K., Zalewski, C.S. and Bowman, J.L.** (2006). Evolution of class III homeodomain–leucine zipper genes in streptophytes. *Genetics* **173**, 373–388.
- Harrison, C.J., Corley, S.B., Moylan, E.C., Alexander, D.L., Scotland, R.W. and Langdale, J.A.** (2005). Independent Recruitment of a Conserved Developmental Mechanism During Leaf Evolution. *Nature* **434**, 509–514.
- Harrison, C.J., Roeder, A.H., Meyerowitz, E.M. and Langdale, J.A.** (2009). Local Cues and Asymmetric Cell Divisions Underpin Body Plan Transitions in the Moss *Physcomitrella Patens*. *Current Biology* **19**, 461–471.
- Kenrick, P. & Crane, P.R.** (1997). *The Origin and Early Diversification of Land Plants. A Cladistic Study*. Washington, London: Smithsonian Institution Press, 441.
- Kofuji, R. and Hasebe, M.** (2014). Eight types of stem cells in the life cycle of the moss *Physcomitrella patens*. *Current opinion in plant biology* **17**, 13–21.
- Lucas, H., Feuerbach, F., Kunert, K., Grandbastien, M. and Caboche, M.** (1995). RNA-mediated transposition of the tobacco retrotransposon Tnt1 in *Arabidopsis thaliana*. *The EMBO journal* **14**, 2364.
- Puttick, M.N., Morris, J.L., Williams, T.A., Cox, C.J., Edwards, D., Kenrick, P., Pressel, S., Wellman, C.H., Schneider, H., Pisani, D. et al.** (2018). The interrelationships of land plants and the nature of the ancestral embryophyte. *Current Biology* **28**, 733–745.
- Sakakibara, K., Nishiyama, T., Deguchi, H. and Hasebe, M.** (2008). Class 1 KNOX genes are not involved in shoot development in the moss *Physcomitrella patens* but do function in sporophyte development. *Evolution & development* **10**, 555–566.
- Sundås-Larsson, A., Svenson, M., Liao, H. and Engström, P.** (1998). A homeobox gene with potential developmental control function in the meristem of the conifer *Picea abies*. *Proceedings of the National Academy of Sciences* **95**, 15118–15122.
- Tomescu, A.M.** (2009). Megaphylls, microphylls and the evolution of leaf development. *Trends in plant science* **14**, 5–12.
- Wright, I.J., Reich, P.B., Westoby, M., Ackerly, D.D., Baruch, Z., Bongers, F., Cavender-Bares, J., Chapin, T., Cornelissen, J.H., Diemer, M. et al.** (2004). The worldwide leaf economics spectrum. *Nature* **428**, 821.
- Yip, H.K., Floyd, S.K., Sakakibara, K. and Bowman, J.L.** (2016). Class III HD-Zip activity coordinates leaf development in *Physcomitrella patens*. *Developmental biology* **419**, 184–197.
- Zimmermann, W.** (1952). Main results of the telome theory. *Palaeobotanist* **1**, 456–470.

1 Introduction

1.1 Evolution of leaves in plants

Leaves are highly specialized organs primarily for light harvesting and photosynthesis; leaf tissue is flattened to various degrees and arranged in a species-specific phyllotactic pattern in order to optimize the light-intercepting leaf area per unit biomass invested (Wright *et al.*, 2004). To efficiently utilize the harvested light energy for carbon fixation, leaves have evolved C3 or C4 anatomy and metabolism (Sleewinski, 2013). Apart from the photosynthetic mesophyll cells, strategically organized stomatal pores in the epidermal layer help in water uptake from soil and gaseous exchange. Reticulate or parallel venation helps in transport of water and photoassimilate. Apart from these basic features, depending on their niche specialization, leaves have evolved many family- or species-specific adaptations such as trichomes, thorns, leaf-teeth and waxy layer. Different combinations of these features contribute to the vast repertoire of leaf forms employed by plants to survive in a myriad of environmental niches on the Earth (Figure 1.1)

The strong selection pressure on leaves has resulted in numerous independent origins of leaf innovation in vascular plant lineages. Among them, small enations with a simple ventilation that are microphylls of lycophytes and complex venations on large megaphylls of euphyllophytes are the two major lineages (Figure 1.2 A) (Tomescu, 2009). It was proposed that microphylls form a monophyly and have evolved from the leafless ancestors of the extinct clade, zosterophyll (Figure 1.2 B). The enation theory suggests that the small enations found on the leafless stems of zosterophylls were vascularised and evolved into microphylls (Bower, 1935), whereas an alternative theory considered them as sterilized sporangia (Kenrick, 1997). Widely accepted Zimmermann's telome theory (Zimmermann, 1952) states that megaphylls have evolved from the extinct leafless ancestors of trimerophytes (Figure 1.2 C). This process is hypothesized to begin with a series of changes that causes the lateral branches to become determinate (overtopping), followed by lateral branches forming on a two-dimensional plane (planation) and the branches were covered with photosynthetic tissue (webbing) (Zimmermann, 1952; Beerling and Fleming, 2007). Phylogeny construction for megaphylls of euphyllophytes based on extant plants suggests a monophyly group. However, the incorporation of fossil evidence divides them into a series of paraphyletic groups (Rothwell and Nixon, 2006). Both approaches suggest up to nine independent origins for megaphylls, comprising two extinct and extant fern origins, two progymnosperm origins, remaining were in seed plants. Like the megaphylls and microphylls of vascular plant sporophytes, gametophores of extant bryophytes also have leaf-like organs.

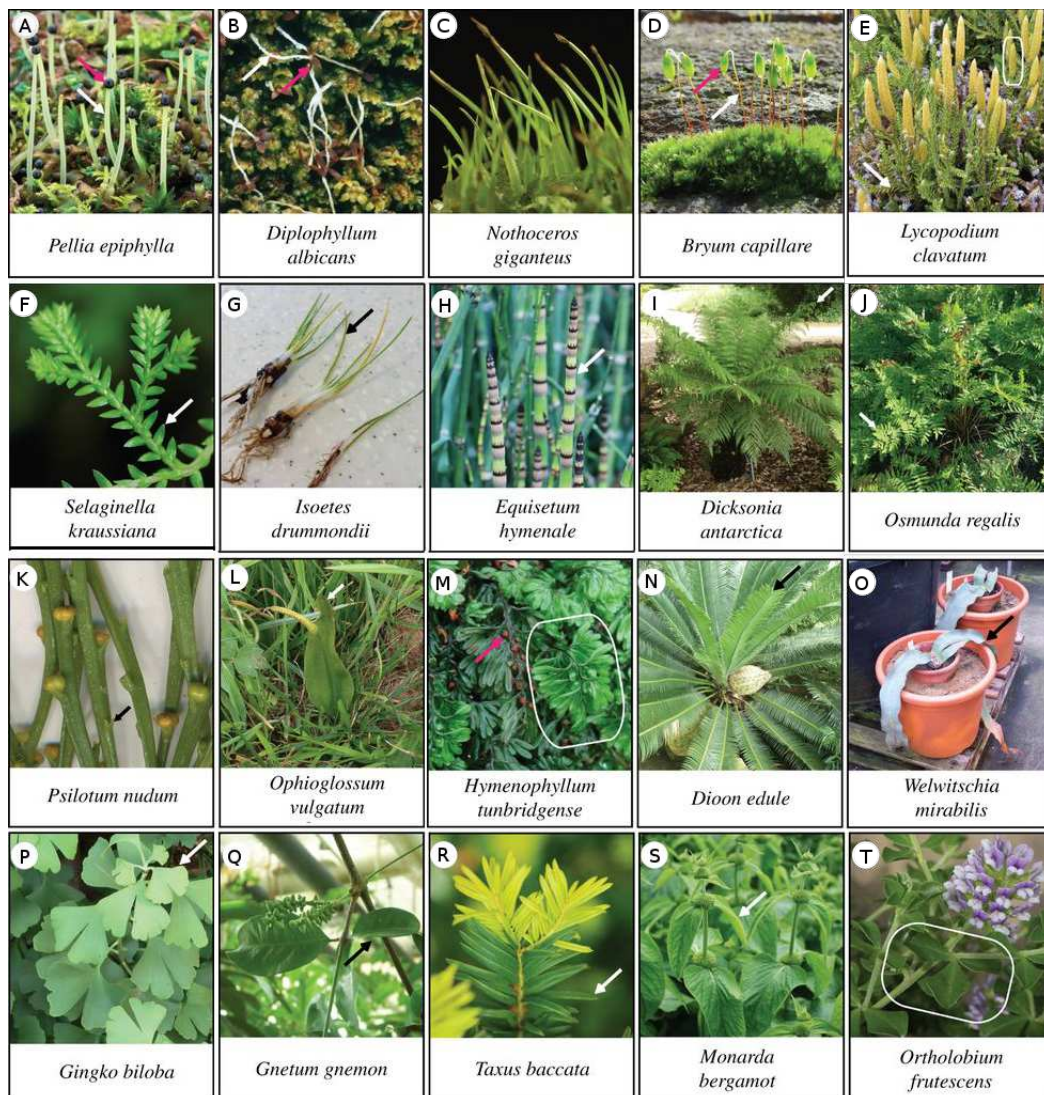


Figure 1.1: The morphological variation of shoot and leaf among major clades of living land plants. Bryophyte lineages including thalloid liverwort (A), leafy-liverwort (B), hornwort (C) and moss (D) showing sporophytes comprising of a single axis (white arrows) that terminates in sporangium formation and capsule development (pink arrows). Shoots of clubmosses (E), spike mosses (F) and quillworts (G) represent a deep divergence within the lycophyte lineage and have microphylls. Diverse leaf morphologies of living monilophytes (H-M) comprise horsetails (H), polypod ferns (I, J), whisk ferns (K), ophioglossid ferns (L) and filmy ferns (M). White and black arrows mark leaves and pink arrow points to sporangium. Different leaf forms from gymnosperm (N-R). Simple and compound leaves of the flowering plant (S-T). (Harrison and Morris, 2018) - *Reproduced with permission from CC-BY 4.0 license.*

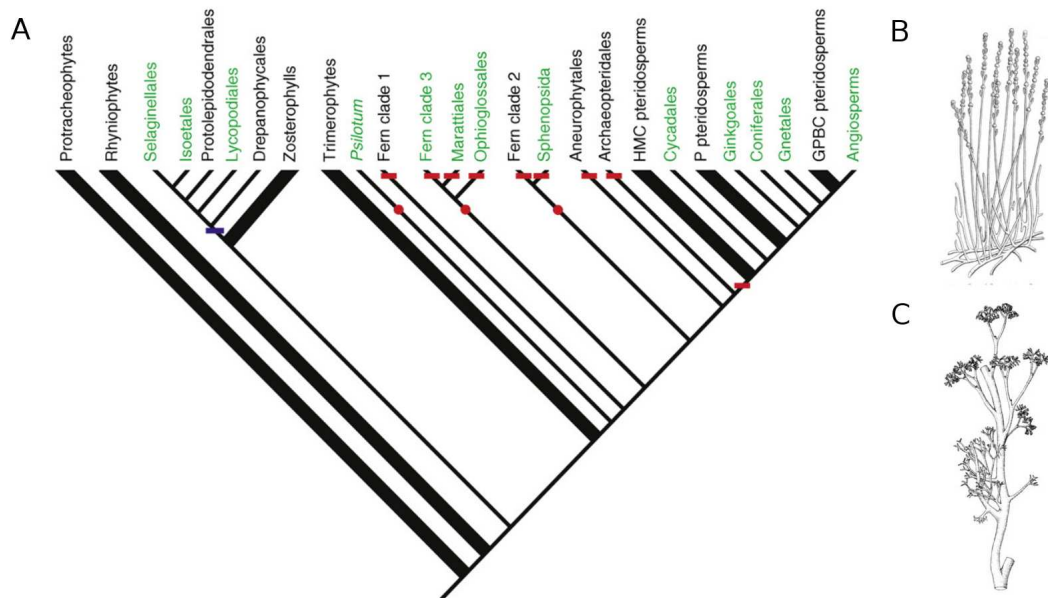


Figure 1.2: Independent origins of leaf evolution. (A) Single origin of microphylls in Lycopodiophyta (blue line) as well as the leafless ancestor group (Zosterophylls) are depicted. Multiple independent origins of megaphylls are represented as red lines and dots along with the leafless ancestor trimerophytes. Lineages with extant representatives are written in green, and extinct lineages are in black. (B) *Zosterophyllum* - a representative of the extinct Zosterophylls. (C) *Psilophyton* - a representative from the extinct leaf ancestor group trimerophytes. (Tomescu, 2009; Harrison and Morris, 2018) - Reproduced with permission from Elsevier and CC-BY 4.0 license.

1.1.1 Phyllids (leaves) in bryophytes

The origin and evolution of miniature leaf-like organs (phyllids) of bryophyte gametophytes (moss and liverworts) is not yet studied. In the bryophytes monophyly, moss and liverwort are closely related than hornworts (Puttick *et al.*, 2018). It is also argued that the thalloid body of liverworts has resulted from the loss of many land plant characters rather than representing primitive basal land plant features (Puttick *et al.*, 2018). In line with the argument, all the moss and leafy-liverwort (*Jungermanniales*) gametophores develop phyllids. However, it is not clear whether the phyllids of moss and leafy-liverworts share a common origin or not? Further phylogenetic and functional studies are necessary to conclude about the origin of phyllids.

It is intriguing to compare phyllids with true leaves (megaphylls and microphylls) of vascular plants. In the sporophytic generation, megaphylls and microphylls share the following defining features: vascularization, determinate growth, bilateral symmetry and definite arrangement (phyllotaxis) (Tomescu, 2009). Phyllids of moss and leafy-liverworts (*Jungermanniales*)

are remotely orthologous to the sporophytic true-leaves in form and function. Phyllids share some basic features of a sporophytic leaf, but still, their tissue architecture remains simple: single leaf apical-cell derived leaf-blade with a single layer of cells, simple midrib (3 layers of cells) reminiscent of leaf-vasculature, and absence of stomatal pores. Given these morphological and anatomical similarities, the compelling question is how much hormonal and genetic factors have been co-opted to develop phyllids and true leaves.

To understand this, we would discuss in the following sections the tissue organization and the contribution of environmental cues, phytohormones, and genetic networks of true leaves in detail and compare with the limited knowledge available on phyllids to identify important open-ended questions for future investigations.

1.2 Developmental events in SAM

Plant leaves have evolved from multiple origins, but their basic developmental process is strikingly similar. In general, vascular plant leaf development progresses in the following phases: a dome of actively dividing and self-renewing shoot apical cells produce new cells at the growing tip of the plant. Auxin maxima emerge on few cells on flanks of the meristem in a pattern that is specific to the phyllotaxy of the species. Eventually, these cells differentiate to become determinate cells and divide further to produce a leaf primordia. As leaf primordium grows further, it obtains multiple axes of polarities like adaxial-abaxial, proximo-distal, and medial-lateral. Further, leaf blade expands in a highly coordinated manner to achieve the final shape and size. As leaf blade matures, many other tissue types like vasculature, stomata, and trichome differentiate and becomes functional. Throughout this process many environmental cues, phytohormone signals modulate the genetic networks to cope up and grow successfully in the ever-changing environment. The striking similarities and deviations in the development of megaphylls, microphylls, and phyllids will be discussed below.

1.2.1 Shoot meristem organization in plants

In all plants, shoot grows from the shoot apex and the lateral branch apex (Wolff, 1759) but the apical meristem organization and maintenance are different among plant lineages. Among angiosperms, dicots have triangular dome-shaped meristems and while monocot meristems are of finger-like shape (Barton, 2010). Widely studied angiosperm dicotyledonous model plant

such as *Arabidopsis* shoot apical meristem (SAM) has three layers of cells in which, outer L1 and L2 layers of cells (tunica) divide into two planes and form a sheet-like tissue overlay, while the L3 layer (carpus) divides in all orientation (duplex meristem) (Figure 1.3 A) (Szymkowiak and Sussex, 1996; Evans and Barton, 1997). As observed in monocotyledons, maize SAM has only two layers of cells, L1 and L2 (Abbe *et al.*, 1951; Steffensen, 1968). Based on cytological studies angiosperm apical meristem is divided into the central zone (CZ) having stem cell population, the organizing center (OC) which controls stem cell population size, the peripheral zone (PZ) with fast dividing cells and differentiating organ primordia (OP) (Figure 1.3 B).

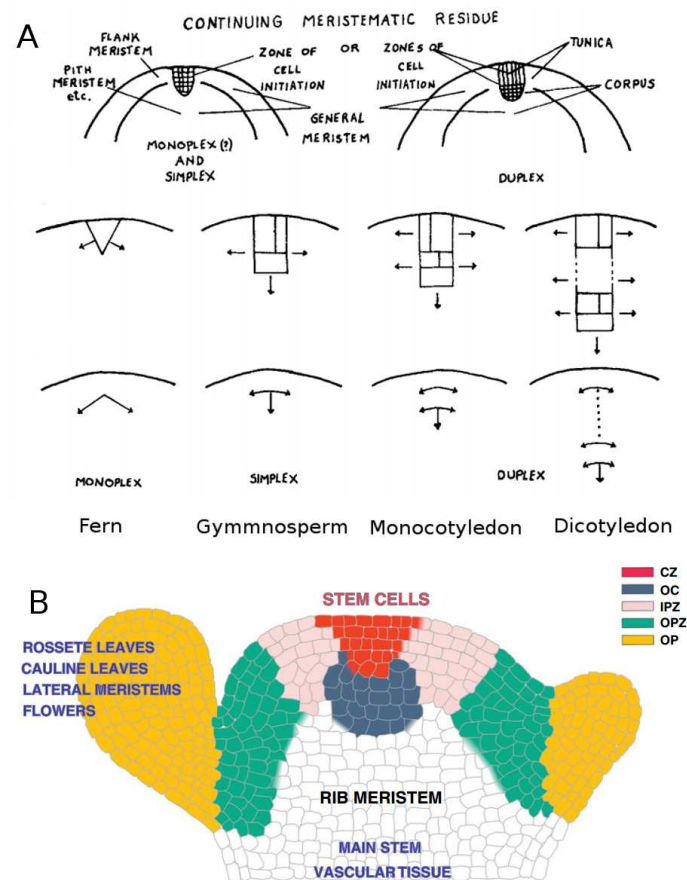


Figure 1.3: Different layers and zones of vascular shoot apical meristem (SAM). (A) The cell division pattern in cytohistologically distinct layers of the meristem is described. Monocotyledon and dicotyledon SAM has two and three distinct layers, respectively (Duplex). Gymnosperm meristem has only one layer (Monoplex) while fern meristem does not have such distinct cell division layers. B) Based on the cell division pattern and the developmental fate of the cells, dicotyledon meristem is divided into different zones like central zone (CZ), organizing center (OC), internal and outer peripheral zone (IPZ and OPZ) and organ primordia (OP). (Gifford and Corson, 1971; Perales and Reddy, 2012) - Adapted with permission from new york botanical garden press.

Among gymnosperms, conifer meristem is divided into the summit and peripheral zones (Gifford and Corson, 1971; Conway and Drinnan, 2017). Summit zone apical cells initially divide anticlinally which results in isotropic growth at the surface. Only summit zone cells can divide periclinally and contribute to inner tissue of the meristem (Simplex meristem) (Figure 1.3 A). Cells from the summit zone divide transverse anticlinally and form the peripheral zone (Conway and Drinnan, 2017). Though cytohistochemical evidence suggests that the fern meristem (McAlpin and White; 1974; Stevenson, 1976 b) and lycophyte meristem (Freeberg and Wetmore, 1968; Stevenson, 1976 a) are multicellular with different zones, but recent literature consider a single apical cell in the place of meristem (Harrison *et al.*, 2005; Sano *et al.*, 2005, Banks, 2015). However, it is clear that extant vascular plant shoot apex has a single stem cell or very few apical cells and follow the monoplex division pattern (Figure 1.3 A).

Moss and liverworts have gametophytic shoot whose apex also has a single apical cell (Figure 1.4 A) (Kofuji and Hasebe, 2014). The gametophore apical cell of moss divides to form a derivative cell which further divides to form leaf apical cell (Figure 1.4 B). A striking similarity among haploid shoot apical cells of bryophytes and diploid shoot apical cells of lycophyte and moniliophyte is that they do not divide periclinally. Unlike seed plants, non-seed land plant meristems do not have distinct layers (Philipson, 1990; Piazza *et al.*, 2005). Though the SAM architecture varies significantly among land plants, their response to environmental cues is determined by hormonal and genetic regulators.

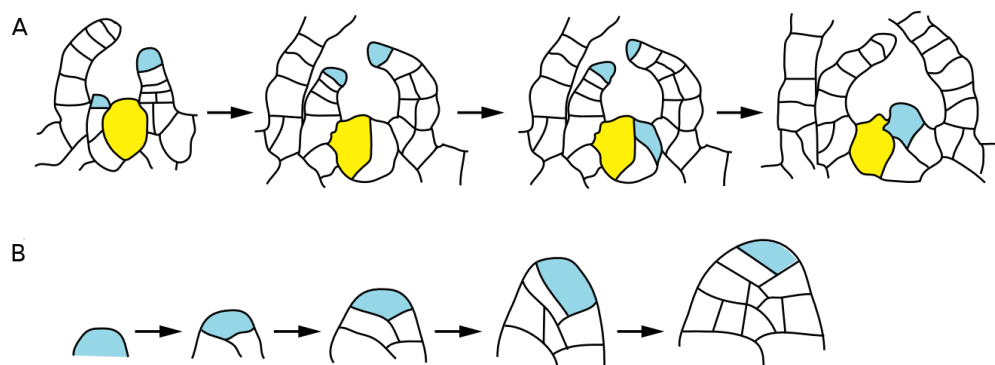


Figure 1.4: Formation of the moss leaf apical cell and leaf growth. (A) The schematic representation explains the longitudinal section of a gametophore and shows the gametophore apical cell (yellow) and the leaf apical cell (blue). (B) The asymmetric cell division of leaf apical cell initiates leaf development on moss gametophores. (Kofuji and Hasebe, 2014)- *Reproduced with permission from Elsevier.*

1.2.2 Shoot meristem maintenance and regulation

In all plant lineages, SAM senses the external environment and mount a highly plastic response through phytohormone signaling and genetic networks. In *Arabidopsis*, *SHOOT MERISTEMLESS* (*STM*) gene encodes a class I *KNOTTED-like homeobox* (*KNOX*) transcription factor which is essential and sufficient for SAM formation (Barton and Poethig, 1993). *STM* expression in SAM enhances cytokinin (CK) accumulation which promotes proliferation of pluripotent stem cells through the well-studied *WUSCHEL-CLAVATA* feedback loop (Figure 1.5) (Mayer *et al.*, 1998; Schoof *et al.*, 2000; Brand *et al.*, 2000). On the other hand, *STM* promotes gibberellin (GA)-deactivator gene *Gibberellin 2- β -dioxygenase 2* (*AtGA2ox2*) and suppresses the GA biosynthetic gene *Gibberellin 20 oxidase 1* (*AtGA20ox1*), thus preserving the totipotency of stem cells (Hay *et al.*, 2002; Jasinski *et al.*, 2005). The intricate details of *Arabidopsis* SAM maintenance are thoroughly reviewed by Barton, (2010) and Perales *et al.*, (2012). Class I *KNOX* transcription factors are conserved throughout land plants and their expression in the SAM is conserved in all vascular plants but varies significantly in organ primordia (Table 1.1) (Sundås-Larsson *et al.*, 1998; Bharathan *et al.*, 2002; Harrison *et al.*, 2005; Sano *et al.*, 2005; Ambrose and Vasco, 2016). Though class I *KNOX* genes regulate sporophyte development in *Physcomitrella patens* (*P. patens*), it is not involved in gametophytic shoot development (Sakakibara *et al.*, 2008). However, the orthologs of AP2-type transcription factors were shown to be essential for moss gametophore apical cell formation (Aoyama *et al.*, 2012).

1.2.3 Events of leaf founder cells formation in SAM

In general, the slow dividing stem cells population in SAM contributes to fast dividing PZ cells (Figure 1.3 B), where they finally become leaf founder cells. The onset of leaf primordium in dicotyledonous species begins as a small portion of L2 layer cells divide with spindles aligned perpendicular to the meristem surface (periclinal), while the division of L1 and L3 layers remain unchanged (Barton, 2010). These changes create a lump on the flanks of the meristem, which becomes leaf primordia. While L1 and L3 layers mostly contribute to leaf epidermis and vasculature associated tissue, respectively, the L2 layer forms the rest of the leaf tissues (Poethig, 1987). In maize apical meristem, such a lump tissue appears at the presumptive midrib and extends laterally to include leaf blade initials. Unlike angiosperms, leaf development in all the non-seed plants begins with a few leaf initial cells from the flanks of the meristem (Steeves and Sussex, 1989).

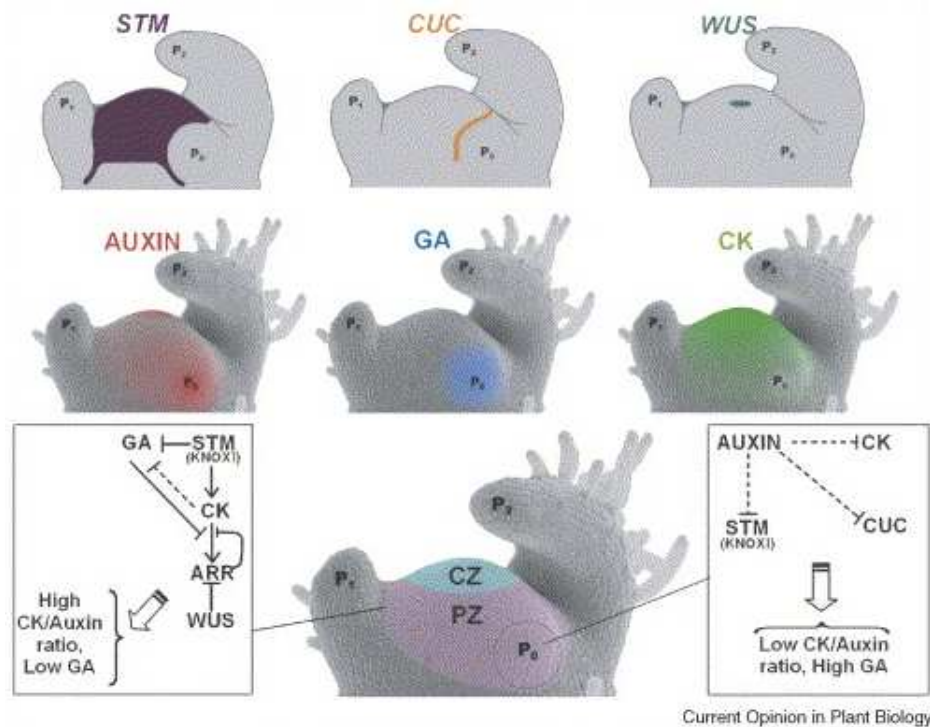


Figure 1.5: Interaction domains of critical players regulating shoot apical meristem (SAM) development. First row: the expression domain of *STM*, *CUC* and *WUS* are depicted. Second row: hypothetical distribution of major phytohormones auxin, gibberellin (GA) and cytokinin (CK) are also represented on a tomato SAM. P_0 indicates future leaf primordia while P_1 is the youngest primordia and P_2 is the next primordium. Third row: a simplified model of interaction between hormonal and genetic factor at the SAM and organ primordium. *STM* expression domain marks undifferentiated cells, where *STM* represses GA biosynthesis and induces GA catabolism and CK biosynthesis. *WUS* also induces CK activity locally. The resulting high CK accumulation and low GA concentration cause indeterminate growth. At the future leaf primordia (P_0 region), auxin accumulates at a very high concentration and suppress *STM* and *CUP-SHAPED COTYLEDON* (*CUC*) expression, and CK biosynthesis. This leads to low CK and high level of GA, which initiate the lateral organ formation. (Shani et al., 2006). - Reproduced with permission from Elsevier.

In bryophyte gametophore apex, a single apical cell divides to form a daughter cell (Figure 1.4). In case of moss, the daughter cell undergoes a periclinal division and then anticlinal division to form leaf apical cell and stem epidermal initials (Crandall-Stotler, 1980). This apical cell develops a leaf primordium as described by Harrison *et al.*, (2009) and Kofuji and Hasebe, (2014) (Figure 1.4). In contrast to moss, daughter cell derived from liverwort apical cell divides only anticlinally leading to the formation of two leaf apical cells (Crandall-Stotler, 1980). It is clear that the complexity of shoot apical meristem reduced drastically in moss in comparison to *Arabidopsis*. Not only that the cell division patterns leading to the formation of

Table 1.1: Conservation of crucial genetic players regulating SAM among plant lineages.(Plackett *et al.*, 2015) - Reproduced with permission under CC-BY license.

Gene Family	Mosses		Lycophytes		Monilophytes		Angiosperms	
	<i>Physcomitrella patens</i>		<i>Selaginella spp.</i>		<i>Ceratopteris richardii</i>		<i>Arabidopsis thaliana</i>	
Gene Family	Expression Pattern	Gene Function	Expression Pattern	Gene Function	Expression Pattern	Gene Function	Expression Pattern	Gene Function
<i>WUSCHEL</i> -related <i>Homeobox</i> (<i>WOX</i>)	Gametophore (AC)	Unknown	Unknown	Unknown	Unknown	Unknown	SAM (Central zone)	SAM identity; indeterminate cell fate
<i>CLAVATA</i> (<i>CLV</i>)	Not present	-	Unknown	Unknown	Unknown	Unknown	SAM (Peripheral zone)	Antagonises <i>WUSCHEL</i> ; restricts central zone
Class I <i>KNOX</i>	Gametophore (AC); zygote; sporophyte (AC and intercalary meristem)	Sporophyte cell division; no gametophyte phenotype	Shoot apex (core domain); internodes (<i>S. kraussiana</i>)	Unknown	Shoot apex (AC); frond primordium; vasculature; gametophyte	Unknown	SAM	SAM identity
<i>ASYMMETRIC LEAVES1</i> , <i>ROUGH SHEATH</i> , <i>PHANTASTICA</i> (<i>ARP</i>)	Not present	-	Shoot apex; microphyll primordia (<i>S. kraussiana</i>)	Unknown	Unknown	Unknown	Leaf primordium	Antagonises <i>KNOX</i> ; leaf primordia identity
<i>PINFORMED</i> auxin efflux carrier (<i>PIN</i>)	Gametophore shoot apex; sporophyte	Organogenesis; sporophyte development and branching	Shoot apex (core domain) (<i>S. moellendorffii</i>)	Microphyll AC boundary formation; rhizophore root fate specification (<i>S. kraussiana</i>)	Unknown	Unknown	SAM (Peripheral zone)	Organogenesis; leaf primordia outgrowth
Class III Homeodomain-Leucine Zipper (<i>HD-Zip</i>)	Detected in gametophyte and sporophyte (RT-PCR)	Unknown	Shoot apex (AC); microphyll primordium (adaxial); vasculature (<i>S. kraussiana</i>)	Unknown	Unknown	Unknown	SAM; leaf primordium (adaxial); vasculature	SAM initiation and maintenance; leaf adaxial identity; vasculature specification
<i>KANADI</i> (<i>KAN</i>)	Unknown	Unknown	Shoot apex (core domain) (<i>S. moellendorffii</i>)	Unknown	Unknown	Unknown	SAM; leaf primordia (abaxial); vasculature	Antagonises <i>HD-Zip</i> ; leaf abaxial identity; vasculature specification
<i>LEAFY</i> (<i>LFY</i>)	Gametophore (shoot apex); archegonium; zygote; sporophyte	Zygotic cell division; no gametophyte phenotype	Unknown	Unknown	Detected in gametophyte and sporophyte (shoot apex and reproductive frond primordia) (RT-PCR)	Unknown	SAM; IM; FM	Phase change (vegetative to flowering); FM identity and early development
<i>MADS</i> -box (<i>MIKC^c</i>)	Gametophyte all tissues (protonema, gametophore, gametangia); sporophyte all tissues	Gametophore gametangia and phyllidia development; sporophyte development	Unknown	Unknown	Detected in gametophyte (RT-PCR); sporophyte shoot AC; frond primordia; frond apex and vasculature; developing sporangia	Unknown	FM; floral organs	Floral whorl identity and floral organ development

leaf founder cell is also strikingly simple. Whether this gradual reduction of complexity reflects in the upstream and downstream molecular networks is of immense scientific interest.

1.2.4 Role of auxin in leaf founder cell formation in SAM

As observed in basal land plants, the position of leaf primordia formation can be determined by the formative cell divisions of the apical cell itself, or it can be independent of the stem cell division planes as in higher plants. On the flanks of the *Arabidopsis* SAM, convergent polar localization of PINFORMED1 (PIN1) auxin efflux carrier proteins leads to channeling of auxin fluxes to form local auxin maxima (Reinhardt *et al.*, 2003). Experimental evidence and extensive mathematical modelling studies predicted a feedback loop from the auxin concentration (Smith *et al.*, 2006) and the mechanical stress on cell walls are necessary for the convergent polar localization of PIN1 (Hamant *et al.*, 2008; Heisler *et al.*, 2010; Braybrook and Peaucelle, 2013). Studies on floral meristem revealed localized expression of an auxin-responsive transcription factor *MONOPTEROS* (*MP*) at incipient primordia even before convergent PIN1 localization (Figure 1.6) (Bhatia *et al.*, 2016). A unifying hypothesis is that the expression of auxin-responsive *MP* activates cell wall loosening enzymes. The neighboring cells sense the mechanical stress and respond by localization of PIN1 on plasma membrane towards the stressed wall (Bhatia *et al.*, 2016; Bhatia and Heisler, 2018). Among the meristematic cells, the cells that are marked by the auxin maxima have to differentiate in order to develop into a leaf primordium which is regulated by another conserved set of genes.

Auxin plays an essential role in shoot development of all land plant lineages. However, the role of polar auxin transport (PAT) is not conserved. Treatment with PAT inhibitors or auxin efflux carrier loss of function mutants in *Arabidopsis* and tomato developed shoots without leaves (Reinhardt *et al.*, 2000; Reinhardt *et al.*, 2003) (Figure 1.7 B). Another study conducted by Sanders and Langdale, (2013) showed that treatment with PAT inhibitor did not arrest the microphyll development in *Selaginella*, but the SAM was lost. However, inhibition of PAT did not affect auxin distribution in along gametophore axis *P. patens* (Fujita *et al.*, 2008). Also, loss of function mutants of *pinA* and *pinB* single and double mutants did not affect gametophore apex and phyllid development but caused differential expression of the auxin-responsive promoter (Bennett *et al.*, 2014) (Figure 1.8). Together these data suggest that the role of polar auxin transport in shoot development is not fully conserved among plant lineages.

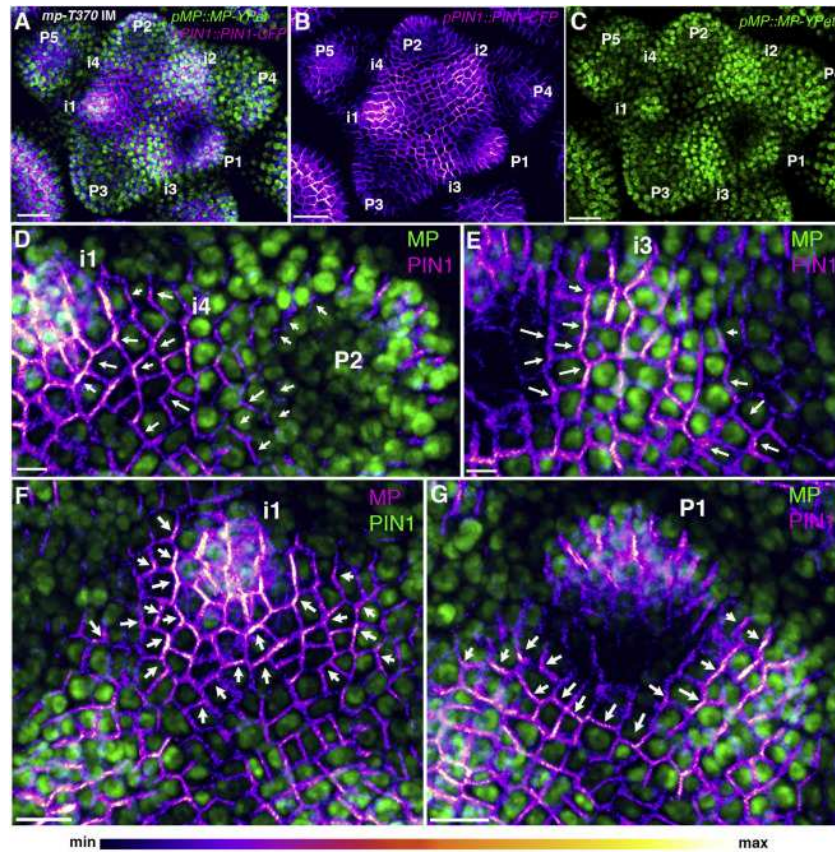


Figure 1.6: MP accumulates before convergent polar localization of PIN1 around incipient primordia. (A) Expression and localization of pMP::MP-YFPet (green) and pPIN1::PIN1-CFP (magenta) in the *mp* mutant (*mp*-T370) inflorescence meristem (IM); expression of pPIN1::PIN1-CFP alone (B) and pMP::MP-YFPet expression alone (C and D). MP accumulates around i4 stage and after i3 stage, PIN1 polarity converges. PIN1 polarity direction within the cells. Primordium (P) and incipient primordium (i) stages are numbered i4-P5. Scale bars, 30 μ m (A-C), 5 μ m (D and E), and 10 μ m (F and G). (Bhatia *et al.*, 2016) - *Reproduced with permission under CC-BY NC ND license.*

1.2.5 Molecular events in formation of leaf primordia

It was first observed in maize (*KNOTTED1*) and later in *Arabidopsis* (*STM*) and Norway spruce that stem-cell fate promoting class I *KNOX* gene expression reduces at the site of presumptive organ primordia (Figure 1.5) (Smith *et al.*, 1992; Jackson *et al.*, 1994; Lincoln *et al.*, 1994; Sunds-Larsson *et al.*, 1998). In *stm* mutants, seedlings had no SAM (Figure 1.7 A and B) (Barton and Poethig, 1993). Interestingly, this phenotype can be rescued by the loss of function mutations of a MYB class transcription factor *ASYMMETRIC LEAVES1* (*AS1*) (Figure 1.7 F and G) (Byrne *et al.*, 2000). *Arabidopsis* *AS1* and its orthologs *ROUGH SHEATH2* (*RS2*) from maize and *PHANTASTICA* (*PHAN*) from Antirrhinum, collectively known as *ARP* genes,

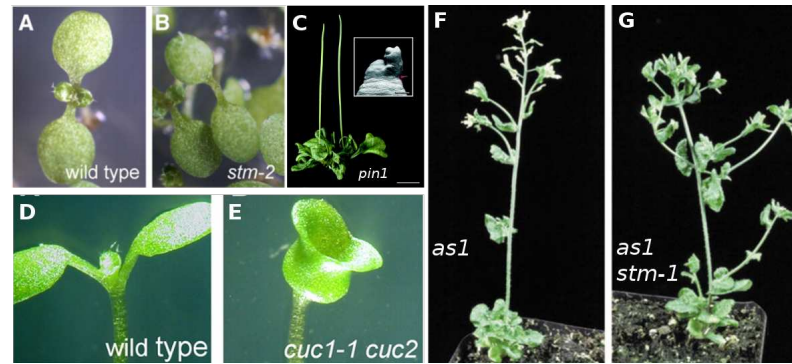


Figure 1.7: *Arabidopsis* mutant lines that are defective in organ primordia formation. (A and D) Wild-type *Arabidopsis* seedling is showing SAM. (B) *stm* seedling lacks SAM. (C) lateral organs were suppressed in the *pin1* mutant lines. (E) Cup-shaped cotyledons developed on the *cuc1 cuc2* mutant seedling. (F) *as1* mutant lines with lobed leaves and flowers on the main and lateral shoot. (G) *stm* phenotype is rescued by the *stm as1* double knock-out line. (Byrne *et al.*, 2000; Kuhlemeier and Reinhardt, 2001; Belles-Boix *et al.*, 2006). - Reproduced with permission from American Society of Plant Biologists, Elsevier and Springer Nature.

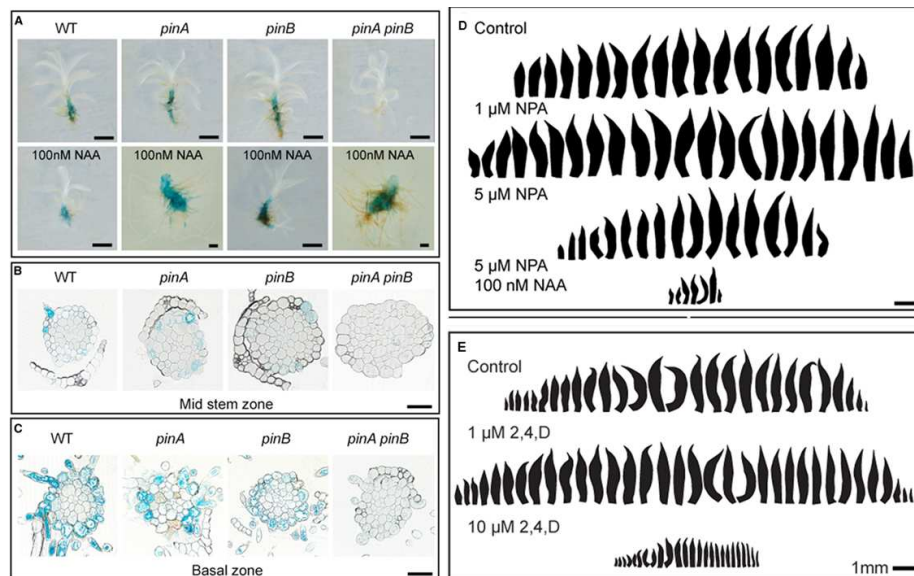


Figure 1.8: Effect of loss of function *pin* mutant and perturbation of auxin concentration on phyllid and phyllotaxy of moss gametophores. Effect of *pinA* and *pinB* single and double mutants on auxin-responsive *GH3::GUS* expression pattern (A-C). In *pinA* and *pinB* single mutants, the GUS expression has moved towards the apex. In double knock out lines, GUS expression is observed in the inner layers of gametophore stem. Treatments with PAT inhibitors NPA (N-1-Naphthylphthalamic Acid) (D) and synthetic auxin analogs like NAA (1-Naphthaleneacetic acid) or 2,4-D (2,4-Dichlorophenoxyacetic acid) affect the size of phyllids by not the phyllotaxy (Bennett *et al.*, 2014). - Reproduced with permission under CC-BY license.

express in the organ primordium alongside auxin maxima. A number of reports have demonstrated that these genes negatively regulate class I *KNOX* gene expression at the leaf primordia (Figure 1.5) (Waites *et al.*, 1998; Marja CP *et al.*, 1999; Tsiantis *et al.*, 1999; Byrne *et al.*, 2000; Ori *et al.*, 2000; Hay *et al.*, 2006). In *stm* mutants, due to lack of inhibition from *STM*, *AS1* expression domain overcomes the CZ and OZ meristem regions and differentiate the stem cells. In *stm as1* double knockout, another class I *KNOX* gene *BREVIPEDICELLUS* (*BP*) expresses in meristem and rescues shoot development (Douglas *et al.*, 2002; Venglat *et al.*, 2002). Both class I *KNOX* and *ARP* genes are evolutionarily conserved, and they maintain stem cell fate and facilitate cell differentiation, respectively.

The *KNOX/ARP* gene module defines distinct meristem and organ primordia tissue types in the fern shoot apex as well. Unlike the mutually exclusive expression pattern found in angiosperms, in the royal fern (*Osmunda regalis*) however, *KNOX* and *ARP* genes are expressed throughout meristem and leaf primordium, and their domains overlap (Harrison *et al.*, 2005). This particular failure to repress *KNOX* in fern leaf primordium is thought to be the reason for the delayed onset of determinacy in its leaves. Interestingly, these studies suggest that the *KNOX/ARP* module is independently recruited to govern shoot apex of vascular plant sporophyte development (Vasco *et al.*, 2013). Similarly, independently recruited *ARP* genes express in the microphyll primordium of *S. kraussiana* and probably contribute to the determinacy of the leaf which is consistent with megaphylls (Harrison *et al.*, 2005). But in *S. kraussiana* meristem the expression pattern of *KNOX* and *ARP* overlap, which could cause repression of *KNOX* expression at the middle of the meristem, followed by bifurcation of the meristem (Harrison *et al.*, 2005). Class I *KNOX* genes were required for the sporophyte development in *P. patens*, but they do not have any role gametophore development as demonstrated by Sakakibara *et al.*, (2008). *ARP* family genes are not present in *P. patens* genome.

The *CUP-SHAPED COTYLEDON1 to 3* (*CUC*) gene regulates at least two crucial events of *Arabidopsis* shoot development. As the name suggests mutant seedlings of *CUC* developed cup-shaped cotyledons, which are fused along the periphery of the embryo (Figure 1.7 D and E) (Aida *et al.*, 1997). The phenotype of *CUC* mutants can be phenocopied by treating with PAT inhibitors (Liu *et al.*, 1993) indicating the negative interaction between *CUC* and auxin. At the globular stage of embryo development, *CUC* expresses in a domain that extends over the apex causing suppression of auxin signaling. *CUC* expression activates *STM* expression at the apical region leading to the formation of the shoot apical meristem (Aida *et al.*, 1997). On the flanks of the meristem, *STM* activates *CUC1* by directly binding to its

promoter, and the resulting expression pattern of *CUC* is necessary to suppress cell growth in the boundary region between organ primordia and central zone as well as between organ primordia (Figure 1.5) (Aida *et al.*, 1997; Spinelli *et al.*, 2011). *CUC* genes are conserved among angiosperms, but their presence in other plant lineages is not apparent (Souer *et al.*, 1996; Weir *et al.*, 2004). Though orthologs of *CUC* genes are present in *P. patens* genome, they are not yet characterized (Larsson *et al.*, 2012). Tissue morphology, anatomy, hormone accumulation pattern and gene expression domains of angiosperm SAM have been studied extensively but to understand the ability of SAM in self-organizing the spatial periodicity of organ primordia (phyllotaxy) would certainly require detailed quantitative analyses.

1.2.6 Understanding phyllotaxy in land plants

Modularity is a fundamental feature of land plants' body plan. Modules are semi-autonomous, often repetitive, functional or structural units like leaves. Immature leaves of fern or flowering plants that are excised from the meristem are capable of developing into small mature leaves, if grown on proper nutrient media, indicating the semi-autonomous nature of leaves as explained by Steeves and Sussex, (1957). These repetitive modular leaves arise from self-organizing spatially-regulated leaf primordia known as phyllotaxy. Extensive experimental studies on the formation of leaf primordia have already been discussed above, but quantitative mathematical models are required to understand the full details of the self-organizing capability. Experimental studies revealed the importance of polar localized PIN1 mediated "up-the-gradient" auxin transport in organ primordia initiation (Figure 1.7 C) (Heisler *et al.*, 2010; Bayer *et al.*, 2009). Initial theoretical studies have developed abstract models, with the assumption of "up-the-gradient" auxin transport and successfully reproduced the phyllotactic patterns (Jönsson *et al.*, 2006; Smith *et al.*, 2006). A significant finding from these abstract models is the requirement of feedback from auxin concentration to PIN1 localization pattern as suggested by Smith *et al.*, (2006). Experimental studies have proposed few candidates such as auxin-responsive transcription factor *MONOPTEROS* (Figure 1.6) (Bhatia *et al.*, 2016). Further research has improved the working models by incorporation of more realistic features, such as extracellular space (Fujita and Kawaguchi, 2018). These models are capable of reproducing alternate, opposite and spiral phyllotactic patterns observed in nature and could be useful to explain phyllotaxy in lower vascular plants such as *Selaginella*, wherein disruption of PAT found to affect phyllotaxy (Sanders and Langdale, 2013). Interestingly, phyllotaxy of *P. patens* gametophores was not affected upon treatment with PAT inhibitors as well as in *pinA* and *pinB* single and double

knockout lines (Bennett *et al.*, 2014) (Figure 1.8) suggesting that a new model is needed to explain the phyllotaxy in moss.

1.3 Leaf development: Acquisition of symmetry axes

An organ primordium is merely a radial outgrowth on the flank of the apical meristem, which acquires adaxial-abaxial, proximal-distal and medial-lateral polarities before maturing into a fully functional leaf (Figure 1.9). The adaxial-abaxial polarity is clearly observable in the multi-layered tissues of megaphylls and microphylls. In the case of phyllids, the leaf blade is uni-stratose, and the midrib tissue is multi-stratose. Hence, abaxial-adaxial polarity of phyllids can be observed in the outer cell wall characteristics of lamina (Biasuso, 2007) and the epidermal cells of midrib (Sakakibara *et al.*, 2003). The proximal-distal and medial-lateral polarities are found in true leaves as well as in phyllids.



Figure 1.9: Symmetries of a leaf. *Arabidopsis* plant leaf marked to show the abaxial-adaxial, proximal-distal, and medial-lateral (M-L) axes. (Piazza *et al.*, 2005) - Reproduced with permission from John Wiley and Sons.

1.3.1 Adaxial and abaxial polarity determination in leaves

The adaxial and abaxial symmetry translates into functionally distinct layers of leaf; adaxial side or the upper side is specialized in light capturing, whereas, the abaxial side has special-

ized tissues for gaseous exchange. Also, the inherent design of leaf development is such that adaxial-abaxial polarity essential for leaf blade outgrowth (Waites and Hudson, 1995; Zoulias *et al.*, 2011). In potato and other flowering plants, an incision in the shoot meristem at the future leaf primordium caused loss of adaxial-abaxial symmetry and formed an abaxialized centric leaf (Figure 1.10 A) (Sussex, 1955; Hanawa, 1961; Reinhardt *et al.*, 2003). These surgi-

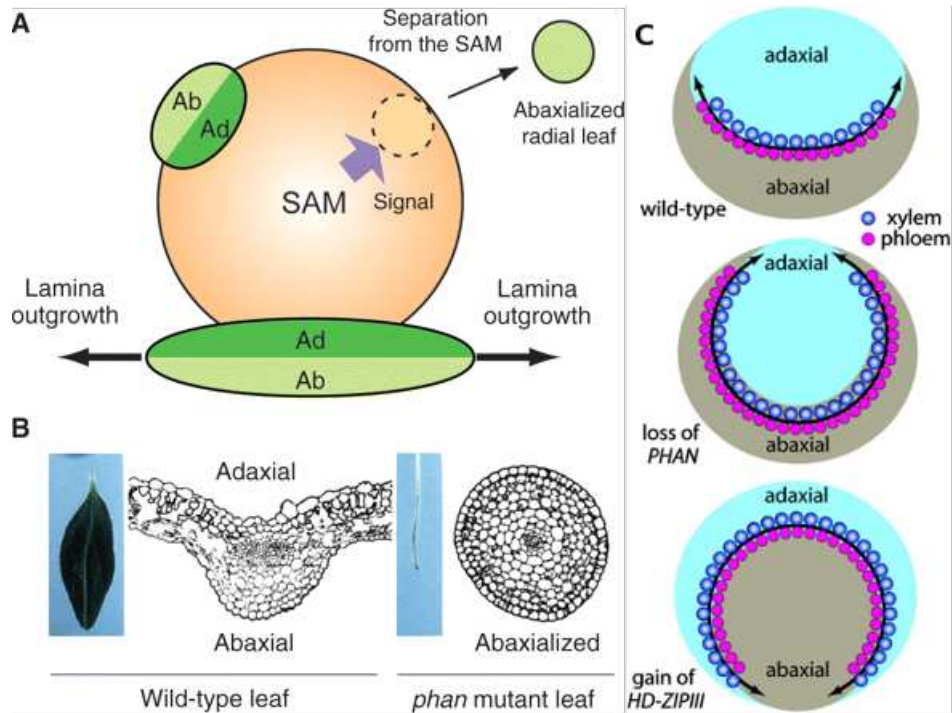


Figure 1.10: Surgical and genetic studies on the adaxial-abaxial polarity of a leaf. (A) Schematics showing the organization of shoot apex and the appearance of adaxial and abaxial polarity on leaf primordium. A surgical incision causes radialized leaf formation. (B) Comparison of morphological and anatomical differences between wild-type and *phan* mutant leaves of *Antirrhinum majus*. (C) Schematic explaining the changes in xylem and phloem arrangement in the midvein and petiole of adaxialized and abaxialized leaves. (Eckardt, 2004; Yamaguchi *et al.*, 2012) - Adapted with permission from Oxford University Press and American Society of Plant Biologists.

cal experiments suggest that the adaxial polarity arises as a consequence of the influence of the meristem on leaf primordium (Wardlaw, 1943). Similar abaxialized leaf phenotype (phloem surrounding xylem) was first observed in *phantastica* (*phan*) mutants of *Antirrhinum majus* (Figure 1.10 B). *PHAN* locus codes for a MYB transcription factor family protein that belongs to *ARP* genes described before (Waites *et al.*, 1998). Unlike *PHAN*, *as1* and *rs2* loss-of-function mutants do not exhibit an abaxialised leaf (Figure 1.8 F), but AS1 protein interaction partner *ASYMMETRIC LEAVES2* (*AS2*) and its maize ortholog *INDETERMINATE GAMETOPHYTE1* (*IG1*) provide the necessary information (Guo *et al.*, 2008). The adaxial specific gene, *AS2*

overexpression caused adaxialization of the leaf (xylem surrounding phloem), and the maize *igl1* mutant leaf midrib developed small flaps which had its own abaxial-adaxial polarity (Figure 1.10 C) (Lin *et al.*, 2003; Evans, 2007; Iwakawa *et al.*, 2007). These studies suggest the presence of parallel pathways regulating adaxial identity in angiosperms. Role of *ARP* genes in adaxial-abaxial symmetry formation in lower vascular plants is not yet clearly understood though *SkARPI* gene from *Selaginella kraussiana* could completely rescue the *as1* mutant phenotype and repress the class I *KNOX* expression in leaves (Harrison *et al.*, 2005). *ARP* group of genes are absent in *P. patens* genome.

The adaxial and abaxial boundary demarcation also involves a mutually inhibiting adaxial- and abaxial- specific genes like the interaction between class I *KNOX* and *ASI* genes (Figure 1.11 A). The dominant mutants of class III *HOMEODOMAIN-LEUCINE ZIPPER* (*HD-ZIP III*) such as *PHABULOSA* (*PHB*), *PHAVOLUTA* (*PHV*) and *REVOLUTA* (*REV*), in which the miR165/166 binding site is disrupted, exhibit adaxialized radial leaves. While in loss-of-function mutants, cotyledons were abaxialized and sometimes SAM was lost (Figure 1.11 B-E) (McConnell *et al.*, 2001; Otsuga *et al.*, 2001). These *HD-ZIP III* genes express throughout the initial leaf primordium but later restricted to adaxial side of the developing leaf in *Arabidopsis*, due to the abaxial-specific expression of miR165/166 (McConnell *et al.*, 2001; Rhoades *et al.*, 2002; Mallory *et al.*, 2004). *HD-ZIP III* transcription factors are evolutionarily conserved in all land plants and have a similar expression pattern in *Ginkgo* and *S. kraussiana* (Table 1.1) (Floyd *et al.*, 2006). Loss of function lines of *PpHD-ZIP III* gene was developed in *P. patens* by ectopical expressing of miRNA 166. In contrast to the vascular plants, *PpHD-ZIP III* gene plays a role only in transient meristems of *P. patens* such as the gametophore leaf base meristem and sporophytic seta meristem (Yip *et al.*, 2016).

Over-expression and loss-of-function of abaxial fate promoting *KANADI* (*KAN*) genes have the opposite phenotype of adaxial fate promoting *HD-ZIP III* genes (Figure 1.11 F and G) (Eshed *et al.*, 2001; Kerstetter *et al.*, 2001). Many genes that function downstream to *KAN* genes in adaxial fate determination are also further regulated by abaxial specific genes. Auxin response factors, *AUXIN RESPONSE FACTOR 3* and *4* (*ARF3* and *ARF4*) genes are abaxial side-specific, and they are considered to function downstream of *KAN* genes (Eshed *et al.*, 2004; Pekker *et al.*, 2005; Stahle *et al.*, 2009). *ARF3* and *ARF4* genes are post-transcriptionally suppressed by adaxial specific trans-acting small RNA (tasi-RNA) loci as has been shown by a number of reports (Garcia *et al.*, 2006; Nogueira *et al.*, 2007; Chitwood *et al.*, 2009). *YABBY* gene family also acts downstream of *KANADI* but regulates lamina out-

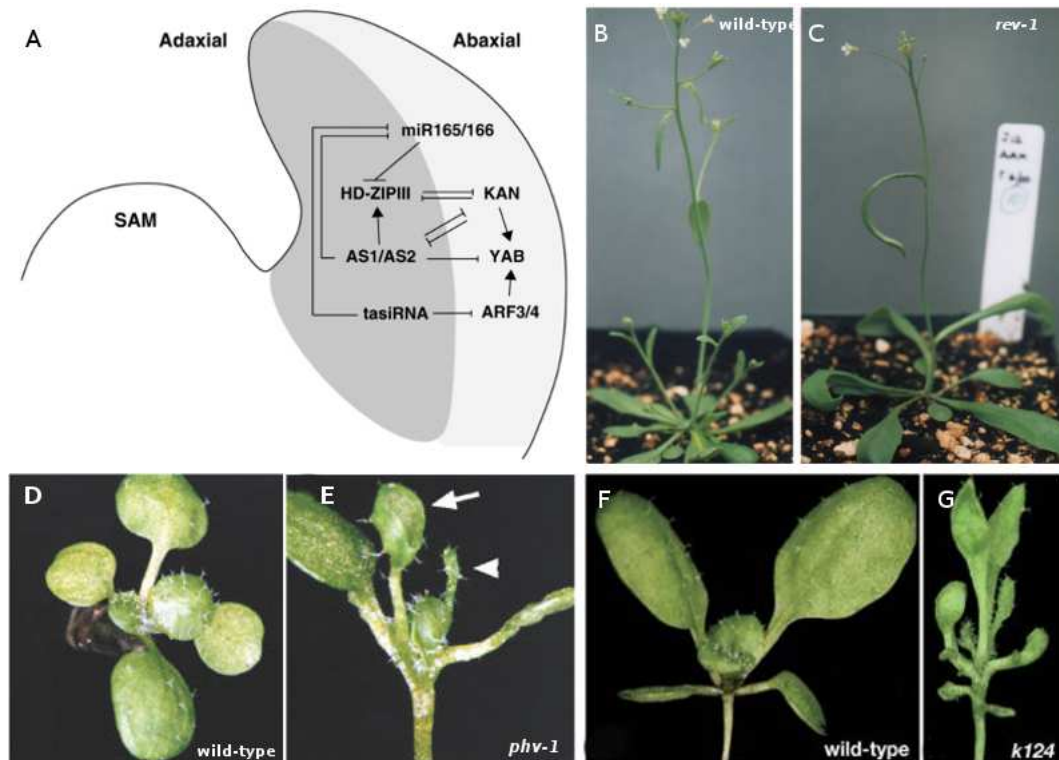


Figure 1.11: *Arabidopsis* mutants defective in adaxial-abaxial leaf patterning. (A) Schematic is describing the mutually inhibiting genetic interaction between class III *HD-ZIP* genes and *KANADI* genes. (B) Wild-type and (C) *REVOLUTA* mutant lines showing a defect in leaf patterning and axillary branch growth. (D) Wild-type seedling and (E) *PHAVOLUTA* mutant seedlings showing trumpet (arrow) and radial (arrowhead) leaves. (F) Wild-type seedling and (G) *KANADI* triple knock out (*kan1 kan2 kan4*) seedlings showing severe leaf patterning defect. (Talbert *et al.*, 1995, McConnell *et al.*, 2001, Izhaki and Bowman, 2007) - adapted with permission from Springer Nature and American Society of Plant Physiologists

growth (Eshed *et al.*, 2004). In *kan1 kan2* double knockout lines, the leaf had ectopic patches of adaxial and abaxial identity (Eshed *et al.*, 2001) but minimal organ outgrowth was observed mainly due to the reduced levels of adequately oriented *YABBY* genes expression. In *kan1 kan2 fil yab3* quadruple mutant line, where *FILAMENTOUS FLOWER (FIL)* and *YABBY3 (YAB3)* genes were also mutated, the leaves became radial (Eshed *et al.*, 2004). In many flowering plants, *YABBY* gene expression was observed in the boundary between adaxial and abaxial domains (Juarez *et al.*, 2004; Gleissberg *et al.*, 2005; Tononi *et al.*, 2010). These results led to the opinion that the lamina outgrowth requires juxtaposition of adaxial and abaxial domains (Waites and Hudson, 1995). Homologs of *KANADI* genes were present in *Selaginella* and *P. patens*, but they are not characterized yet (Floyd and Bowman, 2007).

1.3.2 Medial-Lateral Polarity determination in leaves

Our literature survey indicated that the establishment of the medial-lateral (M-L) axis of leaves is not discussed separately in many scientific literatures. It could be because of the medial-lateral axis is reflected as the width of adaxial and abaxial domains. A study performed on compound leaved-species, tomato, supports this perspective (Zoulias *et al.*, 2011). In the anti-sense lines of tomato (*Solanum lycopersicum*) *slPHAN*, petioles were abaxialized, and needle or cup-shaped lamina was developed (Figure 1.12 I, J, and K) (Kim *et al.*, 2003). In *anti-slPHAN* mutants loss of adaxial domain in the rachis caused loss of leaflet formation as observed in *Arabidopsis*. The authors tried to find out the reason for absence of lamina in wild type petiole and rachis despite the presence of both the adaxial-abaxial domain and the *PHAN* expression. In the *slPHAN* constitutive over-expression lines, leaflets were formed on the petiole and rachis as well (Zoulias *et al.*, 2011). It is interpreted that the *slPHAN* overexpression has increased the width of the adaxial domain compared to wild-type and caused the lamina outgrowth on rachis (Figure 1.12 N). Similarly, in *Arabidopsis*, *WUS*-related homeobox genes (*WOX1* and *WOX3*) specifically expressed in the lateral leaf domain and controlled the leaf outgrowth and margin specific growth. It was observed that in the *wox1 wox3* mutant, leaf blade growth was profoundly affected (Matsumoto and Okada, 2001). Similar phenotypes were observed in *WOX3* family maize mutants *ns1 ns2* (*NARROW SHEATH1* and 2) (Nardmann *et al.*, 2004) (Figure 1.12 L and M). In all these mutants though adaxial-abaxial polarity is not compromised, but the leaf blade growth was affected (Figure 1.12); hence, *WOX1* and *WOX3* are termed as lateral leaf specific genes. In case of the *P. patens*, the M-L polarity of phyllids is shown to be affected by exogenous auxin, PAT inhibitors, and *pinA pinB* loss of function mutants (Bennett *et al.*, 2014) (Figure 1.7).

1.3.3 Proximal-distal polarity determination in leaves

The proximal-distal polarity is evident from the petiole on the proximal end and the leaf blade tip on the distal end of a typical leaf (Byrne, 2005). Studies on maize and tobacco (*Nicotiana glauca*) orthologs of *PHAN* gene are not entirely consistent with results of *as1* (*Arabidopsis*) and *phan* (*Antirrhinum*) mutants; instead, offer a different interpretation of these mutant phenotypes as explained (Schneeberger *et al.*, 1998; McHale and Koning, 2004). In maize *rs2* mutant leaves, the adaxial-abaxial polarity was not compromised. Instead, the highly pronounced phenotype was the displacement of sheath-blade boundary towards the distal end; evident from

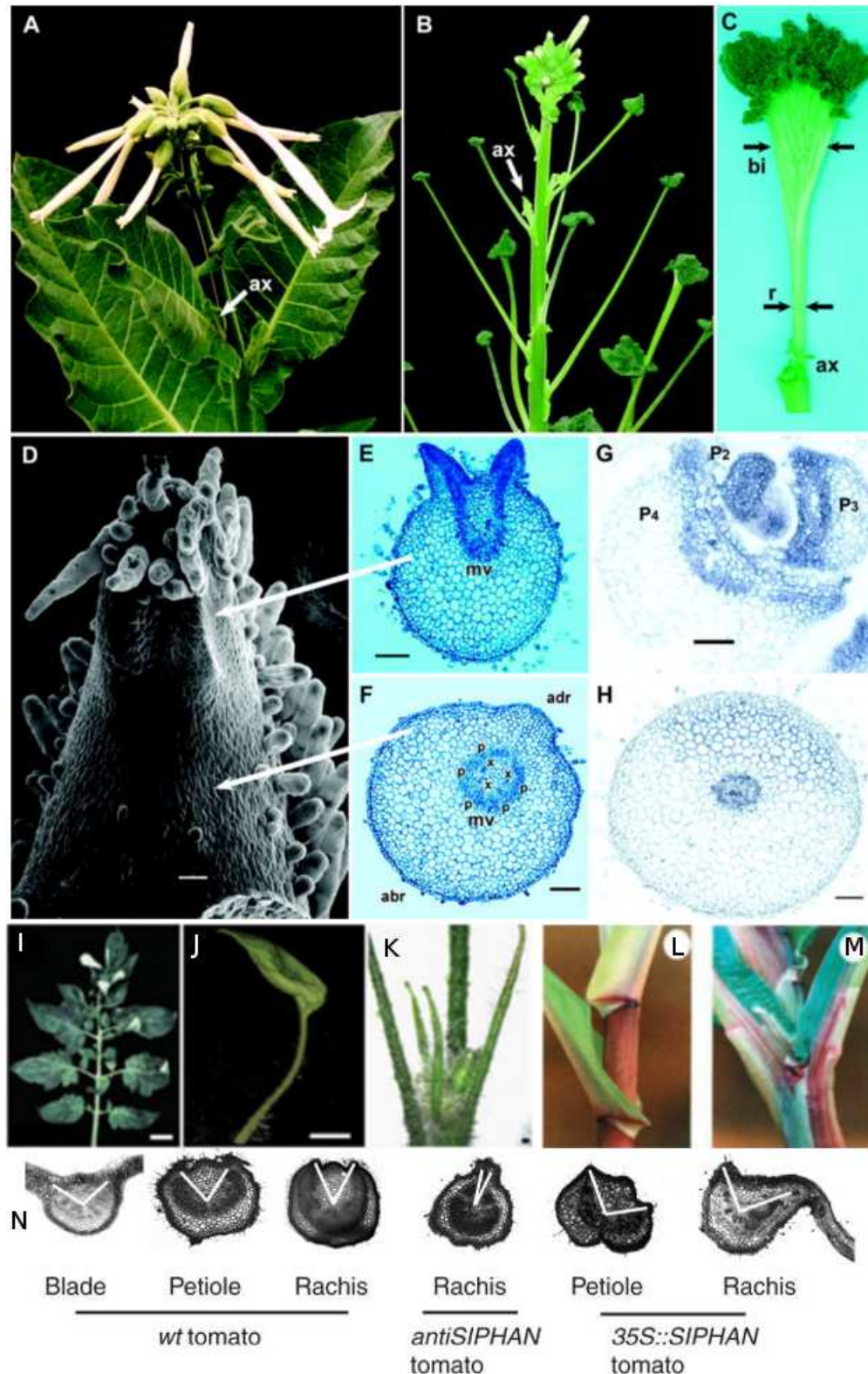


Figure 1.12: Mutants defective in proximo-distal and M-L leaf patterning.

(A) An adult wild-type tobacco plant at flowering stage. Arrow indicates an axillary branch.

(continued)

Figure 1.12: continued

(B) Mature *nsPHAN* mutant plant showing the axillary branch (arrow) and leaves with leaf blade at the distal tip. (C) A single *nsphan* leaf exhibiting radial growth (arrows) at the proximal end and bilateral symmetry (arrows) towards distal tip. (D) Electron micrograph of developing primordia and its cross-section at the distal tip (E) and base (F). (G) *in situ* hybridization of *PHAVOLUTA* probe hybridizing throughout primordia (P2) but (H) in later stages hybridization is restricted to only midvein and adaxial regions. (I) Wild-type tomato leaf and (J) cup-shaped or (K) needle-shaped leaves of antisense *sphan* leaves. (L) Wild-type maize leaf and (M) aberrant proximo-distal patterning in *ns* leaf. (N) The width of the adaxial domain in wild-type, *antiPHAN*, and *35S::SIPHAN*. (Kim *et al.*, 2003; McHale and Koning, 2004; Zoulias *et al.*, 2011) - adapted with permission from Springer Nature and American Society of Plant Physiologists and Oxford University Press.

the location of sheath-specific features such as ligule and auricle along the proximo-distal axis (Figure 1.12 L and M). Based on this observation, a fascinating alternate interpretation is that in *phan* mutants of *Antirrhinum*, proximal petiole or stem features extended and transformed the distal leaf blade (Tsiantis *et al.*, 1999). Characteristics of tobacco *nsphan* mutant phenotype further strengthen this interpretation (McHale and Koning, 2004) (Figure 1.12 A-H). The base of *nsphan* mature leaf petioles are radialised with phloem surrounding xylem (abaxialization)(Figure 1.12 D and E); however, leaves still develop axillary meristem (Figure 1.12 A and B) and show expression of adaxial specific gene *NSPHV* (Figure 1.12 G and H) (McHale and Koning, 2004). Interestingly, bilateral symmetry re-emerges along the proximo-distal axis, and petiole-leaf blade junction is displaced to the distal end (Figure 1.12 C). Thus, *RS2* and *NSPHAN* genes are involved in primary proximo-distal leaf patterning, followed by growth gradients that decide the final shape of the leaf. In phyllids of *P. patens*, perturbation of auxin concentration through exogenous auxin, PAT inhibitors, and *pinA pinB* loss of function affected the proximo-distal growth (Bennett *et al.*, 2014) (Figure 1.7).

1.4 Control of leaf size

In plants, organ size is critical for survival, and it is highly influenced by genetic factors than the environment. In leaves, usually growth occurs by two phases: cell proliferation and cell expansion. Cell proliferation phase has a high rate of cell division coupled with cell expansion, whereas during cell expansion phase, merely cell expands due to turgor pressure and

endoreduplication (Cosgrove, 2005; Schopfer, 2006). During endoreduplication, cells increase the ploidy level without cell division (Breuer *et al.*, 2010). In most of the model angiosperms, basipetal growth is observed where entire organ primordium is under the proliferation phase, but slowly cells at the distal end enter the cell expansion phase (Nath *et al.*, 2003). The dynamic boundary between the two-phase of growth is called ‘arrest front’ (Figure 1.13) (White, 2006; Andriankaja *et al.*, 2012). A simple experiment revealed that other types of growth forms such as acropetal, bidirectional and diffused growth also exists in nature (Gupta and Nath, 2015).

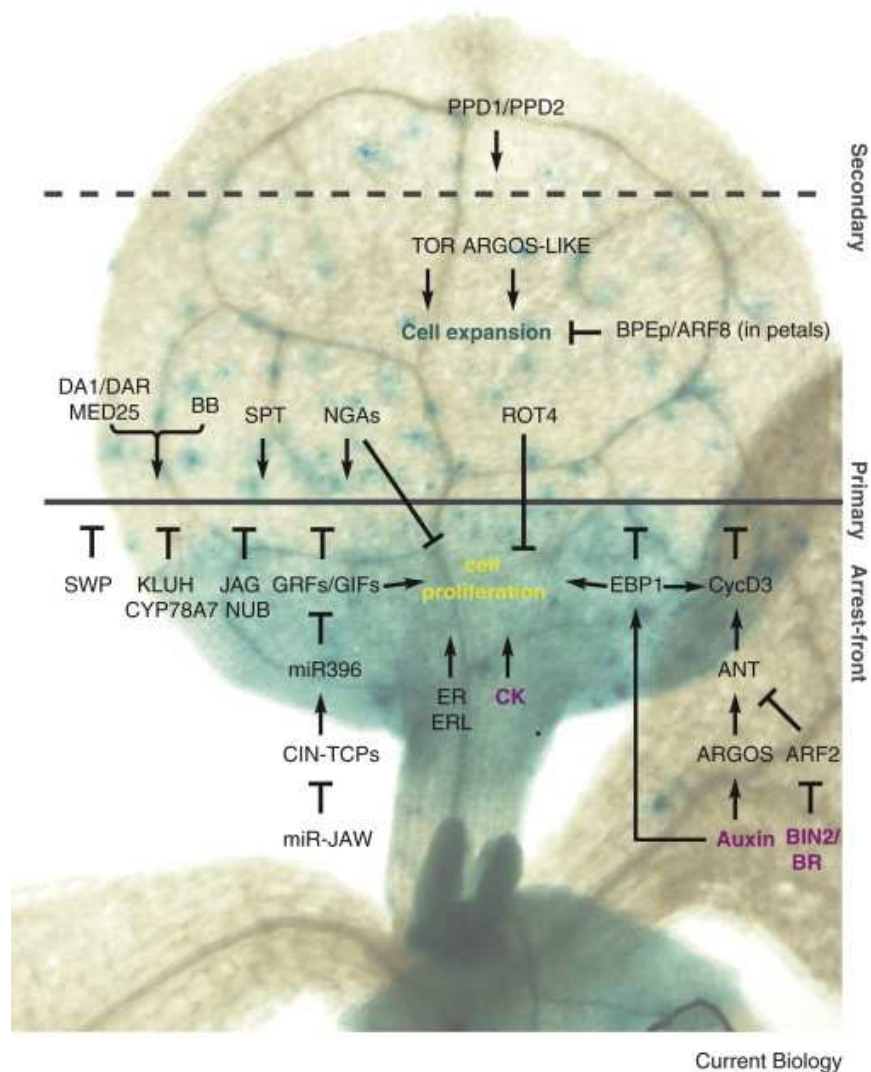


Figure 1.13: Phytohormones and genes involved in the regulation of the cell proliferation ‘arrest front’ dynamics. The *Arabidopsis* pCycB1;1::CDB-GUS lines showing the cells undergoing mitotic divisions. Essential genes and their functions in leaf size regulation are discussed in the main text. Arrow mark and T-shapes indicated enhancing and inhibitory interactions, respectively. (Powell and Lenhard, 2012) - *Reproduced with permission from Elsevier.*

Intuitively, final leaf size could be influenced by the number of SAM cells recruited to

form primordia, the duration and the rate of cell proliferation and expansion phases. It has been shown that maize *NARROW SHEATH* gene positively regulates the number of cells contributing to leaf primordia formation (Poethig, 1984; Scanlon and Freeling, 1997). In *Arabidopsis*, a basic helix-loop-helix transcription factor, *SPATULA* negatively regulates the size of the meristematic region in leaf primordia thus restricting the final leaf size (Ichihashi *et al.*, 2009). The growth-inhibiting property of abscisic acid (ABA) is mediated by the ABA-inducible *DA* gene (a Ubiquitin receptor) (Li *et al.*, 2008). Reports suggest that the *DA* gene in parallel with *BIG BROTHER (BB)*, an E3 ubiquitin ligase negatively regulates the duration of cell proliferation (Disch *et al.*, 2006; Li *et al.*, 2008). Interestingly, *ANGUSTIFOLIA3/ GRF INTERACTING FACTOR1 (AN3/GIF1)* protein, synthesized in the inner mesophyll layer of the leaf, moves to the epidermal layer and enhances the cell proliferation phase (Figure 1.13) (Kawade *et al.*, 2013). As the name suggests, *AN3/GIF1* transcription co-regulator has been shown to interact with *GROWTH REGULATING FACTOR5 (GRF5)*, which also enhances the cell proliferation phase in developing leaves (Horiguchi *et al.*, 2005). Auxin induces the expression of *ARGOS (AUXIN-REGULATED GENE INVOLVED IN ORGAN SIZE)* which promotes the expression of *AINTEGUMENTA (ANT)*, a member of the *AP2/ERF* transcription factor family (Figure 1.13) (Hu *et al.*, 2003; Feng *et al.*, 2011). *ANT* positively regulates the duration of cell proliferation phase by enhancing the expression of the *CYCD3;1* (Krizek, 1999; Mizukami and Fischer, 2000; Hu *et al.*, 2003; Dewitte *et al.*, 2007). Multiple positive and negative regulators control cell proliferation rate and duration. Similarly, the cell expansion phase is also under tight regulation by molecular factors.

An ever-advancing ‘arrest front’ separates actively proliferating cells from cells undergoing expansion and endo-reduplication. The dynamics of the arrest front is determined mainly by miR319-*TCPs (TEOSINTE BRANCHED1, CYCLOIDEA, PROLIFERATING CELL FACTORS)* and miR399-*GRF(GROWTH-REGULATING FACTOR)* modules (Figure 1.13). A family of miRNA319 genes shown to express prominently in the proliferating cells, suppress the cell-expansion phase by restricting the accumulation of *TCP* family transcription factor to the distal side of the leaf (Nath *et al.*, 2003; Palatnik *et al.*, 2003; Ori *et al.*, 2007; Nag *et al.*, 2009). At the distal side of the developing *Arabidopsis* leaf, *TCPs* are shown to induce the expression of miR396 (Rodriguez *et al.*, 2010). The miR396 restricts its targets, such as cell-proliferation-promoting *GRF* to the proximal side of the ‘arrest front’ (Rodriguez *et al.*, 2010; Wang *et al.*, 2011; Debernardi *et al.*, 2012). The concept ‘arrest front’ is applicable for the majority of cell types (epidermis and mesophyll cells); however, other dispersed meristematic cells (DMC), contributing to stomatal and vascular tissues, continue to divide in the distal

elongation side. DMC cell division is regulated by *PEAPOD* genes (*PPD1* and *PPD2*) (Figure 1.13) (White, 2006). From the above examples, it is quite clear that a highly coordinated gene network controls the leaf size in plants.

Very little work has been done regarding the leaf growth of non-seed land plants. In case of moss leaves, the leaf apical cells undergo few asymmetric divisions before it ceases to divide (Figure 1.4). During leaf growth, each cell develops into a segment (Harrison *et al.*, 2009). Naturally, the number of the asymmetric cells could determine the size of the leaf. However, no known mutant has been reported yet with an increased number of segments. Perturbation of auxin concentration through exogenous auxin, PAT inhibitors, and *pinA pinB* loss-of-function mutants shown to affect the overall size of *P. patens* leaves (Figure 1.7) (Bennett *et al.*, 2014). Only future research can reveal the regulators of phyllid growth in moss.

1.4.1 Leaf complexity

In compound-leaved species, the lamina is further divided into leaflets. A leaflet does not have an axillary meristem. Hence, it is not equivalent to a leaf (Smith and Hake, 1992). Extensive studies have been performed on the development of compound leaf in tomato. A well-established fact in the field is that the class I *KNOX* expression is absent in leaf primordia (Lincoln *et al.*, 1994); however, in tomato and other compound-leaved species (except pea) class I *KNOX* expression resumes during the leaf development (Hareven *et al.*, 1996). In tomato and *Cardamine*, ectopic expression of *KNOX* produced ultra-compound leaves (Figure 1.14 A-C) (Hareven *et al.*, 1996; Hay and Tsiantis, 2006) by suppressing GA signaling (Hay *et al.*, 2002). Interestingly, a number of reports have suggested that in pea and other Leguminaceae family members, leaf complexity is controlled by *FLORICULA* / *LEAFY* genes and not by *KNOX* genes (Figure 1.14 D-E) (Champagne *et al.*, 2007; Di Giacomo *et al.*, 2008; Wang *et al.*, 2008). Surprisingly, GA treatment prolonged the proliferative phase of pea leaves (Goliber *et al.*, 1998). Despite all these efforts, the question that remains unanswered is - why ectopic *KNOX* expression increases leaf complexity in compound leaved-species but not in simple leaved-species? This could be explained by the marginal blastozone (MB) concept (Hagemann and Gleissberg, 1996). MB refers to the marginal group of transiently indeterminate cells that has organogenesis capacity, which explains the simple lobed leaf and the dissected compound leaf development (Hagemann and Gleissberg, 1996). Compound leaved-species enter the organogenesis phase after formation of leaf primordia, wherein lateral blastozones form the

axis of lamina development. In case of simple, lobed leaves, MB forms the axis of growth while organogenesis phase is absent in most simple, entire leaves (Piazza *et al.*, 2005). Overexpression of class I *KNOX* gene increases the spatiotemporal duration of these marginal and lateral blastozones and causes ultra compound leaf formation as shown by Hagemann and Gleissberg, (1996) and Bar and Ori, (2014). *Cardamine hirsuta* is a compound-leaved species in Brassicaceae family and closely related to *Arabidopsis thaliana*. *C. hirsuta* has a homeobox gene *REDUCED COMPLEXITY (RCO)* which helps the formation of lateral blastozone by inhibiting cell proliferation between leaflets (Vlad *et al.*, 2014). Also, in *Arabidopsis thaliana*, which does not have the *RCO* in the genome, produced lobed leaves upon expression of *C. hirsuta RCO* gene.

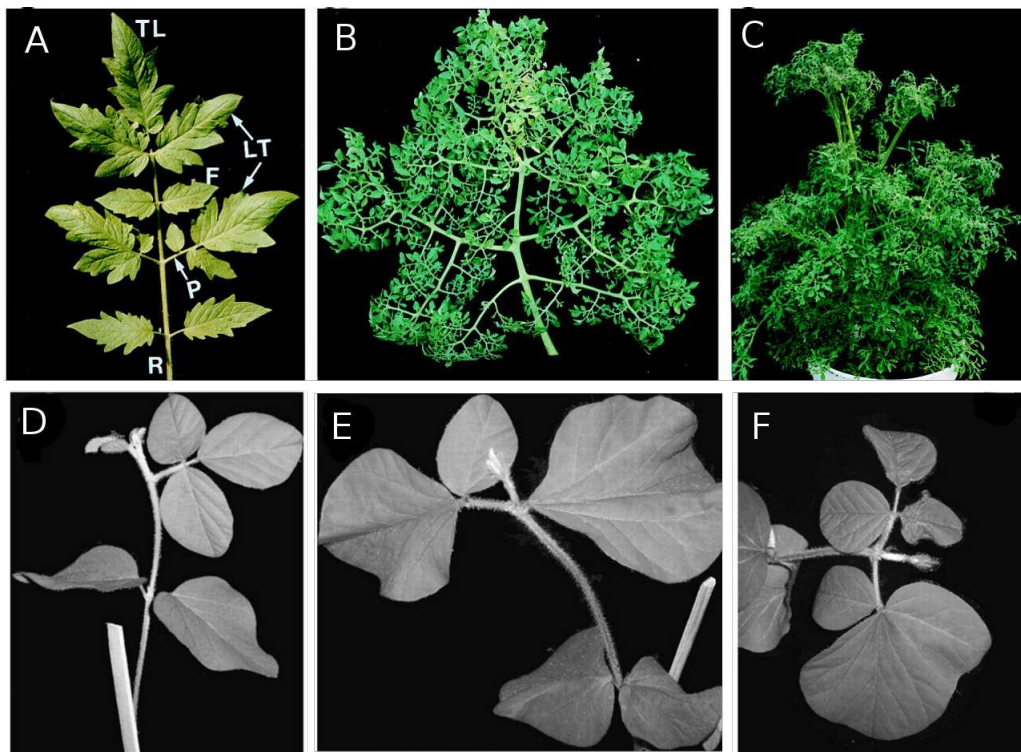


Figure 1.14: Regulation of angiosperm complexity by class I *KNOX* and *FLO/LFY*. (A) Tissue types of wild-type leaves of tomato leaf marked as rachis (R), petiole (P), folioles (F), lateral leaflet (LT), and terminal leaflet (TL). (B and C) Super compound leaf developed on a *KNOX1* overexpression line. (E) Wild-type soybean plant is showing the simple leaf on the first node and compound leaf on the second node. (E and F) *LFY* RNAi lines showing simple or fused compound leaves on the second node. (Hareven *et al.*, 1996; Champagne *et al.*, 2007) - Reproduced with permission from Elsevier and American Society for Plant Biologists.

Many other genes have been discovered to participate in crucial events of compound leaf development. Auxin efflux carrier PIN1 localization converges to form auxin maxima at future leaflets on leaf primordia (DeMason and Polowick, 2009; Koenig *et al.*, 2009). Role

of tomato *ARP* gene, *sIPHAN*, in enhancing adaxial domain size and its influence on leaflet formation has been discussed already (Figure 1.12) (Zoulias *et al.*, 2011). A tomato ortholog of *TCPs* family gene *LANCEOLATE* (*LA*) enhances the differentiation. Hence, gain-of-function *la* mutants cause precocious lateral blastozone differentiation and simple leaf development (Ori *et al.*, 2007; Shleizer-Burko *et al.*, 2011; Bar and Ori, 2014). Apart from megaphylls, both microphylls and phyllid form simple structures as well.

1.4.2 Leaf vasculature

Vascularisation of leaf begins at the primordial stage itself, as vascular strands carry essential resources like water, food, and long distance signaling molecules. Leaf vasculature is created *de novo* unlike the vascular system of the main stem (Scarpella and Meijer, 2004). Pre-procambial cells are recruited from the mesophyll cells, and they are distinguishable only by the marker genes like *ARABIDOPSIS THALIANA HOMEODOMAIN GENE8* (*AtHB8/ CORONA*) - a class III *HOMEODOMAIN-LEUCINE ZIPPER* gene. Sub-epidermal cells in the leaf primordium that express *AtHB8* gene grow narrow and become meristematic vascular tissue which is known as the procambium (Foster, 1952). Leaf vascularisation is also influenced by auxin. Increased vascular tissue formation was observed in auxin -overproduction lines and in leaves treated with exogenous auxin (Jacobs, 1952). Similarly, when PIN-mediated auxin transport is disrupted in growing leaves, increased number of vascular strands were observed though the cells were not correctly aligned (Mattsson *et al.*, 1999). High plasticity of vascular patterning could be observed from mature leaves that develop new vascular strands in response to wounding (Sachs, 1989). This self-organizing mechanism intrigued a lot of mathematical modelling studies concerning the PIN-mediated auxin transport. The most popular models follow the canalization of auxin flow hypothesis, which assumes that polar auxin efflux from a cell progressively increases the capacity of auxin efflux leading to the formation of auxin canals (Mitchison, 1980; Sachs, 1991; Nelson and Dengler, 1997; Rolland-Lagan and Prusinkiewicz, 2005). Microphylls and phyllids form simple venation pattern. Disruption of *PAT* has been noticed to affect venation of *Selaginella* but not in *P. patens* (Fujita *et al.*, 2008; Sanders and Langdale, 2013; Bennett *et al.*, 2014).

Until now, we have described the multiple origins of leaf-like organs followed by the description of shoot apical meristem development and maintenance. Thereafter, we have summarized the information available on the leaf founder cell formation, phyllotaxy, acquisition of

polarity axes by leaf primordia, regulation of leaf size and complexity and finally the vasculature. It was quite clear from the literature survey that numerous transcription factors, genes, and hormones not only govern the fate of stem cells and their derivatives to develop shoot and leaf-like organs, but a spatiotemporal expression of these molecular players also play a crucial role in boundary formation and organ development.

Given our primary interest in moss gametophore shoot development, it was evident from the literature survey that the bryophyte leaf development is distinct from microphylls and megaphylls. The bryophyte shoot apex organization is elementary, wherein the multicellular leaf primordium is replaced with a single leaf apical cell. The gametophore apical cell divides into three cutting planes, causing leaf apical cells to develop spirally around the main stem (Crandall-Stotler, 1980; Harrison *et al.*, 2009; Kofuji and Hasebe, 2014). It is conceivable that mechanisms like PIN protein-mediated auxin maxima to define future leaf primordia formation and class I *KNOX*, *ARP* genes and *CUC* mediated boundary demarcation between stem cells and leaf apical cells are not required for moss shoot apex. For the same reason, phyllid initiation and phyllotaxy were not affected in *pinA pinB* double knockout lines of *P. patens* (Bennett *et al.*, 2014) and the orthologs of *CUC* are not yet characterized. Unlike leaf primordia of higher plants, phyllid development is governed by a determinate leaf apical cell (Harrison *et al.*, 2009; Kofuji and Hasebe, 2014). Hence, the identity and the determinacy of leaf apical cells must be regulated by specific genetic and hormonal players.

However, there are no reports on mutants that are defective in formation of leaf apical cell in bryophytes. Availability of genetic information is scarce among bryophytes. As the genomic sequences of *P. patens* and *Marchantia polymorpha* do not have orthologs of *ARP* genes, a forward genetic screen could possibly help to dissect out the shoot/leaf apical cell development in these organisms. In the following sections, we describe in detail the phylogeny of moss, phyllid diversity among bryophytes and present moss (*P. patens*) as a suitable model organism to study gametophore shoot/phyllid development.

1.5 Diversity and development of phyllids in bryophytes

Alternation of generations between gametophytic (haploid) and sporophytic (diploid) phase is a unique characteristic of the plant life cycle (Hofmeister, 1851). Among gametophytes of plant lineages, moss and liverworts have the highest tissue diversity (Figure 1.15). The miniature leaf-like organs on gametophores of bryophytes (moss and liverworts) are known as phyllids

(Figure 1.16 A and B). At the apex, a gametophore apical cell-derived cell becomes a leaf apical cell, which divides and differentiates into a unistratose lamina with a multistratose midrib (costa) (Kofuji and Hasebe, 2014). While moss phyllids are arranged spirally, leafy-liverwort leaves are arranged in two-ranked or three-ranked phyllotaxy (Figure 1.16 A and B) (Crandall-Stotler, 1984). Also, the midrib is absent in leafy-liverworts, while moss exhibits heteroblasty - old, basal leaves lack the midrib, but other relatively young leaves develop midrib. The schematic diagram (below) is prepared to explain the diversity of tissue types between haploid and diploid generation (Figure 1.15).

1.5.1 Lamina diversity in Bryophytes

Though phyllids are simple organs with few tissue types, huge diversity can be observed among 12,000 species of mosses. Hereafter, phyllids will be referred to as "leaves" in the entire thesis to be consistent with the modern scientific literature. All the moss species have simple leaf except for the class Takakiopsida (contains only 2 species), whose leaves are deeply divided into cylindrical lobes (Jia *et al.*, 2003). In few moss species, the lamina is multistratose (e.g., *Syntrichia pseudodesertorum*) or curved (e.g., *Weissia sterilis*) (Atherton *et al.*, 2010). An exceptional lamina modification can be seen in the genera *Fissidens* (Figure 1.16 C). On the adaxial side, proximal leaf blade has two flaps which clasp the stem. These flaps believe to be useful to retain water on the plant surface. Leaves of Polytrichaceae and Bartramiaceae clasp their stem which provides extra support and capillary spaces for water conduction (References). Another modification of lamina can be seen in the *Schistostega*, where the leaves are connected at the base by a continuous lamina (Figure 1.16 D). Many moss species have serrations and dentations on their lamina margins. Interestingly, the miniature leaves of *Buxbaumia* seem to have a basal meristem rather than from a single apical cell. Surprisingly, the leaves of *Syrrhopodon prolifer* can grow to a majestic length of 6 cm (Goffinet, 2007). Literature suggest that *Hypnum* moss lamina base contains hyaline, thin-walled and inflated cells which are known as alar cells. These cells are believed to regulate the osmosis between cell content and external water, thus, influencing the leaf orientation (Grout, 1908). Modifications at the cellular level include cell lumina protruding outside the cell (Mammillae) and solid cell wall protruding above the surface (papillae) to increase gaseous and water exchange (Goffinet, 2007).

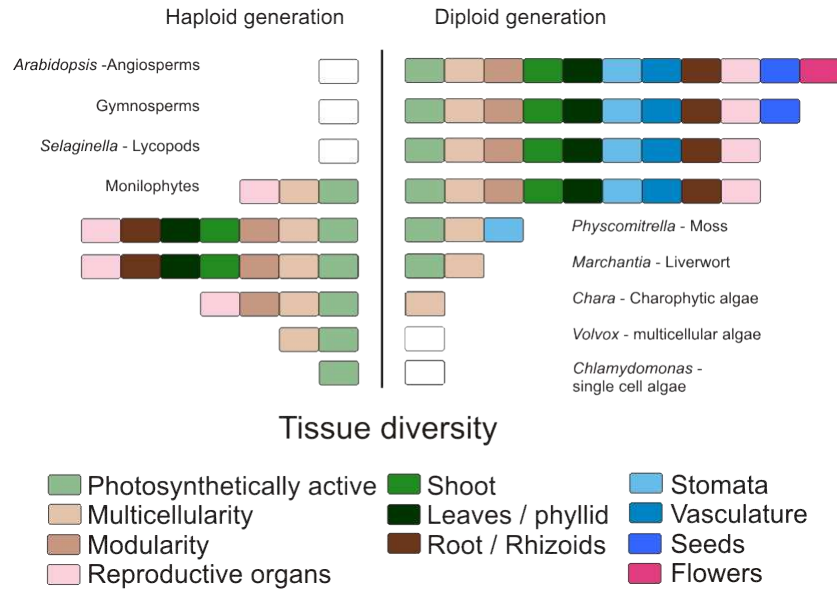


Figure 1.15: Peak of leaf diversity.

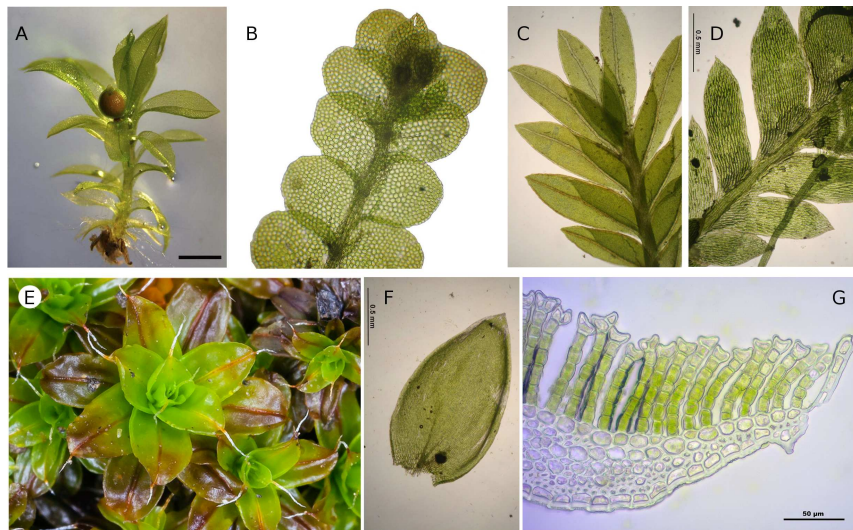


Figure 1.16: Phyllid diversity in bryophytes. (A) *Physcomitrella patens* gametophore with spirally arranged phyllids and a sporophyte at the apex. (B) Leaves of the leafy-liverwort species *Lejeunea trinitensis* arranged in a two-ranked phyllotaxy. (C) Lamina of *Fissidens* clasps the stem. (D) Leaves of *Schistostega* forms a continuous lamina. (E) The midrib of *Syntrichia ruralis* leaves extends beyond lamina. (F) The midrib of *Plagiothecium cavifolium* is short and divided. (G) Parallel sheets of photosynthesis cells arranged in the midrib of *Polytrichum* (Demko *et al.*, 2014).- Reproduced with permission from American Society of Plant Biologists. *Lejeunea trinitensis* by Scott Zona and *Fissidens rufulus*, *Schistostega pennata*, *Plagiothecium cavifolium* and *Polytrichum perigoniale* by Hermann Schachner and *Syntrichia princeps* by John Game are licensed under CC BY 2.0.

1.5.2 Midrib diversity in bryophytes

A multistratose midrib runs at the center of the leaf. Midrib provides mechanical strength to the lamina, which generally starts from the base to apex and sometimes beyond apex (e.g., *Syntrichia ruralis*) (Figure 1.16 E) (Atherton *et al.*, 2010). In some species, midrib is short, restricted to the base and double (Figure 1.16 F) (e.g., *Plagiothecium cavifolium*) or branched (e.g., *Antitrichia*) or extremely broad (e.g., *Leucobryum*). There are evidence of moss families that have diverged before the origin of *Oedipodium* that lack midrib (e.g., *Hedwigia ciliata*) (Blockeel and Stevenson, 2006; Biasuso, 2007). Moss leaves exhibit striking heteroblasty in terms of the midrib. Mostly, basal leaves of a gametophore lack midrib, while at the apex even the youngest leaf develops midrib. Adaxial-abaxial polarity is observed in *Polytrichum*, where on the adaxial side of the *polytrichum* midrib, photosynthetic cells are arranged as parallel sheets called lamellae (Figure 1.16 G). Each lamella is of six to seven cell height (Thomas *et al.*, 1996). Many moss phyllids have external cell projections (papillae) on the cell wall, which increases the leaf surface area for gas and water uptake. Interestingly scanning electron microscopic (SEM) examination of *Hedwigia* genus revealed consistent variation in papillae arrangement between the adaxial and abaxial side of the lamina (Biasuso, 2007). Many exciting heterophylly characters have also been observed in moss leaves. Further, it is observed that many costate moss species do not develop midrib when grown in submerged conditions (Goffinet, 2017). Another extreme modification of a moss leaf is stenophylls, which help in asexual reproduction (Reese, 2000). A stenophyll is a leaf with rod-shaped midrib flanked by a minimum lamina and holding gemma at the tip. Despite the vast diversity of bryophytes and their role as basal land plants, very few studies have focused on bryophyte leaf development.

1.5.3 The moss - *Physcomitrella patens*, as a suitable model organism to study evolutionary questions

Among mosses, *Sphagnum* belongs to an early divergent clade (Figure 1.17). Phylogenetic position of the peculiar moss *Takakia*, which is found on the Himalayas and morphologically similar to liverworts, has not been resolved yet (Smith and Davison, 1993). Morphology of sporophyte is at the heart of moss phylogeny especially peristomes. The sporophyte of extant moss species has a ring of teeth-like structures at the tip.

P. patens belongs to such basal moss species having primitive peristome (Figure 1.17

A). *P. patens* belongs to the family Funariaceae, placed in the order Funariales, which belongs to Bryopsida class (Goffinet, 2007). The genus name - *Physcomitrella*, comes from its morphological similarity to *Physcomitrium* moss. But *Physcomitrella* members are much smaller than *Physcomitrium*. Hence, the Latin word ‘*lla*,’ meaning diminutive, is added (Goffinet, 2007). *P. patens* (Hedw.) Bruch and Schimper is described as small plants of five mm height with ovate-lanceolate, acuminate mature phyllids measuring up to 2.5 mm length. Distal phyllid margin is serrated, and the midrib develops till apex. *Physcomitrella* is distinguished from other Funariaceae family members by its immersed capsules that lack peristome (Figure 1.17 B and C).

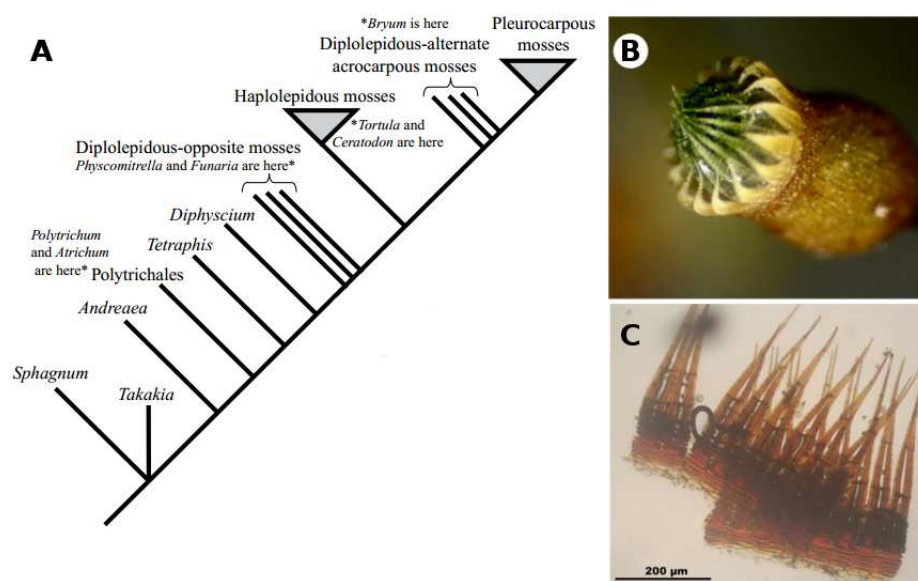


Figure 1.17: The phylogenetic relationship among moss species is depicted in a cladogram. (A). Early phylogenetic classifications were based on the characteristics of sporophyte (B) and the peristomes (C) of *Ceratodon purpureus* located at the tip of the sporophyte. (Mishler *et al.*, 2009). - Reproduced with permission from John Wiley and sons. Images B and C were taken by George Shepherd and Hermann Schachner and distributed under CC-BY license.

Moss has fascinated plant biologists for its resilience to extreme environmental stresses, high regeneration capacity and its position in the plant evolutionary lineage. The desiccation tolerance limits of diverse moss species and various related parameters are well documented (Hosokawa and Kubota, 1957; Hinshiri and Proctor, 1971; Oliver *et al.*, 2005; Proctor *et al.*, 2007). Many moss species can tolerate water level as low as 5 to 10% of total dry weight (Alpert, 2006, Xiao *et al.*, 2018). Moss can also withstand very low temperatures as freezing stress is similar to desiccation in terms of water availability (Oldenhof *et al.*, 2006). Interestingly, the moss *Chorisodontium aciphyllum*, which was frozen for 1533-1697 years in an Antarctic glacier was able to revive when cultured under laboratory condition (Roads *et al.*,

2014). Another remarkable ability of moss is its high regeneration capacity. Interestingly, moss phyllids, if detached from the gametophore and kept on regular growth medium, will regenerate and produce protonemal filaments within three days as demonstrated by Giordano *et al.*, (1996). All the above-discussed characters of mosses could be exploited to staple food crops for agronomical benefit as well as to understand the mechanism of resilience. Mosses are also placed in a critical position in plant evolutionary lineage making them an attractive group to understand the evolution of various genetic networks. Out of all plant lineages, mosses pose maximum tissue diversity in the haploid generation such as distinct shoot, rhizoids, phyllids and reproductive organs. Initially studies were performed on *P. patens*, *Funaria hygrometrica*, *Syntrichia ruralis* and few other moss species. The ability to grow in simple chemically defined media, three-month life cycle under laboratory conditions, genetic crossing techniques, somatic hybridization and high-efficiency homologous recombination protocols made *Physcomitrella patens* as a model organism of choice for many reverse genetics studies (Schaefer and Zrýd, 1997).

1.5.4 Life cycle of moss (*P. patens*) and stem cells involved in its body plan

The gametophytic phase of *P. patens* life cycle begins with the germination of the haploid spore (Figure 1.18 A and B). A protonemal apical cell forms upon the first cell division of spore (Menand *et al.*, 2007). Further tip growth from the protonema apical cell results in one-dimensional protonemal filaments. There are two types of protonemal filaments: chloroplast rich chloronemal filaments produced by chloronemal apical cell and rapidly elongating caulonemal filaments derived from a caulonemal apical cell (Figure 1.18 C, D, F, and G). When a spore germinates, it forms a chloronemal apical cell. Chloronemal filaments branch by developing new chloronemal apical cells (Figure 1.18 E). After a week, chloronemal apical cells acquire the caulonemal apical cell fate and form caulonemal filaments to spread the colony (Figure 1.18 F) (Cove, 2005). Caulonemal filaments form side branch initial which has the potential to obtain either a protonemal (one-dimensional growth) or a gametophore apical cell (three-dimensional growth) fate (Figure 1.18 I) (Cove and Knight, 1993). Around five percentage of side branch initials swell and divide in more than one plane to form a bud having a tetrahedral gametophore apical cell (Figure 1.18 K) (Harrison *et al.*, 2009). Continuous divisions along three-cutting faces of the indeterminate gametophore apical cell give rise to derivative cells and determine the spiral phyllotaxy of *P. patens* phyllids. These derivative cells undergo two rounds of asymmetric divisions and form two shoot initial cells and a determinate

leaf apical cell that is formed in a spiral phyllotaxy (Figure 1.18 M) (Crandall-Stotler, 1980). Leaf apical cell having two-cutting faces undergoes few asymmetric divisions and then cease to divide (Figure 1.18 N). The resulting phyllid primordium divides further to form a planar leaf (Figure 1.18 O). A rhizoid apical cell is initiated from epidermal cells at the base of the bud and nodes of the gametophore (Figure 1.18 P and Q) (Sakakibara *et al.*, 2003). A brown pigmented filament with immature plastids called rhizoid is developed from the rhizoid apical cell (Figure 1.18 Q). Low temperature and short day condition induce antheridia and archegonia formation at the gametophore apex (Hohe *et al.*, 2002). These gametangia are formed by the determinate antheridium and archegonium apical cell of unknown origin. As these gametangia apical cells have two cutting faces, their asymmetric divisions produce two rows of cells from which functional antheridium and archegonium will be developed (Figure 1.18 R-V) (Kofuji *et al.*, 2009). Upon fertilization, the zygote undergoes an asymmetric division forming a sporophyte apical cell with two cutting faces and a basal cell. Asymmetric divisions of the sporophyte apical cell form 12 cells in two rows from which the sporophyte develops (Figure 1.18 W). Moss is the earliest divergent land plant group whose sporophyte develops stomata (Maizel *et al.*, 2005; Tanahashi *et al.*, 2005). Though the immature sporophytes do photosynthesis, sporophytes in general largely depend on gametophyte for nutrients and energy (Figure 1.18 X). Upon maturation, sporophyte releases spores to begin the next cycle (Figure 1.18 Y).

1.5.5 Resources available for *P. patens* research

Over the years, a handful of ecotypes proven worthy to different aspects of moss genomics. The Gransden ecotype isolated in 2004 is used for genome sequencing and also for regular molecular studies (Rensing *et al.*, 2008). Another ecotype Villersexel K3 acts as the closest ecotype for Gransden isolate and used to develop the genetic map for *P. patens* (Kamisugi *et al.*, 2008). The sporophyte is inherently less in Gransden ecotype. Hence, few laboratories have used Reute ecotype to study sporophyte development (Hiss *et al.*, 2017). The monoicous moss, *P. patens*, has $n = 27$ chromosomes containing 518 Mbp genetic material (Schween *et al.*, 2003) whose whole genome has been sequenced by international moss community (Rensing *et al.*, 2008, Lang *et al.*, 2018), and well-annotated (Lang *et al.*, 2005). The moss genomics resources are available at www.cosmoss.org and regular culturing protocols were shared through moss.nibb.ac.jp (PhyScobase).

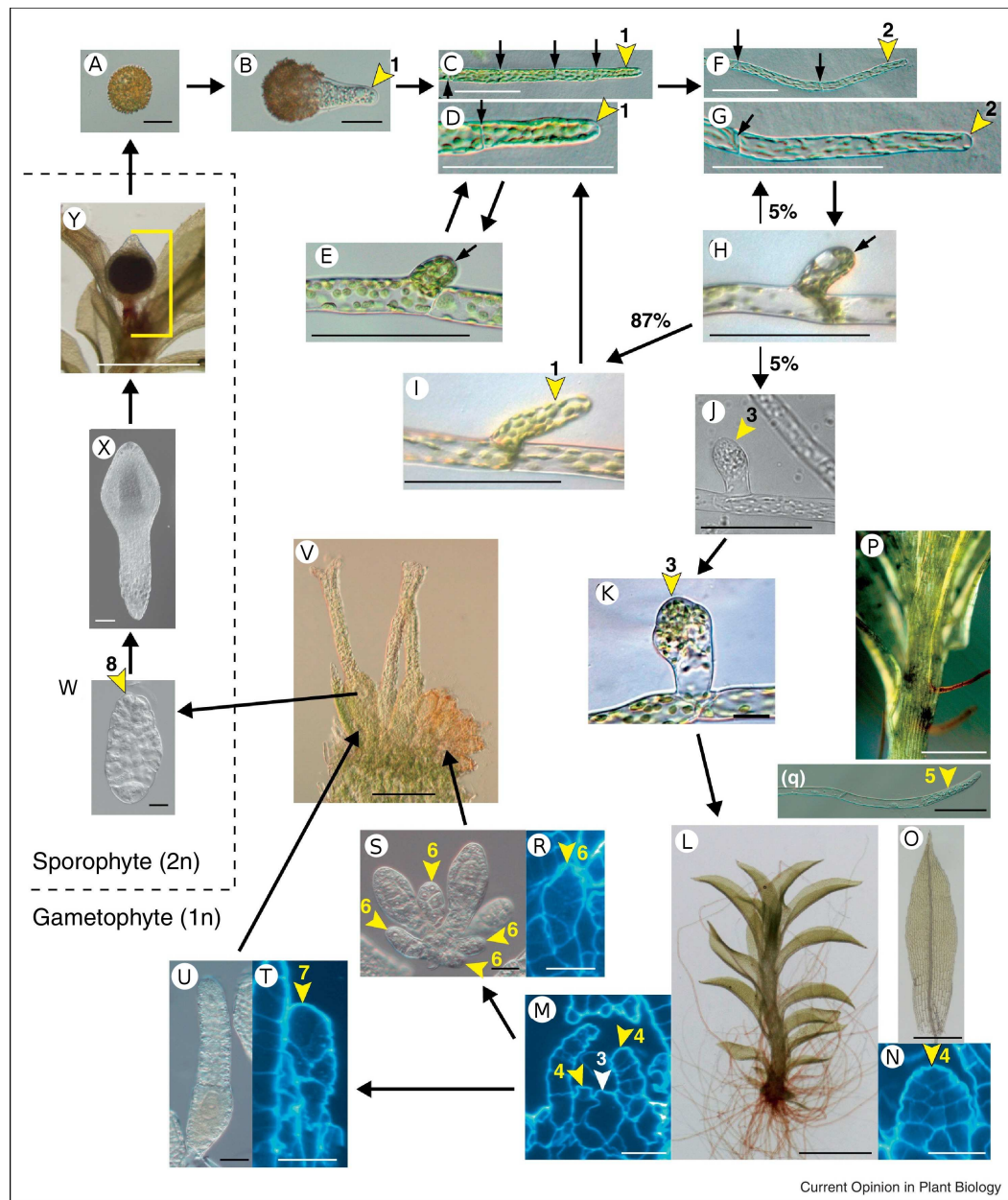


Figure 1.18: *P. patens* life cycle and the stem cells involved in its body plan. *P. patens* life cycle begins with the germination of a haploid spore (A) and produces chloronema apical cell (yellow arrowhead 1) (B). Chloronema apical cell forms chloronemal filaments (C and D) and arrows point the cell division plane. A side branch initial cell from the chloronemal filament develops another chloronemal filament (E). Chloronema apical cell differentiates to form a caulonema apical cell (yellow arrowhead 2) (F and G) and arrows point the oblique cell divisions. A side branch initial cell (h) from a caulonema cell can develop into a chloronema or caulonema, or it could swell (J) and develop a bud (K). The yellow arrowhead 3 denotes the gametophore apical cell which forms a gametophore (L).

Figure 1.18: continued

The gametophore apical cell-derived cell (yellow arrowhead 4) obtains the fate of leaf apical cell (M) which undergoes a series of asymmetric divisions to form a leaf (N and O). The gametophore epidermal cells dedifferentiate to form rhizoid apical cell (yellow arrowhead 5) which develops rhizoids (P and Q). At the gametophore apex, antheridia (R and S) and archegonia apical cells (T) (yellow arrowhead 6,7) which undergo asymmetric divisions to develop antheridium and archegonium respectively (R-V). Yellow arrowhead 8 shows the diploid sporophyte apical cell on a 12 cell stage sporophyte (W). An immature (X) and a mature sporophyte (Y) have undergone meiosis and would release spores to begin next life cycle - *Reproduced with permission from Elsevier.*

1.6 Hypothesis and objectives

Our literature survey revealed the many unexplored paths in the evolution of shoot development in land plants. Recent studies indicate the independent origin of leaves (Megaphylls, microphylls, and phyllids) across plant lineages. The telome and enations theories were proposed to explain the megaphyll and microphyll evolution respectively. Even though phyllids are present in the gametophyte of leafy-liverworts and all moss species, their origin and evolution are not studied yet. Whether the leaf-like organs of leafy-liverwort and moss share a common ancestor or not? remains unanswered. Interestingly, the anatomically simple phyllids have the basic features of megaphylls and microphylls (true leaves), however, the phyllid development is strikingly different from true leaves. In moss, a single tetrahedral gametophore apical cell form the leaf apical cell. Hence, the phyllotaxy is not affected by hormonal and environmental cues. Unlike true leaves, a single leaf apical cell forms the primordia for phyllid development. Also, the highly conserved *KNOX/ARP* network of vascular plant shoot development has known to have no role in gametophore development, which reflects the independent origin of phyllids. Our literature survey suggests that the current knowledge on phyllid development is still primitive. Hence, we began to focus on the genetic network governing the developmental events of bryophyte leaves or phyllids (hereafter leaves).

Considering the independent evolution of phyllids and the lack of conservation in developmental processes and role of genetic networks, the ideal approach to study moss leaf development would be a forward genetic screen. When we began our study, there was no efficient mutagenesis protocol available for *P. patens*. Considering the high gene preference of Tnt1 transpositions, demonstrated in heterologous angiosperm species, we chose Tnt1 as

a mutagen for our forward genetic screen and decided to develop a mutagenesis protocol for protonemal explants. We hypothesize that such a forward genetic approach would benefit from both haploid nature of the explant and the preferential transposition of Tnt1 into gene-rich regions. One of our goal was to screen for mutant lines defective in gametophore or phyllid development. A parallel aim was to look for candidate genes that likely to be involved in gametophore shoot development. Earlier, we have narrated the role of *AP2*-type transcription factors for gametophore apical cell development. Considering the fact that the role of genetic network are distinct between haploid and diploid generations, we hypothesize that GRAS domain containing transcription factors such as *SCARECROW* and *SHORTROOT* that genetically interact with *AP2*-type transcription factors in *Arabidopsis* root development could also be involved in gametophore shoot development in moss. Hence, we also took a reverse genetics approach to dissect the role of these transcription factors.

The following objectives were designed for the thesis work.

- To develop an efficient Tnt1 retrotransposon mutagenesis protocol and screen for mutants
- To characterize Tnt1 insertional mutants defective in gametophore shoot and leaf development.
- To study the function of a GRAS domain TF in gametophore shoot development by a reverse genetic approach.

2 Development of Tnt1 retrotransposon as a mutagenesis tool and screening of *P. patens* mutants

2.1 Introduction

Forward genetic screens have enabled biologists not only to understand phenotype of interest at a molecular level, but they have also facilitated the discovery of novel genes. The efficiency of any forward genetic screen is influenced by choice of mutagen and nature of the screen. A mutagen with a known nucleotide sequence tag is always desirable (Page and Grossniklaus, 2002). For this reason, transfer DNA (T-DNA) insertions have been preferred over traditional chemical mutagenesis tools, since known T-DNA borders aid in identifying the mutated locus in the genome. T-DNA insertions are random (Kim *et al.*, 2007) and mostly integrate into noncoding regions because the majority of plant genomes contain a large number of repetitive sequences (up to 85% of the genome). A mutagenesis tool that preferably integrates into genic regions would reduce the required size of the mutant population to saturate plant genomes.

2.1.1 Tnt1 retrotransposon as a mutagenesis tool

Retrotransposons are class I transposable elements which resemble a retrovirus in gene structure and mode of replication. Long terminal repeat (LTR) - retrotransposons contains genes essential for translocation activity and are flanked by direct repeats of LTR sequences (Finnegan, 2012). These sequences act as both promoter and terminator for the synthesis of intermediate RNA transcripts. Retrotransposon encodes multiple proteins including a reverse-transcriptase and an integrase to synthesize DNA from the RNA intermediate, and this integrates into a host genome leading to an increase in the copy number (Finnegan, 2012). This autonomous mode of retrotransposition process is dependent on host transfer RNA (tRNA), and it is complementary to the primer binding site (PBS) to initiate the reverse transcription process (Feuerbach *et al.*, 1997). Earlier, Tnt1 retrotransposon has been isolated from tobacco (Grandbastien *et al.*, 1989) and its transposition activity was studied extensively (Pouteau *et al.*, 1991; Casacuberta and Grandbastien 1993; Mhiri *et al.*, 1997; Vernhettes *et al.*, 1997). It has also been demonstrated that Tnt1 retrotransposon actively transposes in several heterologous angiosperm hosts like Arabidopsis (Lucas *et al.*, 1995), Medicago (d'Erfurth *et al.*, 2003), soybean (Cui *et al.*, 2013) and potato (Duangpan *et al.*, 2013) and shown to preferentially transpose into gene-rich regions. Yet, a major challenge has been the possibility of occasional translocation events of the retrotransposon in the mutant lines for the gene of interest.

2.1.2 *Physcomitrella patens* as a model organism to understand gametophyte evolution

Moss (*P. patens*), a member of the bryophytes, has a simple body plan yet its growth is regulated by many complex developmental phenomena like apical dominance (Fujita *et al.*, 2008), phototropism (Jenkins and Cove, 1983a) and gravitropism (Jenkins *et al.*, 1986). Also, mosses have the highest gametophytic tissue diversity [including spores, chloronema, caulonema, bud, rhizoid, gametophore axis, phyllids (blade and midrib), antheridium and archegonium] among all green plant lineages (Kofuji and Hasebe, 2014). High regeneration capacity, desiccation tolerance, availability of well-annotated genome sequence and the capacity for gene targeting techniques have established *P. patens* as a unique model organism for understanding the evolution of developmental traits in land plants (Prigge and Bezanilla, 2010). High homologous recombination frequency observed in *P. patens* has allowed extensive reverse genetics studies on several orthologs of angiosperm genes (Schaefer and Zrýd 1997). For example, characterization of orthologs of *KNOX* (class I and II) transcription factors, *EPF* (extra-cellular peptides), *TMM/ERECTA* (transmembrane receptors) and *SMF1* (transcriptional regulator) in moss have revealed that the gene regulatory networks controlling the development of haploid and diploid phases of plant lineages are distinct (Sakakibara *et al.*, 2008, 2013; Caine *et al.*, 2016; Chater *et al.*, 2016). These studies indicate the challenges associated with candidate gene selection for studying gametophytic developmental processes in moss based on the knowledge available from the diploid phase of angiosperms. This further suggests that there is an urgent need for an efficient forward genetic screen to identify novel genes and to complement the reverse genetics approach. In this regard, the haploid dominant life phase of *P. patens* is an interesting feature as even a recessive allele will reveal the phenotype. Previously, Perroud *et al.*, (2011) have developed an efficient fluorescent marker-based crossing system to identify hybrid sporophytes in *P. patens* to allow segregation analysis of the phenotype of interest. Small colony size and simple growth conditions of *P. patens* provide added advantages in carrying out a forward genetic screen. Cryostorage of mutant moss populations and maintenance of mutant lines with minimum effort have also been demonstrated (Schulte and Reski, 2004).

2.1.3 Other mutagenesis tools in *P. patens*

Earlier, chemical mutagenesis of moss has resulted into many auxotrophic, phototropic, polarotropic and various phytohormone resistant and sensitive lines (Ashton *et al.*, 1979; Jenkins and Cove, 1983b). Further studies on these mutant lines have implicated the role of hormones

in moss and their functional conservation in non-vascular plants. Nishiyama *et al.*, (2000) developed a shuttle mutagenesis tool for *P. patens* that specifically targets expressed regions of the genome. However, complicated multiple insertions made difficult for the identification of a causal insertion (Hayashida *et al.*, 2005). Using UV-C (Ultraviolet C)-based mutagenesis and a positional cloning approach, the first successful characterization of a mutant in *P. patens* has been recently reported (Stevenson *et al.*, 2016). When we began this study, there was no study regarding the usage of Tnt1 retrotransposon as a tool for mutagenesis of *P. patens*. Recently, Vives *et al.*, (2016) have shown that a two-component system derived from Tnt1 retrotransposon is capable of efficient transposition into the *P. patens* genome. These researchers have demonstrated that modified Tnt1 eliminates further translocation activity in moss. However, our approach is significantly different as we used an intact retrotransposon carried by *Agrobacterium* to mutagenize protonemal filaments and relied on a cryostorage method to reduce the occasional possibility of transposition. Haploid protonemal filaments, high gene preference of Tnt1 and the cryostorage of mutant lines have offered unique advantages to moss forward genetic studies. Another advantage of using protonemal explants instead of protoplasts is that it eliminates the risk of the diploid formation. In this study, using *Agrobacterium*-mediated transformation of protonemal filaments, we have developed a Tnt1 insertional mutant population and validated its transposition activity in *P. patens*. We have also analyzed the transposition preference of Tnt1 insertions. Additionally, LTR::GUS lines were developed to evaluate the transcriptional regulation of tobacco Tnt1 in moss. Our forward genetic screen has identified several novel moss mutants related to moss leaf development, hormonal and gravity response and phenotypes associated with gamete development. Using sequence-specific amplified polymorphism (SSAP-PCR), we have demonstrated the stability of Tnt1 insertions and the viability of our Tnt1 mutagenesis protocol respectively. Our results suggest that *Agrobacterium tumefaciens* mediated Tnt1 insertional mutagenesis could also generate moss mutants for forward genetic studies to enable novel gene discovery.

2.2 Materials and methods

2.2.1 Moss culture and maintenance

Physcomitrella patens ecotype ‘Gransden’ was procured from International Moss Stock Center (IMSC), University of Freiburg, Germany and maintained *in vitro* as described by Cove *et al.*, (2009). Homogenized protonemal tissue was grown on cellophane-overlaid BCDAT agar

medium. Post homogenization, tissues were incubated for 4-5 days in tissue culture incubators at 16:8 hour light:dark cycle at 24 °C for all the experiments.

2.2.2 Methionyl-tRNA_i sequence analysis

All the available green plant genomes (55 species) from Phytozome ver. 12.0 (<https://phytozome.jgi.doe.gov/pz/portal.html>) (Goodstein *et al.*, 2012) were downloaded to analyze if *P. patens* has necessary host factors for the successful Tnt1 transposition. *Klebsormidium nitens* draft genome was downloaded from the project website (Hori *et al.*, 2014). Transfer RNA genes were predicted from the genomic sequences using tRNAscan-SE ver. 1.3.1 (Pavesi *et al.*, 1994) with default parameters. Predicted methionyl-tRNA (Met-tRNA) (initiator and elongator) sequences were further tested for the stability of the tRNA acceptor arm by checking the 7 bp complementarity between the 5' (5' ATCAGAG 3') and the 3' ends (3' A-TAGTCTC 5'). Verified Met-tRNA 3' end sequences were analyzed for the degree of complementarity with the 9 bp of Tnt1 PBS (5' TGG-TATCAGAGC 3'). The remaining first 3 bp (5' TGG-TATCAGAGC 3') complementarity was not assessed since the 3' end CCA is not coded in the tRNA gene but is subsequently added by an enzymatic reaction. Representative organisms were arranged on a cladogram using PhyloT online tool (<http://phylot.biobyte.de/>) and visualized in iTOL (www.itol.embl.de). PhyloT tool generates trees based on the NCBI taxonomy database.

2.2.3 Cloning and moss transformation

Using *Agrobacterium tumefaciens* mediated transformation, pCAMBIA-1391Xc-Tnt1 (a kind gift from Prof. Pascal Ratet, IPS, CNRS, France) (vector Entrez accession number: AF234311.1 and Tnt1-94 element Entrez accession number: X13777) vector was used to transform into *P. patens* protonema, as described in PHYSCObase (www.moss.nibb.ac.jp/protocol.html). Moss tissue surviving hygromycin selection (20 mg/ L) was further subjected to PCR confirmation using Tnt1 (LTR_F and LTR_R) and *hygromycin phosphotransferase II* (*HPTII*) gene-specific primers (Hyg_F and Hyg_R) (Table 2.1). Confirmed Tnt1 mutant lines were propagated independently on the BCDAT medium. To generate LTR::GUS lines, the LTR promoter of Tnt1 was amplified from pCAMBIA-1391Xc-Tnt1 using primers XbaI_LTR_F and XmaI_LTR_R as forward and reverse primers, respectively (Table 2.1). A 610 bp amplified product was digested with *XbaI* and *XmaI* restriction enzymes (RE) and ligated into the bi-

nary vector pBI101 upstream to the *GUS* gene. LTR::GUS-pBI101 construct was introduced into wild-type (WT) *P. patens* protonemal tissue using *Agrobacterium*-mediated transformation. Mutants were cryopreserved for long-term storage as described by Schulte and Reski, (2004) and revived when required.

Table 2.1: List of primers used in this study.

S.No	Primer name	Sequences 5' to 3'
Tnt1 line confirmation		
1	LTR_F	TGATGATGTCCATCTCATTGAAG
2	LTR_R	TGTTGGGAATAAACCCTTACCA
3	Hyg_F	GATCCCAATACGAGGTCGCCAACAT
3	Hyg_R	CCGGATCGGACGATTGCGTCGCATCG
4	ACT F	ACCGAGTCCAACATTCTACC
5	ACT R	GTCCACATTAGATTCTCGCA
Southern blot		
6	sb_Tnt1_LTR_F	TGATGATGTCCATCTCATTGAAGAAG
7	sb_Tnt1_194_R	TCACCCTCTAAAGCCTACAATATTT
8	sb_Hyg_F	GGATCGGACGATTGCGTCGC
9	sb_Hyg_R	CAGGCTCTCGATGAGCTGATG
TAIL-PCR		
10	LTR3	AGTTGCTCCTCTCGGGGTCG
11	LTR 4	TACCGTATCTCGGTGCTACAT
12	LTR 7	TATTATTCCGCTTTATTACCGTGA
13	AD1	NGTCGASWGANAWGAA
14	AD2	TGWGNAGSANCASAGA
15	AD3	AGWGNAGWANCAWAGG
16	AD4	STTGNTASTNCTNTGC
17	AD5	NTCGASTWTSWGTT
18	AD6	WGTGNAGWANCANAGA
LTR::GUS cloning		
19	XbaI-LTR_F	TAGGTACCTGATGATGTCCATCTCATTGAAG
20	XmaI-LTR_R	CCCGGGTGTGGGAATAAACCCTTACCA
SSAP analysis		
21	Csp6I adapter1	CTGGACGATGAGTCCTGAGA
22	Csp6I adapter2	TATCTCAGGACT
23	C00	CTGGACGATGAGTCCTGAGATAC

2.2.4 Southern hybridization

Genomic DNA was extracted from protonemal tissues using the modified cetyltrimethylammonium bromide (CTAB) method (Doyle, 1990). Approximately ten micrograms were digested using *EcoRI* and *HindIII* REs and resolved on a 0.8% agarose gel. Digested DNA was then transferred to Hybond Nylon membrane using neutral transfer protocol (Sambrook *et al.*, 1989). *HPTII* gene specific Hyg (384 bp) probe was amplified from the pCAMBIA-1391Xc-Tnt1 vector using sb_Hyg_F, sb_Hyg_R primer pairs (Table 2.1). The probe was radioactively labeled with $\alpha^{32}\text{P}$ -dATP using Prime-a-gene labeling system (Promega, Madison, USA). Hybridization (over-night) and one stringent with two additional washes were performed at 57°C and 60°C, respectively (Sambrook *et al.*, 1989). Hybridized blots were exposed for 24 hrs on storage phosphor screen for autoradiography. All radiographic images were recorded through phosphor imager (Typhoon, GE, USA) and interpreted as explained in Figure 2.3 A.

2.2.5 Sequence Specific Amplified Polymorphism-PCR (SSAP-PCR)

To further analyze the number of Tnt1 insertions, we utilized SSAP-PCR. Altogether, four different SSAP analyses were carried out with mutant lines. In the beginning, three mutant lines (1, 3 and 6) were subjected to SSAP for Tnt1 insertion events. To determine the stability of Tnt1 insertions in transformed tissue, we tested (i) individual protonemal colonies established from randomly selected protonemal filaments of Tnt1 lines (1 and 3) maintained independently over ten homogenization cycles; (ii) tissue regenerated from single gametophore leaves for 10 cycles and (iii) individual cryopreserved mutant lines (after 12 months cryostorage) by SSAP using 500 ng CTAB-extracted genomic DNA (Doyle 1990) digested with *Csp6I*. This was ligated with a *Csp6I* adapter prepared by annealing the *Csp6I* adapter1 primer and the 5' phosphorylated *Csp6I* adapter2 primer (Syed *et al.*, 2006). The adapter-ligated DNA was pre-amplified with adapter-specific primer C00, and finally, SSAP-PCR was performed with $\gamma^{32}\text{P}$ -dATP end labeled OL13 primer and C00 primer (Waugh *et al.*, 1997; Tam *et al.*, 2005). PCR products were resolved in a 3.5% UREA-PAGE gel along with a 50 bp ladder (B7025; New England Biolabs, UK) and detected by autoradiography.

2.2.6 Thermal Asymmetric Interlaced PCR (TAIL-PCR)

TAIL-PCR was performed to determine the Tnt1 insertion loci in the transgenic lines. Three nested primers (LTR3, LTR4, and LTR7) were designed from the known LTR sequence and used in consecutive reactions together with one of the arbitrary degenerate primers (AD1 to AD6) (Table 2.1). Genomic DNA (50 ng) isolated from each Tnt1 mutant line was used in primary PCR reaction using HiMedia *Taq* polymerase as described by the manufacturer's protocol (HiMedia, India). A four-fold diluted primary PCR product (1 μ L) was used as a template in consecutive (secondary and tertiary) PCR reactions. The tertiary TAIL-PCR products were cloned into pGEM-T Easy vector (Promega, MA, USA) and sequenced. The sites of Tnt1 insertion were identified by BLASTN analysis of the *Physcomitrella* genome (www.cosmoss.org) (Lang *et al.*, 2005).

2.2.7 GC content analysis

In order to assess, if Tnt1 has specificity for GC-rich regions, altogether 72 Tnt1 retrotransposon insertion sites in the moss genome were used for GC content analysis. We have used 26 insertion data from the published report of Vives *et al.*, (2016) in addition to 37 insertions reported in the present study to increase the robustness of this analysis. The nature of the insertion (gene or intergene) and the GC content of insertion sites over a span of 10, 20, 30 and 50 bp were calculated since GC content distribution would vary depending on the fragment size. In an in silico experiment 10, 20, 30 and 50 bp were randomly chosen ($n = 100000$) from the *P. patens* genome, and their GC content was calculated. Further, the nature of the randomly chosen site (gene or intergene) was determined using the *P. patens* genome annotation ver. 3.3 (Lang *et al.*, 2018). In this study, coding regions along with 1000 bp up and downstream were considered as genic regions and the remaining genome as intergenic. Student's t-test was performed between the simulated random insertions and experimentally determined Tnt1 insertions based on the mean of local GC content of genic, intergenic and combined insertions. All the simulations and calculations were performed using NumPy 1.11.2 - a Python scientific computing package (Walt *et al.*, 2011). The data was plotted using Matplotlib 2.0 - a Python 2D plotting library (Hunter 2007).

2.2.8 Tnt1 retrotransposon expression analysis

To assess, if Tnt1 retrotransposon is inducible upon CuCl₂ treatment, seven days old cultures of WT (strain Gransden) and mutants (LTR-GUS line 1 and line 4) of *P. patens* were transferred for 24 hrs to liquid BCDAT medium containing 0, 0.5 and 2.0 μM CuCl₂. For GUS assay, tissue was transferred to a GUS-staining buffer and incubated at 37 °C overnight (Jefferson *et al.*, 1987). Images were obtained using a Leica S8 APO Stereomicroscope (Leica, Wetzlar, Germany). For microtome sectioning, alcohol was serially replaced with xylene and then paraffin wax. Thin (10 μm) sections were taken using a Leica RM2265 Microtome (Leica). Sections were counterstained with Safranin-O to increase the visibility of background tissue and imaged using a Zeiss ApoTome microscope (Zeiss, Oberkochen, Germany).

For qRT-PCR analysis, total RNA was extracted from CuCl₂-treated protonemal tissue using RNAiso Plus (Takara Bio USA Inc., CA, USA). Crude RNA samples were incubated with Ambion® DNase I (Thermo Fisher Scientific, MA, USA) to remove residual genomic DNA. Two micrograms of the DNA-free RNA samples were reverse-transcribed using oligo dT primers and M-MLV reverse transcriptase (Invitrogen, CA, USA). Specific PCR primers (Table 2.1) were designed to detect endogenous β-Actin (Act F, Act R) and *GUS* gene (Gus F, Gus R) transcripts. cDNA was diluted to 1:10 concentration only during β-Actin transcript amplification and relative quantification of transcripts were performed using the Bio-Rad CFX96 Touch Real-Time PCR Detection System (Bio-Rad, CA, USA). Cycling conditions were as: 95 °C for 10 sec; 40 cycles of 95 °C for 5 sec and 60 °C for 30 sec and an additional step for melting curve analysis at 95 °C for 10 sec. SYBR green used for the detection of transcripts through SYBR Premix Ex Taq II (Tli RNaseH Plus) from Takara (Takara Bio USA Inc., USA). Each plate was run with samples including no template control. Relative target gene expression levels were carried out using β-Actin as a reference gene, and fold-change (sample value/ reference value) was calculated based on the $2^{-\Delta\Delta C_t}$ method of Schmittgen and Livak, (2008).

2.2.9 Screening of Tnt1 insertion lines

Moss tissue was homogenized and grown for five days to get homogeneous protonemal filaments and was subjected to hormone assay. Protonemal explants were inoculated on BCDAT medium with and without BAP (1 μM) or NAA (1 μM) and grown for two weeks at 24 °C, under the continuous light before analyzing the phenotype. For gravitropism experiments, 5 days

old protonemal tissue was pre-cultured on BCDAT agar plates that were supplemented with glucose (0.5%) and incubated at 24 °C in a tissue culture incubator under continuous light conditions for 10 days. Post incubation, plates were arranged vertically in the dark for two weeks for scoring the phenotype (Cove and Quatrano, 2006). WT was inoculated next to mutant lines in Petri dishes for all the assays.

2.3 Results

2.3.1 Tobacco Tnt1 is functional in *P. patens*

Because tobacco Tnt1 retrotransposon is a useful mutagenesis tool in many heterologous angiosperm model organisms like *Arabidopsis*, *Medicago*, etc, we aimed to use it to mutagenize the bryophyte model plant *P. patens*. Therefore, we analyzed if *P. patens* has the necessary host factors critical for successful transposition. In our analysis, Met-tRNA_i from all heterologous model organisms, in which Tnt1 has been shown to transpose successfully, was found to have absolute complementarity with PBS of Tnt1 (Figure 2.1). Despite the evolutionary distance between bryophytes and angiosperms, the 3' end of Met-tRNA_i was found to be conserved in *P. patens*, *Sphagnum fallax*, and *Marchantia polymorpha*, but not in algal species (Figure 2.1).

Using *Agrobacterium*-mediated transformation, T-DNA harboring intact Tnt1-94 retroelement and a hygromycin selection cassette (*HPTII*) from the pCAMBIA-1391Xc binary vector was introduced into *P. patens* protonemal filament. These filaments were subjected to medium containing hygromycin (20 mg/ L) for two weeks followed by antibiotic-free relaxation incubation for additional two weeks. Out of 84 lines subjected to second selection on hygromycin medium (20 mg/ L), 75 stable transgenic lines were generated harboring Tnt1 retrotransposon. These lines were confirmed for the presence of Tnt1 retrotransposon fragments (LTR) as well as the *hygromycin (Hyg) phosphotransferase II (HPTII)* gene (Figure 2.2 A). All these mutant lines were cryopreserved and revived when required for further study (Figure 2.2 B-E). Southern hybridization was performed to detect the number of T-DNA insertions carrying Tnt1 retrotransposon. For the Hyg probe, each band indicates an independent T-DNA integration. All the three lines that we analyzed had one band marking a single stable integration of T-DNA containing Tnt1 in the genome (Figure 2.3 B). Since Southern blotting could not resolve the number of Tnt1 insertions reliably, we additionally employed the SSAP-PCR approach, which is more robust and extensively used to detect Tnt1 retrotransposon insertions

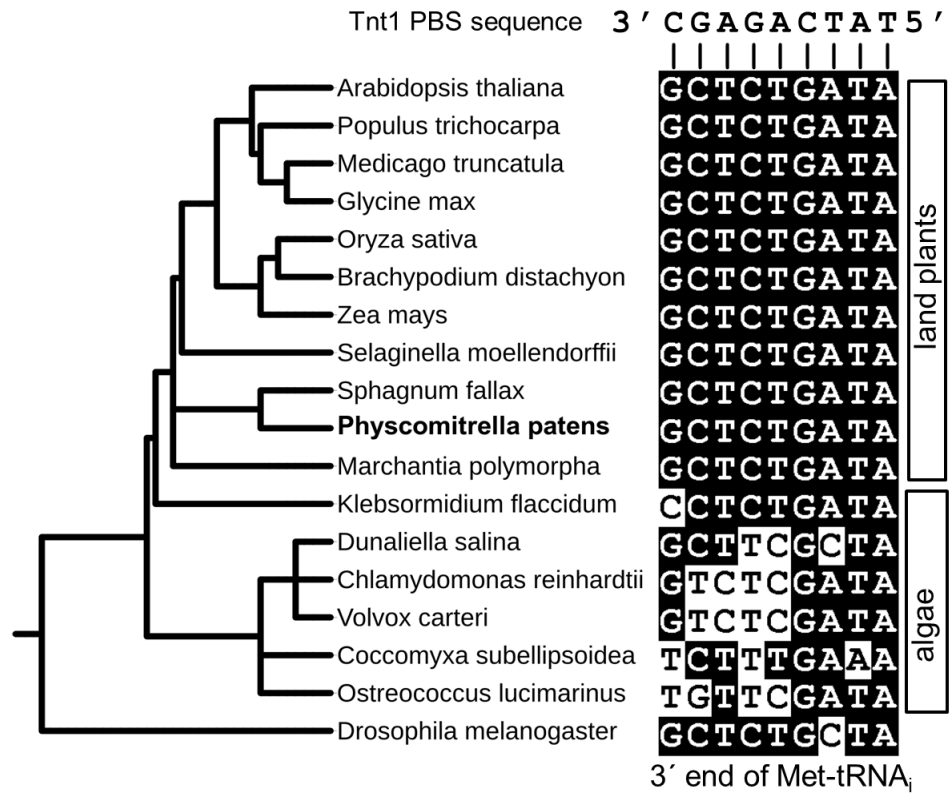


Figure 2.1: *P. patens* has the necessary host factor for Tnt1 transposition activity. Sequence alignment of 3' end Met-tRNA_i gene from representative organisms of Viridiplantae and their degree of sequence complementarity with 9 bp from the 3' end of Tnt1 PBS 5' TGGTATCAGAGC 3'. *Drosophila melanogaster* sequence was used as an outgroup.

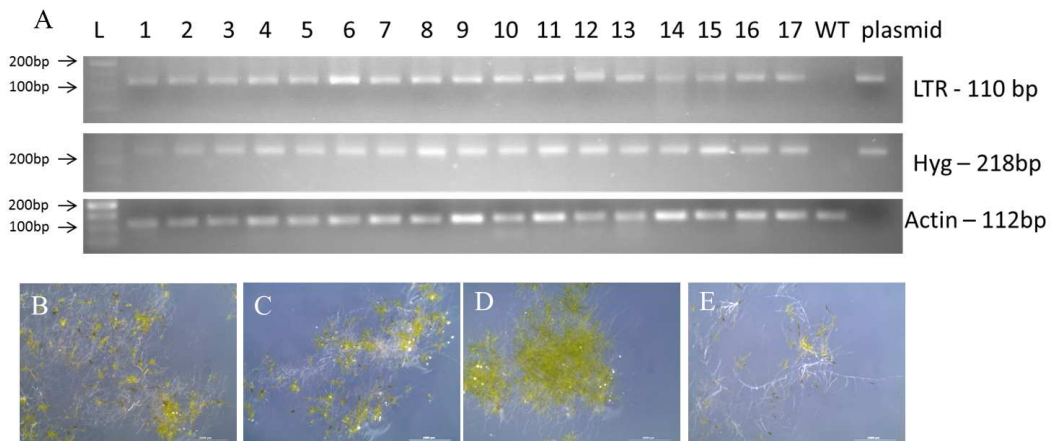


Figure 2.2: PCR screening of *P. patens* lines harboring pCAMBIA-1391Xc-Tnt1 and revival of cryo-stored mutant lines. (A) Transgenic lines screened for the presence of LTR sequence (top) and *HPTII* gene (middle). *Actin* gene (bottom) was used as genomic DNA control. Cryopreserved moss lines re-growing on BCDAT medium 5 days after thawing; WT (B), and Tnt1 insertional lines 5, 9, 26 (C, D, and E). (Scale bar size: 1mm).

(Waugh *et al.*, 1997; Courtial *et al.*, 2001; Tam *et al.*, 2005; Vives *et al.*, 2016). Line 1 and 3 showed the characteristic 388 bp and 426 bp bands amplified indicating the proper T-DNA integration (Figure 2.3 C). Line 8 had a rare incomplete T-DNA integration, where only the 388 bp band was observed (Figure 2.3 C). Apart from the low-intensity nonspecific bands, two insertions for line 1, and five insertions for line 3 were observed indicating that tobacco Tnt1 has transposed in the moss genome from the initial T-DNA insertion. Line 8, which had an incomplete T-DNA integration, did not show any specific Tnt1 insertion (Figure 2.3 C).

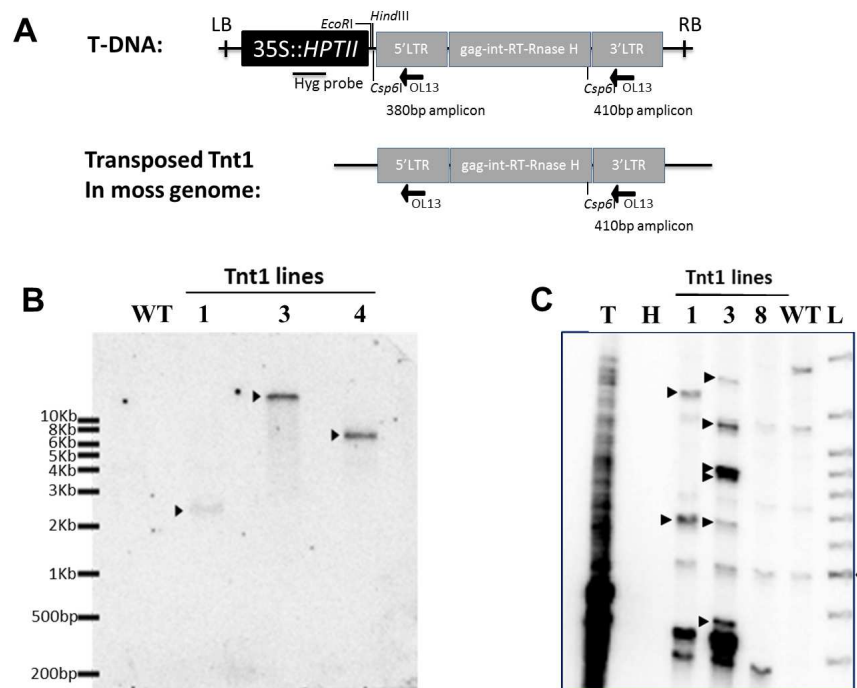


Figure 2.3: Detection of Tnt1 transposition activity in mutant lines of moss generated by *Agrobacterium*-mediated transformation. (A) Schematic diagram of pCAMBIA-1391Xc-Tnt1 insertion cassette and a transposed Tnt1 element. Mutant moss genomic DNA digested with *HindIII* and *EcoRI* and probed with Hyg probe produced one variable size band per T-DNA insertion, according to the insertion locus in the genome (LB -left border; RB - right border). For SSAP analysis, mutant moss genome was digested by the *Csp6I* enzyme, and Tnt1 LTR specific primer (OL13) was used. OL13 and *Csp6I* adapter primers amplified 410 bp and 388 bp bands from T-DNA-linked Tnt1 and only 410 bp band from a transposed Tnt1. (B) Southern blot analysis of wild-type (WT) and Tnt1 lines 1, 3 and 4 using a Hyg probe (arrowheads denote the bands). (C) SSAP analysis of WT and Tnt1 lines 1, 3 and 8. *Nicotiana benthamiana* (T), water (H) and 50 bp ladder (L) were used as positive control, negative control and DNA ladder, respectively. Arrowheads denoted unique Tnt1 insertions and the arrow indicated 500 bp band.

2.3.2 Tnt1 preferentially transposes into genes and GC-rich regions in *P. patens* genome

To identify the Tnt1 transposed loci in moss genome, TAIL-PCR analysis was performed on stable T-DNA insertion lines containing a Tnt1 retrotransposon. Out of 37 insertions detected, 26 were found to be in the genic regions [including promoter (1), exon (11), and intron (12)], which were dispersed among 17 chromosomes of *P. patens* (Figure 2.4) (Table 2.2). Though the moss genome has only 22.74% genic region, we found 70.2% of Tnt1 insertions in gene-rich regions indicating preferential transposition. The total number of insertions per individual line varied from 1 to 9. In Tnt1 line 23, all the 9 insertions were found to be dispersed over 8 chromosomes indicating a lack of hot spot (Figure 2.4) (Table 2.2).

To understand, if there is a GC content bias in Tnt1 transposition events, we compared the local GC content of Tnt1 insertion loci with the simulated random insertions. In all fragment sizes (10, 20, 30 and 50 bp) that were analyzed, mean GC content was significantly different between combined random insertions and combined Tnt1 insertions (Figure 2.5) suggesting the GC bias. In all simulations, the mean GC content of genic regions of random insertions and Tnt1 insertions were also significantly different. Intergenic insertions were further compared to distinguish GC preference from the gene preference. We found a significant difference in the mean GC content of intergenic regions between random insertions and Tnt1 insertions (Figure 2.5) indicating the preference for GC-rich regions. From this analysis, a critical GC value (GC*) of 44-57% was determined as the cutoff (Figure 2.6). If Tnt1 transposition site is chosen only based on local GC content, then any insertion below GC* would more likely be intergenic (I) than genic (G) and vice versa. Tnt1 insertion data indeed showed a considerable increase in intergenic insertions, whose local GC content value was below GC*. However, in both categories (above and below GC*), the number of genic insertions were higher than intergenic insertions. This suggested that high GC content was not the sole criteria in Tnt1 insertion site preference, but it might act parallel to other factors resulting in higher selectivity for genic regions.

Table 2.2: List of primers used in this study.

Line No.	Chromosome No.	Tnt1 insertion	Insertion type	COSMOSS ID
1	1	28983778	exon	Pp3c1_41480V3.2
1	8	17924095	5' UTR	Pp3c8_25561V3.1
1	25	5097100	exon	Pp3c25_7810V3.3
2	3	5850479	exon	Pp3c3_8390V3.3
Continued on next page				

Table 2.2 – continued from previous page

Line No.	Chromosome No.	Tnt1 insertion	Insertion type	COSMOSS ID
2	4	19725463	exon	Pp3c4_26051
2	12	7020224	5' UTR	Pp3c12_10290
2	14	8397712	5' UTR	Pp3c14_13110V3.2
2	21	13098133	intergenic	Pp3c21_20150V3.2
2	23	5312508	5' UTR	Pp3c23_7920V3.5
3	12	12020704	intergenic	Pp3c12_18530V3.1
3	18	5999016	exon	Pp3c18_8530V3.1
3	19	1060700	intergenic	Pp3c19_2080V3.2
7	7	108637	exon	Pp3c7_120V3.3
7	8	11354571	intergenic	
7	9	15510110	intergenic	
7	9	15556193	5' UTR	Pp3c9_22930V3.2
7	18	12651339	intron	Pp3c18_17630V3.3
7	18	12651388	exon	Pp3c18_17630V3.3
17	5	6482514	5' UTR	Pp3c5_8770V3.2
17	7	1253013	3' UTR	Pp3c7_1990V3.2
18	5	9661976	exon	Pp3c5_13510V3.2
22	15	2909938	exon	Pp3c15_4650V3.3
22	17	1881395	intron	Pp3c17_2440V3.2
22	17	9774735	intergenic	Pp3c17_14100V3.2
23	1	9303842	intergenic	Pp3c1_12730V3.2
23	1	6546128	exon	Pp3c1_9020V3.4
23	3	978787	intergenic	Pp3c3_1540V3.2
23	4	1305096	intron	Pp3c4_2150V3.1
23	8	7308388	exon	Pp3c8_11260V3.2
23	13	5730472	intergenic	Pp3c13_8600V3.2
23	19	5775983	intergenic	Pp3c19_9410V3.1
23	23	12361810	Intron	Pp3c23_18780V3.2
23	25	3901634	3' UTR	Pp3c25_5951V3.1
41	1	428810	5' UTR	Pp3c1_670
48	3	1870302	promoter	Pp3c3_3180
48	4	6997215	intergenic	Pp3c4_9690

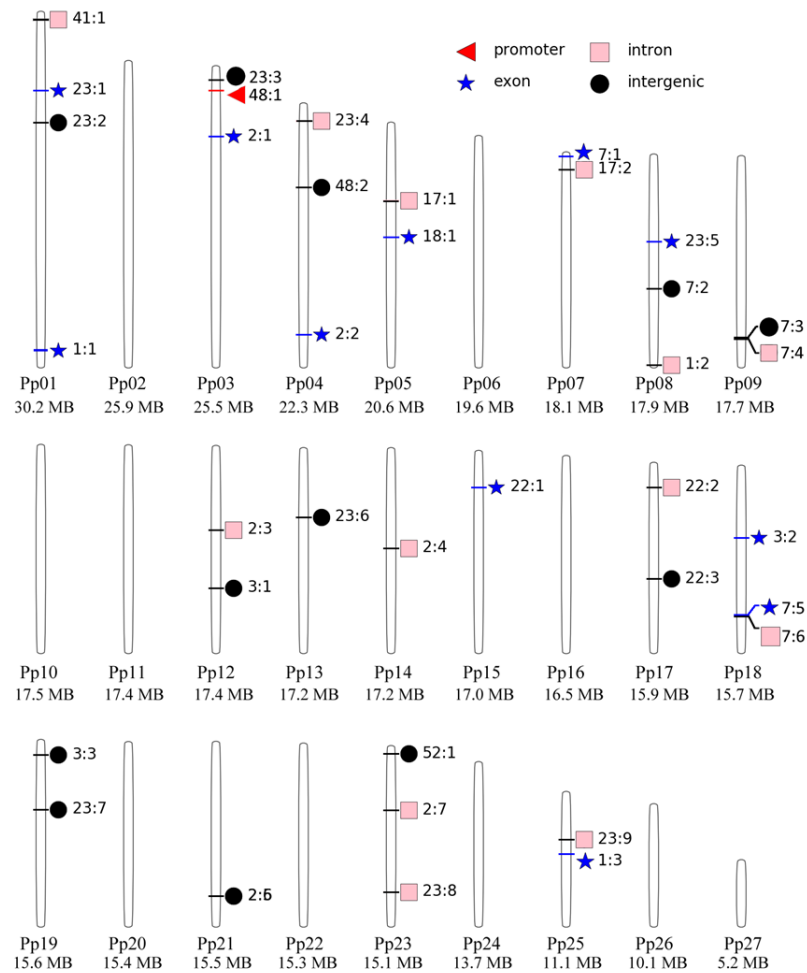


Figure 2.4: Tnt1 retrotransposon insertions in *P. patens* genome determined by TAIL-PCR analysis. Chromosomes are labeled as Pp01 to Pp27, and the insertion coordinates are marked schematically on the chromosomes. Each insertion is labeled as line number: insertion number (23:1 is the 23rd line: first insertion). Red triangle - promoter; blue star - exon; pink square - intron; black circle - intergenic.

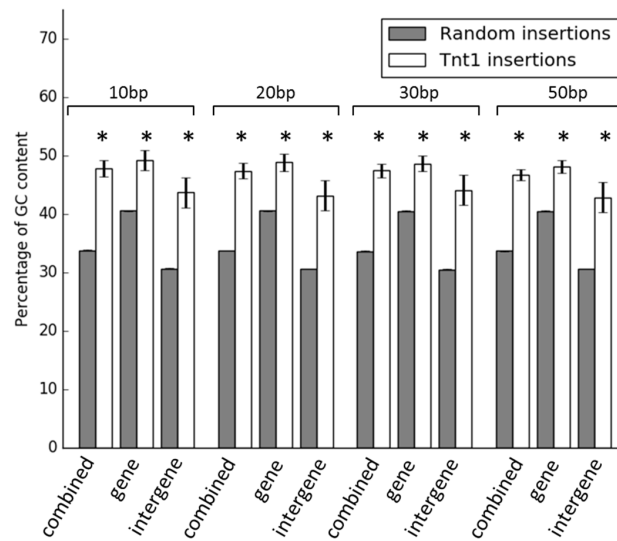


Figure 2.5: Tnt1 transposition sites are biased towards the regions of high local GC content in *P. patens* genome. Grey and white bars represented mean local GC content of simulated random insertions and experimentally determined Tnt1 insertions. Student's t-test was performed to check for the statistically significant difference between the means of random insertions and Tnt1 insertions in different categories combined (genic + intergenic regions), genic regions and intergenic regions. In all 10, 20, 30 and 50 bp sampling fragment sizes, local GC content of combined, genic and intergenic regions was significantly different between simulated insertions and Tnt1 insertions. Error bars indicate SE. Asterisks (*) denotes p -value < 0.001.

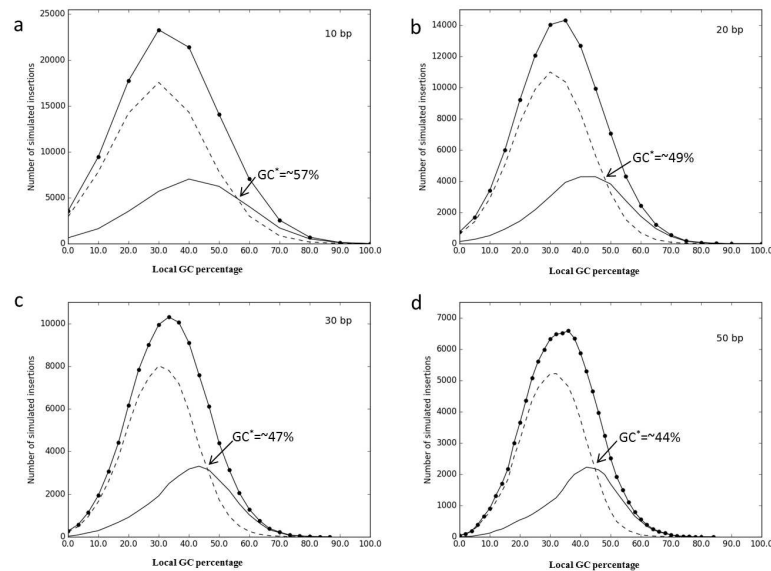


Figure 2.6: Estimation of critical GC value (GC*) of *P. patens* genome. Distribution of local GC content of 10, 20, 30 and 50 bp sequences chosen randomly from moss genome was plotted and labelled accordingly (n = 100000). The curves representing genic and intergenic regions intersect at a critical GC value (GC*).

2.3.3 Tnt1 promoter expression is tissue-specific and inducible

To check the expression pattern of Tnt1, we cloned the entire LTR sequence (610 bp) upstream of the *GUS* reporter gene and generated LTR::*GUS* lines of in *P. patens*. In normal growth conditions, we rarely detect any *GUS* activity in protonemal filaments. Interestingly, gametophores and buds showed expression at apical regions and lateral branches (Figure 2.7 A; ii-iv). This basal tissue-specific expression pattern of LTR promoter was further confirmed by histological studies and *GUS* expression was found to be localized to gametophore lateral branch apex only (Figure 2.7 B). The entire gametophore was treated with 0.5 and 2 μM CuCl_2 to test if the LTR promoter is inducible. The intensity of *GUS* expression increased in apex and lateral branches of the gametophore upon CuCl_2 treatment (Figure 2.7 A; iii-viii) suggesting the inducible nature of Tnt1 promoter. Further, we have analyzed the abundance of *GUS* transcripts by qRT-PCR in uninduced and CuCl_2 induced gametophores of two independent LTR::*GUS* lines (Figure 2.7 C). These lines showed 2.7 and 1.4-fold increase in *GUS* transcript levels, respectively, upon 0.5 μM CuCl_2 induction while both lines showed 2.1 and 0.9-fold change upon induction with 2 μM CuCl_2 (Figure 2.7 C).

2.3.4 Isolation of *P. patens* mutants impaired in gametophyte development

Altogether, 75 mutants were developed and subjected to various screens to identify mutations in the broad gametophyte developmental pathways. Our analyses revealed a *short-leaf* mutant (Tnt1 line 5), which produced shorter leaves compared to the WT (Figure 2.8 A). When all these lines were induced for gametogenesis and sporophyte formation, Tnt1 line 27 formed multiple organs at the gametophore apex (Figure 2.8 C) whereas a single sporophyte was developed in the WT (Figure 2.8 B). These organs appeared to be either unfertilized archegonia that continued to grow mimicking immature sporophyte or they were just poorly developed sporophytes. Various phytohormone assays were performed for the phenotypic characterization. We observed that Tnt1 line 9 showed partial recovery of normal gametophore development even in the presence of 1.0 μM BAP (Figure 2.8 D-G). Tnt1 line 26 showed excessive rhizoid formation and defective gametophore development on BCD minimal media (Figure 2.8 H and I). In the presence of either exogenous 1 μM NAA (Figure 2.8 J, K) or 0.5 mM ammonium tartrate (Figure 2.8 L and M), both WT and Tnt1 line 26 were indistinguishable. Gravitropism analysis revealed that the Tnt1 line 56 protonemal filaments were insensitive to gravity in comparison with WT (Figure 2.8 N and O). Overall, we could isolate five novel phenotypes related to the

gametophyte development out of 75 mutants of *P. patens* identified in this study.

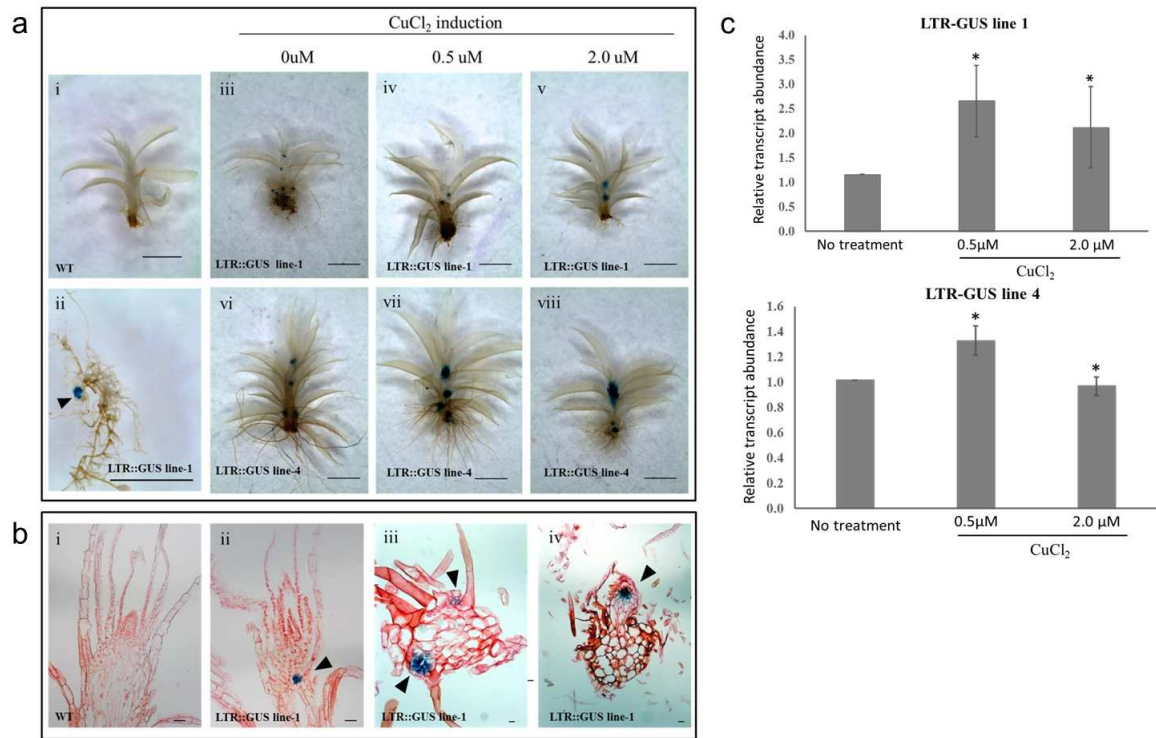


Figure 2.7: Tissue-specific inducible expression pattern of tobacco Tnt1 in *P. patens*.(A) LTR::GUS shows basal expression in bud, gametophore and branch apical cells. Compared to WT (i), LTR promoter showing *GUS* expression pattern of in bud apical cells (arrowhead) (ii) and apex and branching points of gametophore (iii and vi). LTR::GUS line 1 and LTR::GUS line 4 basal LTR promoter expression (iii and vi) and tissue-specific induction using 0.5 μM CuCl₂ (iv and vii) and 2.0 μM CuCl₂ (v and viii) (scale bar = 1 mm). (B) Compared to WT (i) histological sections showing basal *GUS* expression (blue) in LTR::GUS line 1 gametophore stem tangential section (ii) and cross-section at the base of gametophore (iii and iv) (arrowheads denotes the *GUS* expression in lateral branches). All the sections were counterstained with Safranin-O (scale bar = 30 μm). (C) Relative transcript abundance of *GUS* transcripts in LTR-GUS lines (*P. patens*) upon CuCl₂ induction. Asterisk indicates significant level at $p < 0.05$.

2.3.5 Viability of Tnt1 as a mutagenesis tool for *P. patens*

To demonstrate the viability of Tnt1 as a mutagenesis tool, we checked the stability of Tnt1 insertions through SSAP-PCR. Tnt1 transposition activity was analyzed using SSAP-PCR at the protonemal growth stage, gametophore apex stage, and with cryopreserved tissues. The number of insertions for Tnt1 did not change for both line 1 and 3 when we assessed if the protonemal subculturing process was causing any Tnt1 induction (Figure 2.9 A and D). Again,

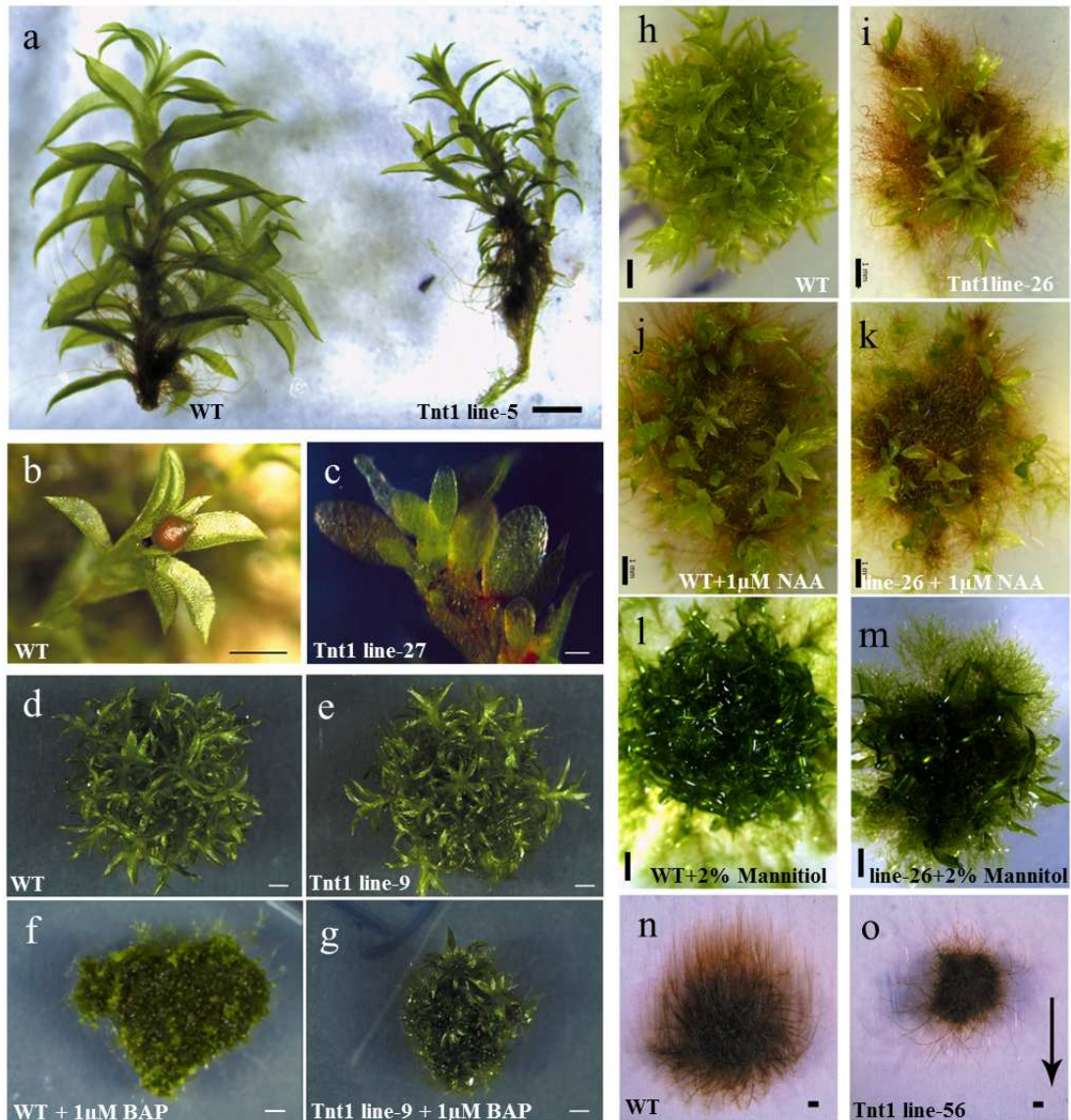


Figure 2.8: Novel phenotypes isolated from the Tnt1 insertional mutant population. (A) Tnt1 line 5 (right) exhibits short-leaf phenotype compared to WT (left). WT (B) gametophore apex bearing mature single sporophyte and Tnt1 line 27 mutant (C) gametophore producing multiple immature sporophytes. (D-G) Tnt1 line 9 shows cytokinin resistance phenotype. WT (D) and Tnt1 line 9 (E) grown without exogenous BAP. WT (F) showing stunted bud development and Tnt1 line 9 mutant (G) showing partial recovery of gametophores when grown in the presence of 1.0 μ M BAP. (H-M) Tnt1 line 26 had conditional rhizoid overproduction phenotype. WT (H-J) and Tnt1 line 26 (I, K, and M) growth in BCD media (H, I), BCD supplemented with 1.0 μ M (J and K) or 0.5 mM ammonium tartrate (L and M). (N and O) Tnt1 line 56 has failed to align to the gravity vector. WT (N) caulonemal filaments grown upwards whereas Tnt1 line 56 mutant (O) caulonemal filaments grown randomly. Arrow indicates the gravity vector (scale bar size is 1 mm).

the number of Tnt1 insertions in line 1 and line 3 remained unchanged when we assessed, if the tissue-specific activity of LTR promoter in gametophore apex correlated to a high mutation load (Figure 2.9 C and E). Similarly, there were no changes in insertional patterns when we revived and tested the 12-months old cryopreserved tissue of moss Tnt1 line 1 and 3 (Figure 2.9 B and D).

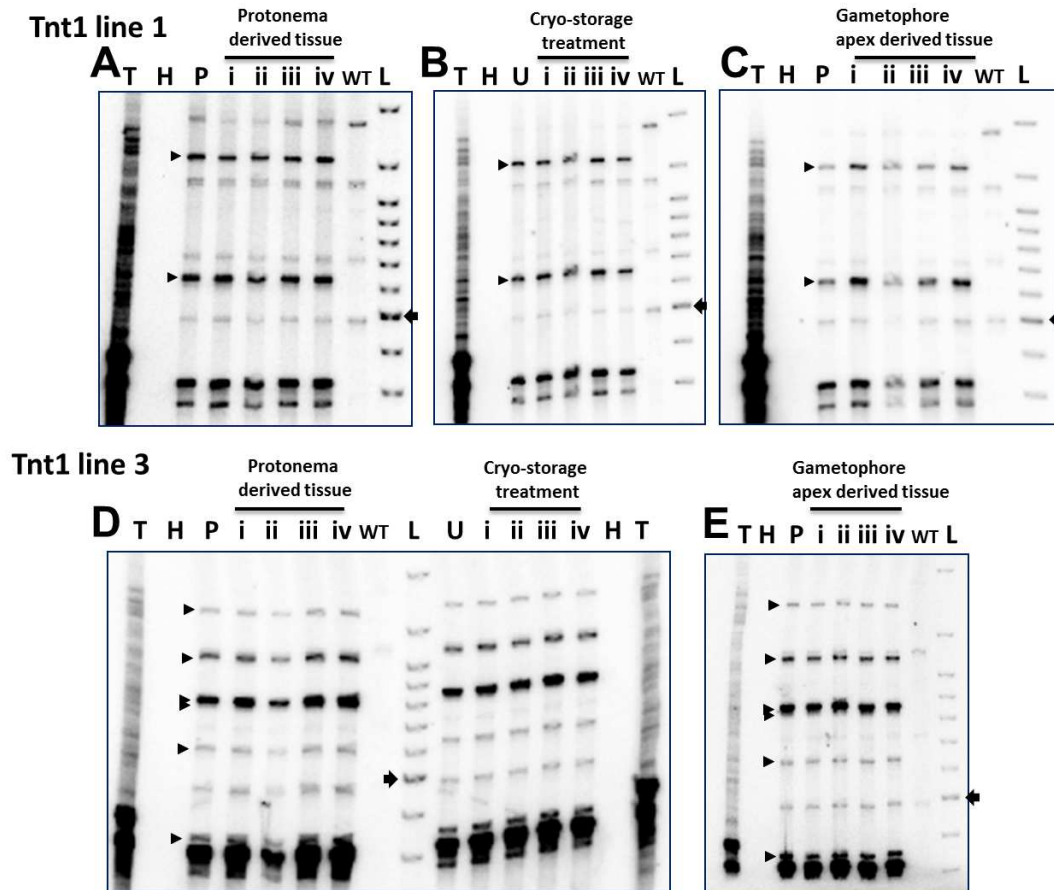


Figure 2.9: SSAP analysis to assess the stability of Tnt1 insertional mutants. SSAP analysis of wild-type (WT) and Tnt1 lines 1 (A to C) and 3 (D and E). Routinely maintained lines (P) or untreated lines (U) of Tnt1 line 1 and 3 were subjected to SSAP analysis along with four biological replicates (i-iv) of clonally propagated lines that were derived from a protonemal plate (A and D). Similarly, tissues revived from a cryo-stock (B and D) or gametophore apex derived tissues (C and E) were analyzed for mutant stability. In all the experiments *Nicotiana benthamiana* (T), water (H) and 50 bp ladder (L) were used as positive control, negative control and DNA ladder, respectively. Arrowheads denoted unique Tnt1 insertions, and arrow marked 500 bp band.

2.4 Discussion

The tobacco Tnt1 retrotransposon is functional in several heterologous angiosperm species (Lucas *et al.*, 1995; d'Erfurth *et al.*, 2003; Cui *et al.*, 2013; Duangpan *et al.*, 2013). During the Tnt1 transposition process, the 3' end of host Met-tRNA_i binds to PBS of Tnt1 and acts as a primer for initial cDNA synthesis (Feuerbach *et al.*, 1997). Considering the evolutionary distance between tobacco and moss, we were interested to determine, if *P. patens* has the necessary host factor for Tnt1 transposition. We noted that the Met-tRNA_i 3' end sequence from all heterologous model organisms, where Tnt1 transposes successfully, exhibited absolute complementarity with PBS, suggesting that Met-tRNA_i is a critical host factor. Further, we also observed that all embryophytes (land plants) including *P. patens* and representative organisms like *Marchantia polymorpha* and *Selaginella moellendorffii* shared this conservation of the 3' end Met-tRNA_i sequence (Figure 2.1). Though basal algal species had multiple mismatches that clearly distinguished algae and embryophytes, only a single mutation was observed in *Klebsoridium nitens* (a charophycean algae), which is consistent with the fact that charophycean algae are sister group to land plants (Hori *et al.*, 2014). Our Met-tRNA_i analysis have suggested that Tnt1 retrotransposon could be potentially used for mutagenesis in all embryophytes.

Though multiple T-DNA integrations per mutant line are possible in *P. patens*, we found only single insertion in the mutant lines as tested by Southern hybridization (Figure 2.3 B). To check the number of Tnt1 insertions, we used SSAP-PCR that indicated five independent transposition events per line (Figure 2.3 C). However, line 8 showed an anomalous result with only the 5'-LTR detectable, and no Tnt1 transposition events (Figure 2.3 C). This indicated the possibility of a rare incomplete T-DNA integration event comprising the left T-DNA border, *HPTII* gene, and 5' LTR but with neither the 3' LTR nor right T-DNA border remaining in the moss genome. Tnt1 has been demonstrated to preferentially transpose into gene-rich regions in the angiosperm model organisms (Lucas *et al.*, 1995; d'Erfurth *et al.*, 2003). Consistent with this and the recent report of Vives *et al.*, (2016), we noted that approximately 70% Tnt1 insertions were in genic regions of *P. patens* genome (Figure 2.4) (Table 2.2). In addition, Tnt1 insertions had a preference for regions of high local GC content independent of gene preference (Figure 2.6). Though high GC preference does not qualify as a sole criterion for choosing transposition site, it may contribute to increasing the chance of transposition into gene-rich regions acting in conjunction with other factors.

The 5' - LTR sequence acts as a promoter that drives the expression of Tnt1 to initiate the first step of transposition process (Grandbastien *et al.*, 1989). Using a *GUS* reporter gene cloned downstream of LTR promoter and the first 25 amino acid coding sequence of Tnt1 (Pouteau *et al.*, 1991), it has been shown that Tnt1 promoter is induced by plant defense signaling and abiotic stress such as CuCl₂ in sporophytic tissues (Pouteau *et al.*, 1994; Mhiri *et al.*, 1997). This response is mainly mediated by the BII sequence repeats present in the U3 region of the LTR promoter (Vernhettes *et al.*, 1997). Hence, we used entire LTR sequence from Tnt1-94 retroelement to characterize its promoter activity. Though all the properties of Tnt1 transposition in *P. patens* were reminiscent of studies on angiosperms, LTR promoter activity was distinct. Surprisingly, in gametophyte of *P. patens*, we observed a basal low expression of LTR::GUS in gametophore apical cell and lateral branch apical cells (Figure 2.7 A; iii-vi) This tissue-specific expression pattern of LTR mimics the previously reported *PpLFY1* and *PpLFY2* expression pattern (Tanahashi *et al.*, 2005) in gametophores of *P. patens*. As previously reported in tobacco (Mhiri *et al.*, 1997), the LTR::GUS promoter was also inducible in *P. patens* by abiotic factors such as CuCl₂. We noticed that the increased *GUS* transcript levels at 0.5 μM and the inhibitory effect at high concentration of CuCl₂ (2 μM) was consistent with the previous studies in tobacco (Vernhettes *et al.*, 1997) (Figure 2.7 C). Though Vives *et al.*, (2016) have reported the expression of Tnt1 in protonemal filaments, we rarely observed *GUS* expression in protonemal filaments in our study. This could be either because of the low expression than the detectable limit or protonemal expression could be regulated by cis-regulatory elements present downstream of LTR promoter.

During this study, five novel mutants were identified out of 75 *P. patens* lines screened that have shown deviation from the WT in different gametophyte developmental pathways (Figure 2.8). Though four out of five mutants exhibited novel phenotypes, agravitropic mutants like that of our Tnt1 line 56 have been earlier isolated from *P. patens* (Jenkins *et al.*, 1986) and *Ceratodon purpureus* (Cove and Quatrano 2006).

Vives *et al.*, (2016) have modified the retrotransposon and developed a two-component system in a mini-Tnt1 retroelement that can transpose only when the required proteins for Tnt1 transposition were supplemented by a separate vector. As we have used an intact Tnt1 retrotransposon for mutagenesis, high-frequency phenotypic deviation that were observed in our mutant population prompted us to study the stability and the number of mutagenic transpositions. We assessed the stability of Tnt1 insertional mutants and found that the Tnt1 insertional pattern did not change over normal subculturing of protonema, gametophore apex

derived tissues where LTR promoter is active, and finally tissues stored via cryopreservation. These results have suggested that Tnt1 transposition is a rare event and could be under post-transcriptional regulation through sRNA mediated pathway like other endogenous moss LTR retrotransposons (Coruh *et al.*, 2015). Even though retrotransposon insertions are rare events, a continuous regular subculture of even WT lines can result in genetic and physiological instability (Kartha and Engelmann, 1994). Hence, we took advantage of the cryopreservation method to avoid undesirable and rare transposition events, since cryo-conditions would likely arrest all metabolic activities. Using Southern blotting and SSAP-PCR, we have shown that the Tnt1 insertions are stable. Together, this demonstrate that *Agrobacterium*-mediated Tnt1 mutagenesis is a promising tool to generate *P. patens* mutant population and could be explored in other non-seed land plants.

In summary, we demonstrate a mutagenesis tool for *P. patens* using an intact tobacco Tnt1 retrotransposon for forward genetic studies. This protocol has an added advantage since we used haploid protonemal filaments for *Agrobacterium*-mediated transformation. Unlike the protoplast transformation used in the previous report, our approach should maintain haploidy throughout the mutagenesis process. Based on the absolute conservation of Met-tRNA_i across all angiosperms, we also propose that Tnt1 could be a common mutagen for all embryophytes. While all major characteristics of Tnt1 retrotransposon appeared to be quite similar between angiosperm and moss, the basal tissue-specific expression pattern of the Tnt1 promoter (LTR) detected in moss was a striking observation. Despite the fact that the moss mutants exhibited on average 4 insertions, we could eventually isolate 5 interesting phenotypes from a total population of 75 individuals. Also, through SSAP analysis, we showed that the high-frequency phenotypes obtained in this study could be because of the high gene preference of Tnt1 transposition in combination with the haploid nature of protonemal filaments of moss. Together, these data suggests that our Tnt1 insertional mutagenesis protocol is a viable approach to perform forward genetics screens in *P. patens*.

Part of this work has been submitted for research publication:

Mohanasundaram B, Rajmane VB, Jogdand SV, Bhide AJ and Banerjee AK, (2018). Analysis of Tnt1 transposition activity in moss (*Physcomitrella patens*) and isolation of mutants with impaired gametophyte development. (**Under revision in Molecular Genetics and Genomics**).

**3 Characterization of Tnt1 insertional *P. patens* mutant line,
short-leaf (shlf), defective in leaf development**

3.1 Introduction

Using our Tnt1 mutagenesis protocol (Mohanasundaram *et al.*, 2018, Under review), we successfully established the Tnt1 insertional moss mutant population in our lab at IISER Pune. Our forward genetics screen yielded several mutants with novel phenotypes. In this chapter, we describe our efforts to phenotypically and genetically characterize one of the Tnt1 insertional mutant termed as *shlf*. Leaf length and various other phenotypic features of the *shlf* mutant were analyzed. Whole genome sequencing (WGS) and phenotype rescue analyses were undertaken to determine the causal gene of this mutant in the present study.

3.1.1 Moss leaf development

Leaf-like organs (phyllids) arise on moss gametophores in a spiral phyllotaxy. The life cycle and body plan of *P. patens* is discussed in detail in section 1.5. The gametophore apical cell divides to form a derivative cell, which further divided to form a leaf apical cell (Kofuji and Hasebe, 2014). A single leaf apical cell gives rise to a leaf primordium. By live microscopy and sector analysis of leaves using X-ray irradiation, the formation of leaf primordium through a series of asymmetric divisions of the leaf apical cell is demonstrated (Harrison *et al.*, 2009). With the first asymmetric division, medial-lateral and proximo-distal polarity are established in the leaf primordium. Number of asymmetric cell divisions (ACD) that form a leaf primordium has a positive correlation with final size of the leaf (Harrison *et al.*, 2009). An acropetal wave of asymmetric anticlinal divisions in the daughter cells increases the cell number along with the medial-lateral axis of the primordium. Further, transverse and longitudinal divisions coupled with elongation within the sectors decide the final shape of the leaf. Harrison *et al.*, (2009) have elaborately shown that the time of exit from cell division cycle varies across the leaf length. The tip cells mature faster than the middle section of the leaf leading to the formation of oblanceolate leaf (Harrison *et al.*, 2009). The proximal cells of a mature leaf are more elongated than the distal cells. The role of external environment on these cell division patterns and the regulation of final leaf shape are discussed in the following section.

3.1.2 Factors influencing leaf shape and size

Moss leaf shape and size are sensitive to environmental conditions and hormonal cues. As observed in vascular plants, moss gametophores etiolate upon sensing darkness (Bao and Ya-

mamoto, 2015). The leaves are being reduced to small scales, and internodal distance is increased in dark-grown etiolated gametophores. Leaves get wider when gametophores are grown on a nitrogen limiting media such as BCD. This phenotype becomes severe upon the cytokinin treatment (Barker, 2011). Auxin has been shown to play a major role in controlling the leaf shape and size. Treatment of *P. patens* gametophores with synthetic auxin analogues like 10 μM 2,4-Dichlorophenoxyacetic acid (2,4,-D) drastically reduce the overall leaf size (Bennett *et al.*, 2014). Treating *P. patens* gametophores with polar auxin transport (PAT) inhibitor such as 5 μM 1-N-Naphthylphthalamic acid (NPA) along with a mild dose of synthetic auxin (100 nM 1-Naphthaleneacetic acid (NAA) produced the most severe reduction in leaf size. As extensively studied and demonstrated in angiosperms, auxin efflux carriers proteins (PIN) are found to be polarly localized in the plasma membranes of moss leaf blade cells (Bennett *et al.*, 2014). These results suggest that PAT could be active in leaves and high auxin accumulation could have caused the leaf size reduction in our *shlf* gametophores.

3.1.3 Auxin metabolism, signaling and transport in *P. patens*

As auxin has a profound influence over the moss leaf development, knowledge over the level of conservation of auxin signaling in moss compared to angiosperm is pre-requisite to understand moss leaf development. Auxin biosynthesis in *P. patens* follows the major pathway of flowering plants, in which tryptophan is converted into indole acetic acid (IAA) through *TAA-1* related enzymes (TARs) and *YUCCA*-related enzymes (Stepanova *et al.*, 2008, Tao *et al.*, 2008, Thelander *et al.*, 2017). *P. patens* genome is found to have six each *TAR* and *YUCCA* paralogs (Rensing *et al.*, 2008). As observed in *Arabidopsis*, the *SHORT INTERNODES/STYLISH* (*SHI/STY*) transcription factors enhance auxin biosynthesis in *P. patens* (Eklund *et al.*, 2010; Landberg *et al.*, 2013). Further, in *P. patens*, IAA is inactivated through amide or glucose conjugation by *GRETCHEN HAGEN3* (*GH3*) or UDP-glucose transferase (Ester Sztain *et al.*, 1999; Ludwig-Müller *et al.*, 2009). IAA is also degraded in moss through oxidization by *oxIAA* (Drábková *et al.*, 2015). The nuclear auxin pathway, which has been extensively studied in angiosperms (Wang and Estelle, 2014; Weijers and Wagner, 2016) is also conserved in *P. patens* (Paponov *et al.*, 2009; Prigge *et al.*, 2010; Causier *et al.*, 2012). The soybean *GH3* promoter has been shown as a better auxin-responsive promoter than the synthetic DR5 promoter in *P. patens* (Fujita and Hasebe, 2009). In flowering plants, PAT controls the shoot branching (Gälweiler *et al.*, 1998; Crawford *et al.*, 2010), a phenomenon is known as the apical dominance. Though decapitation assays demonstrate the presence of apical dominance in moss gametophores, ra-

dioactive auxin feeding assays could not show any basipetal transport of auxin (Fujita *et al.*, 2008). However, *pinA pinB* double mutants of *P. patens* are affected in apical dominance or phyllotaxy (Bennett *et al.*, 2014). A detailed study by Coudert *et al.*, (2015) has proposed an alternate hypothesis that auxin diffuses through plasmodesmata in the moss gametophore. Further studies will provide critical insights for better understanding of the auxin transport in moss.

In our forward genetic screen on the Tnt1 insertional mutant population of *P. patens*, we isolated a novel mutant that produces two times shorter leaves than WT leaves. Earlier it was shown that knockdown lines of class III *HD-ZIP* gene in *P. patens* resulted in the development of miniature leaves (Yip *et al.*, 2016). These leaves however, had highly misoriented cell organization and extremely serrated boundaries. In our observation, *shlf* leaves had proper cell organization and leaf margins. We speculate that *shlf* phenotype could be caused by a gene, which is yet to be characterized in *P. patens*. Based on our literature survey, it is plausible that high auxin accumulation could have caused reduction of leaf size in *shlf* gametophores. To understand short-leaf mutant phenotypically and genetically, the following three approaches were taken in this study.

- Phenotypic characterization of *short-leaf* mutants under various environmental conditions.
- Whole genome sequencing and determination of causal gene(s) for the *short-leaf* mutant.
- Understanding the phylogeny and mechanistic link of the causal gene(s) to short-leaf phenotype.

3.2 Materials and methods

3.2.1 Plant culture and maintenance

Culturing of *Physcomitrella patens* ecotype ‘Gransden’ was performed as described in the section 2.2.1 of this thesis. Takaragaike-1 (Tak-1; Male) and Takaragaike-2 (Tak-2; Female) strains of *Marchantia polymorpha* were grown axenically at 24 °C in half strength Gamborg’s B5 media (Gamborg *et al.*, 1968). Cultures were propagated by means of asexual reproduction via gemma. *Marchantia polymorpha* strains were a kind gift from Prof. Takayuki Kohchi (Kyoto University, Japan).

3.2.2 Phenotypic analysis of *shlf* mutant

Seven-day-old protonemal filaments were inoculated on BCDAT medium and incubated under the standard growth conditions for three weeks (Cove *et al.*, 2009). From the gametophores, ninth leaf from the top (P9) was extracted and imaged. For toluidine blue staining of the cell wall, leaves were cleared using 2M NaOH and then stained in 0.1% toluidine blue solution. Images were taken using Lecia S8 APO (Leica Microsystems, Wetzlar, Germany). Using ImageJ software, various phenotypic measures of the leaf (Schneider *et al.*, 2012) were recorded. The position of the side branch was noted from gametophores of three-week-old colonies and plotted using the Matplotlib package (Hunter, 2007). For the etiolation assay, seven-day-old protonema was inoculated on BCDAT medium supplemented with 0.5% glucose and grown under the standard conditions for two weeks (Cove *et al.*, 2009). Plates were transferred to a dark chamber and incubated vertically (<http://www.physcobase.com>). At regular intervals, the gametophores were scored for etiolation frequency.

3.2.3 Cloning and plant transformation

To develop GH3::GUS-pTFH15.3 construct, the GH3::GUS fragment was amplified from pUC19-GH3::GUS (obtained from Prof. Thomas J. Guilfoyle, University of Missouri, USA) plasmid using GH3_KpnI_F and GH3_NosT_XmaI_R primer pairs (Table 3.1). The polymerase chain reaction (PCR) product was subcloned into pGEM-T vector and sequence verified. Using *KpnI* and *XmaI* enzymes, GH3::GUS DNA fragments were cloned into the pTFH15.3 vector by replacing the rice *Actin* promoter. The construct was finally used for PEG-mediated protoplast transformation in moss. To validate the candidate genes disrupted by Tnt1 insertion, a full-length coding region of Pp3c14_22870.1 (2.1 Kb) was amplified from the *P. patens* genome using the primer pair Tnt1_sl_ins1_F and Tnt1_sl_ins1_R and subcloned into the pGEM-T vector (Table 3.1). PpSHLF-pGEM-T overexpression construct was sequence verified. The *SHLF* was released using *Apal* and *AscI* enzymes and ligated to the pTFH15.3 vector and linearized by the same enzymes. The coding region was released and ligated to the pTFH15.3 vector using *Apal* and *AscI* enzymes. Similarly, full-length *PpExtensin* (Pp3c1_9390V3.1) coding region (1.5 Kb) was amplified from the *P. patens* genome using the primer pair Tnt1_sl_ins2_F and Tnt1_sl_ins2_R and subcloned into the pGEM-T vector (Table 3.1). The PpExt-pGEM-T construct (4.5 Kb) was sequence verified. The *PpExtensin* coding region (1.5 Kb) was released and ligated to the pTFH15.3 vector using *Apal* and *AscI* enzyme.

All the above constructs were transformed into *P. patens* protoplast, and regenerated colonies were selected for G418 resistance as mentioned in the next section.

Table 3.1: List of primers used in this study.

S. No	Primer Name	Sequences 5' to 3'
SHLF Over-expression		
1	Tnt1_sl_ins1_F	GGCGCGCCTATGGCGTCCAGCTCCAGGGCCTTGAC
2	Tnt1_sl_ins1_R	CTAAGCGGATATCGCAATTTCTTTCATC
EXTENSIN Over-expression		
3	Tnt1_sl_ins2_F	GGCGCGCCAATGGCGGAGCAGCTCTGGTTTGCTT
4	Tnt1_sl_ins2_R	GTGGATCAGCCCATGACGTAGTGAAGG
GH3::GUS cloning		
5	GH3_KpnI_F	GGTACCACGAATAAAGAAAATTTAAAAGTCTC-
6	GH3_NosT_XmaI_R	-AACAAATG CCCGGGGATCTAGTAACATAGATGACACCGCG
GH3::GUS cloning		
7	Act_qF	ACCGAGTCCAACATTCTACC
8	Act_qR	GTCCACATTAGATTCTCGCA
9	SHLF_qFP	CTGGAAGCAACCATAGACGCCT
10	SHLF_qRP	TCATCGTCTCCCCGAGCTTGGC
Tnt1 insertion confirmation		
11	LTR_qF	TGATGATGTCCATCTCATTGAAGAA
12	LTR_7	TATTATTCCGCTTTATTACCGTGA

3.2.4 PEG-mediated transformation

PEG-mediated *P. patens* protoplast transformation was performed following the protocol of Nishiyama *et al.*, (2000). In brief, seven-day-old protonema was digested with 1% (w/v) driselase mixture to release protoplasts and washed with 8% mannitol. Protoplast mixture is then transferred to 2% PEG solution containing MgCl₂ and Ca(NO₃)₂ and the desired DNA for transformation. DNA uptake by protoplast was facilitated by a heat shock step at 45 °C for five mins. The osmolarity of protoplast solution was brought back using protoplast regeneration media and incubated under darkness for cell wall regeneration. After five days, regenerated protoplasts were transferred to primary selection media containing G418 (30 mg/ L) and incubated for two weeks. Colonies grown on primary selection media were further transferred to

relaxation media (without antibiotic) and incubated for additional two weeks. Colonies surviving on relaxation media were then transferred to secondary selection media containing G418 (30 mg/L) and incubated up to two-three weeks. Selected colonies were subjected to molecular analysis (PCR) for further verification

3.2.5 GUS assay

One-month-old *P. patens* colonies were grown on BCDAT medium and subjected to β -glucuronidase (GUS) staining assay. In the case of 2-Deoxy-D-Glucose (DDG) treatment, gametophores from one-month-old colonies were incubated in 100 mM DDG solution for seven days. For GUS assay, the moss tissue was fixed in 0.3% formaldehyde solution for 30 mins and washed with BCDAT media. The tissue was transferred to the GUS-staining buffer and incubated at 37 °C for 12 hrs in dark condition (Jefferson *et al.*, 1987). GUS-stained tissues were fixed by 5% (v/v) Formalin for 10 mins followed by incubation in 5% (v/v) Acetic acid for 10 mins. The tissue was dehydrated using a series of ethanol washes (30%, 50%, 70% and 100%). Images were obtained using a Leica S8 APO Stereomicroscope (Leica, Wetzlar, Germany).

3.2.6 Genome sequencing

Genomic DNA (1 μ g) was isolated from *shlf* mutant using the protocol from (PHYSCObase; <http://moss.nibb.ac.jp/protocol.html>) and submitted for whole genome sequencing at Genotypic Technology (Bangalore, Karnataka, India). A 300 to 700 bp fragment library was prepared using NEXTFlex DNA sequencing kit (BIO scientific, Austin, Texas, U.S.A) and 150 bp paired-end sequencing was performed using an Illumina platform (Illumina, CA, U.S.A). Approximately 30X depth raw data were generated and subjected to quality check with FASTQC. Raw data was obtained from Genotypic Technology Pvt. Ltd. A customized bioinformatics in-house pipeline was used to identify the Tnt1 and T-DNA insertion loci in the mutant genome (Annexure 1). In brief, the raw reads were aligned against *P. patens* reference genome, T-DNA sequence (pCAMBIA-1391Xc-Tnt1; Entrez accession number: AF234311.1) and the complete Tnt1 retrotransposon (Entrez accession number: X13777). NGS reads in which one pair matches to moss genome sequence and the other pair matches to either Tnt1 or T-DNA sequences were extracted to locate Tnt1 and T-DNA insertions. Tnt1 and T-DNA insertions detected by WGS were confirmed by the genomic DNA PCR and RT-PCR using the primers pairs Tnt1_sl_ins1_F, LTR_qF (1633 bp) and LTR7, Tnt1_sl_ins1_R (179 bp) for in-

sertion in Pp3C14_22870 and Tnt1_sl_ins2_F, LTR_qF (1147 bp) and LTR7, Tnt1_sl_ins2_R (491 bp) for insertion in Pp3C1_9390. (Table 3.1) (Figures 3.8 and 3.9).

3.2.7 qRT-PCR analysis

For qRT-PCR analysis, total RNA was extracted from protonema and gametophore tissue using RNAiso Plus (Takara Bio USA Inc., CA, USA). Two micrograms of RNA samples were reverse-transcribed using oligo dT primers and SS-IV reverse transcriptase (Invitrogen, CA, USA). Gene specific PCR primers were designed to detect endogenous β -actin (Act_F, Act_R) and *SHLF* gene (SHLF_qFP, SHLF_qRP) transcripts (Table 3.1). cDNA was diluted to 1:10 concentration only during β -actin transcript amplification and relative quantification of transcripts were performed using Bio-Rad CFX96 Touch Real-Time PCR Detection System (Bio-Rad, CA, USA). Cycler conditions were as follows: 95 °C for 10 sec; 40 cycles of 95 °C for 5 sec and 55 °C for 30 sec and an additional step for melting curve analysis at 95 °C for 10 sec. SYBR green used for detection of transcripts was SYBR Premix Ex *Taq* II (Tli RNaseH Plus) from Takara (Takara Bio USA Inc., USA). Each plate was run with samples including no template (RNA) control. Relative target gene expression levels were carried out using β -actin as a reference gene and fold-change (sample value/ reference value) was calculated based on the $2^{-\Delta\Delta C_t}$ method of Schmittgen and Livak, (2008).

3.2.8 Plasmodesmata (PD) associated callose staining using aniline blue

In order to visualize plasmodesmata (PD) associated callose, *P. patens* gametophores were vacuum infiltrated with 0.01% aniline blue solution for four hours on ice. Excess stain was washed off in BCDAT liquid media. Gametophores were mounted on slides and observed under a confocal microscope (Zeiss, Germany) using Plan Apochromat 40X oil immersion lens. Excitation laser of 504 nm and an emission filter of 421-575 nm were used to capture the PD-associated callose. Images were analyzed using ImageJ software (Schneider *et al.*, 2012).

3.2.9 Bioinformatic analysis

To analyze if the *SHLF* protein has homologs in other plant species, the standard protein BLAST was performed at NCBI (Gish *et al.*, 1993). To account for the species, whose tran-

scriptome data is not updated in NCBI databases, all available non-seed plant transcriptomics data (33 species) were downloaded from OneKp project (Matasci *et al.*, 2014). *Sphagnum fallax* transcriptomics data was downloaded from Phytozome v12.0 (<https://phytozome.jgi.doe.gov/pz/portal.html>) (Goodstein *et al.*, 2011). All the transcriptome assemblies were translated and converted into protein BLAST database using BLASTP 2.2.31+ toolkit (Camacho *et al.*, 2009). *SHLF* amino acid sequence was searched against the individual local protein database to find the presence of homologs. Any hit that has a minimum score (bits) of 100 and E-value less than one is considered as a homolog. All the organisms were arranged on a cladogram using PhyloT online tool (<http://phylot.biobyte.de/>) and visualized in iTOL (www.itol.embl.de). PhyloT tool generates trees based on the NCBI taxonomy database.

To check if the *SHLF* locus codes for a protein, the peptidome data of *Physcomitrella patens* from the study by Fesenko *et al.*, (2015) was downloaded and used for our analysis. Individual peptide sequences were formatted to FASTA sequences using GNU Awk 4.1.3 (<https://launchpad.net/ubuntu/+source/gawk>) and then a local protein BLAST database was created using BLASTP 2.2.31+ toolkit (Camacho *et al.*, 2009). The *SHLF* protein sequence was searched against the peptidome BLAST database locally and the hits containing perfect match were chosen. Further, to assess for the uniqueness of hits, the selected peptides were queried against the total protein sequences of moss other than *SHLF* protein of *P. patens*.

3.3 Results

3.3.1 Phenotypic characterization of *short-leaf* (*shlf*) mutant lines

As described in chapter 2, a forward genetic screen on Tnt1 insertional *P. patens* mutant population resulted in the isolation of *short-leaf* (*shlf*) mutant, which developed shorter leaves compared to the wild-type moss (WT). To understand the *shlf* phenotype further, a complete phenotypic study was undertaken. In this report, leaves will be denoted based on their plastochron order (P1, P2 and P3... PN). An array of first nine leaves (P1 to P9) of WT and *shlf* showed that *shlf* leaf length deviated from WT as early as P2 leaf onwards and maximum length of *shlf* leaves was equivalent to P3 of WT (Figure 3.1 A-C). It also showed that the growth along the proximal-distal axis saturated at P9 in both. Hence, all further experiments

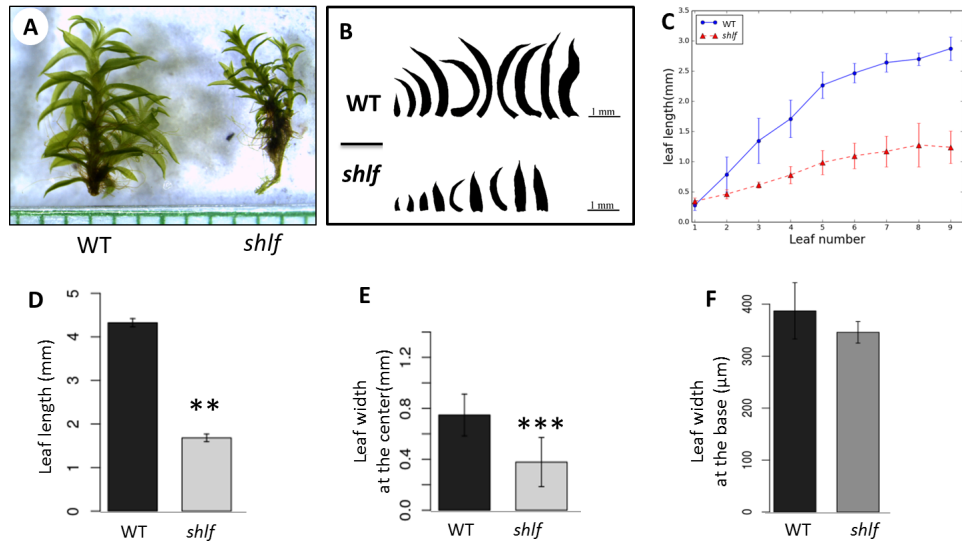


Figure 3.1: *shlf* mutant produces two times shorter leaves than WT. (A) One-month-old gametophores of WT and *shlf* exhibiting the short-leaf phenotype (reproduced from chapter 2). (B) An array of first nine leaves from the apex of WT and *shlf* gametophores (Scale bar size: 1 mm). (C) Line plot showing the gradual increase in the length of WT (circle) and *shlf* (triangle) leaves. (D-F) Comparison of differences in leaf length and width (at the center of the proximal-distal axis as well as at the base) between the ninth leaf of WT and *shlf*. Student's t-test was performed on data with $n = 30$ and asterisk indicate statistical significance where *** is $p < 0.001$ and ** is $p < 0.01$.

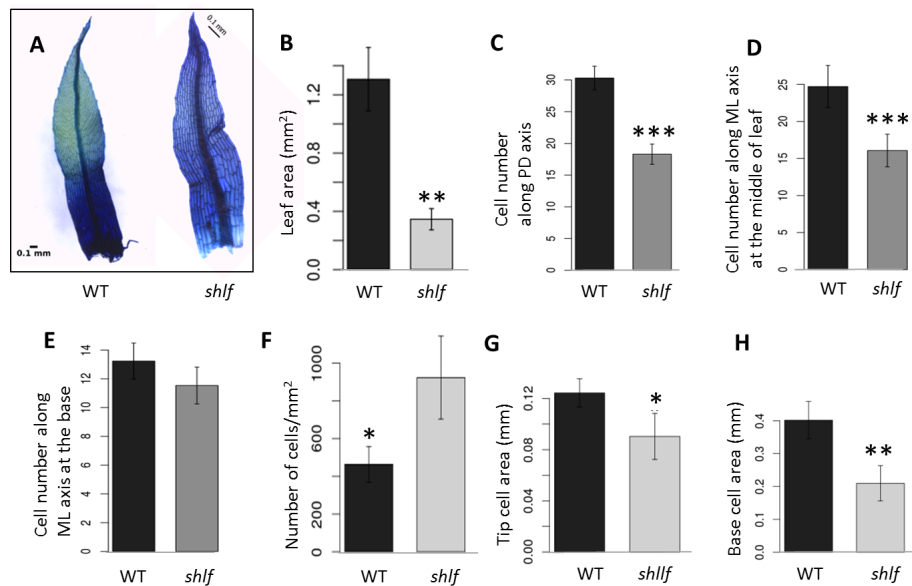


Figure 3.2: Both cell division and elongation are affected in *shlf* leaves. (A) P9 leaves of WT and *shlf* mutant were stained with toluidine blue for enhanced visualization of cell walls under a bright field microscope. Various phenotypes of leaves were analyzed such as total leaf area (B), total number of cells along the proximo-distal axis (C), total number of cells across the width at the middle (D) and base (E) of the leaf, density of cells (F), tip cell area (G) and basal cell area (H). Student's t-test was performed on data with $n = 10$ and asterisk indicate statistical significance where * is $p < 0.05$ ** is $p < 0.01$ and *** is $p < 0.001$.

were performed on P9 leaves of WT and *shlf* mutant. P9 leaves of *shlf* were shorter and narrower (at the middle of the leaf) than WT leaves (Figure 3.1 D and E). However, their width did not vary significantly at the base of the leaf (Figure 3.1 F). Overall, the shape of the WT leaves was oblanceolate (Harrison *et al.*, 2009), while that of *shlf* was lanceolate.

To understand the cause for the reduction in overall leaf size of *shlf*, phenotypes at the cellular level were analyzed. Toluidine blue staining enhanced the visualization of cell walls (Figure 3.2 A). Overall leaf area and the total number of cells per leaf were reduced in the *shlf* mutant (Figure 3.2 B and F). A total number of cells along the proximal-distal axis and medial-lateral axis (at the center of leaf) were reduced (Figure 3.2 C-E). The cell density was higher in *shlf* leaves (Figure 3.2 F). Though the tip cell area was significantly reduced in *shlf* leaves, basal cells reduced more drastically (Figure 3.2 G and H). These results suggested that both cell division and elongation phase is suppressed in *shlf* leaves compared to that of WT leaves.

3.3.2 The response of *shlf* gametophores to temperature and dark conditions

One of the possible reasons for the severe reduction of leaf size of *shlf* mutant could be due to high accumulation of auxin in the shoot. Since auxin accumulation and signaling are known to be linked to being influenced by temperature and light conditions; we tested the response of *shlf* mutant gametophores over a gradient of temperatures and under complete dark condition. We observed that WT leaf length remained unaffected around the standard growth temperature of 24 °C (Figure 3.3 A). However, a gradual reduction in leaf length was observed at 12 °C but rapidly reduced at a higher temperature like 32 °C. Interestingly, *shlf* leaves exhibited a different trend. At lower temperatures (20 °C, 12 °C), leaf length could recover, but at higher temperatures (28 °C, 32 °C) leaf length was observed to reduce further. When WT gametophore apex was grown under standard light conditions, it developed longer leaves and had less internodal length. On the other hand, when gametophore apices were grown in dark condition, they were observed to etiolate (their internodal distance was increased, and leaves were reduced to scales) (Figure 3.3 B). In case of *shlf* mutant, gametophore apices showed etiolation as early as the fourth day, and over 85% gametophores were etiolated by the tenth day on the same condition. However, we find that WT gametophores showed etiolation from sixth day onwards and took more than 10 days for 50% gametophores to etiolate.

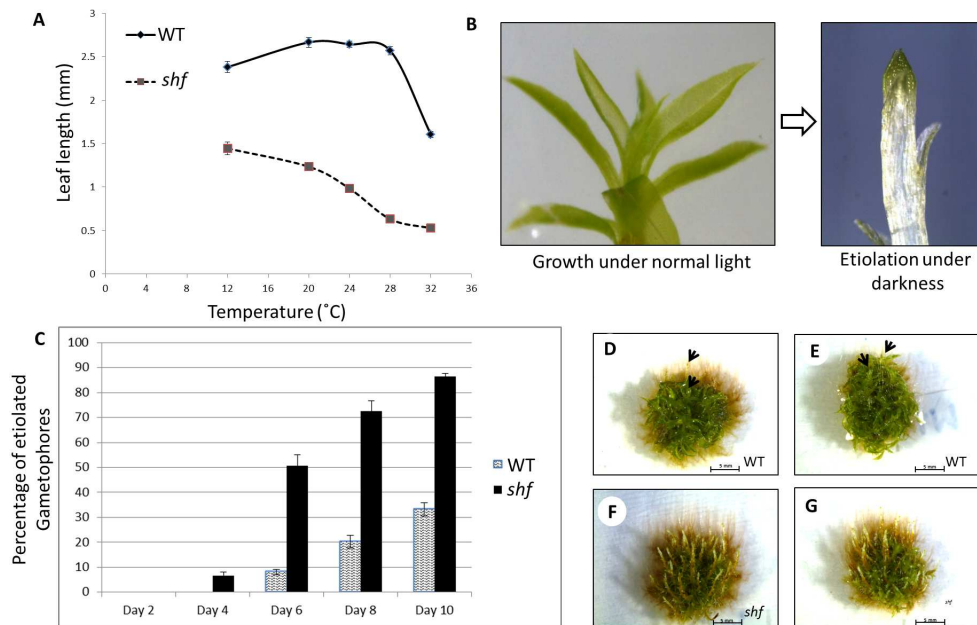


Figure 3.3: *shlf* gametophores and leaves are sensitive to the environmental changes. (A) The effect of growth over the temperature gradient (12, 20, 24, 28 and 30 °C) on WT and *shlf* mutant P9 leaf follow distinct trends. 24 °C is the standard growth temperature. (B) A WT gametophore apex which was grown under normal light conditions (left) and dark-grown etiolated gametophore apex (right). (C) Percentage of gametophore apices showing etiolation in response to darkness was scored by removing a fresh plate every two days interval over two to ten days. (D and E) WT colony showing few etiolated gametophores (arrow) after eight days of dark incubation while most of the *shlf* gametophores (F and G) have been etiolated. Student's t-test was performed on data with $n = 10$. All the comparison between WT and *shlf* are statistically significant with $p < 0.001$.

3.3.3 *shlf* mutant show reduced apical dominance

Morphological observation of WT and *shlf* gametophores indicated a possible defect in branching pattern (Figure 3.4 A). Three different kinds of nodes were observed in *P. patens* gametophores. Nodes at the apex had only leaves whereas; nodes at the base of the gametophore had leaf along with rhizoids. The third type of node was noticed at regular intervals that had branching points in addition to leaves (Figure 3.4 B and C). The mean apical dominance of WT was observed as 14 metamers from the apex, while the apical dominance was reduced to 8 metamers in *shlf* gametophores (Figure 3.4 D and E). In turn, the mean internodal length of *shlf* gametophores has increased significantly compared to WT. (Figure 3.4 F).

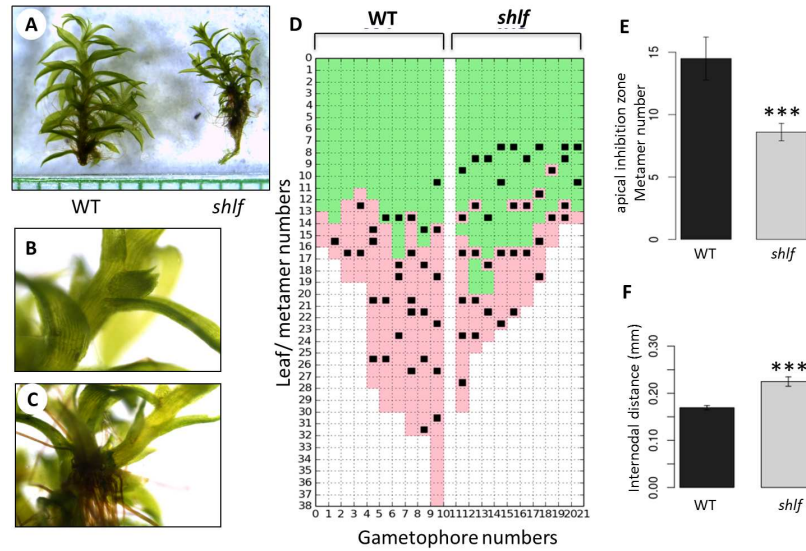


Figure 3.4: *shlf* gametophores exhibit reduced apical dominance. (A) WT and *shlf* gametophores from the one-month-old colony (reproduced from chapter 2). A metamer on a gametophore having leaf and a branch (B) or leaf, branch, and rhizoids (C). (D) Representation of branching along the gametophore main axis. Metamer numbers follow the plastochron number and each green, pink, and black squares represent leaf, rhizoid and branching point respectively. (E) Mean apical inhibition zone of *shlf* gametophores were significantly less than WT (n = 10). (F) Mean of the average internodal distance of *shlf* gametophores were higher than WT (n = 30). Student's t-test was performed, and asterisks indicate statistical significance where * is $p < 0.001$.

3.3.4 Analysis of auxin accumulation pattern in *shlf* gametophore

The phenotypic analysis indicated a possible role for auxin in pleiotropic *shlf* phenotypes. To investigate the differences in auxin accumulation pattern between WT and *shlf* gametophores, soybean auxin-responsive promoter *GH3* was used to drive *GUS* gene. The *GH3::GUS-pTFH15.3* construct was transformed into WT, and *shlf* background (Figure 3.5) and a number of lines were generated. WT-*GH3::GUS* gametophores showed a mild *GUS* expression in apical cells and an intense expression at the base (Figure 3.6 A). However, *shlf-GH3::GUS* gametophores exhibited a different *GUS* expression pattern (Figure 3.6 B). *GUS* expression restricted at the apex only. Leaves and the apex of gametophore were intensely stained, while faint *GUS* expression was observed at the base (Figure 3.6 C and D). We speculate that the differential auxin accumulation in apex and base of the *shlf* mutant could be associated with defective auxin transport through plasmodesmata (PD). Hence, we treated the gametophores (in submerged condition) with DDG solution. DDG inhibits callose biosynthesis and opens the PD connections as shown earlier (Han *et al.* 2014).

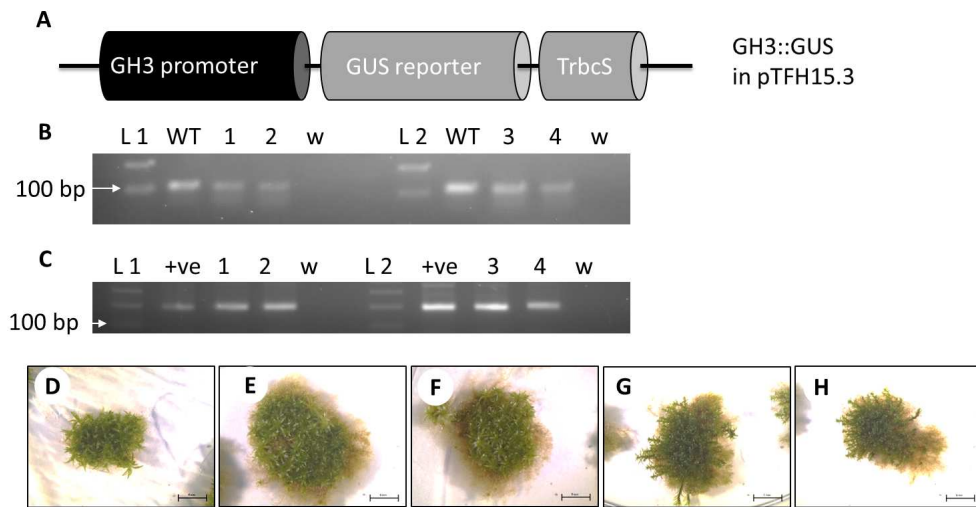


Figure 3.5: Generation of *GH3::GUS* lines in WT and *shlf* backgrounds. (A) Schematics showing the construct design of soybean auxin-responsive (*GH3*) promoter-reporter cassettes in the pTFH15.3 vector backbone. PCR confirmation of *P. patens* lines by PpActin (B) and *GUS* (C) specific primers. Wells are labelled as 100 bp ladder (L1 and L2), wild-type (WT), water control (w), plasmid containing gene of interest (+ve), WT (1 and 2) and *shlf* (3 and 4) background. One-month-old colonies WT (D), *GH3::GUS* lines in WT background (line 1 and 8) (E and F) and *shlf* background (line 3 and 6) (G and H). Scale bar size: 5 mm.

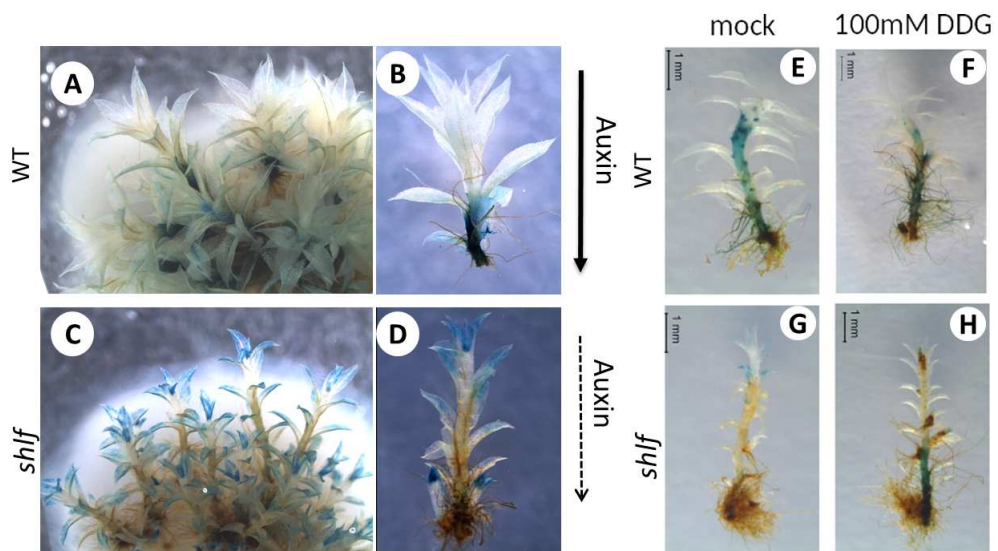


Figure 3.6: Soybean *GH3::GUS* lines revealed the differential auxin accumulation patterns in *shlf* gametophores. *GUS* expression pattern of soybean auxin-responsive promoter-reporter lines (*GH3::GUS*) in the WT background (A and B) and *shlf* background (C and D) when grown on a solid media. *GUS* expression pattern changed when grown under submerged conditions in BCDAT media with (F and H) or without DDG (E and G). Scale bar size: 1 mm.

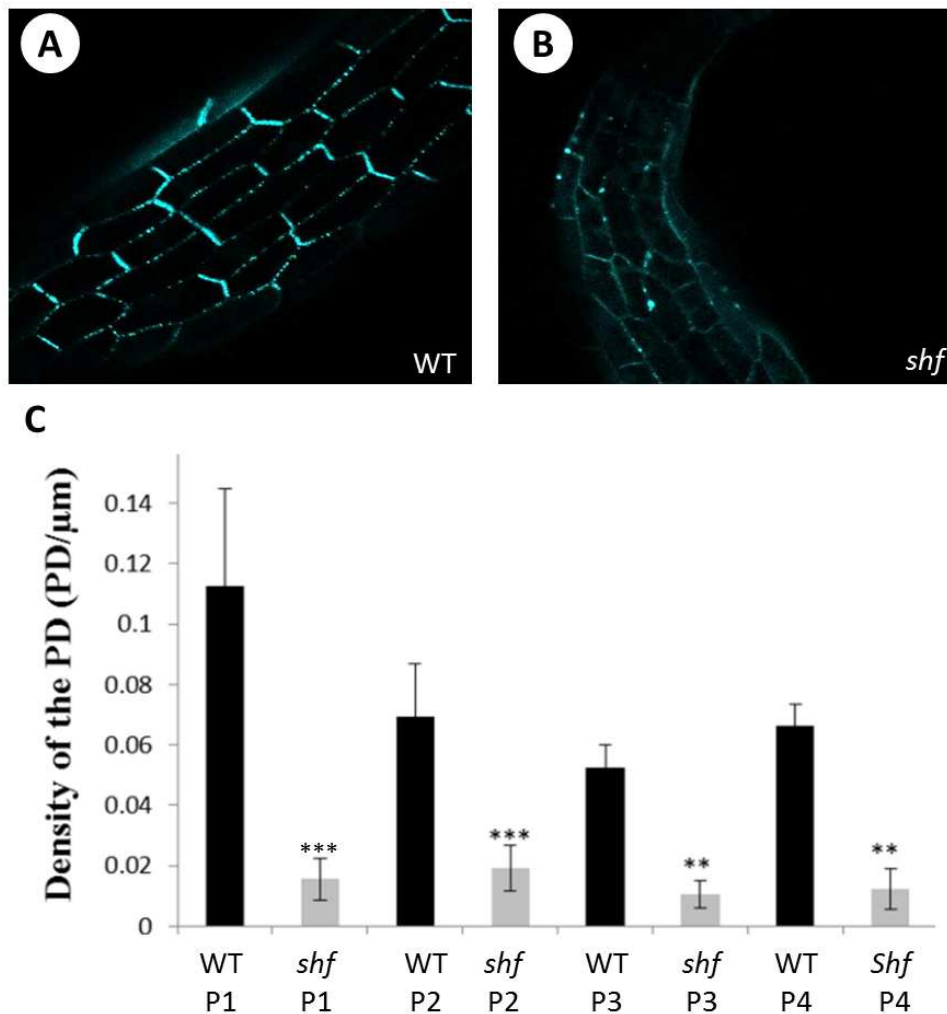


Figure 3.7: Callose staining indicates that the plasmodesmata (PD) density could be low in *shlf* mutant leaves. Aniline blue staining of PD-associated callose in WT (A) and *shlf* (B) leaves. (C) Comparison of PD density of P1 to P4 leaves between WT and *shlf*. PD number is based on PD-associated callose staining. Student's t-test was performed on data n= 10 and asterisks indicate statistical significance where ** is $p < 0.01$ and *** is $p < 0.001$.

Gametophores grown in BCDAT medium without DDG, exhibited *GUS* expression all over the stem in WT-GH3:*GUS* lines compared to those grown on solid BCDAT medium (Figure 3.6 E). While, *shlf* mutant gametophores under the same conditions exhibited *GUS* expression in the young leaves and apex (Figure 3.6 F) only. However, when the *shlf* mutant was incubated with 100 mM DDG, interestingly it showed *GUS* expression at the base of the gametophore. To further understand the probable defect in auxin diffusion, we treated the leaves with aniline blue, (which stains the PD-associated callose) to determine the PD density. We observed that P1 to P4 leaves of *shlf* had a low-density PD-associated callose than those of WT (Figure 3.7 C) lines. All these findings suggested that *shlf* gametophores could have

impaired auxin diffusion mechanism.

3.3.5 WGS and determination of causal gene for the *shlf* mutant

The *shlf* mutant was generated by introducing Tnt1 retrotransposon into *P. patens* through T-DNA insertion. Hence, the mutant phenotype could be due to the T-DNA or Tnt1 insertion. In order to ascertain T-DNA and Tnt1 insertion locations in the *shlf* background, the whole genome was sequenced at a 30X depth and compared with the *P. patens* reference genome using an in-house customized pipeline (for details, please see Annexure 1). Bioinformatics analysis revealed a single T-DNA insertion and three Tnt1 insertions, out of which, two Tnt1 insertions were located in the coding region (Table 3.2). The Tnt1 insertion was found to be at 1000 bp downstream of the start codon of the gene Pp3C1_9390, which codes for an EXTENSIN, a cell wall assembly protein. The insertion was confirmed by genomic DNA PCR but not detected by RT-PCR (Figure 3.8). The second Tnt1 insertion was located 118 bp upstream to the stop codon of the gene Pp3c14_22870 (Figure 3.9 A), which was annotated as coding for an unknown protein. The expression of Pp3C14_22870 gene was detected from protonema and gametophore life stages confirming that it is not a pseudogene (Figure 3.9 B). Tnt1 insertion inside Pp3c14_22870 was confirmed through genomic DNA as well as RT-PCR (Figure 3.9 C, D).

Table 3.2: Tnt1 and T-DNA insertions in *shlf* mutant genome ascertained by WGS

S.No	Genome co-ordinate	Nature of locus	Locus	Mutagen	Comments
1	Chr01:18640862	Intergene		T-DNA	
2	Chr14:14660675	Exon	Pp3c14_22870 (118bp upstream of stop codon)	Tnt1	gene of unknown function
3	Chr01:6877043	Exon	Pp3C1_9390 (1000bp downstream of start codon)	Tnt1	Extensin gene
4	Chr08:11069647	Intergene		Tnt1	

To determine the causal gene for the *shlf* phenotype, both *EXTENSIN* (Pp3c1_9390) and Pp3c14_22870 genes are over-expressed in the mutant background. Both *EXTENSIN* (Pp3c1_9390) and Pp3c14_22870 coding region were cloned under the rice *actin* promoter and introduced into *shlf* protoplasts. Three lines were recovered for each construct, containing

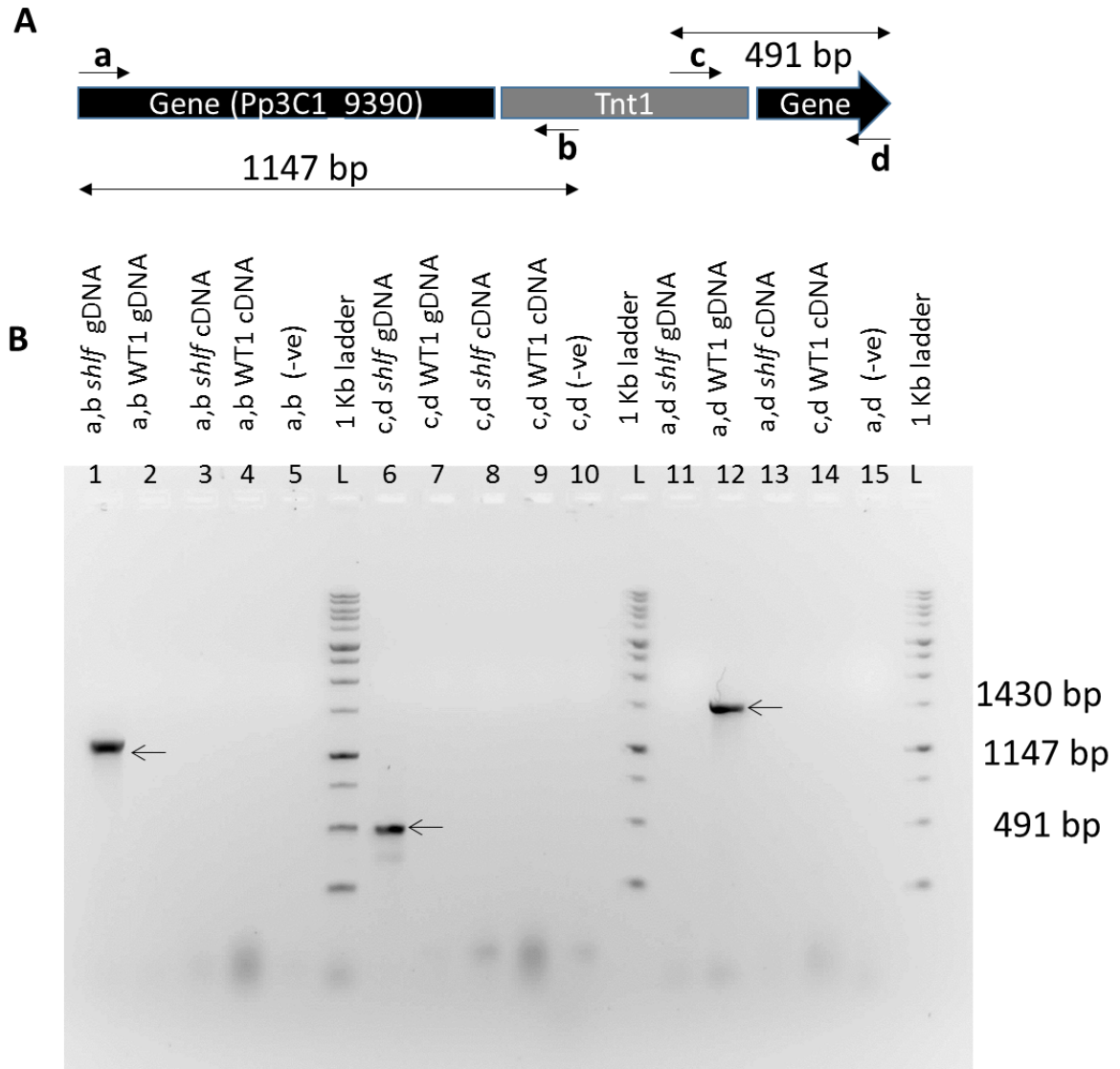


Figure 3.8: PCR confirmation of Tnt1 insertion inside the locus Pp3c1_9390. (A) A schematic diagram showing the Tnt1 insertion inside the coding region and PCR primers binding sites. Primers: a) Tnt1_sl_ins2_F, b) LTR_qR, c) LTR_7 and d) Tnt1_sl_ins2_R. (B) Agarose gel image showing the amplification of 5'(well 1) and 3'(well 6) flanking regions of Tnt1 insertion from *shlf* genomic DNA and full length Pp3c19390 coding region (well 12) from WT genomic DNA (arrows indicate the PCR amplicons).

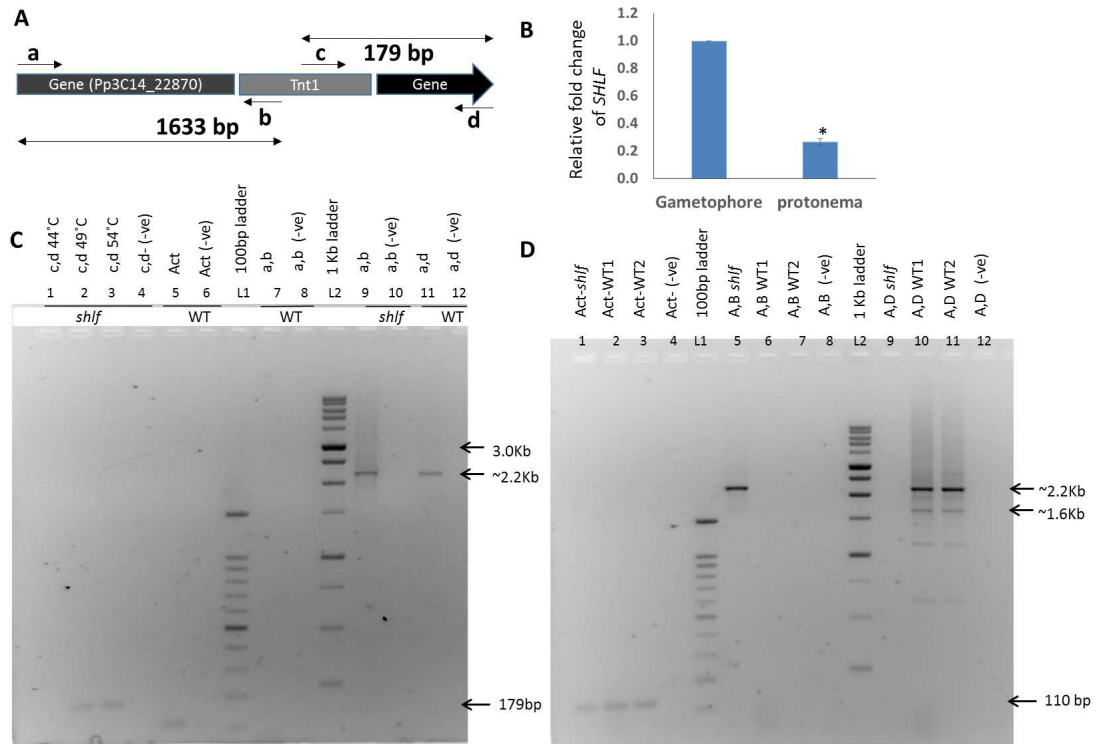


Figure 3.9: PCR confirmation of Tnt1 insertion inside the locus Pp3c14_22870. (A) A schematic diagram showing the Tnt1 insertion inside the coding region and PCR primers binding sites. Primers: a) Tnt1_sl_ins1_F, b) LTR_qR c) LTR_7 and d) Tnt1_sl_ins1_R. (B) Expression pattern of Pp3c14_22870 in gametophore and protonemal tissues. Student's t-test was performed on data n = 3 and asterisks indicate statistical significance where * is $p < 0.05$. (C) Agarose gel image showing the amplification of 3'(wells 2 and 3) and 5'(well 9) flanking regions of Tnt1 insertion from shlf genomic DNA and full-length Pp3c14_22870 coding region (well 11) from WT genomic DNA. (D) Agarose gel image showing the amplification of 5'(well 5) flanking region of Tnt1 insertion from shlf cDNA and full-length Pp3c14_22870 coding region (wells 10 and 11) from WT cDNA. Act (Actin) was used as positive control.

a stable integration of over-expression construct (Figures 3.10 and 3.11). The *PpEXTENSIN* overexpression did not revert the *shlf* phenotype (Figure 3. 10). However, the overexpression of Pp3c14_22870 gene reverted the short-leaf phenotype and produced WT like leaves (Figure 3. 12). In the Pp3c14_22870 over-expression lines, leaf length, width and internodal distance were recovered. Hence, the causal gene for short-leaf phenotype was determined as Pp3c14_22870 and hereafter, will be described as *SHORT-LEAF* (*SHLF*) gene.

3.3.6 Bio-informatic analysis of *SHLF* gene

SHLF gene exhibited unusual sequence features. It had no introns within the 2.1 Kb of coding region. It had four tandem repeats, each of 513 bp in genomic DNA and mRNA, which

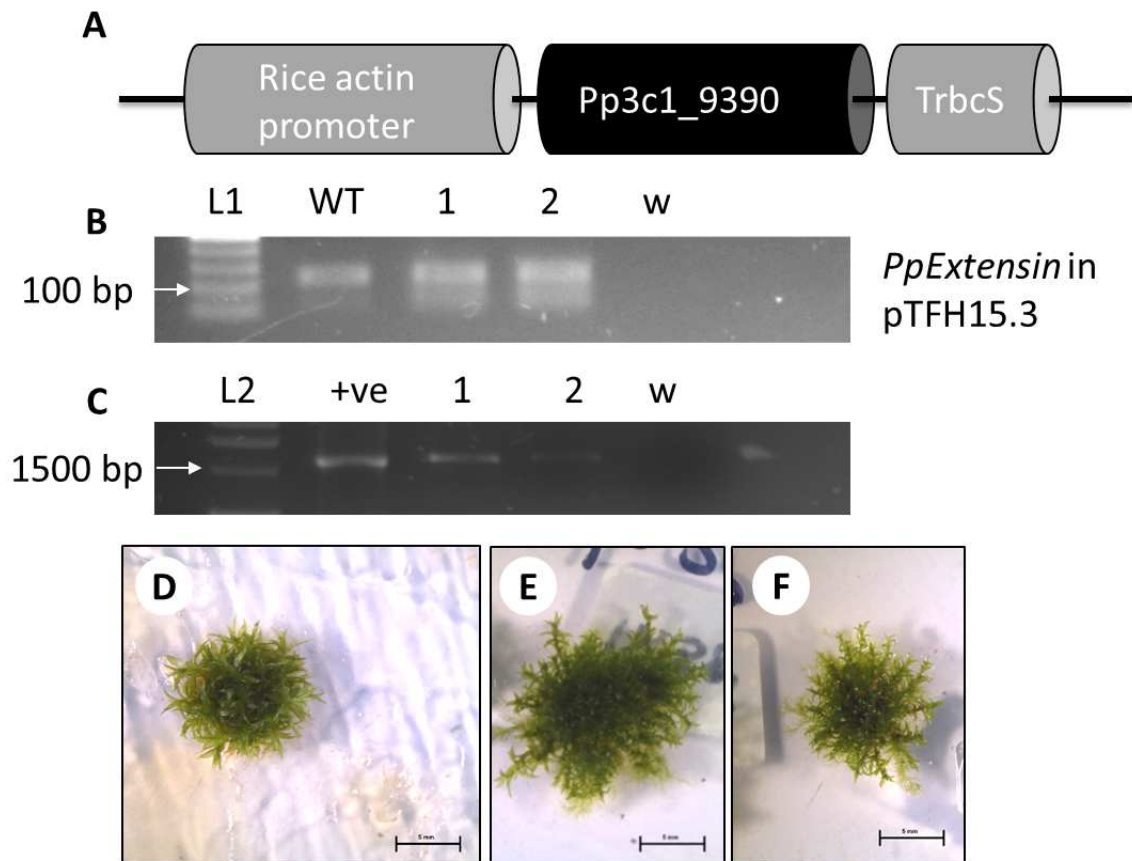


Figure 3.10: Generation of Pp3c1_9390 over-expression lines in the *shlf* background. (A) A schematic diagram showing Pp3c1_9390 over-expression construct in the pTFH15.3 vector backbone. PCR confirmation of *P. patens* lines by *PpActin* (B) and gene-specific (C) primers. Wells are labelled as 50 bp ladder (L1), 100 bp ladder (L2), wild-type (WT), water control (w), plasmid containing gene of interest (+ve), *PpExtensin* over-expression lines (1 and 2). One-month-old colonies of WT (D) and Pp3c1_9390 overexpression lines (line 1 and 2) (E and F) Scale bar size: 5 mm.

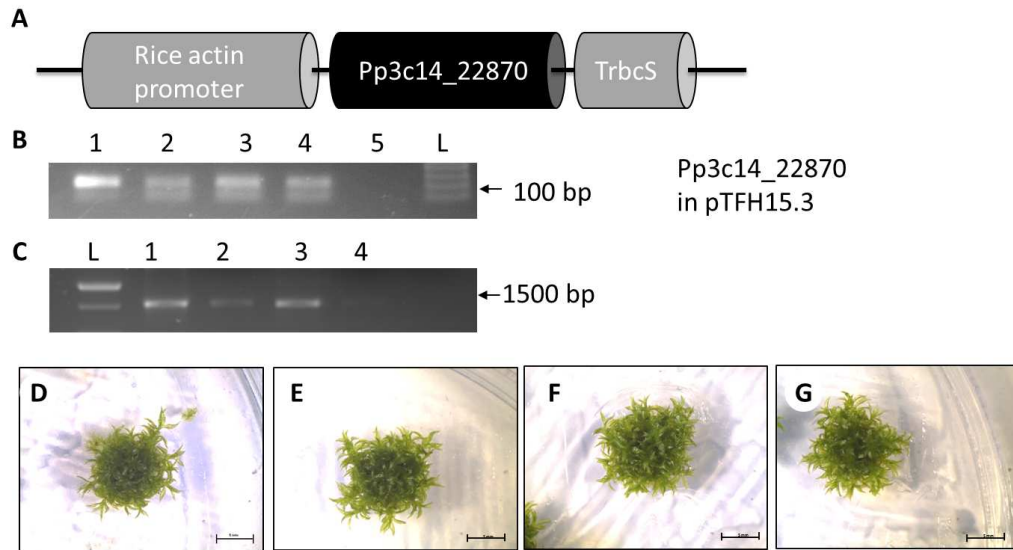


Figure 3.11: Generation of Pp3c14_22870 over-expression lines in the *shlf* background. (A) A schematic diagram showing Pp3c14_22870 overexpression construct in the pTFH15.3 vector backbone. PCR confirmation of *P. patens* lines by *PpActin* (B) and gene-specific (C) primers. Wells are labelled as 50 bp ladder (L1), 100 bp ladder (L2), wild-type (WT), water control (w), plasmid containing gene of interest (+ve), Pp3c14_22870 overexpression lines (1 and 2). One-month-old colonies of WT (D) and Pp3c14_22870 overexpression lines (line 16,33 and 53) (E, F and G). Scale bar size: 5 mm.

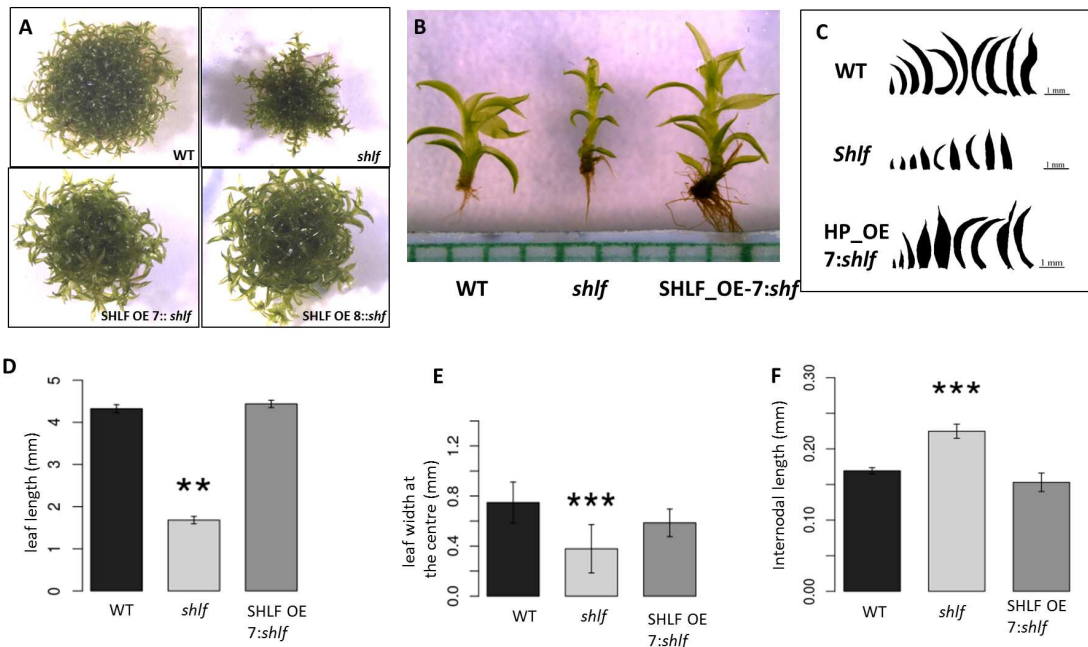


Figure 3.12: Pp3c14_22870 overexpression rescues the *shlf* phenotype. Colonies (A), gametophores (B), the leaf array (C) and barplot on leaf length (D) and width (E) of overexpression line 7 and 8 showing rescue of leaf length compared to *shlf* leaves. (F) The phenotypic difference in internodal length of *shlf* gametophores are also rescued. Student's t-test was performed on data with $n = 10$. All the comparison between WT and *shlf* are statistically significant where * is $p < 0.001$ and ** is $p < 0.01$.

translated into four repeats each of 171 amino acid (aa) in protein (Figure 3.13). We noticed that *SHLF* gene had three 513 bp repeats according to the moss genome assembly version 3 (Lang *et al.*, 2018). However, we found four repeats in the *SHLF* gene using PCR and DNA sequencing. The first repeat had the least similarity, while the other three were near perfect (Figures 3.14 and 3.15).



Figure 3.13: Primary structure of *SHLF* gene and protein. The tandem arrangement of repeats in genomic DNA, mRNA and protein sequences is depicted. A screenshot of NCBI-conserved domain search showing that the *SHLF* has no known conserved domain.

To check if the *SHLF* gene codes for a protein, we analysed the proteome data from Fesenko *et al.*, (2015 and 2017). The *P. patens* peptidome had 100% coverage by unique peptides for the SHLF protein. This confirmed that *SHLF* gene codes for a real protein. The primary sequence features of *SHLF* were carefully analysed. As frequently observed in other proteins, SHLF did not have any tryptophan residue. Our analysis by SecretomeP soft-

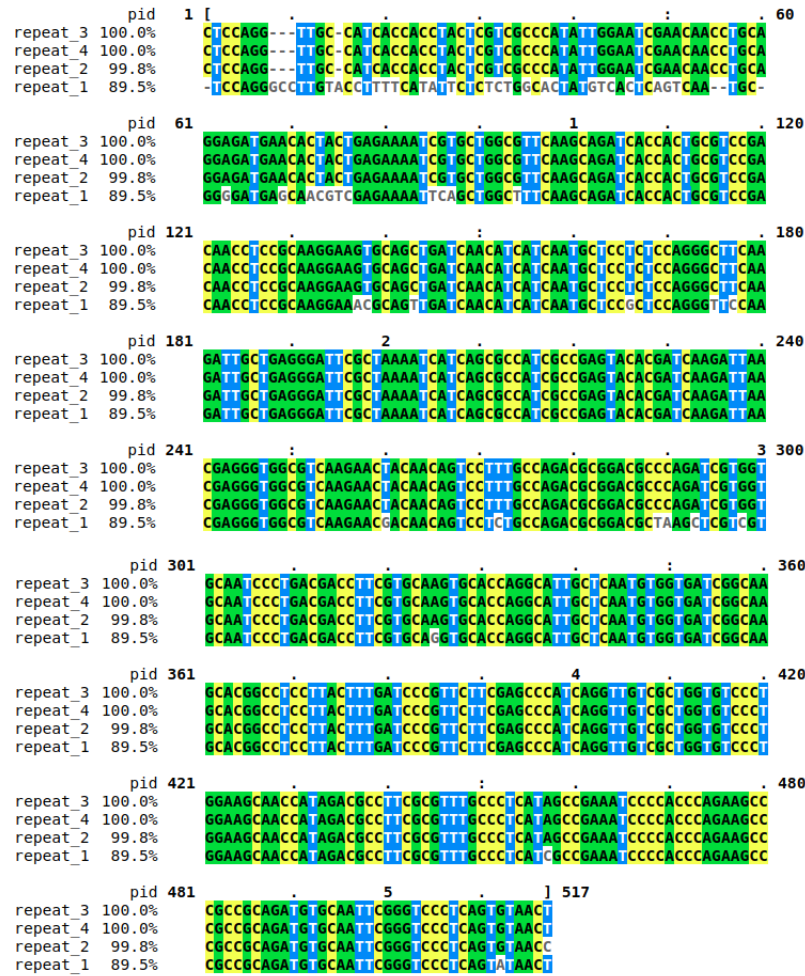


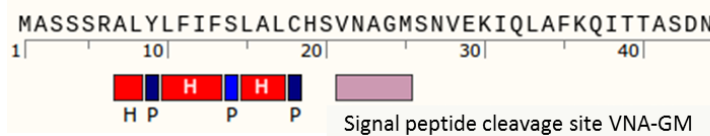
Figure 3.14: Tandem DNA repeats of *SHLF*. The four repeats (repeat_1, repeat_2, repeat_3 and repeat_4) of *SHLF* was aligned using Clustal W software. The percentage of identical residues is mentioned as pid.



Figure 3.15: Tandem amino acid repeats of *SHLF*. The four repeats (repeat_1, repeat_2, repeat_3 and repeat_4) of *SHLF* were aligned using Clustal W software. The percentage of identical residues is mentioned as pid.

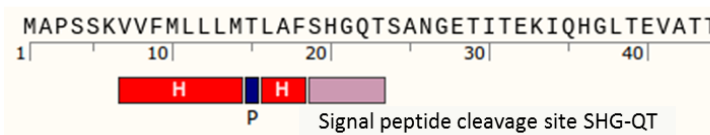
ware (Bendtsen *et al.*, 2004) showed that SHLF has N-terminal endoplasmic reticulum (ER)-targeting signal with high confidence (Figure 3.16). The N-terminal ER-targeting signal is also present in the homologs of SHLF identified from *Marchantia polymorpha* and *Sphagnum fallax*, only available complete transcriptomes in byrophytes. To understand the significance of the ER-targeting signal, a survey on moss proteome (32926 proteins) was performed, which showed that only 1276 proteins (3.87%) have an N-terminal ER-targeting signal.

A *Physcomitrella patens*:



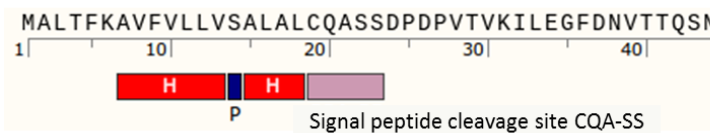
Reliability class:1
SignalP score: 0.848

B *Marchantia polymorpha*:



Reliability class:1
SignalP score: 0.729

C *Sphagnum fallax*:



Reliability class:1
SignalP score: 0.885

Figure 3.16: SHLF has N-terminal ER-targeting signal. Amino acid sequences of SHLF from *P. patens* (A), *Marchantia polymorpha* (B) and *Sphagnum fallax* (C) were analyzed for the presence of ER-targeting signal using the SignalP software. Hydrophobic amino acids are marked as (H), polar amino acids are marked as (P) and the signal peptide cleavage site is also annotated.

To our surprise, when we performed a standard protein BLAST search against NCBI non-redundant protein sequences (nr) database, it showed the presence of homologous sequences only in *Marchantia polymorpha* but not in any of the vascular plants or algae. Also, we did not find any known conserved domain in SHLF (Figure 3.13). To better understand the conservation of SHLF across plant lineages, we collected all the available transcriptomic data from non-seed plants and performed a local blast search (Table 3.3). The cladogram shows that six out of ten moss species and four out of six liverwort species were having a homologous locus for SHLF, while none were found from the chlorophycean algal and vascular plants (Figure 3.17). However, very poor conservation was found in the charophycean algae *Klebsormidium*

nitens. Further, when we expanded our search to the recently published *Chara brunei* genome (Nishiyama *et al.*, 2018), there were no homologs identified. This analysis clearly suggested that *SHLF* represents a novel bryophyte-specific gene family.

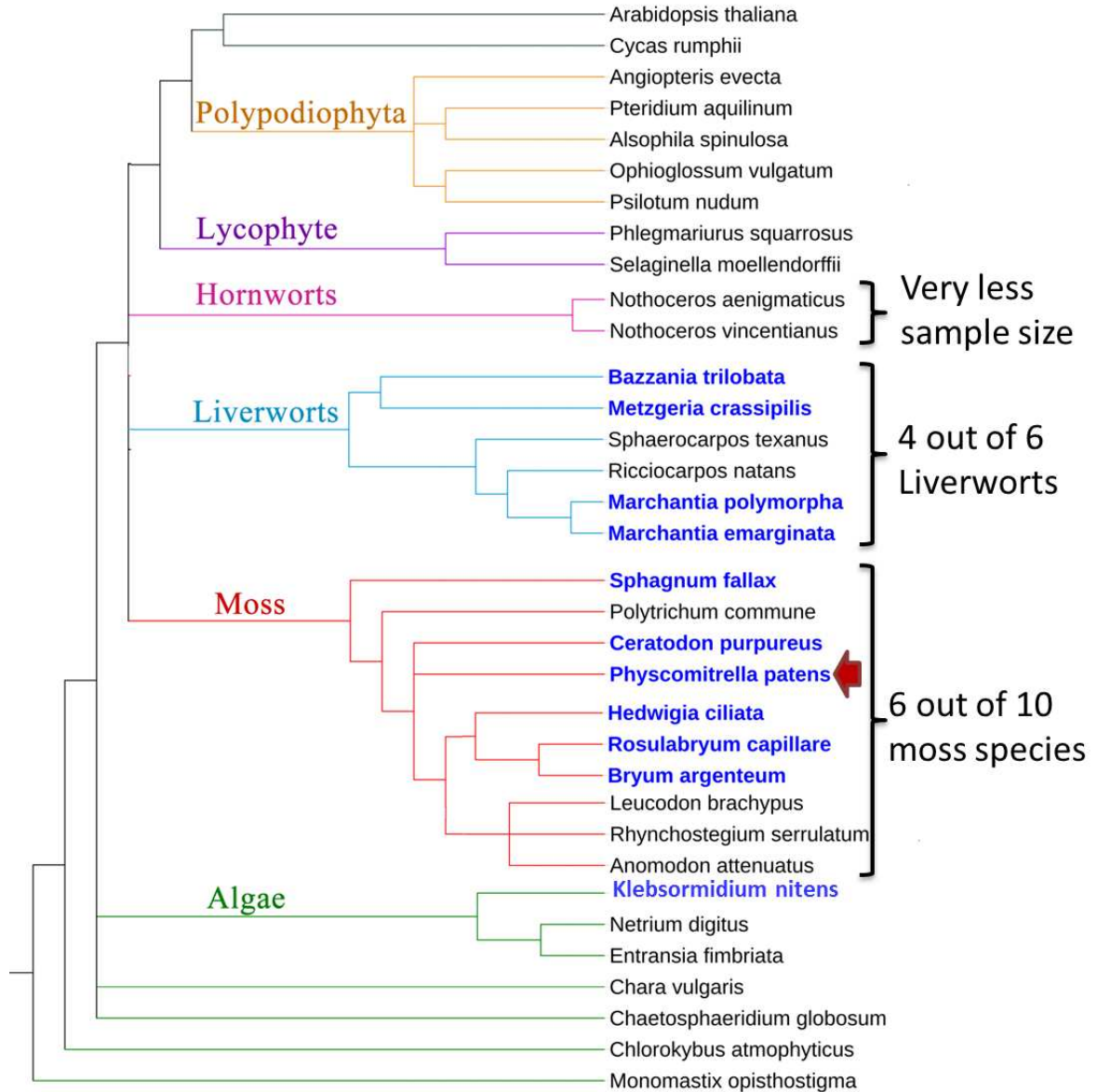


Figure 3.17: *SHLF* is a bryophyte-specific gene. The cladogram is showing the phylogenetic relationship among the species analysed (based on the NCBI Taxonomy database). Organisms containing *Shlf* homologs are in bold and blue colour font.

Our bioinformatic results on the origin and degree of conservation of *SHLF* among plant lineages is summarised in Figures 3.18 and 3.19. Many fully sequenced genomes are available for chlorophycean algae and vascular plants but homologs of *SHLF* were not found to be present in any of them. A poorly conserved homolog (without any repeats) was detected in the only genome sequenced charophycean algae *Klebsormidium nitens*. However, further

Table 3.3: Details of local protein BLAST results for SHLF homolog search.

Plant group	Organism	Highest score (bit)	E-value
Liverwort	<i>Bazzania trilobata</i>	187	2 x 10 ⁻⁵⁶
Liverwort	<i>Metzgeria crassipilis</i>	162	9 x 10 ⁻⁴⁸
Liverwort	<i>Marchantia polymorpha</i>	150	3 x 10 ⁻⁴³
Liverwort	<i>Marchantia emarginata</i>	186	9 x 10 ⁻⁵⁶
Moss	<i>Sphagnum fallax</i>	558	0
Moss	<i>Ceratodon purpureus</i>	191	7 x 10 ⁻⁵⁸
Moss	<i>Hedwigia ciliata</i>	164	4 x 10 ⁻⁴⁸
Moss	<i>Rosulabryum capillare</i>	186	9 x 10 ⁻⁵⁶
Moss	<i>Bryum argenteum</i>	191	1 x 10 ⁻⁵⁷

study would be required to confirm this observation. *SHLF* homologs are present in the only genome-sequenced liverwort species *M. polymorpha*. It had multiple paralogs and as high as five tandem repeats in *M. polymorpha*. Few more homologs were detected from bryophyte transcriptomes available from OneKp database. These results indicated that *SHLF* could be specific to early streptophytes.

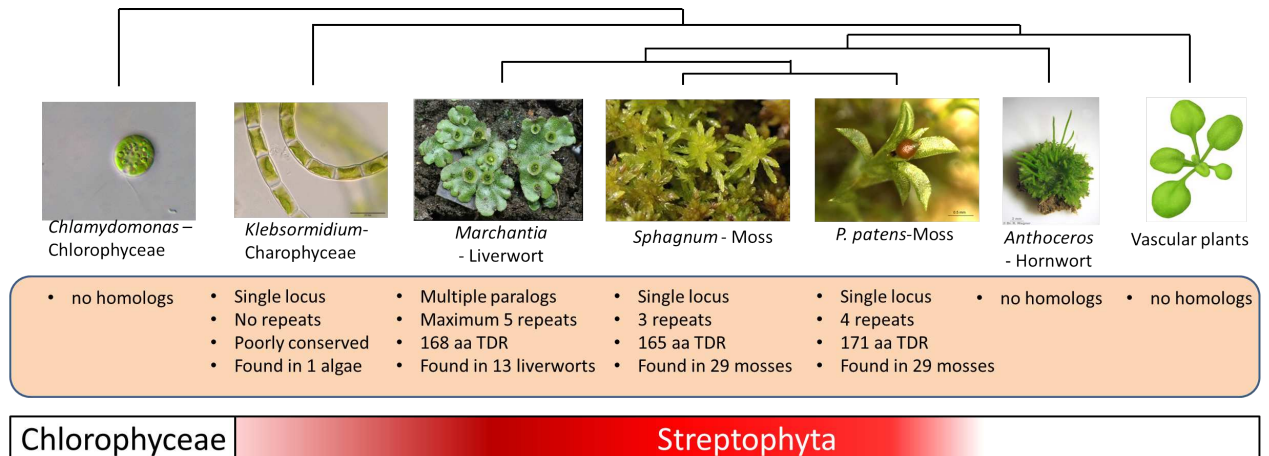


Figure 3.18: *SHLF* gene is conserved among lower streptophytes. A cladogram showing the phylogenetic relationship among plant lineages. *SHLF* homologs were detected from charophycean algae, liverworts and moss (early streptophytes). Early divergent chlorophycean algae, as well as the hornworts and vascular plants, did not have the homologs of *SHLF*.

Interestingly, we could identify five homologs of *SHLF* in *M. polymorpha* genome (Table 3.4). Among them only *MpSHLF50* (Mapoly0112s0050) gene was detected from the cDNA derived from Tak-1 thalloid tissue (Figure 3.19). Hence, we cloned *MPSHLF50* into pTFH15.3 vector and the over-expression lines in the moss *shlf* background are presently being

generated. This cross-species complementation will be helpful to understand the functional conservation of *SHLF* between moss and liverworts.

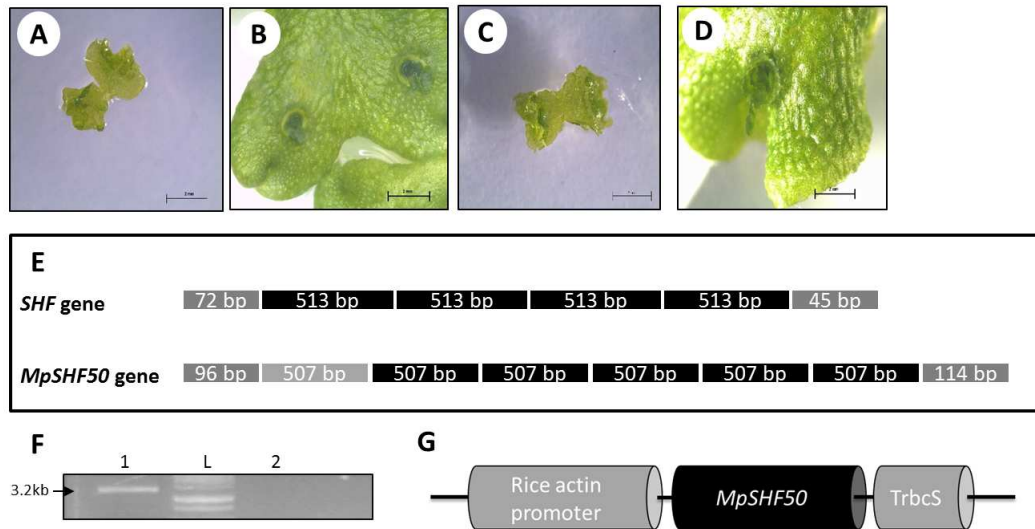


Figure 3.19: Cross-species complementation of *SHLF*. A sporophyll (A and C) and grown thallus (B and D) of Tak-1 (A and B) and Tak-2 (C and D) sexual types of *Marchantia polymorpha*. (E) Comparison of repeat structure between *SHLF* and its homolog in *M. polymorpha* *MpSHLF50*. (F) PCR amplification of the full-length coding region (3.2 Kb) of *MpSHLF50*. (G) A schematic showing the *MpSHLF50* gene cloned under the rice Actin promoter. Scale bar size is 2 mm.

Table 3.4: Details of Marpolbase BLAST results for *SHLF* homolog search.

S. no	<i>M. polymorpha</i> gene ids	Repeat length	Number of repeats
1	Mapoly0112s0050	169 aa	5
2	Mapoly0112s0046	169 aa	4
3	Mapoly0193s0017	169 aa	2
4	Mapoly0120s0049	169 aa	4
5	Mapoly0318s0001	160 aa	3

3.4 Discussion

3.4.1 Phenotypic and molecular characterization of *short-leaf (shlf)* mutant indicate differential auxin accumulation

A comprehensive analysis of *shlf* mutant revealed pleiotropic phenotypes such as leaf size, shape, temperature sensitivity, early etiolation and reduced apical dominance. *shlf* leaf length

deviated from WT as early as P2 indicating that the primary growth of *shlf* leaves was affected (Figure 3.1 A and B). Maximum leaf length of *shlf* lines was comparable to the length of P3 in WT, which clearly established the short-leaf phenotype. Leaves of *shlf* were both short and narrow compared to WT (Figure 3.1 C and D). WT moss develop oblanceolate leaves as a result of persistent cell divisions and growth along the centre of the proximal-distal axis (Harrison *et al.*, 2009). An interesting observation was that the *shlf* leaf were lanceolate and the widest region of the *shlf* leaf is at the base rather than the centre of the proximal-distal axis (Figure 3.1 D and E). This could be due to the uniform exit of the cells from the cell cycle in *shlf* leaves. The overall reduction in leaf area, the total number of cells per leaf and increased cell density in *shlf* leaves indicate that both the cell division and elongation were affected (Figure 3.2 B, C and F). The basal cells of WT leaves are known to be bigger than tip cells. Hence, in *shlf* mutant leaves, the effect of cell elongation suppression was more pronounced in cells at the leaf base than the leaf tip (Figure 3.2 G and H). A similar reduction in leaf size has been reported in *P. patens* by treating the gametophores with PAT inhibitor (5 μ M NPA) along with a synthetic auxin (100 nM NAA) or with only auxin analogue (10 μ M 2,4,-D) (Bennett *et al.*, 2014). It is plausible that auxin accumulation at high concentration in developing leaves could hamper their cell division and elongation, an observation consistent with our *shlf* leaf phenotype.

shlf gametophores varied also in their response to environmental factors in comparison to WT. While WT leaf length reduced at both low and high temperatures, *shlf* leaf length showed a negative correlation to increased temperature (Figure 3.3 A). Auxin is known to be involved in high-temperature stress. When the growth temperature was shifted from 20 °C to 29 °C, *Arabidopsis* plants produced a higher amount of auxin (Gray *et al.*, 1998). Similarly, rice plants also had increased auxin biosynthesis upon heat stress (Du *et al.*, 2013). Not only that, *P. patens* too showed increased auxin-responsive promoter activity (*GH3*) when grown at elevated temperature (28 °C) for 28 days (Mittag *et al.*, 2015). Thus, an increased auxin accumulation in leaves may explain the reduction of leaf length in *shlf* mutant. In our study, as 12 °C does not represent the extreme cold condition, the reduction in WT leaf length could be because of auxin production below the optimum level. Similarly, the early etiolation phenotype of *shlf* could also be due to the high accumulation or hypersensitivity of moss to auxin (Figure 3.3).

Among pleiotropic phenotypes of *shlf* mutant, reduced apical dominance was the most elusive. *shlf* gametophores had a mean apical inhibition zone of 8 metamers, while that of WT had 14 metamers (Figure 3.4). Also, the average internodal distance of *shlf* gametophores

was significantly higher than the WT. In flowering plants, auxin efflux carrier (PIN) proteins-mediated PAT causes apical dominance (Gälweiler *et al.*, 1998; Crawford *et al.*, 2010). Though moss gametophores have apical dominance, surprisingly, PAT was not detected by radioactive auxin feeding assays (Fujita *et al.*, 2008). Also, *pinA pinB* double knockout lines did not alter the branching pattern in *P. patens* (Bennett *et al.*, 2014). Recent report in Arabidopsis have shown that auxin is transported by diffusion through PD connections as well and this particular transport is regulated by the accumulation of callose in PD (Han *et al.*, 2014). Coudert *et al.*, (2015) have shown that, treatment of WT *P. patens* gametophores with callose biosynthesis inhibitor (DDG) can increase the apical inhibition zone. It is believable that auxin can diffuse through PD in moss gametophores and regulate branching patterns. Interestingly, in our study, *shlf* mutant gametophores indicated differential auxin accumulation patterns, where the apex had intense *GUS* expression compared to base (Figure 3.6). Upon DDG treatment of *shlf* gametophores, the *GH3::GUS* expression was higher at the base than the apex (Figure 3.6) suggesting that *shlf* mutant has a probable defect in auxin diffusion mechanism. Aniline blue staining of PD-associated callose suggested that PD density is low in *shlf* leaves (Figure 3.7 C). However, measurement of PD density based on transmission electron microscopy (TEM) could provide foolproof evidence to confirm these findings and can answer the cause of defective auxin diffusion mechanism in *shlf* gametophores.

3.4.2 *SHLF* is the causal gene of *short-leaf* mutant

WGS analysis revealed the T-DNA and Tnt1 insertions in *shlf* genome. As expected the T-DNA insertion was in an intergenic region and two out of three (66%) Tnt1 insertions were in genic region (Table 3.2). One of the insertions was inside the open reading frame of an *PpEXTENSIN* gene (Pp3C1_9390), which could potentially disrupt its function (Figure 3.8 A). EXTENSIN proteins are shown to be involved in the self-assembly of the cell wall (Cannon *et al.*, 2008). Though our results suggested that the *shlf* mutant could be defective in auxin diffusion through PD, the over-expression of *PpEXTENSIN* did not recover the *shlf* phenotype (Figure 3.10). The second candidate is a protein (Pp3C14_22870) with an unknown function, whose over-expression in *shlf* background recovered the short-leaf phenotype (Figure 3.12) and thus we termed it as *SHORT-LEAF* (*SHLF*) gene. This protein is found to have four repeats in genomic DNA/ mRNA (513 bp) and protein (171 aa) (Figure 3.13). Though similar repeat-containing proteins have been reported earlier, they are typically of 5 to 50 aa in length (Jorda *et al.*, 2010). ARMADILLO repeat-containing proteins like poly-ubiquitin is present in all plants, animals

and fungi (Hatzfeld, 1998). Many plant proteins have tandem repeats, which are hypothesized to participate in protein-protein interactions: for example, the tetratricopeptide repeat (34 aa), the Kelch repeat (47 aa), the WD40 repeat (39 aa) and the ankyrin repeat (33 aa) (Groves and Barford, 1999, Adams *et al.*, 2000, Kobe and Kajava, 2001, Stirnimann *et al.*, 2010). However, to our knowledge, protein like SHLF with repeats as long as 171 aa has not been reported till now (Figure 3.15). At this stage, no basic information about the structure of SHLF is available. In general, proteins with repeat length >30 aa are hypothesized to form a bead-on-a-string structure (Lee *et al.*, 1989; Jorda *et al.*, 2010). To verify that *SHLF* is not a pseudogene, it was amplified from cDNA and SHLF specific peptides were detected in *P. patens* proteome. Interestingly, we identified that SHLF protein sequence has an N-terminal ER-targeting signal, which is conserved in *Sphagnum fallax* (Moss) and *Marchantia polymorpha* (Liverwort) (Figure 3. 16). Through bioinformatics analysis, we could infer that the ER-targeting signal in SHLF could have functional relevance, since only 3.8% of moss proteome has been predicted to have an ER-targeting signal. Therefore, in our study, N-terminal and C-terminal fluorescent tagged SHLF transgenic lines were generated. Presently, the microscopic experiments are being optimized to determine the cellular localization and potential function of SHLF protein in *P. patens*.

3.4.3 *SHLF* represents a novel bryophyte-specific gene family

We traced the phylogeny of the *SHLF* to understand its origin and conservation in plants. For this analysis, altogether genomic resources from 18 different species (one each algal and liverwort genomes, transcriptomes from ten mosses and six liverwort species) were used. This showed the presence of *SHLF* homologs in 6 mosses and 4 liverworts (Table 3.3) (Figure 3.17). Poor quality of transcriptomic data could be the reason for the absence in some of the bryophytes. We also detected a poorly conserved *SHLF* homolog-like gene from the genome sequence of *Klebsormidium nitens* (Figure 3.18). However, this observation would require further analysis to conclude. Since no homologs were detected in chlorophycean algae and higher streptophytes (Hornwort and vascular plants), we speculate that *SHLF* could be specific for early streptophytes. Conservation of *SHLF* only among these early streptophytes could suggest that it might have played a key role in colonization of land.

To validate the functional conservation of *SHLF* across early streptophytes a cross-species complementation (an attempt to revert the *shlf* phenotype using *MpSHLF50*) is

presently in progress (Figure 3.19). *SHLF* gene does not have any paralog in the 511 MB *P. patens* genome although moss genome is reported to have undergone two rounds of genome duplication (Lang *et al.*, 2017). On the other hand, five identified homologs of *SHLF* from 280 MB *Marchantia* genome with a maximum of five repeats (Table 3.4) raises interesting questions about the phylogeny and functions of this novel bryophyte specific protein in evolutionary landscape.

In summary, we showed the characterization of pleiotropic phenotypes of *shlf* mutant such as short-leaf, altered temperature sensitivity, early etiolation response and reduced apical dominance. The differential auxin accumulation patterns revealed by *GH3::GUS* expression could be the cause of these pleiotropic phenotypes as observed in *shlf* moss mutant. Low density PD-associated callose staining and DDG treatments further indicated a probable defect in auxin diffusion through PD. However, a detailed TEM analysis would be necessary for further confirmation of this conclusion. Through WGS and mutant phenotype recovery studies, we have identified the causal gene for *shlf* phenotype. The *SHLF* gene has no known conserved domain but has unique long tandem direct repeats at genomic DNA, mRNA and protein levels. Interestingly, the *SHLF* gene is conserved only among early streptophytes and thus appears to be a potential key player in land plant colonization.

Part of this work has been submitted for research publication:

Mohanasundaram B *et al.*, (2018). *SHORT-LEAF* (*SHLF*) - a bryophyte-specific protein regulates auxin transport in *P. patens* gametophores. (Manuscript under preparation).

**4 A reverse genetic approach to characterize the role of
SCARECROW orthologs of *P. patens* in gametophore
shoot development**

4.1 Introduction

In addition to our forward genetic mutant screen, a parallel reverse genetic approach was also initiated to understand the gametophore shoot development in moss with key GRAS domain transcription factors. *P. patens* orthologs of *SCARECROW* (*SCR*) transcription factor which regulate a crucial asymmetric cell division (ACD) in *Arabidopsis* root were chosen as potential candidates. Using homologous recombination-based knock out strategy, histology and microscopic studies, we attempted to determine the function of *P. patens SCR* (*PpSCR*) in this chapter.

Physcomitrella patens (*P. patens*) has high homologous recombination frequency which enables generation of targeted knockout lines for the gene of interest. With the availability of genome sequence, many essential transcription factors like the class I and II *KNOX*, *CURLY LEAF*, epidermal patterning factors (*EPFs*) and membrane-localised receptors like *ERECTA* that regulate body plan have been characterized in *P. patens* (Sakakibara *et al.*, 2008; Okano *et al.*, 2009; Sakakibara *et al.*, 2013; Caine *et al.*, 2016). The function of *EPFs* and *ERECTA* genes in stomata development is conserved among sporophytes of land plants (Caine *et al.*, 2016). However, the role of class I *KNOX* and *AP2*-type transcription factors are shown to be not conserved between functionally orthologous organs like sporophytic SAM and gametophore apex of moss (Sakakibara *et al.*, 2008; Aoyama *et al.*, 2012). These studies have suggested that the genetic regulatory network governing haploid and diploid body plans are distinct. Hence, to predict the function of a key gene in moss gametophore development based on our knowledge from *Arabidopsis* is appeared to be challenging.

In *Arabidopsis*, *AINTEGUMENTA* (*AIN*), *PLETHORA* (*PLT*) and *BABY BOOM* (*BBM*) (*APB*) genes, collectively known as *AP2*-type transcription factors have been shown to regulate cell proliferation, stem cell niche formation in root apical meristem (RAM) and embryogenesis respectively (Elliott *et al.*, 1996; Boutilier *et al.*, 2002; Aida *et al.*, 2004). *SCARECROW* (*SCR*) transcription factor is known to regulate an asymmetric division in RAM and is a member of gene regulatory network governing root development along with *PLT* genes in *Arabidopsis* (Scheres *et al.*, 1995). However, *P. patens* orthologs of *AP2*-type transcription factors are demonstrated to play role in gametophore apical cell formation (Aoyama *et al.*, 2012) instead of rhizoid development. We hypothesize that the members of *Arabidopsis* RAM regulatory network could be conserved between *P. patens* as well. Therefore, we selected *SCR* transcription factors as candidates to study their role in the moss gametophore shoot develop-

ment.

4.1.1 SCR is a GRAS domain transcription factor

Both SCR and SHORTROOT (SHR) transcription factors have GRAS domain in their protein sequence and part of RAM regulatory network. GRAS domain proteins form a plant-specific protein family with many members and play essential roles in plant growth and development, functioning primarily in transcriptional regulation. It is named after the three genes, *GIBBERELLIC ACID INSENSITIVE (GAI)*, *REPRESSOR of GAI*, and *SCARECROW (SCR)* (Li *et al.*, 2014). The *SCR* transcription factor is required for radial patterning of the *Arabidopsis* root (Scheres *et al.*, 1995). At the RAM, the cortex endodermal initial cell undergoes an asymmetric division to form the ground tissue comprising the cortex and epidermis. In *scr* mutants, due to the loss of an asymmetric periclinal division, a single layer ground tissue was formed with the characters of both cortex and epidermis. Hence, Scheres *et al.*, (1995) suggested that *SCR* transcription factor specifically regulates the asymmetric cell division in *Arabidopsis* root. Along with *SCR*, *SHR* and auxin gradient control the radial patterning and ground tissue development of *Arabidopsis* roots (Benfey *et al.*, 1993; Scheres *et al.*, 1995; Perilli *et al.*, 2012). The *SCR* transcription factor also regulates leaf development. In *scr* mutant, leaf size was heavily reduced because *SCR* is required for prolonging the S-phase duration during the leaf development (Dhondt *et al.*, 2010). Interestingly, *Zea mays* PIN1a proteins were found to be localized to end walls of the bundle sheath cells, which is reminiscent of its localization in the root endodermis (Slewinski *et al.*, 2012). Bundle sheath cells are critical anatomical feature that enables C4 photosynthesis. Authors showed that the *Zea mays scr* mutants had impaired epidermal cell formation and Casparian strip development (Slewinski *et al.*, 2012). This also implied that engineering *SCR* pathway could possibly enable to develop C4 rice as has been proposed by multiple authors (Slewinski, 2013).

4.1.2 Asymmetric divisions and moss gametophore development

Plant cells frequently make developmental decisions using ACD (De Smet and Beeckman, 2011). The microspore of angiosperms divides asymmetrically into a larger vegetative cell and a smaller generative cell (Borg *et al.*, 2009). The apical and basal polarity of the *Arabidopsis* embryo is determined by an ACD (Mayer *et al.*, 1993). The basal cell develops into a hypophysis, which divides asymmetrically, and the smaller daughter cell forms the organizing centre

of RAM (De Smet *et al.*, 2010; Lau *et al.*, 2010). Similarly lateral root formation, stomata development, root ground tissue establishment has also been shown to control by ACD in *Arabidopsis* (Benfey *et al.*, 1993; Scheres *et al.*, 1995; De Smet *et al.*, 2008; Peterson *et al.*, 2010). Recent studies have revealed that ACDs play a crucial role in throughout the moss development (Harrison *et al.*, 2009; Kofuji and Hasebe, 2014).

The tetrahedral apical cell of moss gametophore has been shown to divide in three cutting faces, which leads to the formation of leaf apical cells (LAC) in a spiral arrangement (Crandall-Stotler, 1980). Elegant sector analysis and live-imaging on *P. patens* leaves revealed the further cell division pattern in the leaf development (Harrison *et al.*, 2009). The LAC cell undergoes a series of ACDs and contributes daughter cells basipetally to form the leaf primordium. The secondary growth begins from the base of the leaf primordium as each daughter cell initially undergoes two rounds of ACDs along the medial-lateral axis and finally gives rise to a segment of the mature leaf. This wave of secondary growth moves acropetally and does not reach the distal end segments. Since distal segments are cleaved from LAC much later than those at the base, they have less secondary growth phase than the basal segments. Hence, segments towards the tip occupy less leaf area. Despite many known role of ACD in developmental decisions of gametophore growth in moss, knowledge of the gene regulatory network remains largely unknown.

Hence, to understand the missing links in the development of mature moss gametophore from a single tetrahedral gametophore apical cell, the following approaches were undertaken,

- To identify *P. patens* orthologs of *Arabidopsis SCARECROW (SCR)* gene
- To generate knockout lines of *P. patens* orthologs of *SCR*
- To phenotypically characterize the knockout line of *P. patens* orthologs of *SCR*

4.2 Materials and methods

4.2.1 Phylogenetic tree construction

The GRAS domain-containing protein sequences from *Arabidopsis thaliana* and *P. patens* were retrieved in FASTA format from the plant transcription factor database (Jin *et al.*, 2016). All

the sequences were aligned using the multiple sequence aligner available with Clustal W 2.0 (Larkin *et al.*, 2007). From the multiple sequence alignment, the gaps were excluded and corrected for multiple substitutions. The phylogenetic tree was constructed using the neighbour-joining algorithm and bootstrapped with 1000 iterations using Clustal X version 2.0 (Larkin *et al.*, 2007). The phylogenetic tree was visualized and annotated using Figtree software (www.tree.bio.ed.ac.uk/software/figtree/).

4.2.2 Moss culture and maintenance

Culturing of *Physcomitrella patens* ecotype ‘Gransden’ was performed as described in the section 2.2.1. For leaf width assay, seven-day-old protonemal filaments were inoculated in BCD and BCDAT media containing 10 μ M 6-Benzylaminopurine (BAP). Leaf width was recorded from P9 leaves of one-month-old gametophores.

4.2.3 Cloning and plant transformation

The *Ppscr3* knockout construct was prepared by cloning the 5' and 3' flanking regions of Pp3c19_18560 gene into the pTN186 vector (4.5 Kb). The 5' flanking region (1273 bp) and 3' flanking region were subcloned into pGEM-T vector and sequence confirmed. 5' flanking region was cloned into the pTN186 vector between *KpnI* and *Sall* restriction enzyme (RE) sites, and 3' flanking region was cloned between *SmaI* and *SacI* RE sites. This construct (Figure 4.4) was PCR amplified using the primer pair Pp_s882_5'_Nf and Pp1s882_3'_R (Table 4.1) and used for PEG-mediated protoplast transformation.

4.2.4 PEG-mediated protoplast transformation

PEG-mediated *P. patens* protoplast transformation was performed as described earlier in the section 3.2.4. Five days after transformation, regenerated protoplasts were transferred to primary selection media containing hygromycin (20 mg/ L). After two weeks of incubation, colonies were transferred to relaxation media for two weeks. Colonies surviving on relaxation medium were further transferred to secondary selection medium containing hygromycin (20 mg/ L) for additional two weeks before being subjected to polymerase chain reaction (PCR) to detect 5' and 3' homologous recombination.

Table 4.1: List of primers used in this study.

S.No	Primer name	Sequences 5' to 3'
Knockout line generation		
1	Pp_s882_5'_Nf (KpnI)	GGTACCGAAATATCCATTGGATCATGAGCGG
2	Pp_5882'_5NR (SalI)	GTCGACCCTAGCAGGAGACTTCAACGAACAG
3	Pp1s882_3'_F (SmaI)	CCCGGGTCACCGTATTGCCTGCTCTCCCGAA
4	Pp1s882_3'_R (SacI)	GAGCTCCTATGTTACCAAATTAAGCAGATTA
Knockout line confirmation		
5	SCR3_KO_5' fusion_conf F	TTTGGAAGCATGGCATGTCGTT
6	KO_5'_sGFP_conf R	GTCCTTGAAGAAGATGGTGC
7	KO_APH4_conf_F	AAGATGCTAAGGCAGGGTTGGTT
8	SCR3_KO_5' fusion_conf R	ATCTCACCGACCACAGGTTCAA
qRT-PCR Primers		
9	Act_qF	ACCGAGTCCAACATTCTACC
10	Act_qR	GTCCACATTAGATTCTCGCA
11	PpSCR3_qF	AGAGACTGGGGCTCGTACTAA
12	PpSCR3_qR	TGTAACCTCACCTTCTCTCAGCATC
in situ probes		
13	PpTub_F	GGCAAGGTATCGTCAGAGGAGATGAG
14	PpTub_R	CTACCGTCGTGTCGCTTGGCATG
15	PpSCR3_F	ATGGCTTTGGTATGTCCTAATCCAAG
16	PpSCR3_R	GCTGTGAAAAGGATCTCGCAAGTT

4.2.5 qRT-PCR analysis

For qRT-PCR analysis, total RNA was extracted from protonema and gametophore tissue using RNAiso Plus (Takara Bio USA Inc., CA, USA). Two micrograms of RNA samples were reverse-transcribed using oligo dT primers and SS-IV reverse transcriptase (Invitrogen, CA, USA). Specific PCR primers were designed to detect endogenous β -actin(Act_F, Act_R) and *PpSCR3* gene (PpSCR3_qF, PpSCR3_qR) transcripts (Table 4.1). cDNA was diluted to 1:10 concentration only during β -actin transcript amplification and relative quantification of other transcripts were performed using the Bio-Rad CFX96 Touch Real-Time PCR Detection System (Bio-Rad, CA, USA). Cyclor conditions were as follows 95 °C for 10 sec; 40 cycles of 95 °C for 5 sec and 55 °C for 30 sec and an additional step for melting curve analysis at 95 °C for 10 sec. SYBR green used for detection of transcripts was SYBR Premix Ex *Taq* II (Tli RNaseH

Plus) from Takara (Takara Bio USA Inc., USA). Each plate was run with samples including no cDNA template control. Relative target gene expression levels were carried out using β -actin as a reference gene and fold-change (sample value/ reference value) was calculated based on the $2^{-\Delta\Delta C_t}$ method of Schmittgen and Livak, (2008).

4.2.6 *in situ* hybridization

P. patens tissue (gametophore and protonema) was fixed in histochoice fixative (Sigma., USA) for 3 hrs with 20 mins vacuum infiltration. Fixed *P. patens* gametophores (leaves of moss) were incised with the help of a razor blade into 2 or 3 pieces. Incised leaves were kept for overnight digestion in 1% driselase solution (Sigma) on a rotary shaker at 10 rpm. Chlorophyll was removed from digested *P. patens* tissue by a series of ethanol (Hejátko *et al.*, 2006). *Tubulin* and *PpSCR3* antisense (PpTub_R, PpSCR3_R) and sense (PpTub_F, PpSCR3_F) oligo probes were end-labelled by biotin dCTP (Invitrogen, USA) with TDT enzyme (Takara) according to manufacturer's protocol (Table 4.1). Dot blot assay was carried out to check the labelling efficiency of the biotin labelled sense and antisense probe (Prieto *et al.*, 2007). *P. patens* tissues were added to the pre-hybridization solution containing 2X SSC, 25% formamide and 10% dextran sulfate. 10 μ L (1:10 diluted biotin labelled probe) sense and antisense probe was added in the pre-hybridization solution and kept for 17 hrs at 37 °C. Samples were washed with a solution of 1X phosphate buffer saline (PBS), 0.3 tween 20 and 2X saline sodium citrate (SSC) buffer. Thereafter, samples were placed in 1:250 diluted streptavidin-AP (Life Technologies, USA) for 90 mins in the dark condition. This was followed by rewashing the samples in 1X PBS and 0.3 tween 20 at 37 °C for 15-20 mins. Samples were then incubated in colour developing solution (10 μ L 4-Nitrobluetetrazolium chloride (NBT) and 10 μ L 5-Bromo 4-chloro-3-indolyl-phosphate (BCIP) (Sigma) in 1X PBS overnight for the colour development and finally, the expression pattern of genes of interest was documented under a bright light microscope Leica S8 APO (Leica Microsystems, Wetzlar, Germany).

4.2.7 Microscopy

Live-imaging on *P. patens* myosin XIA-3xEGFP lines was performed to track new cell division in protonema and leaves. Myosin XIA-3xEGFP was a kind gift from Prof. Luis Vidali (Worcester Polytechnique Institute, MA, USA). Protonema and gametophores were mounted on a slide and observed under the confocal microscope Carl Zeiss LSM710 (Zeiss, Oberkochen,

Germany) with the following settings: Laser 488 nm; (35%), 63x lens; (Plan Apo 1.4 OIL DIC M27), MBS 488 beam splitter, 471-544 nm emission, 1 A.U pinhole. Images were taken at every two mins interval and processed using ImageJ software (Schneider *et al.*, 2012).

4.2.8 Histological analysis

For Histology studies, *P. patens* gametophores were fixed in a solution of 10% formaldehyde 50% ethanol 5% acetic acid. Chlorophyll was removed by a series of ethanol washes and was serially replaced with xylene followed by paraffin wax. Thin (10 µm) sections were taken using a Leica RM2265 microtome (Leica Microsystems). Sections were stained with Toluidine blue to increase the visibility of tissue and imaged using a Zeiss ApoTome microscope (Zeiss).

4.3 Results

4.3.1 Identification of *P. patens* orthologs of SCR

A phylogenetic tree of proteins containing GRAS domain from *A. thaliana* and *P. patens* was constructed using the neighbour-joining method. The SCR transcription factor and SCR-like 23 formed a clade with three **P. patens** genes: Pp1s85_139V6.1 (Pp3c21_17650V1.1), Pp1s324_56V6.1 (Pp3c22_13060V1.1) and Pp1s882_1V6.1 (Pp3c19_18560V1.1), which will be referred as *PpSCR1*, *PpSCR2* and *PpSCR3*, respectively. This clade and the sub-clade formed by the *P. patens* proteins had high bootstrap values (969/1000 and 992/1000, respectively) (Figure 4.1).

Out of the three SCR orthologs that we identified, *PpSCR2* and *PpSCR3* were detected by RT-PCR and confirmed with DNA sequencing (Figure 4.2 A). For future studies, the *PpSCR3* gene was selected based on the knockout phenotype. Quantitative RT-PCR analysis showed that *PpSCR3* gene was highly expressed (>4 folds) in protonemal tissues (Figure 4.2 B). To understand the tissue-specific expression pattern of *PpSCR3*, *in situ* hybridization was performed using oligo probes. Because leaves were not permeable for *in situ* probes, an incision was given. *PpSCR3* was found to be expressed in protonema as well as the leaf blade cells (Figure 4.3 B, D, F, and H) an. *PpSCR3* expression was uniform in these tissues and any tissue-specific expression pattern was not observed. *Tubulin* antisense probe showed localization throughout the protonemal and incised leaves while sense probe did not produce any signal

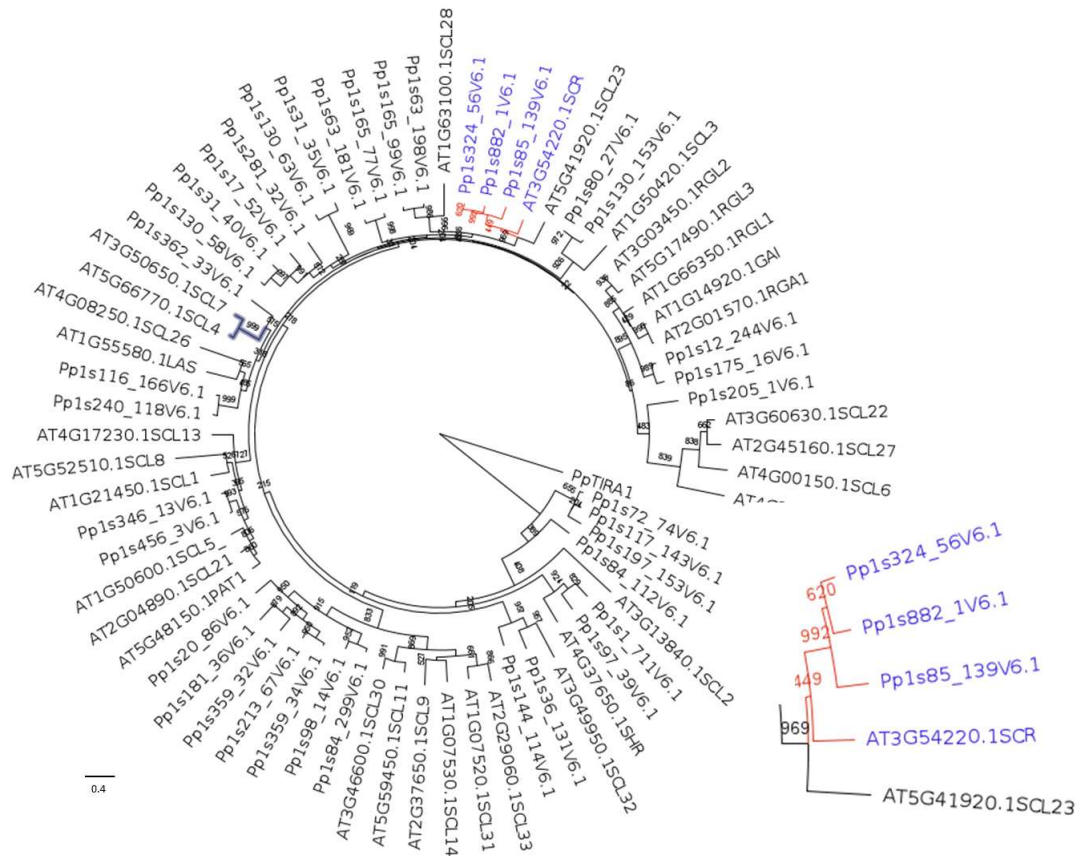


Figure 4.1: Phylogenetic tree of GRAS domain containing transcription factors of *Arabidopsis thaliana* (At) and *Physcomitrella patens* (Pp). A non-GRAS domain-containing protein from *P. patens* TIR1-like auxin receptor (TIRA1) was used as an outgroup. The SCR clade (blue) was zoomed in to show the bootstrap values (red). The bar indicates 0.4 substitutions per site in the main tree.

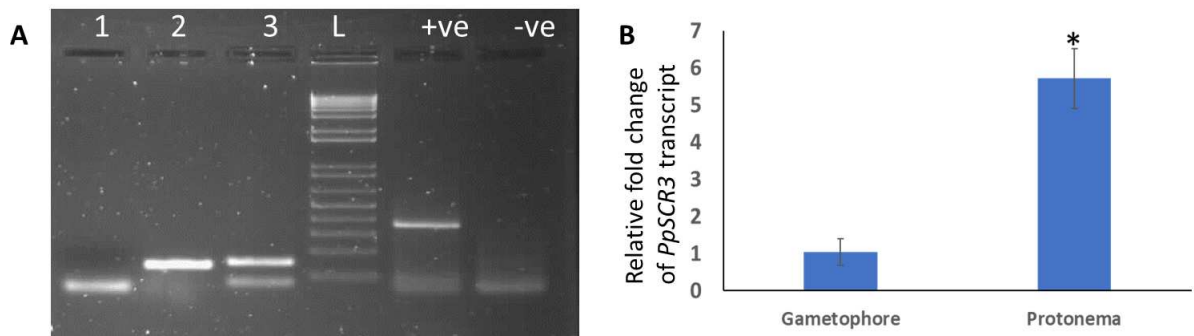


Figure 4.2: Expression analysis of *P. patens* SCARECROW orthologs. (A) RT-PCR detection of *P. patens* orthologs *PpSCR1* (1), *PpSCR2* (2) and *PpSCR3* (3). Wells were loaded as 100 bp ladder (L), *PpActin* as (+ve) and water as (-ve) control. (B) Relative transcript abundance of *PpSCR3* was measured compared to the β -actin reference in gametophore and protonema tissue types. Student's t-test was performed on data $n = 3$, and asterisks indicate statistical significance where * is $p < 0.05$.

(Figure 4.3 A, C, E, and G) and was used as a positive control.

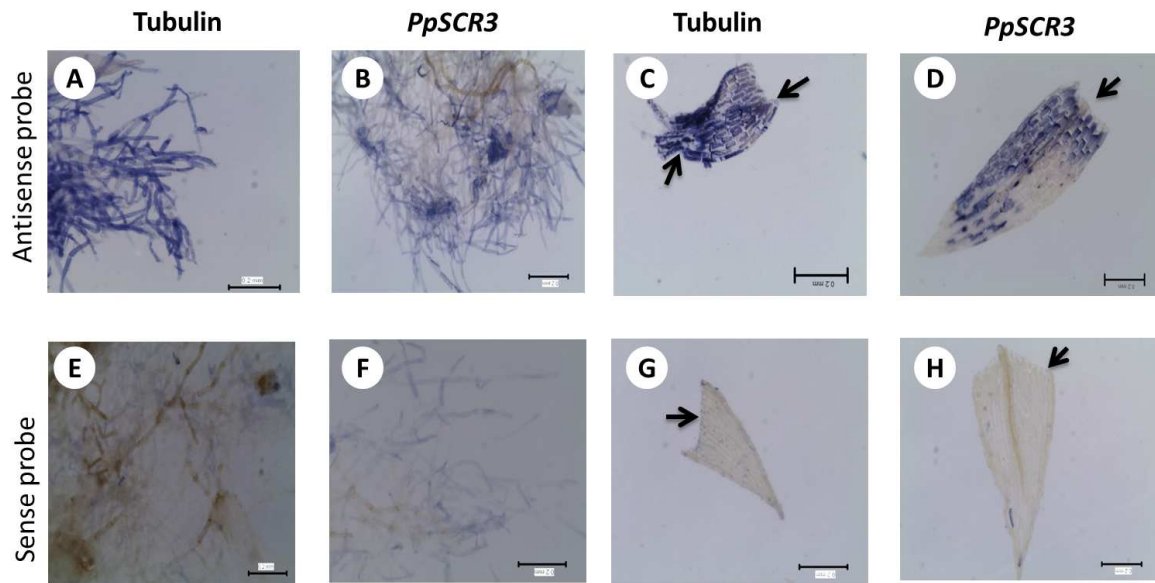


Figure 4.3: *in situ* hybridization to detect the expression pattern of *PpSCR3* In protonemal tissue, sense and antisense probes of tubulin (A and E), *PpSCR3* (B and F) showing their respective expression patterns. Leaves were incised to increase the permeability of the probe (arrow mark). In leaves, both *Tubulin* (C and G) and *PpSCR3* (D and H) expression were detected at the incision site. *Tubulin* was used as positive control. Scale bar is 0.2 mm.

4.3.2 *Ppscr3* knock out lines developed slender-leaves

Homologous recombination-based knockout construct for *PpSCR3* was prepared in pTN186 vector and transformed into *P. patens* protoplast by PEG-mediated transformation (Figure 4.4). All the four lines had successful 5' homologous recombination and developed a slender-leaf phenotype. However, only line 12 had 3' homologous recombination. Hence, line 12 was chosen for further phenotypic and molecular characterization. The *Ppscr3* transformed colonies of moss were visible distinctly from wild-type due to the slender nature of all of the leaves (Figure 4.5 A, B, E, and F). The 9th leaf of the *ppscr3* knocklout line was significantly different in length and width (Figure 4.5 C and D). The leaf width measured at the middle of the proximal-distal axis has reduced up to four times, while the length increased less than two times. These results suggested that the *Ppscr3* might produce slender leaves and detailed histological studies would be required to understand this phenotype.

P. patens leaf width was shown to be sensitive to the availability of nitrogen and exogenous cytokinin (Barker, 2011). When grown in a minimal media without ammonium

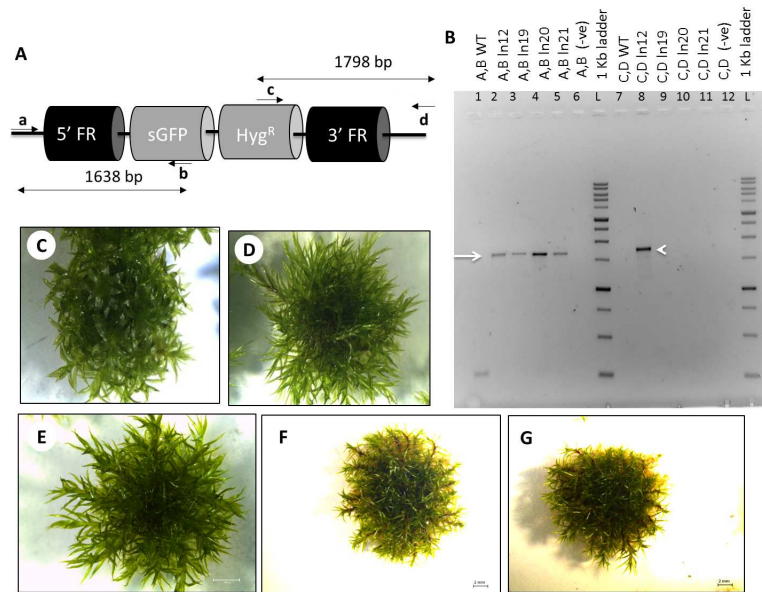


Figure 4.4: Generation of *Ppscr3* knockout lines in moss. (A) schematic diagram showing the *Ppscr3* knockout construct design and PCR confirmation with primers binding sites. Primers: a) *SCR3_KO_5'* fusion_conf F, b) *KO_5'_sGFP_conf_R*, c) *KO_APH4_conf_F*, d) *SCR3_KO_5'* fusion_conf R. (B) Detection of homologous recombination at the 5' flanking region of 1638 bp (wells 2-5 with arrow) and 3' flanking region of 1798 bp (well 8 with arrowhead). WT (C) and *Ppscr3* knock out lines 12, 19, 20 and 21 (D, E, F, and G) used for PCR analysis. Scale bar size 2 mm.

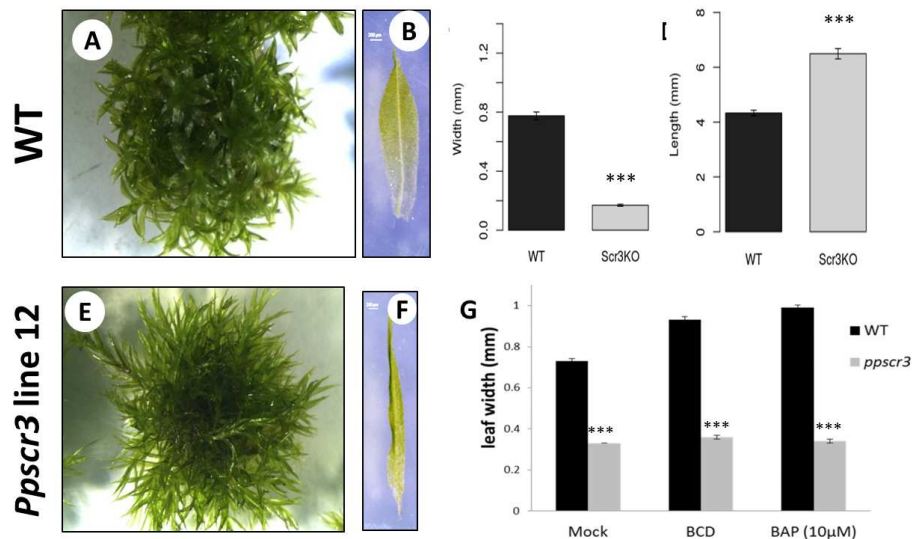


Figure 4.5: *Ppscr3* knockout moss lines produced slender-leaves. Whole colony (A, E), single leaf (B, F), P9 leaf length (C) and width (D). (G) The mean leaf width of WT increased while that of *Ppscr3* lines remained unchanged when grown in minimal BCD media and in the presence of exogenous cytokinin (BAP; 10 µM). Student's t-test was performed on data n = 10 and asterisks indicate statistical significance where * is $p < 0.001$. Scale bar size 2 mm.

source or treatment with exogenous cytokinin (such as BAP), the wild-type (WT) leaf width increased significantly (Figure 4.5 G). However, *Ppscr3* leaf width remained unaffected suggesting that *PpSCR3* functions downstream of genes regulating environmental sensitivity in *P. patens* leaves.

4.3.3 Histological approach to understand the slender-leaf phenotype

P. patens leaves are arranged in a spiral phyllotaxy and have unistratose (single-cell-layer) leaf blade or lamina and multistratose midrib (Figure 4.6 A-C). Hence, it could be possible to track the changes in cell division that might be the cause for the slender-leaf phenotype. Cross section of a gametophore showed the main axis (stem-like) at the centre of the section surrounded by leaves (Figure 4.6 B). Leaf sections revealed the multicell-layered midrib flanked by single-cell-layered leaf blade (Figure 4.6 C). Leaf blade cells near the midrib were bigger than the peripheral cells. Microtome sections of the gametophore apex showed that the spiral phyllotaxy remained unaffected in *Ppscr3*. Cell number of the leaf blade in *Ppscr3* was highly reduced, which perhaps caused the slender-leaf phenotype (Figure 4.6 D and F). Interestingly, the midrib width also increased in the *Ppscr3* leaves compared to WT (Figure 4.6 E and G). These results indicated that the increment in midrib width could have compensated by the reduction in the leaf blade width. Hence, we carried out a detailed histological analysis. Series of microtome sections of leaves of both WT and *Ppscr3* mutant were taken and represented in the leaf tip to base order (Figures 4.7, 4.8, and 4.9).

In general, midrib was absent towards the tip of the WT leaves (Figure 4.7 A). The leaf blade cells were labelled as L1, L2,... and R1, R2,... arbitrarily marking the leaf blades (flanking midrib) as left (L) and right (R). Leaf sections (Figure 4.7 B) showed appearance of a new cell in between L1 and R1, which could have resulted from an anticlinal division of the L1 cell. Further sections showed that this cell-file became a midrib. Hence, it was marked as '0'. Again, figure 4.7 C-E showed that the cell '0' has divided periclinally and resulted in an increment of the number of cell layers at the middle of the leaf blade. The multicell-layered tissue at the middle of the leaf blade is called as midrib. Comparisons of figures 4.7 F and G, showed that a new cell has formed in the midrib, next to the L1 cell. It could be assumed at this stage, that the new small cell came as the daughter cell through an ACD of L1. The daughter cell became multicell-layered by undergoing periclinal and anticlinal divisions (Figure 4.7 G-D). These findings led us to suggest that midrib was developed from the leaf blade cells. As the

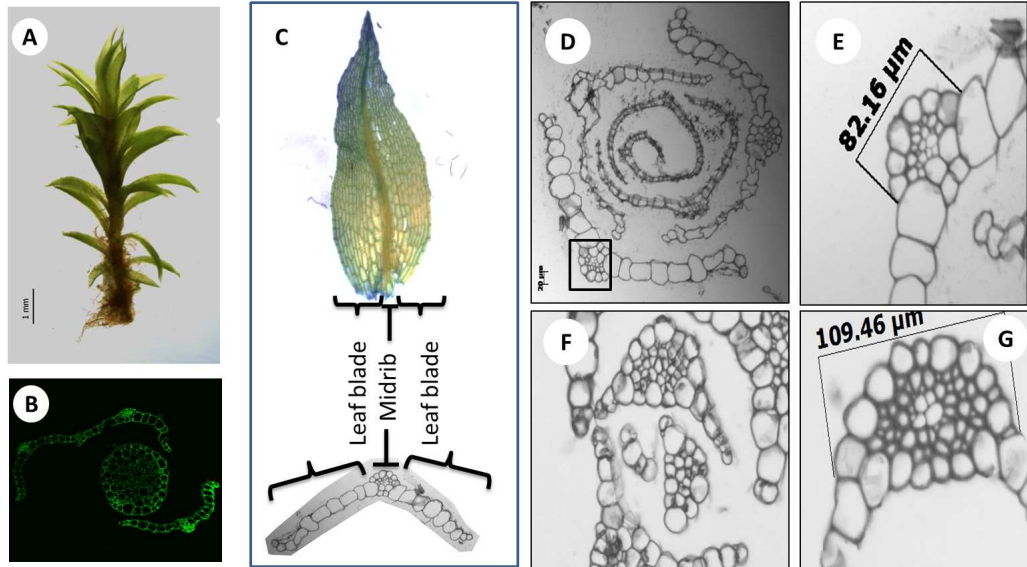


Figure 4.6: Understanding the slender-leaf phenotype with histological sections of leaves. WT gametophore (A), artificially coloured cross-section of gametophore showing the circular mid-axis and the flanking leaves (B). (C) A single leaf of WT partially stained with toluidine blue (top) and the cross-section of the leaf (bottom) showing the midrib flanked by leaf blade. The microtome sections of WT and *Ppscr3* gametophores (D and F) and measurements of the diameter of midrib from leaves (E and G). Scale bar size 1 mm.

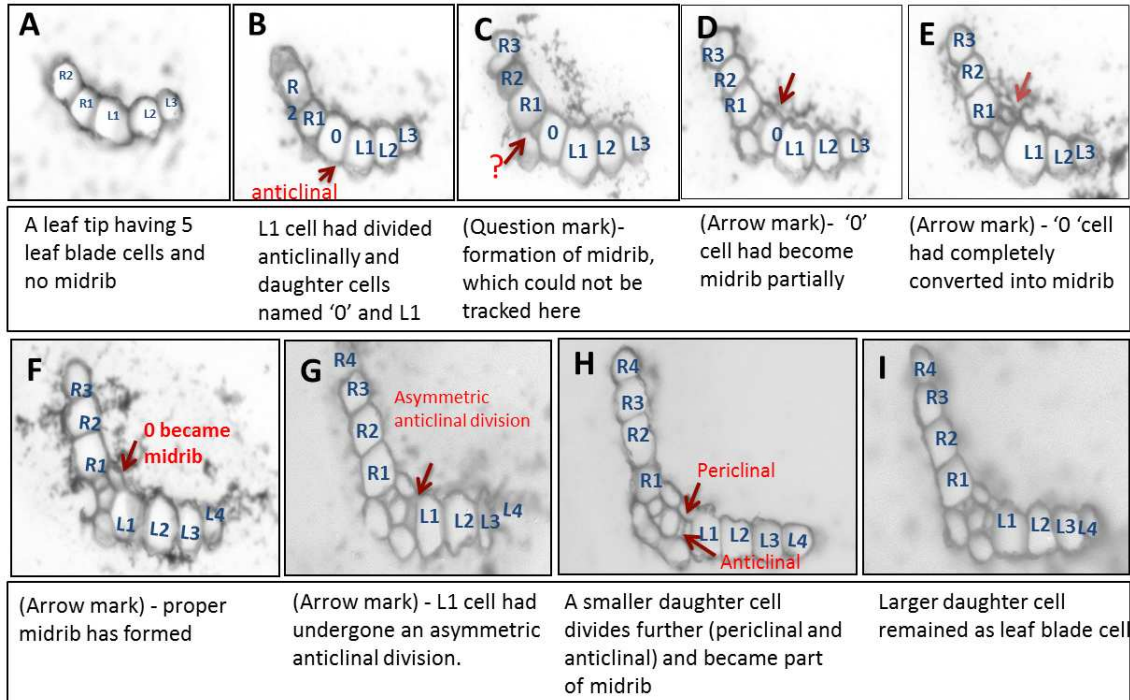


Figure 4.7: Serial cross section of a WT moss leaf from leaf tip to base. (A) At the tip of the leaf, midrib was not developed yet. The anticlinal division of (B, G) first leaf blade cell file (L1) led to increase in leaf blade length. Also, controlled anticlinal and periclinal divisions (D, E and H), contributed to the midrib development. The question mark in (C) represented a sudden increment in the cell layer number.

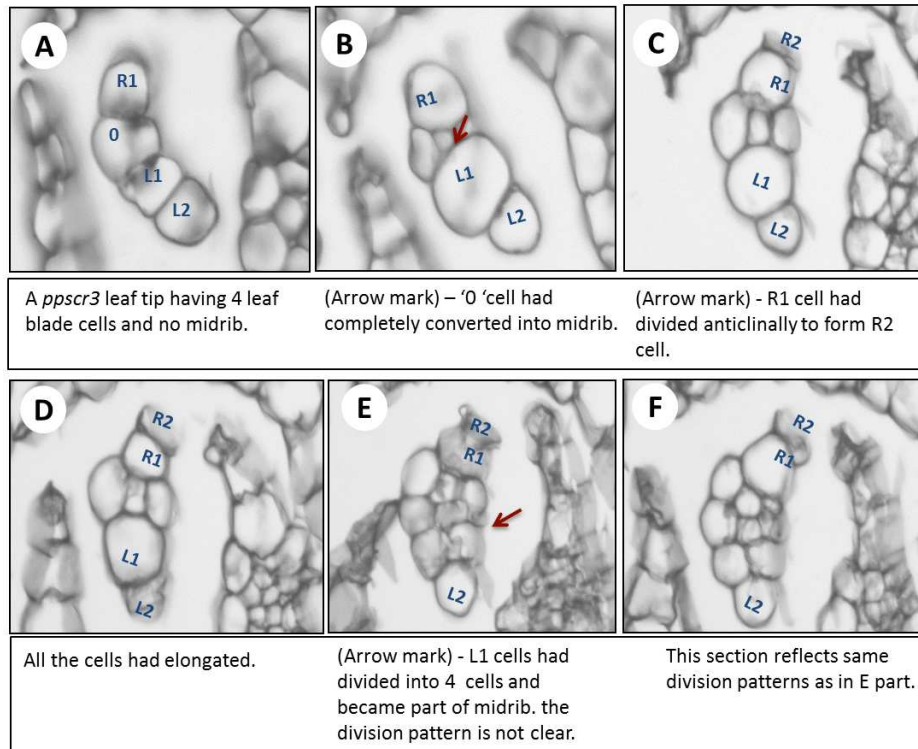


Figure 4.8: Serial cross-sections of a *Ppscr3* mutant leaf from its tip to base. The series of cross-sections from (A) to (F) showed that the L1 leaf blade cell file had undergone a periclinal division instead of anticlinal division (E and F), leading to loss of a leaf blade cell and an increase in midrib cell number and size.

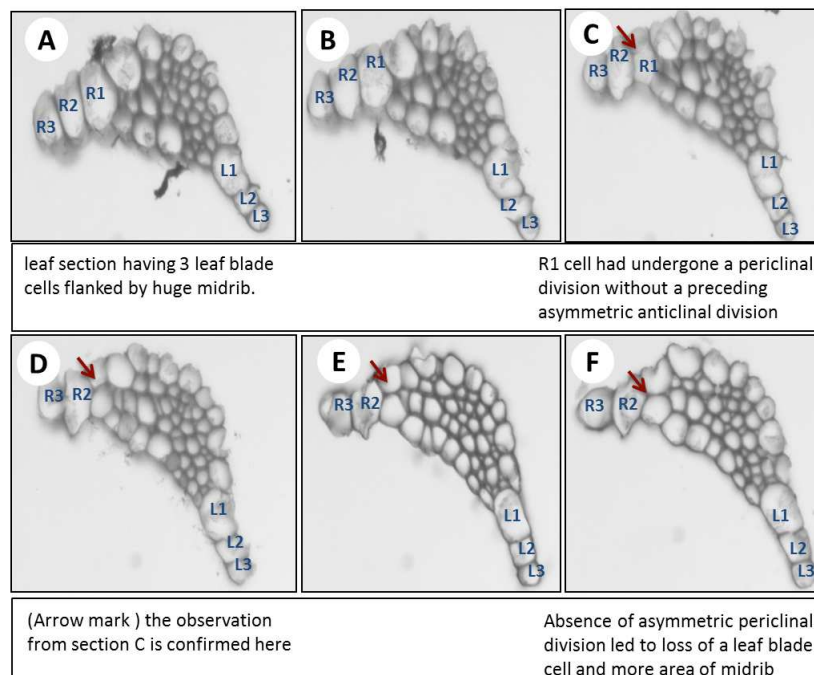


Figure 4.9: Serial cross-sections of a *Ppscr3* leaf at the middle of the proximal-distal axis. The series of images from (A) to (F) showing the first leaf blade cell file (C) dividing periclinally, without any preceding asymmetric anticlinal division leading to increase in size of the midrib.

cell-file concept does not fully apply to *P. patens* leaves, further live-imaging studies would be necessary to draw any final conclusion from these inferences.

Microtome sections of *Ppscr3* leaves were also traced for cell division patterns (Figures 4.8 and 4.9). We could find that the midrib is also absent at the tip of *Ppscr3* leaves (Figure 4.8 A). Leaf blade cells are labelled similar to WT leaf sections. The '0' cell had undergone two periclinal divisions to form a multicell-layered midrib (Figure 4.8 A-D). Surprisingly, further sections indicated that L1 cells had undergone minimum two rounds of cell divisions and became midrib (Figure 4.8 E and F). When sections were taken from the middle of the proximal-distal axis, a wider midrib was observed flanked by merely three to four-leaf blade cells. The entire R1 cell had divided periclinally and became multicell-layered (Figure 4.9). This cell eventually could divide periclinally and become part of the midrib. These results indicated that in *Ppscr3* leaves, leaf blade width had reduced due to less anticlinal divisions, while the midrib width increased due to the periclinal divisions of the first leaf blade cell. As noted before, *P. patens* leaves do not follow a strict cell file concept such as a monocot leaf. However, our literature survey suggested that within a segment of *P. patens* leaves, cell-file concept could be applied. Further, we believe that live imaging of cell division would be necessary to arrive at any definite conclusion.

4.3.4 Live cell imaging of myosin XI-3xEGFP line to study cell division pattern

Live-imaging of cell divisions in *P. patens* leaves has been a challenging task than in protonemal filaments because of the fact that leaf tissue was mostly impermeable to fluorescent dyes like FM4-64. Hence, myosin XI-3xEGFP lines were used to track cell division pattern in leaves. Our overall goal was to use this line as a background and develop a *PpSCR3* knockout line for studying the changes in cell division pattern in slender leaf phenotype. Using these lines, Sun *et al.*, (2018) have already shown that myosin XIA accumulated at the cell plate during protonemal cell division in *P. patens*. At our end, the chloronemal apical cell division was live-imaged (Figure 4.10) and we could reproduce the results of Sun *et al.*, (2018). At 0 min, the EGFP signal was observed throughout the cell plate in an actively dividing cell (Figure 4.10 A). Later, EGFP signal was found only at the periphery of the cell plate (Figure 4.10 B-E) of chloronemal apical cell. After 11 mins, no signal was observed as myosin accumulated specifically in an actively synthesised cell wall (Figure 4.10 F-I). Though these properties of myosin XIA accumulation were ideal for tracking the midrib development, we could not locate

any active cell division in leaves of Myosin XI-3xEGFP line.

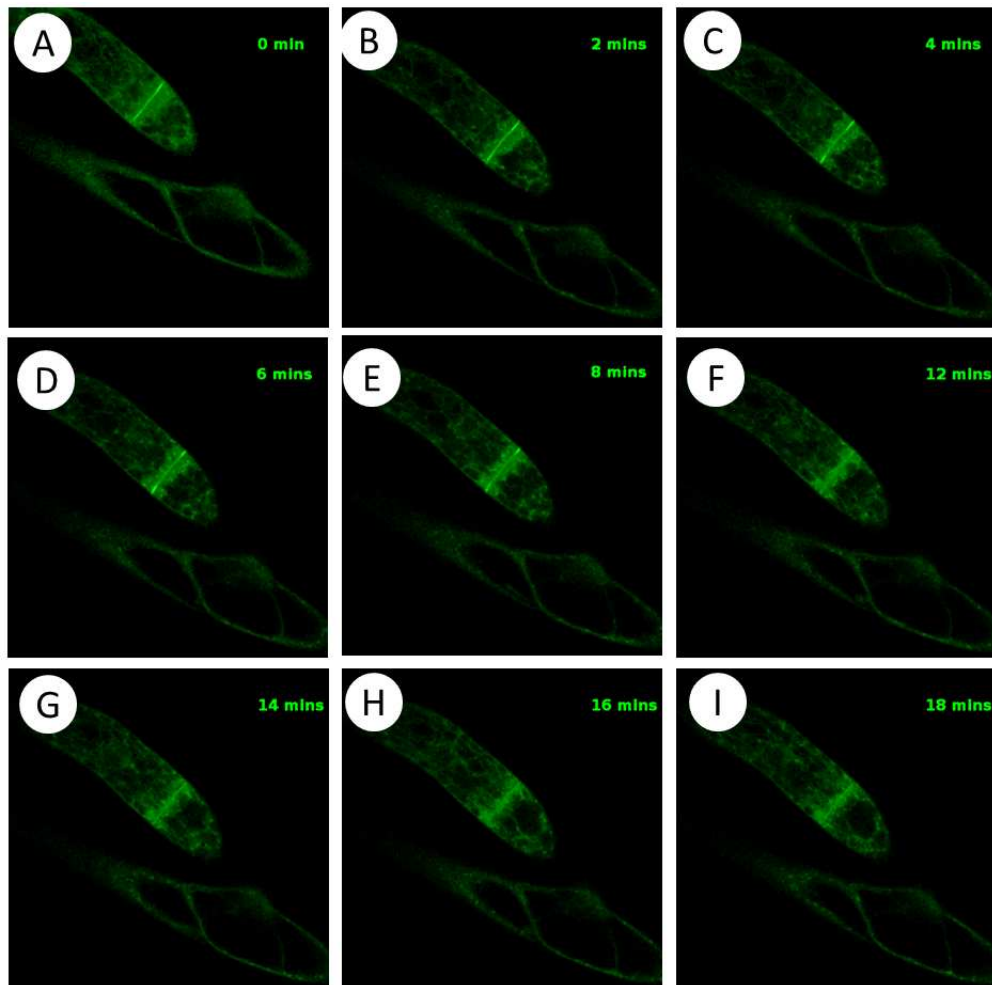


Figure 4.10: Tracking cell division in protonemal filaments using myosin XI-3xEGFP lines. (A) Accumulation of Myosin XIA-3xEGFP on a cell wall being synthesized. Myosin XIA-3xEGFP signal is disappearing from the middle to the periphery of the new cell wall (C - E). Myosin XIA-3xEGFP signal is entirely absent on the newly formed cell wall (F-I).

4.4 Discussion

The phylogenetic tree that we built based on the GRAS domain (amino acid) sequence showed only three orthologs for *SCR* in *P. patens* as opposed to five orthologs based on previous genome annotation (Engstrom, 2011) (Figure 4.1). The *SCR* clade and the subclade formed by the *P. patens* *SCR* orthologs had high bootstrap values reflecting the reliability of our findings. Among these three orthologs, the expression of only two genes was detected from gametophore tissue (Figure 4.2), and one of the orthologs *PpSCR3* was further chosen for the detailed study. An *in situ* hybridization protocol was standardized for *P. patens* protonema and leaf tissues,

which showed that *PpSCR3* expressed in both protonema and leaf tissue (Figure 4.3). *PpSCR3* expression in these tissues was uniform and no tissue-specific expression pattern was observed.

Knockout lines of *Ppscr3* produced slender-leaves, where the mean leaf width was reduced, but the mean leaf length was increased (Figure 4.5). Morphologically, the *Ppscr3* gametophores bearing slender-leaves were similar to the three other moss species such as *Bartramia pomiformis*, *Dicranum scoparium* and *Pleuridium subulatum*. Our literature survey suggest that there are few reports that describe the small or slender-leaf phenotype in angiosperms. In *scr* mutant lines of *Arabidopsis*, the leaf was noted to be small due to an early exit from the cell cycle (Dhondt *et al.*, 2010). In case of rice, loss of function mutation of an auxin biosynthetic gene (YUCCA ortholog) resulted in narrow-leaf phenotype (Fujino *et al.*, 2008). In maize *Dwarf11* mutant, a defect in GA biosynthesis led to the slender-leaf blade development as demonstrated by Wang *et al.*, (2013).

Our histological studies suggested that the number of leaf blade cells along the medial-lateral (ML) axis is highly reduced in *Ppscr3* leaves, and the midrib width has increased (Figure 4.6). Harrison *et al.*, (2009) showed that during leaf development in *P. patens*, each segment initially undergoes two ACD along the ML axis resulting an increase of the leaf width. These divisions are termed as anticlinal divisions because they did not increase the number of cell layers. During the growth phase, further anticlinal divisions along the ML axis contributed to the leaf width. The *Ppscr3* mutant leaves however, lacked anticlinal divisions during the leaf maturation phase resulting into the slender-leaf phenotype. A similar phenotype was observed in maize *rs2* mutant, where the leaf blade was slender, and the midrib was excessively large (Schneeberger *et al.*, 1998). However, in *rs2* mutant, the meristematic cells responsible for the marginal leaf segment were not included among the leaf founder cell population. Hence, the leaf primordium in *rs2* mutant lacked the marginal segment. This also indicates the strict cell-file nature of monocot leaves.

To understand the cause of slender-leaf phenotype and the midrib development, histological sections of WT and *Ppscr3* leaves were studied (Figures 4.7-4.9). Our results indicate that the midrib possibly arises from the leaf blade cells. A competing hypothesis could be that midrib acts as meristem and the leaf blades occur from the midrib. However, this hypothesis could be refuted for the following observations. *P. patens* gametophores have heteroblastic series in which the juvenile leaves at the base of the gametophore lack midrib. Harrison *et al.*, (2009) have showed that due to the ACD of leaf apical cell, leaf segments frequently cross the midrib. Also, cell divisions of the leaf blade cells have been observed during the leaf matu-

ration phase. In an evolutionary perspective, leaves of leafy-liverwort and moss families that has diverged before the origin of *Oedipodium* lack midrib (e.g. *Hedwigia ciliata*) (Blockeel and Stevenson, 2006; Biasuso, 2007). Hence, for moss species, it could be assumed that the leaf blade represents the ground state and the midrib has been innovated later. In flowering plants however, the canalization of the auxin flow hypothesis, which assumes that polar auxin efflux from the developing leaf primordia leads to the formation of mid and lateral veins as explained by a number of reports (Sachs, 1991; Nelson and Dengler, 1997; Rolland-Lagan and Prusinkiewicz, 2005). This suggests that the involvement of auxin in midrib development of moss leaves cannot be ignored and our future studies could provide critical insights in the understanding of moss leaf development.

So far our inferences were based on histological analysis and cell-file concept. Hence, we attempted for live cell imaging as one of the approach to further study cell division pattern using myosin XIA-3xEGFP moss lines. However, our findings suggest that myosin XIA might not be active in leaf cell division. Future studies with alternate cell division markers like *Tubulin* are necessary to visualize and resolve the development of leaf cell division.

At this stage of investigation, we have restricted our analysis of moss leaf development to the histological findings. Based on the current knowledge and the histological observations, we could propose the following model to explain the observed slender-leaf phenotype in *PpSCR3* (Figure 4.10). In WT, anticlinal divisions of leaf blade cells are responsible for an increment of the leaf blade width. The first leaf blade cell (R1) undergoes an ACD, and the smaller cell further divides periclinally (increasing the number of cell layers) to become part of the midrib. However, in *Ppscr3* leaves, the anticlinal divisions of the leaf blade cells are suppressed, which might have resulted the slender leaf blade phenotype. Due to the lack of anticlinal cell divisions in *Ppscr3*, the entire first leaf blade cell undergoes a periclinal division (increasing the number of cell layers) and becomes the part of the midrib. Thus, the lack of an asymmetric anticlinal division could result into development of larger and thick midrib. Only future experiments with live cell imaging may validate this model and our hypothesis.

In summary, we detected three *P. patens* orthologs for the *SCR* transcription factors. *in situ* hybridization for *PpSCR3* showed uniform expression in protonema and leaves. Knock-out lines of *PpSCR3* were developed that produced slender-leaf phenotype. This phenotype was not influenced by the lack of nitrogen source or exogenous cytokinin. Histological analysis advanced our understanding about the midrib developmental patterns in moss. We propose that an ACD of first leaf blade cell contributes to the midrib development. However, this needs

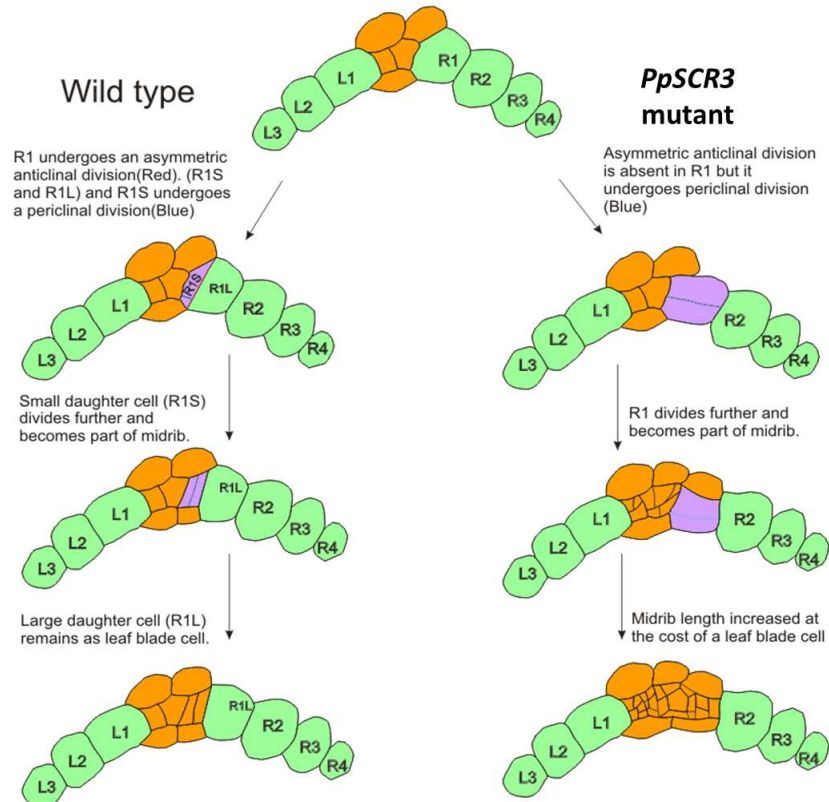


Figure 4.11: Proposed model of cell division patterns and comparison between WT and *Ppscr3* knockout lines.

further validation using live-imaging studies. Though the function of many transcription factors varies between the haploid and diploid phase, *SCR* function in regulating the ACDs appeared to be conserved across plant lineages.

5 Summary and future directions

Leaves are the major photosynthetic organs of a plant. Owing to its contribution to the fitness of the plant, leaf-like organs have evolved independently across plant lineages multiple times, which are majorly grouped as megaphylls, microphylls, and phyllids (Tomescu, 2009). The Zimmerman's telome theory (Zimmermann, 1952) and the enation theory (Bower, 1935) explains the origin and evolution of megaphylls and microphylls from the leaf-less sporophytes. Phyllids are present in the gametophytes of all mosses and leafy-liverworts, and they have high morphological diversity. However, we did not come across any theory of phyllid origin and evolution possibly due to the scarcity of literatures. Though vascular plant leaves and moss leaves are known to be independently evolved, their basic morphological, moss leaves also have midrib flanked by the flat leaf blades with different polarity axes and arranged on a predefined phyllotaxy. However, they vary entirely in the developmental events and genetic regulatory networks. Unlike sporophytic shoot in flowering plants, a single tetrahedral gametophore apical cell divides to form leaf apical cell in a spiral phyllotaxy in moss, which is shown to be robust to exogenous hormone treatments (Crandall-Stotler, 1980; Harrison *et al.*, 2009; Bennett *et al.*, 2014; Kofuji and Hasebe, 2014). In contrast to flowering plants, moss leaf primordium developed by a series of asymmetric cell division of the leaf apical cell. Hence, the total leaf area can be divided into asymmetric segments (Harrison *et al.*, 2009). The major genetic factors regulating shoot apex of flowering plants: such as class I *KNOTTED-HOMEBOX (KNOX)*, *ASYMMETRIC LEAVES1*, *ROUGH SHEATH2*, *PHANTASTICA (ARP)* genes and *CUP-SHAPED COTYLEDON (CUC)* genes are either not involved in gametophore shoot development or not present in moss genome (Sundås-Larsson *et al.*, 1998; Harrison *et al.*, 2005; Floyd *et al.*, 2006; Sakakibara *et al.*, 2008). However, orthologs of *Arabidopsis AP2*-type genes, which are known to be involved in regulating cell proliferation, formation of stem cell niche of root apical meristem (RAM) and embryogenesis (Elliott *et al.*, 1996; Boutilier *et al.*, 2002; Aida *et al.*, 2004) are shown to be necessary for moss gametophore apical cell formation (Aoyama *et al.*, 2012). These studies suggested that the haploid and diploid body plans are distinct.

Hence, we hypothesize that forward genetics would be an ideal approach to study moss gametophore shoot development, and it would benefit from the haploid dominant life cycle of moss. From our literature survey, we find that a number of mutagenesis tools though exist for moss, however, neither this was efficient nor have they been routinely used to develop mutants that can answer gametophore development. It has also been demonstrated that Tnt1 retrotransposon actively transposes in several heterologous angiosperm hosts like *Arabidopsis* (Lucas *et al.*, 1995), *Medicago* (d'Erfurth *et al.*, 2003), soybean (Cui *et al.*, 2013) and potato

(Duangpan *et al.*, 2013) and shown to preferentially transpose into gene-rich regions. At the beginning of our investigation, there was no Tnt1 mutagenesis protocol available for moss. Using *Agrobacterium*-mediated transformation of protonemal filaments, we have developed a Tnt1 insertional mutant population and validated its transposition activity in *P. patens* and characterized mutants defective in gametophore development. Considering the role of orthologs of AP2-type transcription factors (TF) in moss gametophore apical cell development, we also chose orthologs of *SCARECROW* (*SCR*) for a parallel reverse genetic study. It was clear from our literature survey that apart from the knowledge of highly mis-oriented cell arrangement of miniature leaves produced by the class-III *HD-ZIP* knockdown lines of *P. patens* (Yip *et al.*, 2016), there were no other reports that could describe the moss leaf development.

To answer gametophore shoot/leaf development in moss, we laid out the following objectives for this study.

1. To develop an efficient Tnt1 retrotransposon mutagenesis protocol and screen for mutants.
2. To characterize Tnt1 insertional mutants defective in gametophore shoot and leaf development.
3. To study the function of a GRAS domain TF in gametophore shoot development by a reverse genetic approach.

Chapter 1:Introduction

We conducted a thorough literature survey to unravel the different origins and evolution of leaf-like organs across plant lineages. The level of conservation in developmental events and the genetic regulatory network among them were also analyzed. Our literature survey revealed that the origin and evolution of one of the highly diverse leaf-like organ, phyllids, is not understood yet. Though morphologically similar, phyllid developmental events and the genetic regulatory network are distinct from vascular plant leaves. Hence, we have proposed three objectives (stated above) to study the moss gametophore shoot development.

Chapter 2: Development of Tnt1 retrotransposon as a mutagenesis tool and screening of *P. patens* mutants

We chose a forward genetic approach to generate moss mutants defective in gametophore shoot/leaf development. When we began this study, there was no efficient transposition protocol available for *P. patens*. Using *Agrobacterium*-mediated transformation of protonemal filaments, we have developed a Tnt1 insertional mutant population and validated its transposition activity in *P. patens*. We analyzed if *P. patens* could satisfy the host factor requirement for the Tnt1 transposition. We also performed Southern blotting and SSAP-PCR (Sequence Specific Amplified Polymorphism-PCR) to detect Tnt1 transposition events in moss. Thermal Asymmetric Interlaced-PCR (TAIL-PCR) was performed to analyze the transposition preferences of Tnt1 in *P. patens*. Using SSAP-PCR and Tnt1 promoter (Long terminal repeats - LTR) characterization, we examined the stability of Tnt1 insertions. Following were the important findings from the study:

1. Host factor requirement analysis showed that Tnt1 retrotransposon could be functional in all land plants.
2. Southern blot, SSAP-PCR, and TAIL-PCR results confirmed that Tnt1 is functional in *P. patens* and preferentially transposes into gene and GC rich regions.
3. LTR promoter-reporter lines showed that LTR promoter is active in the moss gametophore apical cell. However, SSAP-PCR analysis confirmed that the LTR promoter activity does not reflect in the accumulation of mutagenic load in the mutant genome.
4. Our forward genetic screen yielded many mutants defective in gametophyte development including a *short-leaf* (*shlf*) mutant.

Overall, our results suggest that using protonemal filaments as explants and *Agrobacterium tumefaciens*-mediated Tnt1 insertional mutagenesis tool could also generate moss mutants for forward genetic studies (Mohanasundaram *et al.*, 2018, Under revision).

Chapter 3: Characterization of Tnt1 insertional *P. patens* mutant line, *short-leaf* (*shlf*), defective in leaf development

Our forward genetic screen on Tnt1 insertional mutant population yielded a *short-leaf* (*shlf*) mutant, which had impaired gametophore shoot development. From the literature survey, we came across only the miniature leaves of class III *HOMEODOMAIN-LEUCINE ZIPPER* (*HD-ZIPIII*) knockout lines to be phenotypically similar to *shlf* mutant leaves (Yip *et al.*, 2016). However, leaves of *HD-ZIPIII* knockdown lines had highly mis-oriented cell arrangement, while *shlf* had proper cell arrangement. Hence, we assume that the *shlf* phenotype is caused by a gene, which is not yet characterized in *P. patens*. We began with a complete phenotypic characterization of *shlf* mutant. Using soybean *GRETCHEN HAGEN3* (*GH3*) promoter, we analyzed the auxin accumulation patterns in *shlf* background and also looked at the changes upon callose biosynthesis inhibitor (2-Deoxy-D-Glucose; DDG) treatment. Whole genome sequencing (WGS) was performed to identify the transfer-DNA (T-DNA) and Tnt1 insertions in the *shlf* genome. The two putative candidate genes, disrupted by Tnt1 transposition, were overexpressed in the *shlf* background individually and determined that the phenotype was caused by a hitherto unknown gene. Intensive bioinformatic analyses were performed to identify the origin and phylogeny of the *SHLF* gene. We also attempted to rescue the *shlf* phenotype by overexpressing the *M. polymorpha* homolog to understand the functional conservation across lineages. Following were the important findings from this study:

1. Phenotypic analysis showed that the *shlf* mutant has pleiotropic phenotypes such as small leaf size, shape, temperature sensitivity, early etiolation and reduced apical dominance. The mutant leaves were small due to the suppression of both cell division and cell elongation.
2. Soybean auxin-responsive promoter analysis (*GH3::GUS*) exhibited differential auxin accumulation pattern in *shlf* mutant gametophores. In contrast to wild-type (WT), *shlf* gametophores exhibited high GUS activity in the apex than the base.
3. Differential GUS activity of *shlf* gametophores can be reversed by DDG treatment indicating a possible defect in plasmodesmata-mediated auxin diffusion.
4. Aniline blue staining of plasmodesmata-associated callose revealed that the *shlf* mutant leaves have a low density of plasmodesmata connections.

5. WGS analysis showed one T-DNA insertion and three Tnt1 insertions in *shlf* genome. Two out of three Tnt1 insertions were inside the open reading frame.
6. One of the Tnt1 insertion was found inside a *EXTENSIN* gene which functions in self-assembly of cell wall, whereas the other Tnt1 insertion disrupted a coding region of a gene of unknown function.
7. We observed that *EXTENSIN* overexpression in *shlf* mutant background did not rescue the short-leaf phenotype, however, overexpression of the gene of unknown function rescued the phenotype and determined as the causal gene of the phenotype.
8. Bioinformatic analysis showed that the causal gene (*SHLF*) is novel and has no known conserved domain.
9. Preliminary sequence analyses showed the presence of four unique 513 bp (171 amino acid) repeats in the genomic DNA, mRNA and protein sequences in *SHLF* gene.
10. We could also reveal that *SHLF* is specific for lower streptophytes.
11. Attempts are being made to understand the cellular localization of SHLF protein.

Taken together, our forward genetics approach successfully yielded a novel bryophyte-specific gene, which we believe could answer key questions in colonization of land.

Chapter 4: A reverse genetic approach to characterize the role of *SCARE-CROW* orthologs of *P. patens* in gametophore shoot development

In parallel to a forward genetic approach, we also carried out a reverse genetic approach with key transcription factors (TF) associated with gametophyte shoot development. Literature suggests that AP2-type TFs are necessary for gametophore apical cell development in *P. patens* (Aoyama *et al.*, 2012). In *Arabidopsis*, AP2-type genes, regulate cell proliferation, root apical meristem (RAM) stem cell niche formation, and embryogenesis respectively (Elliott *et al.*, 1996, Boutilier *et al.*, 2002, Aida *et al.*, 2004). SCR TF regulates an asymmetric cell division in RAM and is a member of the gene regulatory network governing root development along with AP2-type TFs. Hence, we hypothesize that the members of this regulatory network could be conserved between *P. patens* and *Arabidopsis*, and selected SCR transcription factors as candidates to study their role in the moss gametophore shoot development. We constructed

a phylogenetic tree of GRAS domain-containing proteins from *P. patens* and *Arabidopsis* to identify the orthologs of *SCR* TF. Knock-out lines were generated for one of the orthologs of *PpSCR3* and were subjected to phenotypic characterization. To understand cellular events leading to the *Ppscr3* phenotype, histological analysis were performed. To further validate our findings, we also attempted live-imaging of the cell division patterns of the WT and *Ppscr3* leaves. Following were the important findings from this study:

1. The phylogenetic tree containing GRAS domain TFs showed that *P. patens* has three orthologs for the *Arabidopsis SCR* TF.
2. A *in situ* hybridization protocol was standardized and *PpSCR3* expression was found to be not tissue-specific.
3. Knockout lines of one of the ortholog *PpSCR3* produced slender-leaves, which had less lamina width and thick midrib.
4. Histological analysis of series of WT and *Ppscr3* leaf sections indicated that the mutant leaves undergo very less anticlinal divisions leading to slender-leaf phenotype (reduced lamina width).
5. Based on histological sections, we proposed a model for midrib development, wherein lack of asymmetric anticlinal divisions in *Ppscr3* mutants leads to the development of thick midrib. However, this cell-division model needs to be validated by live-imaging techniques.

To summarize, we could infer that the role of *SCR* TF in the regulation of asymmetric cell division is conserved across plant lineages and between haploid and diploid body plans.

Future directions

Our forward genetic approach yielded many mutants with interesting phenotypes. Characterization of one of the mutant *shlf* appears to be defective in gametophore auxin transport due to disruption of a novel gene. The gene *SHLF* is found to be conserved only among bryophytes. Undoubtedly, our investigation has opened up new questions that could be explored in future to determine the unknown function of *SHLF* gene.

1. What is the mechanistic link between the *SHLF* gene, auxin and the short-leaf phenotype?
2. Having no known domain, how are the unique repeats present in the *SHLF* protein contribute to its function?
3. Being specific to early streptophytes, what could be its role in colonization on land?
4. How do we validate the proposed model of cell division pattern of moss leaf development?

6 References

- Abbe, E., Phinney, B. and Baer, D.** (1951). The growth of the shoot apex in maize: internal features. *American Journal of Botany* **38**, 744–751.
- Adams, J., Kelso, R. and Cooley, L.** (2000). The kelch repeat superfamily of proteins: propellers of cell function. *Trends in cell biology* **10**, 17–24.
- Aida, M., Beis, D., Heidstra, R., Willemsen, V., Blilou, I., Galinha, C., Nussaume, L., Noh, Y.-S., Amasino, R. and Scheres, B.** (2004). The *PLETHORA* genes mediate patterning of the *Arabidopsis* root stem cell niche. *Cell* **119**, 109–120.
- Aida, M., Ishida, T., Fukaki, H., Fujisawa, H. and Tasaka, M.** (1997). Genes involved in organ separation in *Arabidopsis*: an analysis of the cup-shaped cotyledon mutant. *The Plant Cell* **9**, 841–857.
- Alpert, P.** (2006). Constraints of tolerance: why are desiccation-tolerant organisms so small or rare? *Journal of Experimental Biology* **209**, 1575–1584.
- Ambrose, B.A. and Vasco, A.** (2016). Bringing the multicellular fern meristem into focus. *New Phytologist* **210**, 790–793.
- Andriankaja, M., Dhondt, S., DeBodt, S., Vanhaeren, H., Coppens, F., DeMilde, L., Mühlenbock, P., Skirycz, A., Gonzalez, N., Beemster, G.T. et al.** (2012). Exit from proliferation during leaf development in *Arabidopsis thaliana*: a not-so-gradual process. *Developmental cell* **22**, 64–78.
- Aoyama, T., Hiwatashi, Y., Shigyo, M., Kofuji, R., Kubo, M., Ito, M. and Hasebe, M.** (2012). AP2-type transcription factors determine stem cell identity in the moss *Physcomitrella patens*. *Development* **139**, 3120–3129.
- Ashton, N., Grimsley, N. and Cove, D.** (1979). Analysis of gametophytic development in the moss, *Physcomitrella patens*, using auxin and cytokinin resistant mutants. *Planta* **144**, 427–435.
- Atherton, I., Bosanquet, S.D. and Lawley, M.** (2010). Mosses and liverworts of Britain and Ireland: a field guide. British Bryological Society Plymouth.
- Banks, J.A.** (2015). The evolution of the shoot apical meristem from a gene expression perspective. *New Phytologist* **207**, 486–487.
- Bao, L., Yamamoto, K. T., and Fujita, T.** (2015). Phototropism in gametophytic shoots of the moss *Physcomitrella patens*. *Plant signaling and behavior* **10**(3), e1010900.
- Bar, M. and Ori, N.** (2014). Leaf development and morphogenesis. *Development* **141**, 4219–4230.
- Barker, E.I.** (2011). An examination of leaf morphogenesis in the moss, *Physcomitrella patens*. PhD thesis, Faculty of Graduate Studies and Research, University of Regina.
- Barton, M.** (2010). Twenty years on: the inner workings of the shoot apical meristem, a developmental dynamo. *Developmental biology* **341**, 95–113.
- Barton, M.K. and Poethig, R.S.** (1993). Formation of the shoot apical meristem in *Arabidopsis thaliana*: an analysis of development in the wild type and in the shoot meristemless mutant. *Development* **119**, 823–831.
- Bayer, E.M., Smith, R.S., Mandel, T., Nakayama, N., Sauer, M., Prusinkiewicz, P. and Kuhlemeier, C.** (2009). Integration of transport-based models for phyllotaxis and midvein formation. *Genes & development* **23**, 373–384.

- Beerling, D. and Fleming, A.** (2007). Zimmermann's Telome Theory of Megaphyll Leaf Evolution: a Molecular and Cellular Critique. *Current Opinion in Plant Biology* **10**, 4–12.
- Belles-Boix, E., Hamant, O., Witiak, S.M., Morin, H., Traas, J. and Pautot, V.** (2006). *KNAT6*: an *Arabidopsis* homeobox gene involved in meristem activity and organ separation. *The Plant Cell* **18**, 1900–1907.
- Bendtsen, J. D., Jensen, L. J., Blom, N., Von Heijne, G., and Brunak, S.** (2004). Feature-based prediction of non-classical and leaderless protein secretion. *Protein Engineering Design and Selection*, **17**, 349–356.
- Benfey, P.N., Linstead, P.J., Roberts, K., Schiefelbein, J.W., Hauser, M.-T. and Aeschbacher, R.A.** (1993). Root development in *Arabidopsis*: four mutants with dramatically altered root morphogenesis. *Development* **119**, 57–70.
- Bennett, T.A., Liu, M.M., Aoyama, T., Bierfreund, N.M., Braun, M., Coudert, Y., Dennis, R.J., O'Connor, D., Wang, X.Y., White, C.D. et al.** (2014). Plasma membrane-targeted PIN proteins drive shoot development in a moss. *Current Biology* **24**, 2776–2785.
- Bharathan, G., Goliber, T.E., Moore, C., Kessler, S., Pham, T. and Sinha, N.R.** (2002). Homologies in leaf form inferred from *KNOXI* gene expression during development. *Science* **296**, 1858–1860.
- Bhatia, N., Bozorg, B., Larsson, A., Ohno, C., Jönsson, H. and Heisler, M.G.** (2016). Auxin acts through *MONOPTEROS* to regulate plant cell polarity and pattern phyllotaxis. *Current Biology* **26**, 3202–3208.
- Bhatia, N. and Heisler, M.G.** (2018). Self-organizing periodicity in development: organ positioning in plants. *Development* **145**, dev149336.
- Biasuso, A.B.** (2007). The genus *Hedwigia* (Hedwigiaceae, Bryophyta) in Argentina. *Lindbergia* **32**, 5–17.
- Blockeel, T.L. and Stevenson, C.R.** (2006). *Hypnum cupressiforme* Hedw. var. *heseleri* (Ando & Higuchi) MO Hill (Bryopsida, Hypnales) in Norfolk, new to the British Isles. *Journal of Bryology* **28**, 190–193.
- Borg, M., Brownfield, L. and Twell, D.** (2009). Male gametophyte development: a molecular perspective. *Journal of experimental botany* **60**, 1465–1478.
- Boutilier, K., Offringa, R., Sharma, V.K., Kieft, H., Ouellet, T., Zhang, L., Hattori, J., Liu, C.-M., van Lammeren, A.A., Miki, B.L. et al.** (2002). Ectopic expression of *BABYBOOM* triggers a conversion from vegetative to embryonic growth. *The Plant Cell* **14**, 1737–1749.
- Bower, F.O.** (1935). Primitive land plants. Macmillan And Co.; London.
- Brand, U., Fletcher, J.C., Hobe, M., Meyerowitz, E.M. and Simon, R.** (2000). Dependence of stem cell fate in *Arabidopsis* on a feedback loop regulated by CLV3 activity. *Science* **289**, 617–619.
- Braybrook, S.A. and Peaucelle, A.** (2013). Mechano-chemical aspects of organ formation in *Arabidopsis thaliana*: the relationship between auxin and pectin. *PLoS one* **8**, e57813.

- Breuer, C., Ishida, T. and Sugimoto, K.** (2010). Developmental control of endocycles and cell growth in plants. *Current opinion in plant biology* **13**, 654–660.
- Byrne, M.E.** (2005). Networks in leaf development. *Current opinion in plant biology* **8**, 59–66.
- Byrne, M.E., Barley, R., Curtis, M., Arroyo, J.M., Dunham, M., Hudson, A. and Martienssen, R.A.** (2000). *Asymmetric leaves1* mediates leaf patterning and stem cell function in *Arabidopsis*. *Nature* **408**, 967.
- Caine, R.S., Chater, C.C., Kamisugi, Y., Cuming, A.C., Beerling, D.J., Gray, J.E. and Fleming, A.J.** (2016). An ancestral stomatal patterning module revealed in the non-vascular land plant *Physcomitrella patens*. *Development* **143**, 3306–3314.
- Camacho, C., Coulouris, G., Avagyan, V., Ma, N., Papadopoulos, J., Bealer, K. and Madden, T.L.** (2009). BLAST+: architecture and applications. *BMC bioinformatics* **10**, 421.
- Cannon, M.C., Terneus, K., Hall, Q., Tan, L., Wang, Y., Wegenhart, B.L., Chen, L., Lamport, D.T., Chen, Y. and Kieliszewski, M.J.** (2008). Self-assembly of the plant cell wall requires an extensin scaffold. *Proceedings of the National Academy of Sciences* **105**, 2226–2231.
- Casacuberta, J.M. and Grandbastien, M.-A.** (1993). Characterisation of LTR sequences involved in the protoplast specific expression of the tobacco Tnt1 retrotransposon. *Nucleic acids research* **21**, 2087–2093.
- Causier, B., Lloyd, J., Stevens, L. and Davies, B.** (2012). TOPLESS co-repressor interactions and their evolutionary conservation in plants. *Plant signaling & behavior* **7**, 325–328.
- Champagne, C.E., Goliber, T.E., Wojciechowski, M.F., Mei, R.W., Townsley, B.T., Wang, K., Paz, M.M., Geeta, R. and Sinha, N.R.** (2007). Compound leaf development and evolution in the legumes. *The Plant Cell* **19**, 3369–3378.
- Chater, C.C., Caine, R.S., Tomek, M., Wallace, S., Kamisugi, Y., Cuming, A.C., Lang, D., MacAlister, C.A., Casson, S., Bergmann, D.C. et al.** (2016). Origin and function of stomata in the moss *Physcomitrella patens*. *Nature Plants* **2**, 16179.
- Chitwood, D.H., Nogueira, F.T., Howell, M.D., Montgomery, T.A., Carrington, J.C. and Timmermans, M.C.** (2009). Pattern formation via small RNA mobility. *Genes & development* **23**, 549–554.
- Conway, S.J. and Drinnan, A.N.** (2017). Analysis of Surface Growth in the Conifer Shoot Apical Meristem. *International Journal of Plant Sciences* **178**, 273–287.
- Coruh, C., Cho, S.H., Shahid, S., Liu, Q., Wierzbicki, A. and Axtell, M.J.** (2015). Comprehensive annotation of *Physcomitrella patens* small RNA loci reveals that the heterochromatic short interfering RNA pathway is largely conserved in land plants. *The Plant Cell* , tpc–15.
- Cosgrove, D.J.** (2005). Growth of the plant cell wall. *Nature reviews molecular cell biology* **6**, 850.
- COSMOSS-** The *Physcomitrella patens* resource. *url: <http://www.cosmoss.org>*

- Coudert, Y., Palubicki, W., Ljung, K., Novak, O., Leyser, O. and Harrison, C.J.** (2015). Three ancient hormonal cues co-ordinate shoot branching in a moss. *Elife* **4**, e06808.
- Courtial, B., Feuerbach, F., Eberhard, S., Rohmer, L., Chiapello, H., Camilleri, C. and Lucas, H.** (2001). Tnt1 transposition events are induced by in vitro transformation of *Arabidopsis thaliana*, and transposed copies integrate into genes. *Molecular genetics and genomics* **265**, 32–42.
- Cove, D.** (2005). The moss *Physcomitrella patens*. *Annu. Rev. Genet.* **39**, 339–358.
- Cove, D.J. and Knight, C.D.** (1993). The moss *Physcomitrella patens*, a model system with potential for the study of plant reproduction. *The Plant Cell* **5**, 1483.
- Cove, D.J., Perroud, P.-F., Charron, A.J., McDaniel, S.F., Khandelwal, A. and Quatrano, R.S.** (2009). Culturing the Moss *Physcomitrella patens*. *Cold Spring Harbor Protocols* **2009**, pdb.prot5136.
- Cove, D.J. and Quatrano, R.S.** (2006). Agravitropic mutants of the moss *Ceratodon purpureus* do not complement mutants having a reversed gravitropic response. *Plant, cell & environment* **29**, 1379–1387.
- Crandall-Stotler, B.** (1980). Morphogenetic Designs and a Theory of Bryophyte Origins and Divergence Barbara Crandall-Stotler. *BioScience* **30**, 580–585.
- Crandall-Stotler, B.** (1984). Musci, hepatics, and anthocerotes - an essay on analogues. *New manual of bryology* **2**, 1093–1129.
- Crawford, S., Shinohara, N., Sieberer, T., Williamson, L., George, G., Hepworth, J., Müller, D., Domagalska, M.A. and Leyser, O.** (2010). Strigolactones enhance competition between shoot branches by dampening auxin transport. *Development* **137**, dev-051987.
- Cui, Y., Barampuram, S., Stacey, M.G., Hancock, C.N., Findley, S., Mathieu, M., Zhang, Z., Parrott, W.A. and Stacey, G.** (2013). Tnt1 Retrotransposon Mutagenesis: A Tool for Soybean Functional Genomics. *Plant Physiology* **161**, 36–47.
- DeSmet, I. and Beeckman, T.** (2011). Asymmetric cell division in land plants and algae: the driving force for differentiation. *Nature Reviews Molecular Cell Biology* **12**, 177.
- DeSmet, I., Lau, S., Mayer, U. and Jürgens, G.** (2010). Embryogenesis—the humble beginnings of plant life. *The Plant Journal* **61**, 959–970.
- DeSmet, I., Vassileva, V., DeRybel, B., Levesque, M.P., Grunewald, W., VanDamme, D., VanNoorden, G., Naudts, M., VanIsterdael, G., DeClercq, R. et al.** (2008). Receptor-like kinase ACR4 restricts formative cell divisions in the *Arabidopsis* root. *Science* **322**, 594–597.
- Debernardi, J.M., Rodriguez, R.E., Mecchia, M.A. and Palatnik, J.F.** (2012). Functional specialization of the plant miR396 regulatory network through distinct microRNA–target interactions. *PLoS Genetics* **8**, e1002419.
- DeMason, D.A. and Polowick, P.L.** (2009). Patterns of DR5::GUS expression in organs of pea (*Pisum sativum*). *International Journal of Plant Sciences* **170**, 1–11.

- Demko, V., Perroud, P.-F., Johansen, W., Delwiche, C.F., Cooper, E.D., Remme, P., Ako, A.E., Kugler, K.G., Mayer, K.F., Quatrano, R. et al.** (2014). Genetic analysis of *DEFECTIVE KERNEL1* loop function in three-dimensional body patterning in *Physcomitrella patens*. *Plant physiology* **166**, 903–919.
- d’Erfurth, I., Cosson, V., Eschstruth, A., Lucas, H., Kondorosi, A. and Ratet, P.** (2003). Efficient transposition of the Tnt1 tobacco retrotransposon in the model legume *Medicago truncatula*. *The Plant Journal* **34**, 95–106.
- Deveaux, Y., Toffano-Nioche, C., Claisse, G., Thareau, V., Morin, H., Laufs, P., Moreau, H., Kreis, M. and Lecharny, A.** (2008). Genes of the most conserved *WOX* clade in plants affect root and flower development in *Arabidopsis*. *BMC Evolutionary Biology* **8**, 291.
- Dewitte, W., Scofield, S., Alcasabas, A.A., Maughan, S.C., Menges, M., Braun, N., Collins, C., Nieuwland, J., Prinsen, E., Sundaresan, V. et al.** (2007). *Arabidopsis CYCD3* D-type cyclins link cell proliferation and endocycles and are rate-limiting for cytokinin responses. *Proceedings of the National Academy of Sciences* **104**, 14537–14542.
- Dhondt, S., Coppens, F., DeWinter, F., Swarup, K., Merks, R.M., Inzé, D., Bennett, M.J. and Beemster, G.T.** 2010. *SHORT-ROOT* and *SCARECROW* regulate leaf growth in *Arabidopsis* by stimulating S-phase progression of the cell cycle. *Plant Physiology* **153**.
- DiGiacomo, E., Sestili, F., Iannelli, M.A., Testone, G., Mariotti, D. and Frugis, G.** (2008). Characterization of *KNOX* genes in *Medicago truncatula*. *Plant molecular biology* **67**, 135–150.
- Disch, S., Anastasiou, E., Sharma, V.K., Laux, T., Fletcher, J.C. and Lenhard, M.** (2006). The E3 ubiquitin ligase *BIG BROTHER* controls *Arabidopsis* organ size in a dosage-dependent manner. *Current Biology* **16**, 272–279.
- Douglas, S.J., Chuck, G., Dengler, R.E., Pelecanda, L. and Riggs, C.D.** (2002). *KNATI* and *ERECTA* regulate inflorescence architecture in *Arabidopsis*. *The Plant Cell* **14**, 547–558.
- Doyle, J.J.** (1990). Isolation of plant DNA from fresh tissue. *Focus* **12**, 13–15.
- Drábková, L.Z., Dobrev, P.I. and Motyka, V.** (2015). Phytohormone profiling across the bryophytes. *PLoS One* **10**, e0125411.
- Du, H., Wu, N., Chang, Y., Li, X., Xiao, J., and Xiong, L.** (2013). Carotenoid deficiency impairs ABA and IAA biosynthesis and differentially affects drought and cold tolerance in rice. *Plant molecular biology*, **83**, 475–488.
- Duangpan, S., Zhang, W., Wu, Y., Jansky, S.H. and Jiang, J.** (2013). Insertional Mutagenesis Using Tnt1 Retrotransposon in Potato. *Plant Physiology* **163**, 21–29.
- Eckardt, N.A.** (2004). The role of *PHANTASTICA* in leaf development. *The Plant Cell* **16**, 1073–1075.
- Eklund, D.M., Thelander, M., Landberg, K., Ståldal, V., Nilsson, A., Johansson, M., Valsecchi, I., Pederson, E.R., Kowalczyk, M., Ljung, K. et al.** (2010). Homologues of the *Arabidopsis thaliana SHI/STY/LRP1* genes control auxin biosynthesis and affect growth and development in the moss *Physcomitrella patens*. *Development* **137**, 1275–1284.

- Elliott, R.C., Betzner, A.S., Huttner, E., Oakes, M.P., Tucker, W., Gerentes, D., Perez, P. and Smyth, D.R.** (1996). *AINTEGUMENTA*, an *APETALA2*-like gene of *Arabidopsis* with pleiotropic roles in ovule development and floral organ growth. *The Plant Cell* **8**, 155–168.
- Engstrom, E.M.** (2011). Phylogenetic analysis of GRAS proteins from moss, lycophyte and vascular plant lineages reveals that GRAS genes arose and underwent substantial diversification in the ancestral lineage common to bryophytes and vascular plants. *Plant signaling & behavior* **6**, 850–854.
- Eshed, Y., Baum, S.F., Perea, J.V. and Bowman, J.L.** (2001). Establishment of polarity in lateral organs of plants. *Current Biology* **11**, 1251–1260.
- Eshed, Y., Izhaki, A., Baum, S.F., Floyd, S.K. and Bowman, J.L.** (2004). Asymmetric leaf development and blade expansion in *Arabidopsis* are mediated by *KANADI* and *YABBY* activities. *Development* **131**, 2997–3006.
- Ester Sztein, A., Cohen, J.D., dela Fuente, I. s. G.a. and Cooke, T.J.** (1999). Auxin metabolism in mosses and liverworts. *American Journal of Botany* **86**, 1544–1555.
- Evans, M.M.** (2007). The *indeterminate gametophyte1* gene of maize encodes a LOB domain protein required for embryo sac and leaf development. *The Plant Cell* **19**, 46–62.
- Evans, M.M. and Barton, M.K.** (1997). Genetics of angiosperm shoot apical meristem development. *Annual Review of Plant Biology* **48**, 673–701.
- Feng, G., Qin, Z., Yan, J., Zhang, X. and Hu, Y.** (2011). *Arabidopsis ORGAN SIZE RELATED1* regulates organ growth and final organ size in orchestration with *ARGOS* and *ARL*. *New Phytologist* **191**, 635–646.
- Fesenko, I., Khazigaleeva, R., Kirov, I., Kniazev, A., Glushenko, O., Babalyan, K., Arapidi, G., Shashkova, T., Butenko, I., Zgoda, V. et al.** (2017). Alternative splicing shapes transcriptome but not proteome diversity in *Physcomitrella patens*. *Scientific reports* **7**, 2698.
- Fesenko, I.A., Arapidi, G.P., Skripnikov, A.Y., Alexeev, D.G., Kostryukova, E.S., Manolov, A.I., Altukhov, I.A., Khazigaleeva, R.A., Seredina, A.V., Kovalchuk, S.I. et al.** (2015). Specific pools of endogenous peptides are present in gametophore, protonema, and protoplast cells of the moss *Physcomitrella patens*. *BMC plant biology* **15**, 87.
- Feuerbach, F., Drouaud, J. and Lucas, H.** (1997). Retrovirus-like end processing of the tobacco Tnt1 retrotransposon linear intermediates of replication. *Journal of virology* **71**, 4005–4015.
- FigTree** - Molecular Evolution, Phylogenetics and Epidemiology. *url: <http://tree.bio.ed.ac.uk/software/figtree/>*
- Finnegan, D.J.** (2012). Retrotransposons. *Current Biology* **22**, R432–R437.
- Floyd, S.K. and Bowman, J.L.** (2007). The ancestral developmental tool kit of land plants. *International journal of plant sciences* **168**, 1–35.
- Floyd, S.K., Zalewski, C.S. and Bowman, J.L.** (2006). Evolution of class III homeodomain–leucine zipper genes in streptophytes. *Genetics* **173**, 373–388.
- Foster, A.S.** (1952). Foliar venation in angiosperms from an ontogenetic standpoint. *American Journal of Botany* **39**, 752–766.

- Freeberg, J. and Wetmore, R.** (1968). The Lycopsidea—a study in development. *Phytomorphology* **17**, 78–91.
- Fujino, K., Matsuda, Y., Ozawa, K., Nishimura, T., Koshiba, T., Fraaije, M.W. and Sekiguchi, H.** (2008). NARROW LEAF 7 controls leaf shape mediated by auxin in rice. *Molecular Genetics and Genomics* **279**, 499–507.
- Fujita, H. and Kawaguchi, M.** (2018). Spatial regularity control of phyllotaxis pattern generated by the mutual interaction between auxin and PIN1. *PLoS computational biology* **14**, e1006065.
- Fujita, T. and Hasebe, M.** (2009). Convergences and divergences in polar auxin transport and shoot development in land plant evolution. *Plant signaling & behavior* **4**, 313–315.
- Fujita, T., Sakaguchi, H., Hiwatashi, Y., Wagstaff, S.J., Ito, M., Deguchi, H., Sato, T. and Hasebe, M.** (2008). Convergent evolution of shoots in land plants: lack of auxin polar transport in moss shoots. *Evolution & development* **10**, 176–186.
- Gälweiler, L., Guan, C., Müller, A., Wisman, E., Mendgen, K., Yephremov, A. and Palme, K.** (1998). Regulation of polar auxin transport by AtPIN1 in Arabidopsis vascular tissue. *Science* **282**, 2226–2230.
- Gamborg, O.L., Miller, R. and Ojima, K.** (1968). Nutrient requirements of suspension cultures of soybean root cells. *Experimental cell research* **50**, 151–158.
- Gawk** - GNU Awk 4.1.3. *url: <https://www.gnu.org/software/gawk/>*
- Garcia, D., Collier, S.A., Byrne, M.E. and Martienssen, R.A.** (2006). Specification of leaf polarity in Arabidopsis via the trans-acting siRNA pathway. *Current Biology* **16**, 933–938.
- Gifford, E.M. and Corson, G.E.** (1971). The shoot apex in seed plants. *The Botanical Review* **37**, 143–229.
- Giordano, S., Alfano, F., Esposito, A., Spagnuolo, V., Basile, A. and Cobianchi, R.C.** (1996). Regeneration from detached leaves of *Pleurochaete squarrosa* (Brid.) Lindb. in culture and in the wild. *Journal of Bryology* **19**, 219–227.
- Gish, W. et al.** (1993). Identification of protein coding regions by database similarity search. *Nature genetics* **3**, 266.
- Gleissberg, S., Groot, E.P., Schmalz, M., Eichert, M., Kölsch, A. and Hutter, S.** (2005). Developmental events leading to peltate leaf structure in *Tropaeolum majus* (Tropaeolaceae) are associated with expression domain changes of a YABBY gene. *Development genes and evolution* **215**, 313–319.
- Goffinet, B.** (2007). *Physcomitrella bruch & schimper*. Flora of North America Editorial Committee (eds.) , 194–195.
- Goliber, T., Kessler, S., Chen, J.-J., Bharathan, G. and Sinha, N.** (1998). 8 Genetic, Molecular, and Morphological Analysis of Compound Leaf Development. In *Current topics in developmental biology* vol. 43, pp. 259–290.
- Goodstein, D.M., Shu, S., Howson, R., Neupane, R., Hayes, R.D., Fazo, J., Mitros, T., Dirks, W., Hellsten, U., Putnam, N. and Rokhsar, D.S.** (2012). Phytozome: a Comparative Platform for Green Plant Genomics. *Nucleic Acids Research* **40**, D1178–D1186.

- Grandbastien, M.-A., Spielmann, A. and Caboche, M.** (1989). Tnt1, a mobile retroviral-like transposable element of tobacco isolated by plant cell genetics. *nature* **337**, 376.
- Gray, W.M., Östin, A., Sandberg, G., Romano, C.P. and Estelle, M.** (1998). High temperature promotes auxin-mediated hypocotyl elongation in Arabidopsis. *Proceedings of the National Academy of Sciences* **95**, 7197–7202.
- Grout, A.J.** (1908). Some relations between the habitats of mosses and their structure. *The Bryologist* **11**, 97–100.
- Groves, M.R. and Barford, D.** (1999). Topological characteristics of helical repeat protein. *Current opinion in structural biology* **9**, 383–389.
- Guo, M., Thomas, J., Collins, G. and Timmermans, M.C.** (2008). Direct repression of KNOX loci by the ASYMMETRIC LEAVES1 complex of Arabidopsis. *The Plant Cell* **20**, 48–58.
- Gupta, M.D. and Nath, U.** (2015). Divergence in patterns of leaf growth polarity is associated with the expression divergence of miR396. *The Plant Cell* **27**, 2785–2799.
- Hagemann, W. and Gleissberg, S.** (1996). Organogenetic capacity of leaves: the significance of marginal blastozones in angiosperms. *Plant Systematics and Evolution* **199**, 121–152.
- Hamant, O., Heisler, M.G., Jönsson, H., Krupinski, P., Uyttewaal, M., Bokov, P., Corson, F., Sahlín, P., Boudaoud, A., Meyerowitz, E.M. et al.** (2008). Developmental patterning by mechanical signals in Arabidopsis. *science* **322**, 1650–1655.
- Han, X., Hyun, T. K., Zhang, M., Kumar, R., Koh, E. J., Kang, B. H. et al.,** (2014). Auxin-callose-mediated plasmodesmal gating is essential for tropic auxin gradient formation and signaling. *Developmental cell*, **28**, 132–146.
- Hanawa, J.** (1961). Experimental Studies on Leaf Dorsiventrality in *Sesamum indicum* L. *Shokubutsugaku Zasshi* **74**, 303–309.
- Hareven, D., Gutfinger, T., Parnis, A., Eshed, Y. and Lifschitz, E.** (1996). The making of a compound leaf: genetic manipulation of leaf architecture in tomato. *Cell* **84**, 735–744.
- Harrison, C.J.** (2015). Shooting Through Time: New Insights From Transcriptomic Data. *Trends in Plant Science* **20**, 468–470.
- Harrison, C.J., Corley, S.B., Moylan, E.C., Alexander, D.L., Scotland, R.W. and Langdale, J.A.** (2005). Independent Recruitment of a Conserved Developmental Mechanism During Leaf Evolution. *Nature* **434**, 509–514.
- Harrison, C.J. and Morris, J.L.** (2018). The origin and early evolution of vascular plant shoots and leaves. *Phil. Trans. R. Soc. B* **373**, 20160496.
- Harrison, C.J., Roeder, A.H., Meyerowitz, E.M. and Langdale, J.A.** (2009). Local Cues and Asymmetric Cell Divisions Underpin Body Plan Transitions in the Moss *Physcomitrella Patens*. *Current Biology* **19**, 461–471.
- Hatzfeld, M.** (1998). The armadillo family of structural proteins. In *International review of cytology* vol. 186, pp. 179–224. Elsevier.

- Hay, A., Barkoulas, M. and Tsiantis, M.** (2006). ASYMMETRIC LEAVES1 and auxin activities converge to repress BREVIPEDICELLUS expression and promote leaf development in Arabidopsis. *Development* **133**, 3955–3961.
- Hay, A., Kaur, H., Phillips, A., Hedden, P., Hake, S. and Tsiantis, M.** (2002). The gibberellin pathway mediates KNOTTED1-type homeobox function in plants with different body plans. *Current Biology* **12**, 1557–1565.
- Hay, A. and Tsiantis, M.** (2006). The genetic basis for differences in leaf form between *Arabidopsis thaliana* and its wild relative *Cardamine hirsuta*. *Nature genetics* **38**, 942.
- Hayashida, A., Takechi, K., Sugiyama, M., Kubo, M., Itoh, R., Takio, S., Fujita, T., Hiwatashi, Y., Hasebe, M. and Takano, H.** (2005). Isolation of mutant lines with decreased numbers of chloroplasts per cell from a tagged mutant library of the moss *Physcomitrella patens*. *Plant Biology* **7**, 300–306.
- Heisler, M.G., Hamant, O., Krupinski, P., Uyttewaal, M., Ohno, C., Jönsson, H., Traas, J. and Meyerowitz, E.M.** (2010). Alignment between PIN1 polarity and microtubule orientation in the shoot apical meristem reveals a tight coupling between morphogenesis and auxin transport. *PLoS biology* **8**, e1000516.
- Hejátko, J., Blilou, I., Brewer, P.B., Friml, J., Scheres, B. and Benková, E.** (2006). In situ hybridization technique for mRNA detection in whole mount Arabidopsis samples. *Nature Protocols* **1**, 1939.
- Hinshiri, H. and Proctor, M.** (1971). The effect of desiccation on subsequent assimilation and respiration of the bryophytes *Anomodon viticulosus* and *Porella platyphylla*. *New Phytologist* **70**, 527–538.
- Hiss, M., Meyberg, R., Westermann, J., Haas, F.B., Schneider, L., Schallenberg-Rüdinger, M., Ullrich, K.K. and Rensing, S.A.** (2017). Sexual reproduction, sporophyte development and molecular variation in the model moss *Physcomitrella patens*: introducing the ecotype Reute. *The Plant Journal* **90**, 606–620.
- Hofmeister, W.** (1851). comparative investigations of the germination, development and production of higher cryptogams.(mosses, ferns, equisetaceae, rhizocarpeae and lycopodiaceae)and the seed formation of the conifers, Leipzig Flora**35**,1-10.
- Hohe, A., Rensing, S., Mildner, M., Lang, D. and Reski, R.** (2002). Day length and temperature strongly influence sexual reproduction and expression of a novel MADS-box gene in the moss *Physcomitrella patens*. *Plant biology* **4**, 595–602.
- Hori, K., Maruyama, F., Fujisawa, T., Togashi, T., Yamamoto, N., Seo, M., Sato, S., Yamada, T., Mori, H., Tajima, N. et al.** (2014). *Klebsormidium flaccidum* genome reveals primary factors for plant terrestrial adaptation. *Nature communications* **5**.
- Horiguchi, G., Kim, G.-T. and Tsukaya, H.** (2005). The transcription factor AtGRF5 and the transcription coactivator AN3 regulate cell proliferation in leaf primordia of *Arabidopsis thaliana*. *The Plant Journal* **43**, 68–78.
- Hosokawa, T. and Kubota, H.** (1957). On the osmotic pressure and resistance to desiccation of epiphytic mosses from a beech forest, south-west Japan. *The Journal of Ecology* , 579–591.
- Hu, Y., Xie, Q. and Chua, N.-H.** (2003). The Arabidopsis auxin-inducible gene ARGOS controls lateral organ size. *The Plant Cell* **15**, 1951–1961.

Hunter, J.D. (2007). Matplotlib: A 2d Graphics Environment. *Computing in Science & Engineering* **9**, 90–95.

Ichihashi, Y., Horiguchi, G., Gleissberg, S. and Tsukaya, H. (2009). The bHLH transcription factor SPATULA controls final leaf size in *Arabidopsis thaliana*. *Plant and cell physiology* **51**, 252–261.

iTOL - Interactive Tree Of Life, *url: <https://itol.embl.de/>*

Iwakawa, H., Iwasaki, M., Kojima, S., Ueno, Y., Soma, T., Tanaka, H., Semiarti, E., Machida, Y. and Machida, C. (2007). Expression of the ASYMMETRIC LEAVES2 gene in the adaxial domain of Arabidopsis leaves represses cell proliferation in this domain and is critical for the development of properly expanded leaves. *The Plant Journal* **51**, 173–184.

Izhaki, A. and Bowman, J.L. (2007). KANADI and class III HD-Zip gene families regulate embryo patterning and modulate auxin flow during embryogenesis in Arabidopsis. *The Plant Cell* **19**, 495–508.

Jackson, D., Veit, B. and Hake, S. (1994). Expression of maize KNOTTED1 related homeobox genes in the shoot apical meristem predicts patterns of morphogenesis in the vegetative shoot. *Development* **120**, 405–413.

Jacobs, W.P. (1952). The role of auxin in differentiation of xylem around a wound. *American Journal of Botany* **39**, 301–309.

PhyloT, A phylogenetic tree generator, based on NCBI taxonomy. *url: <https://phylot.biobyte.de/>*

Phytozome, the Plant Comparative Genomics portal. *url: <https://phytozome.jgi.doe.gov/pz/portal.html>*

Jasinski, S., Piazza, P., Craft, J., Hay, A., Woolley, L., Rieu, I., Phillips, A., Hedden, P. and Tsiantis, M. (2005). KNOX action in Arabidopsis is mediated by coordinate regulation of cytokinin and gibberellin activities. *Current Biology* **15**, 1560–1565.

Jefferson, R.A., Bevan M. and Kavanagh, T. (1987). The Use of The *Escherichia Coli* β -glucuronidase Gene As a Gene Fusion Marker for Studies of Gene Expression in Higher Plants. *Biochemical Society Transactions* **15**, 17–18.

Jenkins, G., Courtice, G. and Cove, D. (1986). Gravitropic responses of wild-type and mutant strains of the moss *Physcomitrella patens*. *Plant, cell & environment* **9**, 637–644.

Jenkins, G. I. and Cove, D. J. (1983a). Phototropism and polarotropism of primary chloronemata of the moss *Physcomitrella patens*: responses of the wild-type. *Planta*, **158**, 357-364.

Jenkins, G. I., and D. J. Cove. (1983b). Phototropism and polarotropism of primary chloronemata of the moss *Physcomitrella patens*: responses of mutant strains. *Planta*, **159**, 432-438.

Jia, Y., Wu, P.-C., Wang, M.-Z. and He, S. (2003). Takakiopsida, a unique taxon of bryophytes. *Acta Phytotaxonomica Sinica* **41**, 350–361.

Jin, J., Tian, F., Yang, D.-C., Meng, Y.-Q., Kong, L., Luo, J. and Gao, G. (2017). PlantTFDB 4.0: toward a central hub for transcription factors and regulatory interactions in plants. *Nucleic acids research* **45**

- Jorda, J., Xue, B., Uversky, V. N., and Kajava, A. V.** (2010). Protein tandem repeats—the more perfect, the less structured. *The FEBS journal*, **277**, 2673–2682.
- Jönsson, H., Heisler, M.G., Shapiro, B.E., Meyerowitz, E.M. and Mjolsness, E.** (2006). An auxin-driven polarized transport model for phyllotaxis. *Proceedings of the National Academy of Sciences* **103**, 1633–1638.
- Juarez, M.T., Twigg, R.W. and Timmermans, M.C.** (2004). Specification of adaxial cell fate during maize leaf development. *Development* **131**, 4533–4544.
- Kamisugi, Y., VonStackelberg, M., Lang, D., Care, M., Reski, R., Rensing, S.A. and Cuming, A.C.** (2008). A sequence-anchored genetic linkage map for the moss, *Physcomitrella patens*. *The plant journal* **56**, 855–866.
- Kartha, K. and Engelmann, F.** (1994). Cryopreservation and germplasm storage. In *Plant cell and tissue culture* pp. 195–230. Springer.
- Kawade, K., Horiguchi, G., Usami, T., Hirai, M.Y. and Tsukaya, H.** (2013). ANGUSTIFOLIA3 signaling coordinates proliferation between clonally distinct cells in leaves. *Current Biology* **23**, 788–792.
- Kenrick, P. & Crane, P.R.** (1997). *The Origin and Early Diversification of Land Plants. A Cladistic Study*. Washington, London: Smithsonian Institution Press, 441.
- Kerstetter, R.A., Bollman, K., Taylor, R.A., Bomblies, K. and Poethig, R.S.** (2001). KANADI regulates organ polarity in Arabidopsis. *Nature* **411**, 706.
- Kim, M., McCormick, S., Timmermans, M. and Sinha, N.** (2003). The expression domain of PHANTASTICA determines leaflet placement in compound leaves. *Nature* **424**, 438.
- Kim, S.-I., Veena and Gelvin, S.B.** (2007). Genome-wide analysis of Agrobacterium T-DNA integration sites in the Arabidopsis genome generated under non-selective conditions. *The Plant Journal* **51**, 779–791.
- Kobe, B. and Kajava, A.V.** (2001). The leucine-rich repeat as a protein recognition motif. *Current opinion in structural biology* **11**, 725–732.
- Koenig, D., Bayer, E., Kang, J., Kuhlemeier, C. and Sinha, N.** (2009). Auxin patterns *Solanum lycopersicum* leaf morphogenesis. *Development* **136**, 2997–3006.
- Kofuji, R. and Hasebe, M.** (2014). Eight types of stem cells in the life cycle of the moss *Physcomitrella patens*. *Current opinion in plant biology* **17**, 13–21.
- Kofuji, R., Yoshimura, T., Inoue, H., Sakakibara, K., Hiwatashi, Y., Kurata, T., Aoyama, T., Ueda, K. and Hasebe, M.** (2009). Gametangia development in the moss *Physcomitrella patens*. *Annu Plant Rev* **36**, 167–181.
- Krizek, B.A.** (1999). Ectopic expression of AINTEGUMENTA in Arabidopsis plants results in increased growth of floral organs. *Developmental genetics* **25**, 224–236.
- Kuhlemeier, C. and Reinhardt, D.** (2001). Auxin and phyllotaxis. *Trends in Plant Science* **6**, 187–189.
- Landberg, K., Pederson, E.R., Viaene, T., Bozorg, B., Friml, J., Jönsson, H., Thelander, M. and Sundberg, E.** (2013). The moss *Physcomitrella patens* reproductive organ development is highly organized, affected by the two SHI/STY genes and by the level of active auxin in the SHI/STY expression domain. *Plant physiology* **162**, 1406–1419.

- Lang, D., Eisinger, J., Reski, R. and Rensing, S.** (2005). Representation and high-quality annotation of the *Physcomitrella patens* transcriptome demonstrates a high proportion of proteins involved in metabolism in mosses. *Plant Biology* **7**, 238–250.
- Lang, D., Ullrich, K.K., Murat, F., Fuchs, J., Jenkins, J., Haas, F.B., Piednoel, M., Gundlach, H., VanBel, M., Meyberg, R. et al.** (2018). The *Physcomitrella patens* chromosome-scale assembly reveals moss genome structure and evolution. *The Plant Journal* **93**, 515–533.
- Larkin, M.A., Blackshields, G., Brown, N., Chenna, R., McGettigan, P.A., McWilliam, H., Valentin, F., Wallace, I.M., Wilm, A., Lopez, R. et al.** (2007). Clustal W and Clustal X version 2.0. *bioinformatics* **23**, 2947–2948.
- Larsson, E., Sundström, J.F., Sitbon, F. and von Arnold, S.** (2012). Expression of PaNAC01, a *Picea abies* CUP-SHAPED COTYLEDON orthologue, is regulated by polar auxin transport and associated with differentiation of the shoot apical meristem and formation of separated cotyledons. *Annals of botany* **110**, 923–934.
- Lau, S., Ehrismann, J.S., Schlereth, A., Takada, S., Mayer, U. and Jürgens, G.** (2010). Cell–cell communication in *Arabidopsis* early embryogenesis. *European journal of cell biology* **89**, 225–230.
- Lee, M. S., Gippert, G. P., Soman, K. V., Case, D. A., and Wright, P. E.** (1989). Three-dimensional solution structure of a single zinc finger DNA-binding domain. *Science*, **245(4918)**, 635–637.
- Li, S., Zhao, Y., Zhao, Z., Wu, X., Sun, L., Liu, Q., and Wu, Y.** (2016). Crystal structure of the GRAS domain of SCARECROW-LIKE 7 in *Oryza sativa*. *The Plant Cell*, tpc-00018.
- Li, Y., Zheng, L., Corke, F., Smith, C. and Bevan, M.W.** (2008). Control of final seed and organ size by the DA1 gene family in *Arabidopsis thaliana*. *Genes & Development* **22**, 1331–1336.
- Lin, W.-c., Shuai, B. and Springer, P.S.** (2003). The *Arabidopsis* LATERAL ORGAN BOUNDARIES–domain gene ASYMMETRIC LEAVES2 functions in the repression of KNOX gene expression and in adaxial-abaxial patterning. *The Plant Cell* **15**, 2241–2252.
- Lincoln, C., Long, J., Yamaguchi, J., Serikawa, K. and Hake, S.** (1994). A knotted1-like homeobox gene in *Arabidopsis* is expressed in the vegetative meristem and dramatically alters leaf morphology when overexpressed in transgenic plants. *The Plant Cell* **6**, 1859–1876.
- Liu, C., Xu, Z. and Chua, N.-h.** (1993). Auxin polar transport is essential for the establishment of bilateral symmetry during early plant embryogenesis. *The Plant Cell* **5**, 621–630.
- Lucas, H., Feuerbach, F., Kunert, K., Grandbastien, M. and Caboche, M.** (1995). RNA-mediated transposition of the tobacco retrotransposon Tnt1 in *Arabidopsis thaliana*. *The EMBO journal* **14**, 2364.
- Ludwig-Müller, J., Jülke, S., Bierfreund, N.M., Decker, E.L. and Reski, R.** (2009). Moss (*Physcomitrella patens*) GH3 proteins act in auxin homeostasis. *New Phytologist* **181**, 323–338.

- Maizel, A., Busch, M.A., Tanahashi, T., Perkovic, J., Kato, M., Hasebe, M. and Weigel, D.** (2005). The floral regulator *LEAFY* evolves by substitutions in the DNA binding domain. *Science* **308**, 260–263.
- Mallory, A.C., Reinhart, B.J., Jones-Rhoades, M.W., Tang, G., Zamore, P.D., Barton, M.K. and Bartel, D.P.** (2004). MicroRNA control of *PHABULOSA* in leaf development: importance of pairing to the microRNA 5' region. *The EMBO journal* **23**, 3356–3364.
- Marja, CP, T., Hudson, A., Becraft, P.W., Nelson, T. et al.** (1999). *ROUGH SHEATH2*: a Myb protein that represses *knox* homeobox genes in maize lateral organ primordia. *Science* **284**, 151–153.
- Matasci, N., Hung, L.H., Yan, Z., Carpenter, E.J., Wickett, N.J., Mirarab, S., Nguyen, N., Warnow, T., Ayyampalayam, S., Barker, M. et al.** (2014). Data access for the 1,000 Plants (1KP) project. *Gigascience* **3**, 17.
- Matsumoto, N. and Okada, K.** (2001). A homeobox gene, *PRESSED FLOWER*, regulates lateral axis-dependent development of *Arabidopsis* flowers. *Genes & development* **15**, 3355–3364.
- Mattsson, J., Sung, Z.R. and Berleth, T.** (1999). Responses of plant vascular systems to auxin transport inhibition. *Development* **126**, 2979–2991.
- Mayer, K.F., Schoof, H., Haecker, A., Lenhard, M., Jürgens, G. and Laux, T.** (1998). Role of *WUSCHEL* in regulating stem cell fate in the *Arabidopsis* shoot meristem. *Cell* **95**, 805–815.
- Mayer, U., Buttner, G. and Jurgens, G.** (1993). Apical-basal pattern formation in the *Arabidopsis* embryo: studies on the role of the *gnom* gene. *Development* **117**, 149–162.
- McAlpin, B.W. and White, R.A.** (1974). Shoot organization in the Filicales: the promeristem. *American Journal of Botany* **61**, 562–579.
- McConnell, J.R., Emery, J., Eshed, Y., Bao, N., Bowman, J. and Barton, M.K.** (2001). Role of *PHABULOSA* and *PHAVOLUTA* in determining radial patterning in shoots. *Nature* **411**, 709.
- McHale, N.A. and Koning, R.E.** (2004). *PHANTASTICA* regulates development of the adaxial mesophyll in *Nicotiana* leaves. *The Plant Cell* **16**, 1251–1262.
- Menand, B., Calder, G. and Dolan, L.** (2007). Both chloronemal and caulonemal cells expand by tip growth in the moss *Physcomitrella patens*. *Journal of experimental botany* **58**, 1843–1849.
- Mhiri, C., Morel, J.-B., Vernhettes, S., Casacuberta, J.M., Lucas, H. and Grandbastien, M.-A.** (1997). The promoter of the tobacco *Tnt1* retrotransposon is induced by wounding and by abiotic stress. *Plant molecular biology* **33**, 257–266.
- Mishler, B. D., and Oliver, M. J.** (2009). Putting *Physcomitrella patens* on the tree of life: the evolution and ecology of mosses. *Annual Plant Reviews*, **36**, 1-15.
- Mitchison, G.** (1980). A model for vein formation in higher plants. In *Proc. R. Soc. Lond. B* vol. **207**, 79–109.
- Mittag, J., Gabrielyan, A., and Ludwig-Müller, J.** (2015). Knockout of *GH3* genes in the moss *Physcomitrella patens* leads to increased IAA levels at elevated temperature and in darkness. *Plant Physiology and Biochemistry*, **97**, 339-349.

- Mizukami, Y. and Fischer, R.L.** (2000). Plant organ size control: AINTEGUMENTA regulates growth and cell numbers during organogenesis. *Proceedings of the National Academy of Sciences* **97**, 942–947.
- Mohanasundaram B, Rajmane VB, Jogdand SV, Bhide AJ and Banerjee AK,** (2018). Analysis of Tnt1 transposition activity in moss (*Physcomitrella patens*) and isolation of mutants with impaired gametophyte development. (**Under revision in BMC Plant Biology**).
- Nag, A., King, S. and Jack, T.** (2009). miR319a targeting of TCP4 is critical for petal growth and development in Arabidopsis. *Proceedings of the National Academy of Sciences* **106**, 22534–22539.
- Nardmann, J., Ji, J., Werr, W. and Scanlon, M.J.** (2004). The maize duplicate genes narrow sheath1 and narrow sheath2 encode a conserved homeobox gene function in a lateral domain of shoot apical meristems. *Development* **131**, 2827–2839.
- Nardmann, J., Reisewitz, P. and Werr, W.** (2009). Discrete shoot and root stem cell-promoting WUS/WOX5 functions are an evolutionary innovation of angiosperms. *Molecular biology and evolution* **26**, 1745–1755.
- Nath, U., Crawford, B.C., Carpenter, R. and Coen, E.** (2003). Genetic control of surface curvature. *Science* **299**, 1404–1407.
- Nelson, T. and Dengler, N.** (1997). Leaf vascular pattern formation. *The Plant Cell* **9**, 1121.
- Nishiyama, T., Hiwatashi, Y., Sakakibara, K., Kato, M. and Hasebe, M.** (2000). Tagged mutagenesis and gene-trap in the moss, *Physcomitrella patens* by shuttle mutagenesis. *DNA research* **7**, 9–17.
- Nishiyama, T., Sakayama, H., de Vries, J., Buschmann, H., Saint-Marcoux, et al.,**(2018). The *Chara* Genome: Secondary Complexity and Implications for Plant Terrestrialization. *Cell*, **174**, 448-464.
- Nogueira, F.T., Madi, S., Chitwood, D.H., Juarez, M.T. and Timmermans, M.C.** (2007). Two small regulatory RNAs establish opposing fates of a developmental axis. *Genes & development* **21**, 750–755.
- Okano, Y., Aono, N., Hiwatashi, Y., Murata, T., Nishiyama, T., Ishikawa, T., Kubo, M. and Hasebe, M.** (2009). A polycomb repressive complex 2 gene regulates apogamy and gives evolutionary insights into early land plant evolution. *Proceedings of the National Academy of Sciences* **106**, 16321–16326.
- Oldenhof, H., Wolkers, W.F., Bowman, J.L., Tablin, F. and Crowe, J.H.** (2006). Freezing and desiccation tolerance in the moss *Physcomitrella patens*: an in situ Fourier transform infrared spectroscopic study. *Biochimica et Biophysica Acta (BBA)-General Subjects* **1760**, 1226–1234.
- Oliver, M.J., Velten, J. and Mishler, B.D.** (2005). Desiccation Tolerance in Bryophytes: A Reflection of the Primitive Strategy for Plant Survival in Dehydrating Habitats? 1. *Integrative and Comparative Biology* **45**, 788–799.
- Ori, N., Cohen, A.R., Etzioni, A., Brand, A., Yanai, O., Shleizer, S., Menda, N., Amsellem, Z., Efroni, I., Pekker, I. et al.** (2007). Regulation of LANCEOLATE by miR319 is required for compound-leaf development in tomato. *Nature genetics* **39**, 787.

- Ori, N., Eshed, Y., Chuck, G., Bowman, J.L. and Hake, S.** (2000). Mechanisms that control knox gene expression in the Arabidopsis shoot. *Development* **127**, 5523–5532.
- Otsuga, D., DeGuzman, B., Prigge, M.J., Drews, G.N. and Clark, S.E.** (2001). REVOLUTA regulates meristem initiation at lateral positions. *The Plant Journal* **25**, 223–236.
- Page, D.R. and Grossniklaus, U.** (2002). The art and design of genetic screens: *Arabidopsis thaliana*. *Nature Reviews Genetics* **3**, 124.
- Palatnik, J.F., Allen, E., Wu, X., Schommer, C., Schwab, R., Carrington, J.C. and Weigel, D.** (2003). Control of leaf morphogenesis by microRNAs. *Nature* **425**, 257.
- Paponov, I.A., Teale, W., Lang, D., Paponov, M., Reski, R., Rensing, S.A. and Palme, K.** (2009). The evolution of nuclear auxin signalling. *BMC Evolutionary Biology* **9**, 126.
- Pavesi, A., Conterio, F., Bolchi, A., Dieci, G. and Ottonello, S.** (1994). Identification of new eukaryotic tRNA genes in genomic DNA databases by a multistep weight matrix analysis of transcriptional control regions. *Nucleic acids research* **22**, 1247–1256.
- Pekker, I., Alvarez, J.P. and Eshed, Y.** (2005). Auxin response factors mediate Arabidopsis organ asymmetry via modulation of KANADI activity. *The Plant Cell* **17**, 2899–2910.
- Perales, M. and Reddy, G.V.** (2012). Stem cell maintenance in shoot apical meristems. *Current opinion in plant biology* **15**, 10–16.
- Perilli, S., DiMambro, R. and Sabatini, S.** (2012). Growth and development of the root apical meristem. *Current opinion in plant biology* **15**, 17–23.
- Perroud, P.-F., Cove, D.J., Quatrano, R.S. and McDaniel, S.F.** (2011). An experimental method to facilitate the identification of hybrid sporophytes in the moss *Physcomitrella patens* using fluorescent tagged lines. *New Phytologist* **191**, 301–306.
- Peterson, K.M., Rychel, A.L. and Torii, K.U.** (2010). Out of the mouths of plants: the molecular basis of the evolution and diversity of stomatal development. *The Plant Cell* **22**, 296–306.
- Philipson, W.** (1990). The significance of apical meristems in the phylogeny of land plants. *Plant Systematics and Evolution* **173**, 17–38.
- Piazza, P., Jasinski, S. and Tsiantis, M.** (2005). Evolution of leaf developmental mechanisms. *New Phytologist* **167**, 693–710.
- Plackett, A.R., DiStilio, V.S. and Langdale, J.A.** (2015). Ferns: the missing link in shoot evolution and development. *Frontiers in plant science* **6**, 972.
- Poethig, R.S.** (1987). Clonal Analysis of Cell Lineage Patterns in Plant Development. *American Journal of Botany* **74**, 581–594.
- Poethig, S.** (1984). Cellular parameters of leaf morphogenesis in maize and tobacco. In *Contemporary problems in plant anatomy* pp. 235–259. Elsevier.
- Pouteau, S., Grandbastien, M.-A. and Boccara, M.** (1994). Microbial elicitors of plant defence responses activate transcription of a retrotransposon. *The plant journal* **5**, 535–542.

- Pouteau, S., Huttner, E., Grandbastien, M. and Caboche, M.** (1991). Specific expression of the tobacco Tnt1 retrotransposon in protoplasts. *The EMBO journal* **10**, 1911.
- Powell, A.E. and Lenhard, M.** (2012). Control of organ size in plants. *Current Biology* **22**, R360–R367.
- Prieto, P., Moore, G. and Shaw, P.** (2007). Fluorescence in situ hybridization on vibratome sections of plant tissues. *Nature Protocols* **2**, 1831.
- Prigge, M.J. and Bezanilla, M.** (2010). Evolutionary crossroads in developmental biology: *Physcomitrella patens*. *Development* **137**, 3535–3543.
- Prigge, M.J., Lavy, M., Ashton, N.W. and Estelle, M.** (2010). *Physcomitrella patens* auxin-resistant mutants affect conserved elements of an auxin-signaling pathway. *Current Biology* **20**, 1907–1912.
- Proctor, M.C., Oliver, M.J., Wood, A.J., Alpert, P., Stark, L.R., Cleavitt, N.L. and Mishler, B.D.** (2007). Desiccation-tolerance in bryophytes: a review. *The Bryologist* **110**, 595–621.
- Puttick, M.N., Morris, J.L., Williams, T.A., Cox, C.J., Edwards, D., Kenrick, P., Pressel, S., Wellman, C.H., Schneider, H., Pisani, D. et al.** (2018). The interrelationships of land plants and the nature of the ancestral embryophyte. *Current Biology* **28**, 733–745.
- Reese, W.D.** (2000). Extreme leaf dimorphism in Calymperaceae. *The Bryologist* **103**, 534–540.
- Reinhardt, D., Mandel, T. and Kuhlemeier, C.** (2000). Auxin regulates the initiation and radial position of plant lateral organs. *The Plant Cell* **12**, 507–518.
- Reinhardt, D., Pesce, E.-R., Stieger, P., Mandel, T., Baltensperger, K., Bennett, M., Traas, J., Friml, J. and Kuhlemeier, C.** (2003). Regulation of phyllotaxis by polar auxin transport. *Nature* **426**, 255.
- Rensing, S.A., Lang, D., Zimmer, A.D., Terry, A., Salamov, A., Shapiro, H., Nishiyama, T., Perroud, P.-F., Lindquist, E.A., Kamisugi, Y. et al.** (2008). The *Physcomitrella* genome reveals evolutionary insights into the conquest of land by plants. *Science* **319**, 64–69.
- Rhoades, M.W., Reinhart, B.J., Lim, L.P., Burge, C.B., Bartel, B. and Bartel, D.P.** (2002). Prediction of plant microRNA targets. *cell* **110**, 513–520.
- Roads, E., Longton, R.E. and Convey, P.** (2014). Millennial timescale regeneration in a moss from Antarctica. *Current Biology* **24**, R222–R223.
- Rodriguez, R.E., Mecchia, M.A., Debernardi, J.M., Schommer, C., Weigel, D. and Palatnik, J.F.** (2010). Control of cell proliferation in *Arabidopsis thaliana* by microRNA miR396. *Development* **137**, 103–112.
- Rolland-Lagan, A.-G. and Prusinkiewicz, P.** (2005). Reviewing models of auxin canalization in the context of leaf vein pattern formation in *Arabidopsis*. *The Plant Journal* **44**, 854–865.
- Rothwell, G.W. and Nixon, K.C.** (2006). How does the inclusion of fossil data change our conclusions about the phylogenetic history of euphyllophytes? *International Journal of Plant Sciences* **167**, 737–749.

- Sachs, T.** (1989). The development of vascular networks during leaf development. *Curr. Top. Plant Biochem. Physiol.* **8**, 168–183.
- Sachs, T.** (1991). Cell polarity and tissue patterning in plants. *Development* **113**, 83–93.
- Sakakibara, K., Ando, S., Yip, H.K., Tamada, Y., Hiwatashi, Y., Murata, T., Deguchi, H., Hasebe, M. and Bowman, J.L.** (2013). KNOX2 genes regulate the haploid-to-diploid morphological transition in land plants. *Science* **339**, 1067–1070.
- Sakakibara, K., Nishiyama, T., Deguchi, H. and Hasebe, M.** (2008). Class 1 KNOX genes are not involved in shoot development in the moss *Physcomitrella patens* but do function in sporophyte development. *Evolution & development* **10**, 555–566.
- Sakakibara, K., Nishiyama, T., Sumikawa, N., Kofuji, R., Murata, T. and Hasebe, M.** (2003). Involvement of auxin and a homeodomain-leucine zipper I gene in rhizoid development of the moss *Physcomitrella patens*. *Development* **130**, 4835–4846.
- Sakakibara, K., Reisewitz, P., Aoyama, T., Friedrich, T., Ando, S., Sato, Y., Tamada, Y., Nishiyama, T., Hiwatashi, Y., Kurata, T. et al.** (2014). WOX13-like genes are required for reprogramming of leaf and protoplast cells into stem cells in the moss *Physcomitrella patens*. *Development* **141**, 1660–1670.
- Sambrook, J., Fritsch, E.F., Maniatis, T. et al.** (1989). *Molecular cloning: a laboratory manual*. Number Ed. 2, Cold spring harbor laboratory press.
- Sanders, H.L. and Langdale, J.A.** (2013). Conserved transport mechanisms but distinct auxin responses govern shoot patterning in *Selaginella kraussiana*. *New Phytologist* **198**, 419–428.
- Sano, R., Juarez, C.M., Hass, B., Sakakibara, K., Ito, M., Banks, J.A. and Hasebe, M.** (2005). Knox Homeobox Genes Potentially Have Similar Function in Both Diploid Unicellular and Multicellular Meristems, But Not in Haploid Meristems. *Evolution and Development* **7**, 69–78.
- Scanlon, M.J. and Freeling, M.** (1997). Clonal sectors reveal that a specific meristematic domain is not utilized in the maize mutant narrow sheath. *Developmental biology* **182**, 52–66.
- Scarpella, E. and Meijer, A.H.** (2004). Pattern formation in the vascular system of monocot and dicot plant species. *New Phytologist* **164**, 209–242.
- Schaefer, D.G. and Zrýd, J.-P.** (1997). Efficient gene targeting in the moss *Physcomitrella patens*. *The Plant Journal* **11**, 1195–1206.
- Scheres, B., DiLaurenzio, L., Willemsen, V., Hauser, M.-T., Janmaat, K., Weisbeek, P. and Benfey, P.N.** (1995). Mutations affecting the radial organisation of the Arabidopsis root display specific defects throughout the embryonic axis. *Development* **121**, 53–62.
- Schmittgen, T.D. and Livak, K.J.** (2008). Analyzing real-time PCR data by the comparative C T method. *Nature protocols* **3**, 1101.
- Schneeberger, R., Tsiantis, M., Freeling, M. and Langdale, J.A.** (1998). The rough sheath2 gene negatively regulates homeobox gene expression during maize leaf development. *Development* **125**, 2857–2865.
- Schneider, C.A., Rasband, W.S. and Eliceiri, K.W.** (2012). NIH Image to ImageJ: 25 years of image analysis. *Nature methods* **9**, 671.

- Schoof, H., Lenhard, M., Haecker, A., Mayer, K.F., Jürgens, G. and Laux, T.** (2000). The stem cell population of Arabidopsis shoot meristems is maintained by a regulatory loop between the CLAVATA and WUSCHEL genes. *Cell* **100**, 635–644.
- Schopfer, P.** (2006). Biomechanics of plant growth. *American journal of botany* **93**, 1415–1425.
- Schulte, J. and Reski, R.** (2004). High throughput cryopreservation of 140000 *Physcomitrella patens* mutants. *Plant Biology* **6**, 119–127.
- Schween, G., Gorr, G., Hohe, A. and Reski, R.** (2003). Unique tissue-specific cell cycle in *Physcomitrella*. *Plant Biology* **5**, 50–58.
- Shani, E., Yanai, O. and Ori, N.** (2006). The role of hormones in shoot apical meristem function. *Current opinion in plant biology* **9**, 484–489.
- Shleizer-Burko, S., Burko, Y., Ben-Herzel, O. and Ori, N.** (2011). Dynamic growth program regulated by LANCEOLATE enables flexible leaf patterning. *Development* **138**, 695–704.
- Slewinski, T.L., Anderson, A.A., Zhang, C. and Turgeon, R.** (2012). Scarecrow plays a role in establishing Kranz anatomy in maize leaves. *Plant and Cell Physiology* **53**, 2030–2037.
- Slewinski, T. L.** (2013). Using evolution as a guide to engineer Kranz-type C4 photosynthesis. *Frontiers in plant science* **4**, 212.
- Smith, D.K. and Davison, P.G.** (1993). Antheridia and sporophytes in *Takakia ceratophylla*(Mitt.)Grolle—Evidence for reclassification among the mosses. *Journal of the Hattori Botanical Laboratory* , p263–271.
- Smith, L.G., Greene, B., Veit, B. and Hake, S.** (1992). A dominant mutation in the maize homeobox gene, Knotted-1, causes its ectopic expression in leaf cells with altered fates. *Development* **116**, 21–30.
- Smith, L.G. and Hake, S.** (1992). The initiation and determination of leaves. *The Plant Cell* **4**, 1017.
- Smith, R.S., Guyomarc’h, S., Mandel, T., Reinhardt, D., Kuhlemeier, C. and Prusinkiewicz, P.** (2006). A plausible model of phyllotaxis. *Proceedings of the National Academy of Sciences* **103**, 1301–1306.
- Souer, E., van Houwelingen, A., Kloos, D., Mol, J. and Koes, R.** (1996). The no apical meristem gene of *Petunia* is required for pattern formation in embryos and flowers and is expressed at meristem and primordia boundaries. *Cell* **85**, 159–170.
- Spinelli, S.V., Martin, A.P., Viola, I.L., Gonzalez, D.H. and Palatnik, J.F.** (2011). A mechanistic link between STM and CUC1 during Arabidopsis development. *Plant physiology* **156**, 1894–1904.
- Stahle, M.I., Kuehlich, J., Staron, L., von Arnim, A.G. and Golz, J.F.** (2009). YAB-BYs and the transcriptional corepressors LEUNIG and LEUNIG_HOMOLOG maintain leaf polarity and meristem activity in Arabidopsis. *The Plant Cell* **21**, 3105–3118.
- Steeves, T. and Sussex, I.** (1989). Patterns in Plant Development: Shoot Apical Meristem Mutants of *Arabidopsis thaliana*.

- Steeves, T.A. and Sussex, I.** (1957). Studies on the development of excised leaves in sterile culture. *American Journal of Botany* **44**, 665–673.
- Steffensen, D.M.** (1968). A reconstruction of cell development in the shoot apex of maize. *American Journal of Botany* **55**, 354–369.
- Stepanova, A.N., Robertson-Hoyt, J., Yun, J., Benavente, L.M., Xie, D.-Y., Doležal, K., Schlereth, A., Jürgens, G. and Alonso, J.M.** (2008). TAA1-mediated auxin biosynthesis is essential for hormone crosstalk and plant development. *Cell* **133**, 177–191.
- Stevenson, D.W.** (1976a). The cytohistological and cytohistochemical zonation of the shoot apex of *Botrychium multifidum*. *American Journal of Botany* **63**, 852–856.
- Stevenson, D.W.** (1976b). Observations on phyllotaxis, stelar morphology, the shoot apex and gemmae of *Lycopodium lucidulum* Michaux (Lycopodiaceae). *Botanical Journal of the Linnean Society* **72**, 81–100.
- Stevenson, S.R., Kamisugi, Y., Trinh, C.H., Schmutz, J., Jenkins, J.W., Grimwood, J., Muchero, W., Tuskan, G.A., Rensing, S.A., Lang, D. et al.** (2016). Genetic analysis of *Physcomitrella patens* identifies ABSCISIC ACID NON-RESPONSIVE (ANR), a regulator of ABA responses unique to basal land plants and required for desiccation tolerance. *The Plant Cell* , tpc-00091.
- Stirnemann, C.U., Petsalaki, E., Russell, R.B. and Müller, C.W.** (2010). WD40 proteins propel cellular networks. *Trends in biochemical sciences* **35**, 565–574.
- Sun, H., Furt, F. and Vidali, L.** (2018). Myosin XI localizes at the mitotic spindle and along the cell plate during plant cell division in *Physcomitrella patens*. *Biochemical and biophysical research communications* **1**.
- Sundås-Larsson, A., Svenson, M., Liao, H. and Engström, P.** (1998). A homeobox gene with potential developmental control function in the meristem of the conifer *Picea abies*. *Proceedings of the National Academy of Sciences* **95**, 15118–15122.
- Sussex, I.** (1955). Morphogenesis in *Solanum tuberosum* L.: experimental investigation of leaf dorsiventrality and orientation in the juvenile shoot. *Phytomorphology* **5**, 286–300.
- Syed, N.H. and Flavell, A.J.** (2006). Sequence-specific amplification polymorphisms (SSAPs): a multi-locus approach for analyzing transposon insertions. *Nature Protocols* **1**, 2746.
- Szymkowiak, E.J. and Sussex, I.M.** (1996). What chimeras can tell us about plant development. *Annual review of plant biology* **47**, 351–376.
- Talbert, P.B., Adler, H.T., Parks, D.W. and Comai, L.** (1995). The REVOLUTA gene is necessary for apical meristem development and for limiting cell divisions in the leaves and stems of *Arabidopsis thaliana*. *Development* **121**, 2723–2735.
- Tam, S.M., Mhiri, C., Vogelaar, A., Kerkveld, M., Pearce, S.R. and Grandbastien, M.-A.** (2005). Comparative analyses of genetic diversities within tomato and pepper collections detected by retrotransposon-based SSAP, AFLP and SSR. *Theoretical and Applied Genetics* **110**, 819–831.
- Tanahashi, T., Sumikawa, N., Kato, M. and Hasebe, M.** (2005). Diversification of gene function: homologs of the floral regulator FLO/LFY control the first zygotic cell division in the moss *Physcomitrella patens*. *Development* **132**, 1727–1736.

- Tao, Y., Ferrer, J.-L., Ljung, K., Pojer, F., Hong, F., Long, J.A., Li, L., Moreno, J.E., Bowman, M.E., Ivans, L.J. et al.** (2008). Rapid synthesis of auxin via a new tryptophan-dependent pathway is required for shade avoidance in plants. *Cell* **133**, 164–176.
- Thelander, M., Landberg, K. and Sundberg, E.** (2017). Auxin-mediated developmental control in the moss *Physcomitrella patens*. *Journal of experimental botany* **69**, 277–290.
- Thomas, R.J., Ryder, S.H., Gardner, M.I., Sheetz, J.P. and Nichipor, S.D.** (1996). Photosynthetic function of leaf lamellae in *Polytrichum commune*. *Bryologist* **99**, 6–11.
- Tomescu, A.M.** (2009). Megaphylls, microphylls and the evolution of leaf development. *Trends in plant science* **14**, 5–12.
- Tononi, P., Möller, M., Bencivenga, S. and Spada, A.** (2010). GRAMINIFOLIA homolog expression in *Streptocarpus rexii* is associated with the basal meristems in phyllo-morphs, a morphological novelty in Gesneriaceae. *Evolution & development* **12**, 61–73.
- Tsiantis, M., Schneeberger, R., Golz, J.F., Freeling, M. and Langdale, J.A.** (1999). The maize rough sheath2 gene and leaf development programs in monocot and dicot plants. *Science* **284**, 154–156.
- vander Graaff, E., Laux, T. and Rensing, S.A.** (2009). The WUS homeobox-containing (WOX) protein family. *Genome biology* **10**, 248.
- Vasco, A., Moran, R.C. and Ambrose, B.A.** (2013). The Evolution, Morphology, and Development of Fern Leaves. *Frontiers in Plant Science* **4**, nil.
- Venglat, S., Dumonceaux, T., Rozwadowski, K., Parnell, L., Babic, V., Keller, W., Martienssen, R., Selvaraj, G. and Datla, R.** (2002). The homeobox gene BREVIPEDICELLUS is a key regulator of inflorescence architecture in Arabidopsis. *Proceedings of the National Academy of Sciences* **99**, 4730–4735.
- Vernhettes, S., Grandbastien, M.-A. and Casacuberta, J.M.** (1997). In vivo characterization of transcriptional regulatory sequences involved in the defence-associated expression of the tobacco retrotransposon Tnt1. *Plant molecular biology* **35**, 673–679.
- Vives, C., Charlot, F., Mhiri, C., Contreras, B., Daniel, J., Epert, A., Voytas, D.F., Grandbastien, M.-A., Nogué, F. and Casacuberta, J.M.** (2016). Highly efficient gene tagging in the bryophyte *Physcomitrella patens* using the tobacco (*Nicotiana tabacum*) Tnt1 retrotransposon. *New Phytologist* **212**, 759–769.
- Vlad, D., Kierzkowski, D., Rast, M.I., Vuolo, F., Ioio, R.D., Galinha, C., Gan, X., Hajheidari, M., Hay, A., Smith, R.S. et al.** (2014). Leaf shape evolution through duplication, regulatory diversification, and loss of a homeobox gene. *Science* **343**, 780–783.
- Waites, R. and Hudson, A.** (1995). phantastica: a gene required for dorsoventrality of leaves in *Antirrhinum majus*. *Development* **121**, 2143–2154.
- Waites, R., Selvadurai, H.R., Oliver, I.R. and Hudson, A.** (1998). The PHANTASTICA gene encodes a MYB transcription factor involved in growth and dorsoventrality of lateral organs in *Antirrhinum*. *Cell* **93**, 779–789.
- Walt, S. v.d., Colbert, S.C. and Varoquaux, G.** (2011). The NumPy array: a structure for efficient numerical computation. *Computing in Science & Engineering* **13**, 22–30.

- Wang, H., Chen, J., Wen, J., Tadege, M., Li, G., Liu, Y., Mysore, K.S., Ratet, P. and Chen, R.** (2008). Control of compound leaf development by FLORICAULA/LEAFY ortholog SINGLE LEAFLET1 in *Medicago truncatula*. *Plant Physiology* **146**, 1759–1772.
- Wang, L., Gu, X., Xu, D., Wang, W., Wang, H., Zeng, M., Chang, Z., Huang, H. and Cui, X.** (2011). miR396-targeted AtGRF transcription factors are required for coordination of cell division and differentiation during leaf development in Arabidopsis. *Journal of experimental Botany* **62**, 761–773.
- Wang, R. and Estelle, M.** (2014). Diversity and specificity: auxin perception and signaling through the TIR1/AFB pathway. *Current opinion in plant biology* **21**, 51–58.
- Wang, Y., Deng, D., Ding, H., Xu, X., Zhang, R., Wang, S., Bian, Y., Yin, Z. and Chen, Y.** (2013). Gibberellin biosynthetic deficiency is responsible for maize dominant Dwarf11 (D11) mutant phenotype: physiological and transcriptomic evidence. *PloS one* **8**, e66466.
- Wardlaw, C.** (1943). Experimental and Analytical Studies of Pteridophytes: II. Experimental Observations on the Development of Buds in *Onoclea sensibilis* and in Species of Dryopteris. *Annals of Botany* **7**, 357–377.
- Waugh, R., McLean, K., Flavell, A., Pearce, S., Kumar, A., Thomas, B. and Powell, W.** (1997). Genetic distribution of Bare-1-like retrotransposable elements in the barley genome revealed by sequence-specific amplification polymorphisms (S-SAP). *Molecular and General Genetics MGG* **253**, 687–694.
- Weijers, D. and Wagner, D.** (2016). Transcriptional responses to the auxin hormone. *Annual review of plant biology* **67**, 539–574.
- Weir, I., Lu, J., Cook, H., Causier, B., Schwarz-Sommer, Z. and Davies, B.** (2004). CUPULIFORMIS establishes lateral organ boundaries in Antirrhinum. *Development* **131**, 915–922.
- White, D.W.** (2006). PEAPOD regulates lamina size and curvature in Arabidopsis. *Proceedings of the National Academy of Sciences* **103**, 13238–13243.
- Wolff, C.** (1759). *Theoria generationis*. Germany; University of Halle .
- Wright, I.J., Reich, P.B., Westoby, M., Ackerly, D.D., Baruch, Z., Bongers, F., Cavender-Bares, J., Chapin, T., Cornelissen, J.H., Diemer, M. et al.** (2004). The worldwide leaf economics spectrum. *Nature* **428**, 821.
- Xiao, L., Yobi, A., Koster, K.L., He, Y. and Oliver, M.J.** (2018). Desiccation tolerance in *Physcomitrella patens*: Rate of dehydration and the involvement of endogenous abscisic acid (ABA). *Plant, cell & environment* **41**, 275–284.
- Yamaguchi, T., Nukazuka, A. and Tsukaya, H.** (2012). Leaf adaxial–abaxial polarity specification and lamina outgrowth: evolution and development. *Plant and Cell Physiology* **53**, 1180–1194.
- Yip, H.K., Floyd, S.K., Sakakibara, K. and Bowman, J.L.** (2016). Class III HD-Zip activity coordinates leaf development in *Physcomitrella patens*. *Developmental biology* **419**, 184–197.
- Zimmermann, W.** (1952). Main results of the telome theory. *Palaeobotanist* **1**, 456–470.

Zoulias, N., Koenig, D., Hamidi, A., McCormick, S. and Kim, M. (2011). A role for PHANTASTICA in medio-lateral regulation of adaxial domain development in tomato and tobacco leaves. *Annals of botany* **109**, 407–418.

7 Annexure

Annexure 1

- Building indexes for references (*P. patens* genome, Tnt1, T-DNA with Tnt1, T-DNA WO Tnt1)

```
$ bowtie2-build 'Ppatens_318_v3.fa' mossv3.3
```

```
$ bowtie2-build 'Tnt1.fa' Tnt
```

```
$ bowtie2-build 'T-DNA_with_Tnt1.fa' TDNAwithTnt
```

```
$ bowtie2-build 'TDNA_WO_Tnt1.fa' TDNAWOTnt
```

- Aligning the NGS reads to *P. patens* genome

```
$ bowtie2 -x mossv3.3 -p 6 -1 'NGS_sl_R1.fastq.gz' -2 'NGS_sl_R2.fastq.gz' -q -S  
bow_sl_ongenome.sam
```

```
$ samtools view -h bow_sl_ongenome.sam > bow_sl_ongenome.bam
```

- Aligning the NGS reads Tnt1 and T-DNA without Tnt1 sequences.

```
$ bowtie2 -x Tnt -p 6 -1 'NGS_sl_R1.fastq.gz' -2 'NGS_sl_R2.fastq.gz' -q -S bow_sl_onTnt.sam
```

```
$ bowtie2 -x TDNAWOTnt -p -6 -1 'NGS_sl_R1.fastq.gz' -2 'NGS_sl_R2.fastq.gz' -q  
-S bow_sl_onTDNAWOTnt.sam
```

Extracting Tnt1 singletons.

- Extracting reads mapped to Tnt1.

```
$ samtools view -h -S -F4 bow_sl_onTnt.sam > F4_sl_onTnt1.sam
```

```
$ samtools flagstat F4_sl_onTnt1.sam
```

- Extracting singletons out of total mapped reads.

```
$ samtools view -f 8 -F 4 F4_sl_onTnt1.sam > singleton_F4_sl_onTnt1.sam
```

- Preparing awk query.

```
$ awk '{print "$1 ~ /"$1"\n\n"}' singleton_F4_sl_onTnt1.sam > singleton_sl_Tnt1_list
```

- Extracting singleton mates using awk.

```
$ awk -f singleton_sl_Tnt1_list bow_sl_ongenome.sam > singleton_sl_Tnt1_mate.sam
```

- Adding header and indexing the reads.

```
$ awk '$1 ~ @' bow_sl_ongenome.sam > header
$ echo -e 'Or header\n\n' | ed singleton_sl_Tnt1_mate.sam
$ samtools view -h singleton_sl_Tnt1_mate.sam > singleton_sl_Tnt1_mate.bam
$ samtools sort singleton_sl_Tnt1_mate.bam -o singleton_sl_Tnt1_mate_sorted.bam
$ samtools index singleton_sl_Tnt1_mate_sorted.bam
```

Extracting T-DNA singletons

- Extracted reads mapped to T-DNA.

```
$ samtools view -h -S -F 4 bow_sl_onTDNAWOTnt.sam > F4_sl_onTDNAWO.sam
$ samtools flagstat F4_sl_onTDNAWO.sam
```

- Extracted singletons out of it.

```
$ samtools view -f 8 -F 4 F4_sl_onTDNAWO.sam > singleton_F4_sl_onTDNAWO.sam
```

- Preparing awk query.

```
$ awk '{print "$1 ~ /"$1"\n\n"}' singleton_F4_ln5_onTDNAWO.sam > singleton_ln5_TDNAWO_list
```

- Extraction singleton mates using awk.

```
$ awk -f singleton_sl_TDNAWO_list bow_sl_ongenome.sam > singleton_sl_TDNAWO_mate.sam
```

- Adding header and indexing the reads.

```
$ awk '$1 ~ @' bow_sl_ongenome.sam > header
$ echo -e 'Or header\n\n' | ed singleton_sl_TDNAWO_mate.sam
$ samtools view -h singleton_sl_TDNAWO_mate.sam > singleton_sl_TDNAWO_mate.bam
$ samtools sort singleton_sl_TDNAWO_mate.bam -o singleton_sl_TDNAWO_mate_sorted.bam
$ samtools index singleton_sl_TDNAWO_mate_sorted.bam
```

**ELSEVIER LICENSE
TERMS AND CONDITIONS**

Jul 02, 2018

This Agreement between Mr. Boominathan Mohanasundaram -- Boominathan Mohanasundaram ("You") and Elsevier ("Elsevier") consists of your license details and the terms and conditions provided by Elsevier and Copyright Clearance Center.

License Number	4380600977876
License date	Jul 02, 2018
Licensed Content Publisher	Elsevier
Licensed Content Publication	Trends in Plant Science
Licensed Content Title	Megaphylls, microphylls and the evolution of leaf development
Licensed Content Author	Alexandru M.F. Tomescu
Licensed Content Date	Jan 1, 2009
Licensed Content Volume	14
Licensed Content Issue	1
Licensed Content Pages	8
Start Page	5
End Page	12
Type of Use	reuse in a thesis/dissertation
Portion	figures/tables/illustrations
Number of figures/tables/illustrations	1
Format	both print and electronic
Are you the author of this Elsevier article?	No
Will you be translating?	No
Original figure numbers	Figure 1
Title of your thesis/dissertation	Investigating phyllid development using Tnt1 insertional "short-leaf" and targeted knockout "slender-leaf" mutants of moss (<i>P. patens</i>).
Expected completion date	Jul 2018
Estimated size (number of pages)	150
Requestor Location	Mr. Boominathan Mohanasundaram IISER-PUNE Dr. Homi Bhabha Road, Pashan Pune, Maharashtra 411008 India Attn: Mr. Boominathan Mohanasundaram
Publisher Tax ID	GB 494 6272 12
Total	0.00 USD

[Terms and Conditions](#)

INTRODUCTION

1. The publisher for this copyrighted material is Elsevier. By clicking "accept" in connection with completing this licensing transaction, you agree that the following terms and conditions apply to this transaction (along with the Billing and Payment terms and conditions



Note: Copyright.com supplies permissions but not the copyrighted content itself.

1
PAYMENT

2
REVIEW

3
CONFIRMATION

Step 3: Order Confirmation

Thank you for your order! A confirmation for your order will be sent to your account email address. If you have questions about your order, you can call us 24 hrs/day, M-F at +1.855.239.3415 Toll Free, or write to us at info@copyright.com. This is not an invoice.

Confirmation Number: 11727776
Order Date: 07/02/2018

If you paid by credit card, your order will be finalized and your card will be charged within 24 hours. If you choose to be invoiced, you can change or cancel your order until the invoice is generated.

Payment Information

Boominathan Mohanasundaram
Mr. Boominathan Mohanasundaram
mboominath@students.iiserpune.ac.in
+91 8380098807
Payment Method: invoice

Billing address:
Mr. Boominathan Mohanasundaram
IISER-PUNE
Dr. Homi Bhabha Road,
Pune, Maharashtra 411008
IN

Order Details

Special Orders

The botanical review

Order detail ID: 71277957
Job Ticket: 501411272
ISSN: 0006-8101
Publication Type: Journal
Volume:
Issue:
Start page:
Publisher: NEW YORK BOTANICAL GARDEN
PRESS
Author/Editor: NEW YORK BOTANICAL GARDEN

Permission Status:  **Special Order**
Special Order Update: Checking availability

Permission type:
Republish or display content

Type of use:
Thesis/Dissertation

Requestor type Academic institution

Format Print, Electronic

Portion image/photo

Number of images/photos requested 1

The requesting person/organization IISER-Pune

Title or numeric reference of the portion(s) Figure 7

Title of the article or chapter the portion is from N/A

Editor of portion(s) N/A

**ELSEVIER LICENSE
TERMS AND CONDITIONS**

Jul 25, 2018

This Agreement between Mr. Boominathan Mohanasundaram -- Boominathan Mohanasundaram ("You") and Elsevier ("Elsevier") consists of your license details and the terms and conditions provided by Elsevier and Copyright Clearance Center.

License Number	4396060306034
License date	Jul 25, 2018
Licensed Content Publisher	Elsevier
Licensed Content Publication	Current Opinion in Plant Biology
Licensed Content Title	Stem cell maintenance in shoot apical meristems
Licensed Content Author	Mariano Perales,G Venugopala Reddy
Licensed Content Date	Feb 1, 2012
Licensed Content Volume	15
Licensed Content Issue	1
Licensed Content Pages	7
Start Page	10
End Page	16
Type of Use	reuse in a thesis/dissertation
Portion	figures/tables/illustrations
Number of figures/tables /illustrations	1
Format	both print and electronic
Are you the author of this Elsevier article?	No
Will you be translating?	No
Original figure numbers	Figure 1
Title of your thesis/dissertation	Investigating phyllid development using Tnt1 insertional "short-leaf" and targeted knockout "slender-leaf" mutants of moss (<i>P. patens</i>).
Expected completion date	Jul 2018
Estimated size (number of pages)	150
Requestor Location	Mr. Boominathan Mohanasundaram IISER-PUNE Dr. Homi Bhabha Road, Pashan Pune, Maharashtra 411008 India Attn: Mr. Boominathan Mohanasundaram
Publisher Tax ID	GB 494 6272 12
Total	0.00 USD

**ELSEVIER LICENSE
TERMS AND CONDITIONS**

Jul 19, 2018

This Agreement between Mr. Boominathan Mohanasundaram -- Boominathan Mohanasundaram ("You") and Elsevier ("Elsevier") consists of your license details and the terms and conditions provided by Elsevier and Copyright Clearance Center.

License Number	4392810015251
License date	Jul 19, 2018
Licensed Content Publisher	Elsevier
Licensed Content Publication	Current Opinion in Plant Biology
Licensed Content Title	Eight types of stem cells in the life cycle of the moss <i>Physcomitrella patens</i>
Licensed Content Author	Rumiko Kofuji, Mitsuyasu Hasebe
Licensed Content Date	Feb 1, 2014
Licensed Content Volume	17
Licensed Content Issue	n/a
Licensed Content Pages	9
Start Page	13
End Page	21
Type of Use	reuse in a thesis/dissertation
Portion	figures/tables/illustrations
Number of figures/tables/illustrations	1
Format	both print and electronic
Are you the author of this Elsevier article?	No
Will you be translating?	No
Original figure numbers	Figure 2
Title of your thesis/dissertation	Investigating phyllid development using Tnt1 insertional "short-leaf" and targeted knockout "slender-leaf" mutants of moss (<i>P. patens</i>).
Expected completion date	Jul 2018
Estimated size (number of pages)	150
Requestor Location	Mr. Boominathan Mohanasundaram IISER-PUNE Dr. Homi Bhabha Road, Pashan Pune, Maharashtra 411008 India Attn: Mr. Boominathan Mohanasundaram
Publisher Tax ID	GB 494 6272 12
Total	0.00 USD
Terms and Conditions	

INTRODUCTION

1. The publisher for this copyrighted material is Elsevier. By clicking "accept" in connection with completing this licensing transaction, you agree that the following terms and conditions apply to this transaction (along with the Billing and Payment terms and conditions

**ELSEVIER LICENSE
TERMS AND CONDITIONS**

Jul 02, 2018

This Agreement between Mr. Boominathan Mohanasundaram -- Boominathan Mohanasundaram ("You") and Elsevier ("Elsevier") consists of your license details and the terms and conditions provided by Elsevier and Copyright Clearance Center.

License Number	4380611181832
License date	Jul 02, 2018
Licensed Content Publisher	Elsevier
Licensed Content Publication	Current Opinion in Plant Biology
Licensed Content Title	The role of hormones in shoot apical meristem function
Licensed Content Author	Eilon Shani,Osnat Yanai,Naomi Ori
Licensed Content Date	Oct 1, 2006
Licensed Content Volume	9
Licensed Content Issue	5
Licensed Content Pages	6
Start Page	484
End Page	489
Type of Use	reuse in a thesis/dissertation
Intended publisher of new work	other
Portion	figures/tables/illustrations
Number of figures/tables/illustrations	1
Format	both print and electronic
Are you the author of this Elsevier article?	No
Will you be translating?	No
Original figure numbers	Figure 1
Title of your thesis/dissertation	Investigating phyllid development using Tnt1 insertional "short-leaf" and targeted knockout "slender-leaf" mutants of moss (<i>P. patens</i>).
Expected completion date	Jul 2018
Estimated size (number of pages)	150
Requestor Location	Mr. Boominathan Mohanasundaram IISER-PUNE Dr. Homi Bhabha Road, Pashan Pune, Maharashtra 411008 India Attn: Mr. Boominathan Mohanasundaram
Publisher Tax ID	GB 494 6272 12
Total	0.00 USD
Terms and Conditions	

INTRODUCTION

**SPRINGER NATURE LICENSE
TERMS AND CONDITIONS**

Jul 02, 2018

This Agreement between Mr. Boominathan Mohanasundaram -- Boominathan Mohanasundaram ("You") and Springer Nature ("Springer Nature") consists of your license details and the terms and conditions provided by Springer Nature and Copyright Clearance Center.

License Number	4380630028885
License date	Jul 02, 2018
Licensed Content Publisher	Springer Nature
Licensed Content Publication	Nature
Licensed Content Title	Asymmetric leaves1 mediates leaf patterning and stem cell function in Arabidopsis
Licensed Content Author	Mary E. Byrne, Ross Barley, Mark Curtis, Juana Maria Arroyo, Maitreya Dunham et al.
Licensed Content Date	Dec 21, 2000
Licensed Content Volume	408
Licensed Content Issue	6815
Type of Use	Thesis/Dissertation
Requestor type	academic/university or research institute
Format	print and electronic
Portion	figures/tables/illustrations
Number of figures/tables /illustrations	1
High-res required	no
Will you be translating?	no
Circulation/distribution	<501
Author of this Springer Nature content	no
Title	Investigating phyllid development using Tnt1 insertional "short-leaf" and targeted knockout "slender-leaf" mutants of moss (<i>P. patens</i>).
Instructor name	n/a
Institution name	n/a
Expected presentation date	Jul 2018
Portions	Figure 4
Requestor Location	Mr. Boominathan Mohanasundaram IISER-PUNE Dr. Homi Bhabha Road, Pashan Pune, Maharashtra 411008 India Attn: Mr. Boominathan Mohanasundaram

**ELSEVIER LICENSE
TERMS AND CONDITIONS**

Jul 02, 2018

This Agreement between Mr. Boominathan Mohanasundaram -- Boominathan Mohanasundaram ("You") and Elsevier ("Elsevier") consists of your license details and the terms and conditions provided by Elsevier and Copyright Clearance Center.

License Number	4380620859289
License date	Jul 02, 2018
Licensed Content Publisher	Elsevier
Licensed Content Publication	Trends in Plant Science
Licensed Content Title	Auxin and phyllotaxis
Licensed Content Author	Cris Kuhlemeier,Didier Reinhardt
Licensed Content Date	1 May 2001
Licensed Content Volume	6
Licensed Content Issue	5
Licensed Content Pages	3
Start Page	187
End Page	189
Type of Use	reuse in a thesis/dissertation
Intended publisher of new work	other
Portion	figures/tables/illustrations
Number of figures/tables/illustrations	1
Format	both print and electronic
Are you the author of this Elsevier article?	No
Will you be translating?	No
Original figure numbers	Figure 2
Title of your thesis/dissertation	Investigating phyllid development using Tnt1 insertional "short-leaf" and targeted knockout "slender-leaf" mutants of moss (<i>P. patens</i>).
Expected completion date	Jul 2018
Estimated size (number of pages)	150
Requestor Location	Mr. Boominathan Mohanasundaram IISER-PUNE Dr. Homi Bhabha Road, Pashan Pune, Maharashtra 411008 India Attn: Mr. Boominathan Mohanasundaram
Publisher Tax ID	GB 494 6272 12
Total	0.00 USD
Terms and Conditions	

INTRODUCTION



Note: Copyright.com supplies permissions but not the copyrighted content itself.

1
PAYMENT

2
REVIEW

3
CONFIRMATION

Step 3: Order Confirmation

Thank you for your order! A confirmation for your order will be sent to your account email address. If you have questions about your order, you can call us 24 hrs/day, M-F at +1.855.239.3415 Toll Free, or write to us at info@copyright.com. This is not an invoice.

Confirmation Number: 11733489
Order Date: 07/25/2018

If you paid by credit card, your order will be finalized and your card will be charged within 24 hours. If you choose to be invoiced, you can change or cancel your order until the invoice is generated.

Payment Information

Boominathan Mohanasundaram
Mr. Boominathan Mohanasundaram
mboominath@students.iiserpune.ac.in
+91 8380098807
Payment Method: n/a

Order Details

The plant cell

Order detail ID: 71333587
Order License Id: 4396070050169
ISSN: 1040-4651
Publication Type: Journal
Volume:
Issue:
Start page:
Publisher: AMERICAN SOCIETY OF PLANT
PHYSIOLOGISTS,
Author/Editor: AMERICAN SOCIETY OF PLANT
PHYSIOLOGISTS

Permission Status: **Granted**
Permission type: Republish or display content
Type of use: Republish in a thesis/dissertation

Requestor type Academic institution

Format Print, Electronic

Portion image/photo

Number of images/photos requested 1

The requesting person/organization IISER-Pune

Title or numeric reference of the portion(s) Figure 2

Title of the article or chapter the portion is from N/A

Editor of portion(s) N/A

Author of portion(s) N/A

Volume of serial or monograph N/A

**JOHN WILEY AND SONS LICENSE
TERMS AND CONDITIONS**

May 28, 2018

This Agreement between Mr. Boominathan Mohanasundaram -- Boominathan Mohanasundaram ("You") and John Wiley and Sons ("John Wiley and Sons") consists of your license details and the terms and conditions provided by John Wiley and Sons and Copyright Clearance Center.

License Number	4357980216513
License date	May 28, 2018
Licensed Content Publisher	John Wiley and Sons
Licensed Content Publication	New Phytologist
Licensed Content Title	Evolution of leaf developmental mechanisms
Licensed Content Author	Miltos Tsiantis, Sophie Jasinski, Paolo Piazza
Licensed Content Date	Jun 14, 2005
Licensed Content Volume	167
Licensed Content Issue	3
Licensed Content Pages	18
Type of use	Dissertation/Thesis
Requestor type	University/Academic
Format	Print and electronic
Portion	Figure/table
Number of figures/tables	1
Original Wiley figure/table number(s)	Figure 4
Will you be translating?	No
Title of your thesis / dissertation	Investigating phyllid development using Tnt1 insertional "short-leaf" and targeted knockout "slender-leaf" mutants of moss (<i>P. patens</i>).
Expected completion date	Jul 2018
Expected size (number of pages)	150
Requestor Location	Mr. Boominathan Mohanasundaram IISER-PUNE Dr. Homi Bhabha Road, Pashan Pune, Maharashtra 411008 India Attn: Mr. Boominathan Mohanasundaram
Publisher Tax ID	EU826007151
Total	0.00 USD
Terms and Conditions	



Note: Copyright.com supplies permissions but not the copyrighted content itself.

1
PAYMENT

2
REVIEW

3
CONFIRMATION

Step 3: Order Confirmation

Thank you for your order! A confirmation for your order will be sent to your account email address. If you have questions about your order, you can call us 24 hrs/day, M-F at +1.855.239.3415 Toll Free, or write to us at info@copyright.com. This is not an invoice.

Confirmation Number: 11720516
Order Date: 05/29/2018

If you paid by credit card, your order will be finalized and your card will be charged within 24 hours. If you choose to be invoiced, you can change or cancel your order until the invoice is generated.

Payment Information

Boominathan Mohanasundaram
Mr. Boominathan Mohanasundaram
mboominath@students.iiserpune.ac.in
+91 8380098807
Payment Method: n/a

Order Details

The plant cell

Order detail ID: 71219764
Order License Id: 4358040435314
ISSN: 1040-4651
Publication Type: Journal
Volume:
Issue:
Start page:
Publisher: AMERICAN SOCIETY OF PLANT
PHYSIOLOGISTS,
Author/Editor: AMERICAN SOCIETY OF PLANT
PHYSIOLOGISTS

Permission Status: **Granted**
Permission type: Republish or display content
Type of use: Republish in a thesis/dissertation

Requestor type Academic institution

Format Print, Electronic

Portion cartoon

Number of cartoons 1

The requesting person/organization Boominathan M, Indian
Institute of Science
Education and research
-Pune

Title or numeric reference of the portion(s) Figure 2

Title of the article or chapter the portion is from The role of Phantastica in
leaf development

Editor of portion(s) N/A

Author of portion(s) N/A

Note: This item will be invoiced or charged separately through CCC's **RightsLink** service. [More info](#)

\$ 0.00

**OXFORD UNIVERSITY PRESS LICENSE
TERMS AND CONDITIONS**

May 29, 2018

This Agreement between Mr. Boominathan Mohanasundaram -- Boominathan Mohanasundaram ("You") and Oxford University Press ("Oxford University Press") consists of your license details and the terms and conditions provided by Oxford University Press and Copyright Clearance Center.

License Number	4358031205066
License date	May 29, 2018
Licensed content publisher	Oxford University Press
Licensed content publication	Plant and Cell Physiology
Licensed content title	Leaf adaxial-abaxial polarity specification and lamina outgrowth: evolution and development
Licensed content author	Yamaguchi, Takahiro; Nukazuka, Akira
Licensed content date	May 21, 2012
Type of Use	Thesis/Dissertation
Institution name	
Title of your work	Investigating phyllid development using Tnt1 insertional "short-leaf" and targeted knockout "slender-leaf" mutants of moss (<i>P. patens</i>).
Publisher of your work	n/a
Expected publication date	Jul 2018
Permissions cost	0.00 USD
Value added tax	0.00 USD
Total	0.00 USD
Title	Investigating phyllid development using Tnt1 insertional "short-leaf" and targeted knockout "slender-leaf" mutants of moss (<i>P. patens</i>).
Instructor name	n/a
Institution name	n/a
Expected presentation date	Jul 2018
Portions	Figure 1
Requestor Location	Mr. Boominathan Mohanasundaram IISER-PUNE Dr. Homi Bhabha Road, Pashan Pune, Maharashtra 411008 India Attn: Mr. Boominathan Mohanasundaram
Publisher Tax ID	GB125506730
Billing Type	Invoice

**SPRINGER NATURE LICENSE
TERMS AND CONDITIONS**

May 29, 2018

This Agreement between Mr. Boominathan Mohanasundaram -- Boominathan Mohanasundaram ("You") and Springer Nature ("Springer Nature") consists of your license details and the terms and conditions provided by Springer Nature and Copyright Clearance Center.

License Number	4358000261217
License date	May 29, 2018
Licensed Content Publisher	Springer Nature
Licensed Content Publication	Nature
Licensed Content Title	Role of PHABULOSA and PHAVOLUTA in determining radial patterning in shoots
Licensed Content Author	Jane R. McConnell, John Emery, Yuval Eshed, Ning Bao, John Bowman et al.
Licensed Content Date	Jun 7, 2001
Licensed Content Volume	411
Licensed Content Issue	6838
Type of Use	Thesis/Dissertation
Requestor type	academic/university or research institute
Format	print and electronic
Portion	figures/tables/illustrations
Number of figures/tables /illustrations	1
High-res required	no
Will you be translating?	no
Circulation/distribution	<501
Author of this Springer Nature content	no
Title	Investigating phyllid development using Tnt1 insertional "short-leaf" and targeted knockout "slender-leaf" mutants of moss (<i>P. patens</i>).
Instructor name	n/a
Institution name	n/a
Expected presentation date	Jul 2018
Portions	Figure 1
Requestor Location	Mr. Boominathan Mohanasundaram IISER-PUNE Dr. Homi Bhabha Road, Pashan Pune, Maharashtra 411008 India Attn: Mr. Boominathan Mohanasundaram



Note: Copyright.com supplies permissions but not the copyrighted content itself.

1
PAYMENT

2
REVIEW

3
CONFIRMATION

Step 3: Order Confirmation

Thank you for your order! A confirmation for your order will be sent to your account email address. If you have questions about your order, you can call us 24 hrs/day, M-F at +1.855.239.3415 Toll Free, or write to us at info@copyright.com. This is not an invoice.

Confirmation Number: 11733498
Order Date: 07/25/2018

If you paid by credit card, your order will be finalized and your card will be charged within 24 hours. If you choose to be invoiced, you can change or cancel your order until the invoice is generated.

Payment Information

Boominathan Mohanasundaram
Mr. Boominathan Mohanasundaram
mboominath@students.iiserpune.ac.in
+91 8380098807
Payment Method: n/a

Order Details

The plant cell

Order detail ID: 71333618
Order License Id: 4396070993703

ISSN: 1040-4651
Publication Type: Journal

Volume:
Issue:

Start page:

Publisher: AMERICAN SOCIETY OF PLANT
PHYSIOLOGISTS,

Author/Editor: AMERICAN SOCIETY OF PLANT
PHYSIOLOGISTS

Permission Status: **Granted**

Permission type: Republish or display content

Type of use: Republish in a thesis/dissertation

Requestor type Academic institution

Format Print, Electronic

Portion image/photo

Number of images/photos requested 1

The requesting person/organization IISER-Pune

Title or numeric reference of the portion(s) Figure 1

Title of the article or chapter the portion is from N/A

Editor of portion(s) N/A

Author of portion(s) N/A

Volume of serial or monograph N/A

**SPRINGER NATURE LICENSE
TERMS AND CONDITIONS**

May 29, 2018

This Agreement between Mr. Boominathan Mohanasundaram -- Boominathan Mohanasundaram ("You") and Springer Nature ("Springer Nature") consists of your license details and the terms and conditions provided by Springer Nature and Copyright Clearance Center.

License Number	4358070401612
License date	May 29, 2018
Licensed Content Publisher	Springer Nature
Licensed Content Publication	Nature
Licensed Content Title	The expression domain of PHANTASTICA determines leaflet placement in compound leaves
Licensed Content Author	Minsung Kim, Sheila McCormick, Marja Timmermans, Neelima Sinha
Licensed Content Date	Jul 24, 2003
Licensed Content Volume	424
Licensed Content Issue	6947
Type of Use	Thesis/Dissertation
Requestor type	academic/university or research institute
Format	print and electronic
Portion	figures/tables/illustrations
Number of figures/tables /illustrations	1
High-res required	no
Will you be translating?	no
Circulation/distribution	<501
Author of this Springer Nature content	no
Title	Investigating phyllid development using Tnt1 insertional "short-leaf" and targeted knockout "slender-leaf" mutants of moss (<i>P. patens</i>).
Instructor name	n/a
Institution name	n/a
Expected presentation date	Jul 2018
Portions	Figure 1
Requestor Location	Mr. Boominathan Mohanasundaram IISER-PUNE Dr. Homi Bhabha Road, Pashan Pune, Maharashtra 411008 India Attn: Mr. Boominathan Mohanasundaram
Billing Type	Invoice



Note: Copyright.com supplies permissions but not the copyrighted content itself.

1
PAYMENT

2
REVIEW

3
CONFIRMATION

Step 3: Order Confirmation

Thank you for your order! A confirmation for your order will be sent to your account email address. If you have questions about your order, you can call us 24 hrs/day, M-F at +1.855.239.3415 Toll Free, or write to us at info@copyright.com. This is not an invoice.

Confirmation Number: 11720520
Order Date: 05/29/2018

If you paid by credit card, your order will be finalized and your card will be charged within 24 hours. If you choose to be invoiced, you can change or cancel your order until the invoice is generated.

Payment Information

Boominathan Mohanasundaram
Mr. Boominathan Mohanasundaram
mboominath@students.iiserpune.ac.in
+91 8380098807
Payment Method: n/a

Order Details

The plant cell

Order detail ID: 71219773
Order License Id: 4358050844985
ISSN: 1040-4651
Publication Type: Journal
Volume:
Issue:
Start page:
Publisher: AMERICAN SOCIETY OF PLANT
PHYSIOLOGISTS,
Author/Editor: AMERICAN SOCIETY OF PLANT
PHYSIOLOGISTS

Permission Status: **Granted**
Permission type: Republish or display content
Type of use: Republish in a thesis/dissertation

Requestor type: Academic institution

Format: Print, Electronic

Portion: chart/graph/table/figure

Number of charts/graphs/tables/figures: 1

The requesting person/organization: Boominathan M, Indian Institute of Science Education and research -Pune

Title or numeric reference of the portion(s): Figure 4

Title of the article or chapter the portion is from: PHANTASTICA Regulates Development of the Adaxial Mesophyll in Nicotiana Leaves

Editor of portion(s): N/A

Note: This item will be invoiced or charged separately through CCC's **RightsLink** service. [More info](#)

\$ 0.00

**OXFORD UNIVERSITY PRESS LICENSE
TERMS AND CONDITIONS**

May 29, 2018

This Agreement between Mr. Boominathan Mohanasundaram -- Boominathan Mohanasundaram ("You") and Oxford University Press ("Oxford University Press") consists of your license details and the terms and conditions provided by Oxford University Press and Copyright Clearance Center.

License Number	4358061293479
License date	May 29, 2018
Licensed content publisher	Oxford University Press
Licensed content publication	Annals of Botany
Licensed content title	A role for <i>PHANTASTICA</i> in medio-lateral regulation of adaxial domain development in tomato and tobacco leaves
Licensed content author	Zoulias, Nicholas; Koenig, Daniel
Licensed content date	Dec 19, 2011
Type of Use	Thesis/Dissertation
Institution name	
Title of your work	Investigating phyllid development using Tnt1 insertional "short-leaf" and targeted knockout "slender-leaf" mutants of moss (<i>P. patens</i>).
Publisher of your work	n/a
Expected publication date	Jul 2018
Permissions cost	0.00 USD
Value added tax	0.00 USD
Total	0.00 USD
Title	Investigating phyllid development using Tnt1 insertional "short-leaf" and targeted knockout "slender-leaf" mutants of moss (<i>P. patens</i>).
Instructor name	n/a
Institution name	n/a
Expected presentation date	Jul 2018
Portions	Figure 1
Requestor Location	Mr. Boominathan Mohanasundaram IISER-PUNE Dr. Homi Bhabha Road, Pashan Pune, Maharashtra 411008 India Attn: Mr. Boominathan Mohanasundaram
Publisher Tax ID	GB125506730
Billing Type	Invoice

**ELSEVIER LICENSE
TERMS AND CONDITIONS**

May 30, 2018

This Agreement between Mr. Boominathan Mohanasundaram -- Boominathan Mohanasundaram ("You") and Elsevier ("Elsevier") consists of your license details and the terms and conditions provided by Elsevier and Copyright Clearance Center.

License Number	4358590075676
License date	May 30, 2018
Licensed Content Publisher	Elsevier
Licensed Content Publication	Current Biology
Licensed Content Title	Control of Organ Size in Plants
Licensed Content Author	Anahid E. Powell,Michael Lenhard
Licensed Content Date	8 May 2012
Licensed Content Volume	22
Licensed Content Issue	9
Licensed Content Pages	8
Start Page	R360
End Page	R367
Type of Use	reuse in a thesis/dissertation
Intended publisher of new work	other
Portion	figures/tables/illustrations
Number of figures/tables /illustrations	1
Format	both print and electronic
Are you the author of this Elsevier article?	No
Will you be translating?	No
Original figure numbers	Figure 2
Title of your thesis/dissertation	Investigating phyllid development using Tnt1 insertional "short-leaf" and targeted knockout "slender-leaf" mutants of moss (<i>P. patens</i>).
Expected completion date	Jul 2018
Estimated size (number of pages)	150
Requestor Location	Mr. Boominathan Mohanasundaram IISER-PUNE Dr. Homi Bhabha Road, Pashan Pune, Maharashtra 411008 India Attn: Mr. Boominathan Mohanasundaram

**ELSEVIER LICENSE
TERMS AND CONDITIONS**

Jul 20, 2018

This Agreement between Mr. Boominathan Mohanasundaram -- Boominathan Mohanasundaram ("You") and Elsevier ("Elsevier") consists of your license details and the terms and conditions provided by Elsevier and Copyright Clearance Center.

License Number	4392871306868
License date	Jul 20, 2018
Licensed Content Publisher	Elsevier
Licensed Content Publication	Cell
Licensed Content Title	The Making of a Compound Leaf: Genetic Manipulation of Leaf Architecture in Tomato
Licensed Content Author	Dana Hareven, Tamar Gutfinger, Ania Parnis, Yuval Eshed, Eliezer Lifschitz
Licensed Content Date	Mar 8, 1996
Licensed Content Volume	84
Licensed Content Issue	5
Licensed Content Pages	10
Start Page	735
End Page	744
Type of Use	reuse in a thesis/dissertation
Portion	figures/tables/illustrations
Number of figures/tables/illustrations	1
Format	both print and electronic
Are you the author of this Elsevier article?	No
Will you be translating?	No
Original figure numbers	Figure 1
Title of your thesis/dissertation	Investigating phyllid development using Tnt1 insertional "short-leaf" and targeted knockout "slender-leaf" mutants of moss (<i>P. patens</i>).
Expected completion date	Jul 2018
Estimated size (number of pages)	150
Requestor Location	Mr. Boominathan Mohanasundaram IISER-PUNE Dr. Homi Bhabha Road, Pashan Pune, Maharashtra 411008 India Attn: Mr. Boominathan Mohanasundaram
Publisher Tax ID	GB 494 6272 12
Total	0.00 USD

[Terms and Conditions](#)

INTRODUCTION

1. The publisher for this copyrighted material is Elsevier. By clicking "accept" in connection with completing this licensing transaction, you agree that the following terms and conditions



Note: Copyright.com supplies permissions but not the copyrighted content itself.

1
PAYMENT

2
REVIEW

3
CONFIRMATION

Step 3: Order Confirmation

Thank you for your order! A confirmation for your order will be sent to your account email address. If you have questions about your order, you can call us 24 hrs/day, M-F at +1.855.239.3415 Toll Free, or write to us at info@copyright.com. This is not an invoice.

Confirmation Number: 11732068
Order Date: 07/20/2018

If you paid by credit card, your order will be finalized and your card will be charged within 24 hours. If you choose to be invoiced, you can change or cancel your order until the invoice is generated.

Payment Information

Boominathan Mohanasundaram
Mr. Boominathan Mohanasundaram
mboominath@students.iiserpune.ac.in
+91 8380098807
Payment Method: invoice

Billing address:
Mr. Boominathan Mohanasundaram
IISER-PUNE
Dr. Homi Bhabha Road,
Pune, Maharashtra 411008
IN

Order Details

Special Orders

The plant cell

Order detail ID: 71319818
Job Ticket: 501415413
ISSN: 1040-4651
Publication Type: Journal
Volume:
Issue:
Start page:
Publisher: AMERICAN SOCIETY OF PLANT
PHYSIOLOGISTS,
Author/Editor: AMERICAN SOCIETY OF PLANT
PHYSIOLOGISTS

Permission Status:  **Special Order**
Special Order Update: Checking availability

Permission type:
Republish or display content

Type of use:
Republish in a thesis/dissertation

Requestor type Academic institution

Format Print, Electronic

Portion image/photo

Number of images/photos requested 1

The requesting person/organization Boominathan M

Title or numeric reference of the portion(s) Figure 6

Title of the article or chapter the portion is from Compound Leaf Development and Evolution in the Legumes

Editor of portion(s) N/A



Note: Copyright.com supplies permissions but not the copyrighted content itself.

1
PAYMENT

2
REVIEW

3
CONFIRMATION

Step 3: Order Confirmation

Thank you for your order! A confirmation for your order will be sent to your account email address. If you have questions about your order, you can call us 24 hrs/day, M-F at +1.855.239.3415 Toll Free, or write to us at info@copyright.com. This is not an invoice.

Confirmation Number: 11720724
Order Date: 05/30/2018

If you paid by credit card, your order will be finalized and your card will be charged within 24 hours. If you choose to be invoiced, you can change or cancel your order until the invoice is generated.

Payment Information

Boominathan Mohanasundaram
Mr. Boominathan Mohanasundaram
mboominath@students.iiserpune.ac.in
+91 8380098807
Payment Method: n/a

Order Details

Plant physiology

Order detail ID: 71220668
Order License Id: 4358570872255

ISSN: 1532-2548
Publication Type: e-Journal

Volume:

Issue:

Start page:

Publisher: AMERICAN SOCIETY OF PLANT BIOLOGISTS

Author/Editor: American Society of Plant Biologists ; American Society of Plant Physiologists

Permission Status: **Granted**

Permission type: Republish or display content
Type of use: Republish in a thesis/dissertation

Requestor type Academic institution

Format Print, Electronic

Portion image/photo

Number of images/photos requested 1

The requesting person/organization Boominathan M, Indian Institute of Science Education and research -Pune

Title or numeric reference of the portion(s) Figure 2

Title of the article or chapter the portion is from Genetic Analysis of DEFECTIVE KERNEL1 Loop Function in Three-Dimensional Body Patterning in Physcomitrella patens

Editor of portion(s) N/A

Note: This item will be invoiced or charged separately through CCC's **RightsLink** service. [More info](#)

\$ 0.00

**JOHN WILEY AND SONS LICENSE
TERMS AND CONDITIONS**

Jun 01, 2018

This Agreement between Mr. Boominathan Mohanasundaram -- Boominathan Mohanasundaram ("You") and John Wiley and Sons ("John Wiley and Sons") consists of your license details and the terms and conditions provided by John Wiley and Sons and Copyright Clearance Center.

License Number	4360030459097
License date	Jun 01, 2018
Licensed Content Publisher	John Wiley and Sons
Licensed Content Publication	Wiley Books
Licensed Content Title	Putting Physcomitrella patens on the Tree of Life: The Evolution and Ecology of Mosses
Licensed Content Date	Jul 10, 2009
Licensed Content Pages	15
Type of use	Dissertation/Thesis
Requestor type	University/Academic
Format	Print and electronic
Portion	Figure/table
Number of figures/tables	1
Original Wiley figure/table number(s)	Figure 1.2
Will you be translating?	No
Title of your thesis / dissertation	Investigating phyllid development using Tnt1 insertional "short-leaf" and targeted knockout "slender-leaf" mutants of moss (<i>P. patens</i>).
Expected completion date	Jul 2018
Expected size (number of pages)	150
Requestor Location	Mr. Boominathan Mohanasundaram IISER-PUNE Dr. Homi Bhabha Road, Pashan Pune, Maharashtra 411008 India Attn: Mr. Boominathan Mohanasundaram
Publisher Tax ID	EU826007151
Total	0.00 USD
Terms and Conditions	

TERMS AND CONDITIONS

This copyrighted material is owned by or exclusively licensed to John Wiley & Sons, Inc. or one of its group companies (each a "Wiley

**ELSEVIER LICENSE
TERMS AND CONDITIONS**

Jun 07, 2018

This Agreement between Mr. Boominathan Mohanasundaram -- Boominathan Mohanasundaram ("You") and Elsevier ("Elsevier") consists of your license details and the terms and conditions provided by Elsevier and Copyright Clearance Center.

License Number	4363460050200
License date	Jun 07, 2018
Licensed Content Publisher	Elsevier
Licensed Content Publication	Current Opinion in Plant Biology
Licensed Content Title	Eight types of stem cells in the life cycle of the moss <i>Physcomitrella patens</i>
Licensed Content Author	Rumiko Kofuji, Mitsuyasu Hasebe
Licensed Content Date	Feb 1, 2014
Licensed Content Volume	17
Licensed Content Issue	n/a
Licensed Content Pages	9
Start Page	13
End Page	21
Type of Use	reuse in a thesis/dissertation
Portion	figures/tables/illustrations
Number of figures/tables/illustrations	1
Format	both print and electronic
Are you the author of this Elsevier article?	No
Will you be translating?	No
Original figure numbers	Figure 1
Title of your thesis/dissertation	Investigating phyllid development using Tnt1 insertional "short-leaf" and targeted knockout "slender-leaf" mutants of moss (<i>P. patens</i>).
Expected completion date	Jul 2018
Estimated size (number of pages)	150
Requestor Location	Mr. Boominathan Mohanasundaram IISER-PUNE Dr. Homi Bhabha Road, Pashan Pune, Maharashtra 411008 India Attn: Mr. Boominathan Mohanasundaram
Publisher Tax ID	GB 494 6272 12
Total	0.00 USD
Terms and Conditions	

INTRODUCTION

1. The publisher for this copyrighted material is Elsevier. By clicking "accept" in connection with completing this licensing transaction, you agree that the following terms and conditions apply to this transaction (along with the Billing and Payment terms and conditions

Boominathan MOHANASUNDARAM

PERSONAL DATA

PLACE, DOB and GENDER: Coimbatore, TN, India | 01 March 1989 | Male
WORK ADDRESS: Molecular Plant Biology Lab, IISER-Pune, Maharashtra, India – 411008.
PERMANENT ADDRESS: 541/1433, Gandhimanagar, Peelamedu post, India - 641004.
PHONE: +918380098807
EMAIL: mboominath@students.iiserpune.ac.in

ACADEMIC PROFILE

- CURRENT Ph.D in BIOLOGICAL SCIENCE, **IISER-Pune**, Maharashtra
working since *August, 2011* in Molecular Plant Biology Lab.
Thesis title: “Investigating phyllid development using Tnt1 insertional
“short-leaf” and targeted knockout “slender-leaf” mutants of moss (*P. patens*)”
Advisor: Dr. Anjan K. BANERJEE | CGPA: 9.5/10
- JUNE 2010 *Bachelor of Technology Degree* in BIOTECHNOLOGY
Agricultural College and Research Institute, Coimbatore.
Tamil Nadu Agricultural University, Coimbatore
OGP: 8.65/10
- MARCH 2006 Higher Secondary Course Certificate at **Sri Gopal Naidu Hr Sec School**, Coimbatore
PERCENTILE: 90.08
- APRIL 2004 Secondary School Leaving Certificate at **Sri Gopal Naidu Hr Sec School**, Coimbatore
PERCENTILE: 95.2

SCHOLARSHIPS AND CERTIFICATES

- AUG. 2011 Junior Research Fellowship - CSIR NET (Rank: 98)
FEB. 2011 Graduate Aptitude Test in Engineering -GATE (Score: 43)

PUBLICATIONS

- Mohanasundaram, B.**, Rajmane, Jogdand, S., Bhide, A., and Banerjee, A. (2018). Analysis of Tnt1 transposition activity in moss (*Physcomitrella patens*) and isolation of mutants with impaired gametophyte development. **Molecular Genetics and Genomics**. under review.
- Ghadge, A.G., Karmakar, K., Devani, R.S., Banerjee, J., **Mohanasundaram, B.**, Sinha, R.K., Sinha, S. and Banerjee, A.K., 2014. Flower development, pollen fertility and sex expression analyses of three sexual phenotypes of *Coccinia grandis*. **BMC plant biology**, 14(1), p.325.

SEMINARS AND CONFERENCES

- Presented a Poster on “A novel bryophyte-specific gene ‘Short-leaf’ regulates gametophore development in *P. patens*” in the Biannual EMBO conference “New Shores in Land Plant Evolution”, held at Lisbon, 2018.

2. Presented a Poster on "Conserved role of SCARECROW (SCR) in regulation of asymmetric cell division (ACD) involved in leaf shape control of *P. patens*." in the Biannual EMBO conference "New Shores in Land Plant Evolution", held at Lisbon, 2018.
3. Presented a Poster on "Understanding moss leaf development through Tnt1 insertional "short-leaf" and targeted knockout "slender-leaf" mutants" in International Conference on Plant Developmental Biology (ICPDB-2017), held at NISER, Bhubaneswar.
4. Delivered oral presentation on "Recent developments in pteridophyte biology" at the national symposium on "The genomic age challenges and opportunities in taxonomy and biology of Indian Pteridophytes" organised by BSI and Indian fern society, held at Pune, 2017

WORK EXPERIENCE

- | | |
|------------------------|--|
| JULY 2010 - JULY 2011 | <p><i>Junior Research Fellow</i> at Molecular Ecology Lab, TNAU, Coimbatore
 Worked under the guidance of <i>Dr. S. Mohankumar</i>, focusing on barcoding and mitochondrial genome sequencing of mealy bug species infesting agronomically important crop species.</p> |
| SEPT. 2009 - APR. 2010 | <p><i>Project Trainee</i> at CPMB, TNAU, Coimbatore
 Worked on the project Engineering bouganin gene to eliminate cytotoxicity under the guidance of <i>Dr. R. Balasaraswathi</i>.</p> |

WET-LAB SKILLS

- An up to date knowledge on working with *Physcomitrella patens*.
- Experience in tissue culturing of *Marchantia* and *Tocacco*.
- Expertise on molecular biology techniques.
- Experience in handling radio-active materials (P32) for DNA marker analysis.

COMPUTER SKILLS

Basic Knowledge: Bash, GNU Emacs and \LaTeX
 Intermediate Knowledge: LINUX, Python, R, sed and AWK
 Bioinformatics: Genome analysis, NGS data analysis, Phylogenetic tree construction.

INTERESTS AND ACTIVITIES

Programming and Mathematical models
 Tinkering with electronic gadgets
 Trekking and Wild life census

DECLARATION

I do hereby declare that the particulars of information and facts stated herein above are true, correct and complete to the best of my knowledge and belief.

Place : Pune
 Date : 15-11-2018

Name : BOOMINATHAN. M